



UNIVERSITY OF
LEICESTER

Synthesis of Teixobactin Analogues: Cyclic Peptidomimetics to Combat Antibiotic Resistance

Thesis submitted for the degree of
Doctor of Philosophy
at the University of Leicester, UK

Georgina Claire Girt MSc

Department of Chemistry, University of Leicester

Initial Submission September 2017

Final Submission March 2018

Abstract

Synthesis of Teixobactin Analogues: Cyclic Peptidomimetics to Combat Antibiotic Resistance – Georgina Claire Girt, MSc

The development of bacterial resistance over time combined with the lack of novel compounds has resulted in a drastic need for new antibiotic drugs. The structure of teixobactin, a cyclic undecapeptide, was published in January 2015 in a paper describing the use of an “iChip” to successfully grow a number of previously uncultivable bacteria. Teixobactin, a cyclic depsipeptide made up of 11 amino residues, containing the unproteinogenic amino acid L-*allo*-enduracididine, was found to have μM activity against many Gram-positive bacteria, including *Clostridium difficile* and methicillin-resistant *Staphylococcus aureus* (MRSA).

This research aimed to both further elucidate the mechanism of action of teixobactin by examining the structure-activity relationship of various moieties of the compound; and to create related compounds that could be synthesised simply and economically, whilst retaining potency against Gram-positive bacteria. These focused particularly on investigating the role of residues 1-7; the linear hydrophobic tail, and variation of the nonproteinogenic residue by replacement with genetically encoded variants. To form the native macrocycle, a simple synthetic route towards L-*allo*-enduracididine was required; a novel route using Ni(II) Schiff base complex was attempted.

The formation of the 13-membered macrocyclic core of teixobactin was attempted with multiple methods of cyclisation, using both solution-phase and on-resin approaches, ultimately resulting in an effective route providing 100% conversion of linear precursors in 20 minutes.

Nineteen analogues were synthesised and submitted for biological assays. These compounds were acetylated, prenylated or lipidated in place of residues 1-7, with L-*allo*-enduracididine mutated to seven different residues varying in functionality, basicity and structure. Of the compounds tested, four were found to have antibiotic activity, with one compound displaying high potency with a minimum inhibitory concentration (MIC) value ($0.5 \mu\text{g}/\text{mL}$), comparable to native teixobactin itself.

Acknowledgements

First and foremost, I would like to thank Dr Andrew Jamieson for offering me the opportunity to work on this project and for all support and guidance he has given me throughout my PhD. I would also like to thank the other members of the Jamieson group, and the students and academics of the chemical biology lab at Leicester for providing me with such a stimulating and interesting working environment during my time here.

This research would not have been possible without funding from the European Regional Development Fund (ERDF) Innovation through the Research Support Accelerator (IRSA), the University of Leicester and Pepceuticals Ltd, from which I would particularly like to thank Dr Kamal Badiani for his generosity.

Thank you to Prof Marco Oggioni for his expertise and ideas regarding the biological testing of the peptide analogues, and for Zaaïma Al-Jabri and Megan De Ste Croix for carrying out all the MIC assay work. Thanks to Mick Lee and Gerry Griffiths for helping me with numerous LCMS and NMR throughout the course of my PhD.

To my good friends at Leicester: Thalassa, Marian, Todd, Shannon, Alex, Javier and Tom – thank you for being such delightful people, for joining me on Friday nights at the pub (and sometimes later at the student union), and for helping me keep my sanity. To my friends who travelled further afield to do their PhDs, particularly Dan Francis - thanks for sharing the experience, and for providing me with many articles from obscure journals.

Finally, I'd like to express my gratitude to my family: my amazing parents and my wonderful sister Susannah, who have always supported me throughout all my endeavours. Without them, this would not have been possible.

Abbreviations

Ahx	6-Aminohexanoic acid
AMP	Antimicrobial peptide
AMR	Antimicrobial resistance
Boc	<i>tert</i> -Butyloxycarbonyl
Cbz	Carboxybenzyl
COSY	Correlation spectroscopy
CRE	Carbapenem-resistant Enterobacteriaceae
Da	Daltons
DCC	<i>N,N'</i> -Dicyclohexylcarbodiimide
DCM	Dichloromethane
DIC	<i>N,N'</i> -Diisopropylcarbodiimide
DIPEA	<i>N,N'</i> -diisopropylethyl amine (Hunig's base)
DMAP	4-(Dimethylamino)pyridine
DMF	<i>N,N'</i> -dimethylformamide
DMSO	Dimethylsulfoxide
DNA	Deoxyribonucleic acid
End	Enduracididine
ESI-MS	Electrospray ionisation mass spectrometry
EtOAc	Ethyl acetate
Farn	Farnesyl
FITC	Fluorescein isothiocyanate
Fmoc	Fluorenylmethyloxycarbonyl
Ger	Geranyl
GerGer	Geranylgeranyl
HATU	1-[Bis(dimethylamino)methylene]-1H-1,2,3-triazolo[4,5-b]pyridinium 3-oxide hexafluorophosphate
HBTU	O-(Benzotriazol-1-yl)- <i>N,N,N',N'</i> -tetramethyluronium hexafluorophosphate
HCTU	O-(6-Chlorobenzotriazol-1-yl)- <i>N,N,N',N'</i> -tetramethyluronium hexafluorophosphate
HPLC	High-performance liquid-chromatography

HRMS	High resolution mass spectrometry
HTS	High-throughput screening
LCMS	Liquid chromatography – mass spectrometry
MBC	Minimum bactericidal concentration
MeCN	Acetonitrile
1-Melm	1-Methylimidazole
MeOH	Methanol
MHz	Megahertz
MIC	Minimum inhibitory concentration
Mmt	Monomethoxytrityl
mRNA	Messenger ribonucleic acid
MRSA	Methicillin-resistant <i>Staphylococcus aureus</i>
MS	Mass spectrometry
Mtt	4-Methyltrityl
MW	Microwave
NAG	<i>N</i> -Acetylglucosamine
NAM	<i>N</i> -Acetylmuramic acid
NBS	Nitrobenzenesulfonyl
NMP	<i>N</i> -methylpyrrolidine
NMR	Nuclear magnetic resonance
Pbf	2,2,4,6,7-Pentamethyldihydrobenzofuran-5-sulfonyl
PBP	Penicillin-binding proteins
PE	Petroleum ether
PG	Protecting group
ppm	Parts per million
PTM	Post-translational modification
PyBOP	Benzotriazol-1-yl-oxytripyrrolidinophosphonium hexafluorophosphate
RBF	Round-bottomed flask
RP-HPLC	Reverse-phase high performance liquid chromatography
RNA	Ribonucleic acid
rt	Room temperature
SAR	Structure-activity relationship

SPPS	Solid phase peptide synthesis
Su	Succinimide
T _R	Retention time
tBu	<i>Tert</i> -butyl
TES	Triethylsilane
THF	Tetrahydrofuran
TFA	Trifluoroacetic acid
TFE	Trifluoroethanol
THF	Tetrahydrofuran
Trt	Trityl
VISA	Vancomycin-intermediate <i>Staphylococcus aureus</i>
VRE	Vancomycin-resistant Enterococci
VRSA	Vancomycin-resistant <i>Staphylococcus aureus</i>

Memorandum

Work within this thesis has been presented at the following meetings:

Poster presentation at 5th International Meeting on Antimicrobial Peptides (IMAP) – 7th to 8th September 2015 – Burlington House, London

Poster presentation at the RSC Chemical Biology Symposium 2016 – 27th April 2016 – Burlington House, London

Poster presentation at the RSC Chemical Biology and Bio-Organic Chemistry Postgraduate Symposium - University of Nottingham - 19th May 2016

Finalist for poster presentation at STEM for Britain – 13th March 2017 – Houses of Parliament, London

Poster presentation at the RSC Organic Division Midlands Meeting – 5th April 2017 – University of Leicester

Winner of 1st prize for best poster presentation

Oral presentation at RSC Chemical Biology and Bio-Organic Group Postgraduate Symposium – 25th May 2017

Runner up prize for best oral presentation

Poster presentation at the American Peptide Symposium – 17th June to 22nd June 2017 – Whistler, Canada

Semi-finalist of poster competition and recipient of travel award

Contents

Abstract	i
Acknowledgements	ii
Abbreviations.....	iii
Memorandum	vi
1. Introduction.....	1
1.1 Bacteria and antibiotics.....	1
1.1.1 Antibiotics: discovery and biological mechanisms of action	1
1.1.2 Antimicrobial resistance (AMR).....	5
1.1.3 Mechanisms of antibiotic resistance	7
1.1.4 Structure and origins of bacteria	9
1.1.5 Peptidoglycan biosynthesis and lipid II	11
1.1.6 β -lactam antibiotics	14
1.1.7 Antimicrobial peptides.....	16
1.2 Teixobactin (42)	35
1.2.1 Discovery of teixobactin (42)	35
1.2.2 Structure and biosynthesis	36
1.2.3 Mechanism of action and therapeutic potential	37
1.2.4 Enduracididine (43) and enduracidin (45).....	39
1.2.5 Total synthesis of teixobactin (42)	45
1.2.6 Teixobactin analogues.....	52
1.3 Aims of the project	60
2. Towards a novel synthesis of L- <i>allo</i> -enduracididine (43)	62
2.1 Introduction	62
2.2 Aims of the chapter	62
2.3 Synthesis design with a nickel (II) glycine Schiff base complex.....	64
2.4. Initial alkylation reactions and electrophile optimisation.....	69

2.5. Reactions of (S)-Ni-Gly-2FBPB (138) with tri-Cbz protected cyclic iodoguanidine (158)	73
2.6. Alkylation of (S)-Ni-Gly-2FBPB (138) under optimised conditions	78
2.7 Complexation of less substituted electrophiles in optimised conditions...	84
2.8 Conclusions	85
3. Synthesis of teixobactin analogues using on-resin cyclisation	87
3.1 Introduction	87
3.2 Aims of the chapter	95
3.3 Loading of safety-catch resins	96
3.4 Initial synthesis of teixobactin macrocycle analogues.....	100
3.5. Synthesis of teixobactin macrocycle with trityl-based side chain protection	106
3.5.1 Design of protection strategy	106
3.5.2 Determination of trityl stability with linker activation conditions	107
3.5.3 Epimerisation study of loading to safety-catch resin.....	109
3.5.4 On-resin cyclisation reaction optimisation	111
3.6 Optimised synthesis of teixobactin macrocycle with Ala-loading	114
3.7 Conclusions	116
4. Synthesis of teixobactin analogues using solution-phase cyclisation	118
4.1 Introduction	118
4.2 Aims of the chapter	118
4.3 Solution-phase macrolactonisation	119
4.3.1 Studies on depsipeptide macrocyclisation	119
4.3.2 Determination of Gln(Trt) and Thr(Trt) protection lability	121
4.3.3 Methods of depsipeptide formation.....	123
4.3.3.1 Macrolactonisation of linear peptide Ac-tAR(Pbf)I-OH (256)	126
4.4 Cyclisation via solution-phase macrolactamisation.....	130
4.5 Synthesis of truncated, acetylated macrocyclic analogues	134

4.6	Synthesis of teixobactin lipopeptidomimetics.....	137
4.6.1	Prenylation of peptides and proteins	138
4.6.2	Synthesis of <i>N</i> -terminus prenylated teixobactin analogues	142
4.6.3	Synthesis of cysteine-prenylated teixobactin analogues	148
4.6.4	Synthesis of analogues with a positively-charged hydrocarbon tail 155	
4.7	Attempted synthesis of fluorescent active teixobactin analogues	160
4.8	Antibiotic activity of truncated and lipidated teixobactin analogues ..	162
4.9	Conclusions	167
5.	Final conclusions and future work	170
6.	Experimental	173
6.1	General information	173
6.2	Chemical syntheses	174
6.3	Peptide syntheses.....	185
6.3.1	General procedure for automated peptide synthesis.....	185
6.3.2	General procedures for resin loading	185
6.3.3	General procedures for Fmoc-SPPS	187
6.3.4	Peptide cleavage from resin	188
6.3.5	Solution phase macrolactamisations	190
6.3.6	Modifications of cyclic peptides	191
6.3.7	Peptide content determination	191
6.3.7.1	Determination of peptide content by UV-Vis	191
6.3.7.2	Determination of peptide content by ¹ H NMR	192
6.3.8	Syntheses of individual peptides.....	192
6.3.9	Characterisation of peptides	199
6.3.9	NMR spectroscopy of peptides	203
6.4	MIC and MBC assays	210

6.4.1	Bacterial strains.....	210
6.4.2	Microdilution method for susceptibility testing to antimicrobials ...	210
6.4.3	MIC and MBC Assays.....	210
7.	References	212

1. Introduction

1.1 Bacteria and antibiotics

1.1.1 Antibiotics: discovery and biological mechanisms of action

The serendipitous discovery of penicillin **1** (Figure 1) by Alexander Fleming in 1928 is generally considered the rudiment of antibiotic drug discovery in the modern age.¹ Whilst Fleming noted that regions of germ culture plates containing growth of the mould *Penicillium notatum* inhibited the formation of *Staphylococcus*, it was Howard Florey who realised the significance of this discovery, and worked on the small-scale manufacture and the first clinical trials of penicillin, which was the first FDA approved antibiotic in 1943.

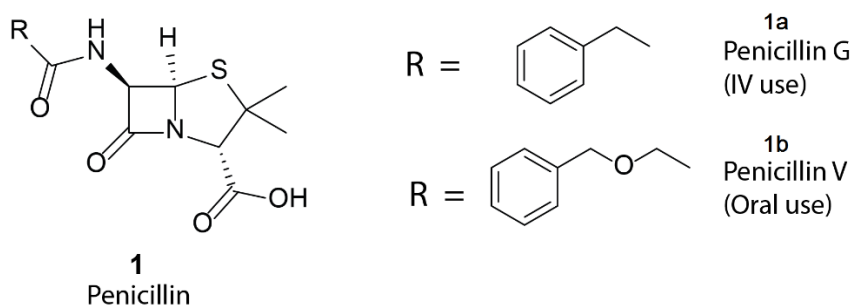
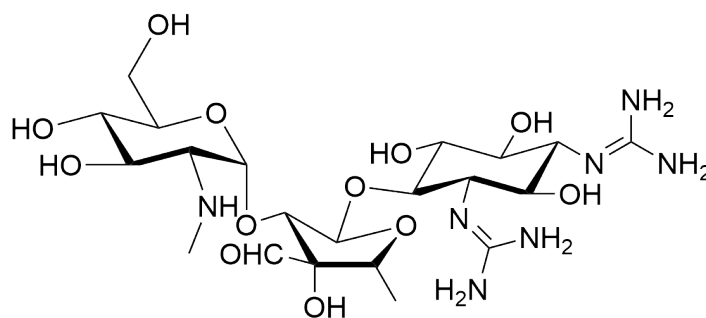


Figure 1 - General structure of penicillin antibiotics with two common therapeutic forms (Penicillin G **1a** and Penicillin V **1b**).

The golden age of antibiotic discovery commenced in the 1940s, when Waksman began screening soil bacteria, particularly *Actinomyces*, for natural product antibiotics.² Lead species were identified by the presence of growth inhibition zones surrounding single colonies of bacteria under various conditions, and these were then tested against specifically targeted pathogenic bacteria.

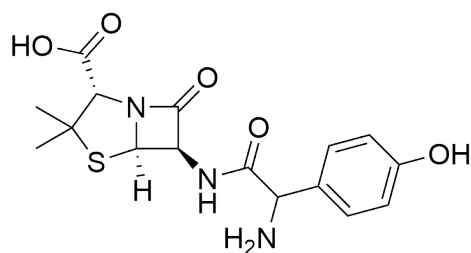
From this screening, around twenty novel antibiotic compounds were identified, of which 15 came to market. This included streptomycin **2**, both the first antibiotic to treat tuberculosis and the first identified aminoglycoside (Figure 2). After twenty years of success, this screening platform diminished mainly due to the restrictions of the methodology: solely detecting the formation of metabolites by known species within a specific environment only provided a limited number of hits.³



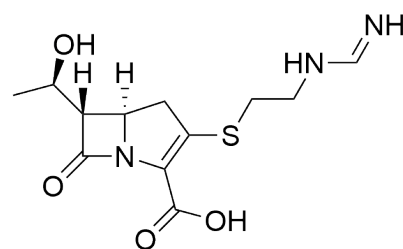
Streptomycin **2**

Figure 2 - Structure of streptomycin **2**, an antibiotic discovered in 1943 by Waksman, produced by *Streptomyces griseus*.

The 1970s marked the beginning of the medicinal chemistry era, where novel antibiotics were mainly discovered via synthetic alteration of previously identified natural products to produce new compounds (Figure 3). This was facilitated by considerable advances in screening and chemical methodologies. Desired native and mutated proteins were now accessible in high yields and purity from recombinant DNA expression, rather than extraction from native species, and this facilitated investigations to determine drug mechanism of action. Protein-structure determination by crystallography and NMR enabled rational drug design, robotics greatly increased the speed and efficiency of large library screenings, and developments in computing allowed access to, and faster analysis of, large data sets.



Amoxicillin 3



Imipenem 4

Figure 3 - Structures of antibiotics approved in the 1970s for therapeutic use: amoxicillin 3, derived from penicillin 1, and imipenem 4, derived from thienamycin 5.

These advances ultimately led to target-based screening, however this was met with narrow success.⁴ The sequencing of *Haemophilus influenza* in 1995, the first complete bacterial genome, revived interest in the field of antibiotic discovery, providing hundreds of new genes to evaluate as potential drug targets.⁵ GlaxoSmithKline (GSK) spent seven years examining over 300 genes, of which 160 were found to be essential to the survival of the cell, through 70 high-throughput screening (HTS) campaigns.⁶ Like most target-based screens before it, synthetic derivatives of original HTS hits usually resulted in reduced antibiotic activity, generally attributed to unsuitable drug mechanism and pharmacokinetic profiles such as poor cell permeability, narrow-spectrum efficacy or lack of activity against resistant or hard-to-treat strains.⁷ Since the 1960s, only the antibiotics linezolid 6 and daptomycin 7 (Figure 4) were found to belong to new classes introduced into clinical practice (oxazolidinones and lipopeptides, respectively), with most novel drugs being derivatives of known active compounds. No new classes of antibiotics targeting Gram-negative bacteria have been developed for over four decades.⁸

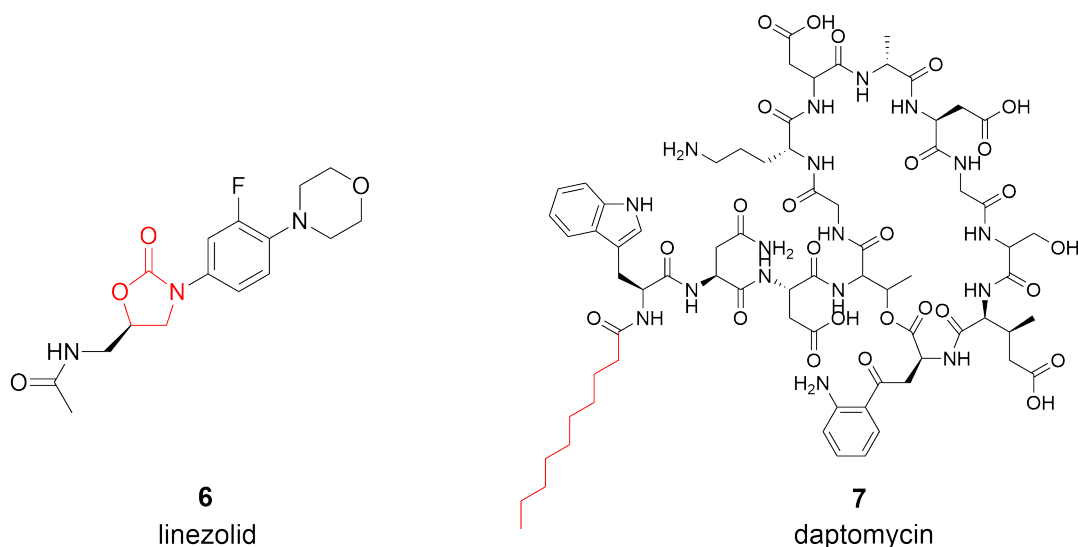


Figure 4 - Structures of the antibiotics linezolid **6** and daptomycin **7**, with class-determining regions highlighted in red.

Current research largely focuses on the discovery of new antibiotic pathways: providing new targets to elicit the inhibition of bacterial growth and survival. This has been attempted via the cultivation of unusual bacterial strains from non-standard environments,⁹ and the identification of novel secondary metabolites through microbial genome exploration.¹⁰ Due to the global crisis of antimicrobial resistance, there is a dire need for novel antibiotics and classes. The gravity of the situation has been cemented largely by two reports. In 2015, resistance via horizontal gene transfer to colistin **8**, the “last-resort” antibiotic, has been identified in *E. coli* and *Klebsiella pneumoniae*,¹¹ triggering almost 150 papers in under a year on the causative *mcr-1* gene. Perhaps most significantly in 2017, a patient was diagnosed with a strain of *Klebsiella pneumoniae* that was found to be resistant to all 26 antibiotics tested against it, including aminoglycosides and polymyxins, and subsequently died of septic shock.¹²

1.1.2 Antimicrobial resistance (AMR)

The development and proliferation of antibiotic resistance combined with the lack of novel antibiotic compounds has become a major problem worldwide. In the USA, multidrug resistant bacterial infections are estimated to have cost the economy over \$55 billion per year in excess health care and societal costs, and over 8 million additional hospital days.¹³ Many current antibiotics have become prone to resistance by multiple different strains of bacterial species. The development of antibiotic resistance has been observed as early as 1944, a year after the introduction of penicillin to the market; with Kirby reporting particular strains of *Staphylococcus aureus* isolated from hospital patients to be producing penicillinases, thus rendering the drug ineffective.¹⁴ Within several years, this resistance amplified and became apparent in the majority of hospital isolates, particularly in patients that had previously been treated with penicillin **1** or another β -lactam antibiotic.¹⁵ Since this time, resistance has been observed against every known clinical antibiotic (Figure 5).¹⁶ Often resistance has been observed within as little as a year of introduction of the drug, as in the cases of levofloxacin **9** (marketed 1996; resistance observed in the same year),¹⁷ and linezolid **5** (marketed in 2000 with resistance seen in 2001).¹⁸ Even vancomycin **10**, a glycopeptide antibiotic introduced in 1972 that was thought to be immune from resistance development, was found to have reduced efficacy against an MRSA isolate in 1997,¹⁹ and since then strains such as VISA (vancomycin-intermediate *S. aureus*) and VRSA (vancomycin-resistant *S. aureus*) have become exponentially more common.²⁰

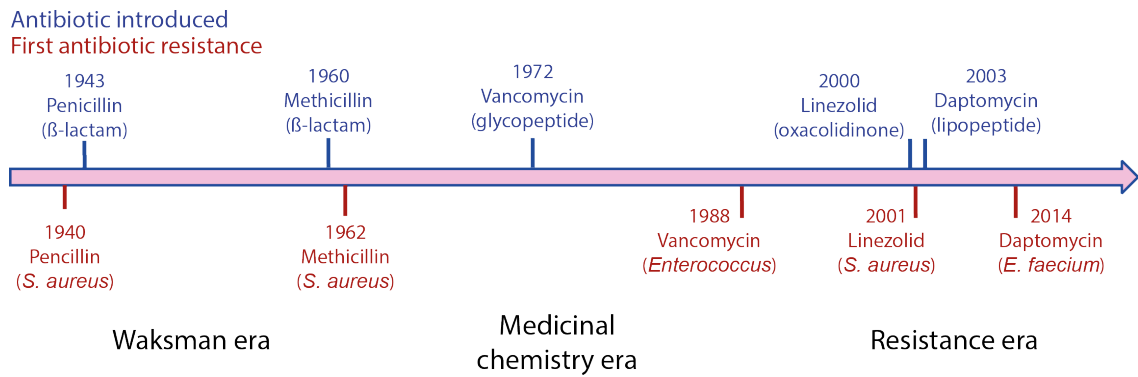


Figure 5 - Timeline showing clinical approval of key antibiotics and their class (blue) compared with the first documented antibiotic resistance, and within which species it was observed (red).

The rise of resistant bacteria has been attributed a number of different factors. Most prominently, this has been linked to the overuse and misuse of antibiotic medication.²¹ Epidemiological evidence indicates a clear trend between the level of antibiotic consumption per capita and the incidence of resistant bacteria.²² Antibiotics eradicate only drug-susceptible bacteria, leaving behind resistant counterparts, and therefore promoting their growth and proliferation. The overuse of antibiotics is partially due to inappropriate prescribing, with studies showing that antibiotics are wrongly prescribed in 30–60% of cases,²³ either with an inappropriate choice of agent; mistakenly according to presentation of symptoms, or with incorrect duration of treatment – although a recent article has suggested that the requirement for the completion of an antibiotic course lacks robust evidence.²⁴ In many countries, antibiotics are readily available over the counter without a prescription, making them easily accessible. Aside from human consumption, antibiotics are used as growth supplements in livestock in both developing and developed countries, with around 80% of total antibiotics sales in the USA being for use in animal agriculture.²⁵ Resistant bacteria which develop directly in these animals can then be transmitted to humans through a number of routes, such as consumption of undercooked meat.¹¹

To combat the rise of resistant bacteria, a continual stream of novel drugs is required. However, the slow pace of drug development over the last century has not been able to keep up with the rapid rate at which resistance occurs.²⁶ Most of the largest pharmaceutical companies have now left the antibiotic research

market entirely.²⁷ Aside from the limited range of techniques available to find new drug candidates, the production and marketing of new antibiotic drugs is not economical. Until resistance becomes more widespread and generic medications are no-longer viable, drugs such as penicillin **1** and amoxicillin **3** are likely to be preferentially be prescribed over newer, more expensive alternatives. Antibiotics are used as short courses and are curative, and are therefore much less profitable than drugs for chronic and often incurable illnesses such as cancer, diabetes, and auto-immune diseases.²⁸

The Infectious Diseases Society of American (IDSA) has created the acronym “ESKAPE”, referring to six of the leading Gram-positive and negative pathogens responsible for nosocomial infections: *Enterococcus faecium*, *S. aureus*, *Klebsiella pneumoniae*, *Acinetobacter baumannii*, *Pseudomonas aeruginosa* and the *Enterobacter* genus as a whole.²⁹ Infection by these species in immunocompromised individuals within a hospital can often be life-threatening. Between these species of bacteria there are a multitude of pathogenicity, resistance and transmission mechanisms to be addressed, and much current research is focused on circumventing the resistance processes to create novel, effective therapeutic options.³⁰

1.1.3 Mechanisms of antibiotic resistance

Some bacterial resistance is intrinsic, and a result of a species having an inherent structure or function that prevents the action of an antibiotic from working. Usually this is due to the lack of a particular cellular target, the presence of an enzyme or protein that promotes the degradation or efflux of the compound, or a structural factor that prevents penetration of the outer membrane into the cell.³¹ Antibiotic resistance can also be acquired through horizontal gene transfer and spontaneous mutations in chromosomal DNA (Figure 6).

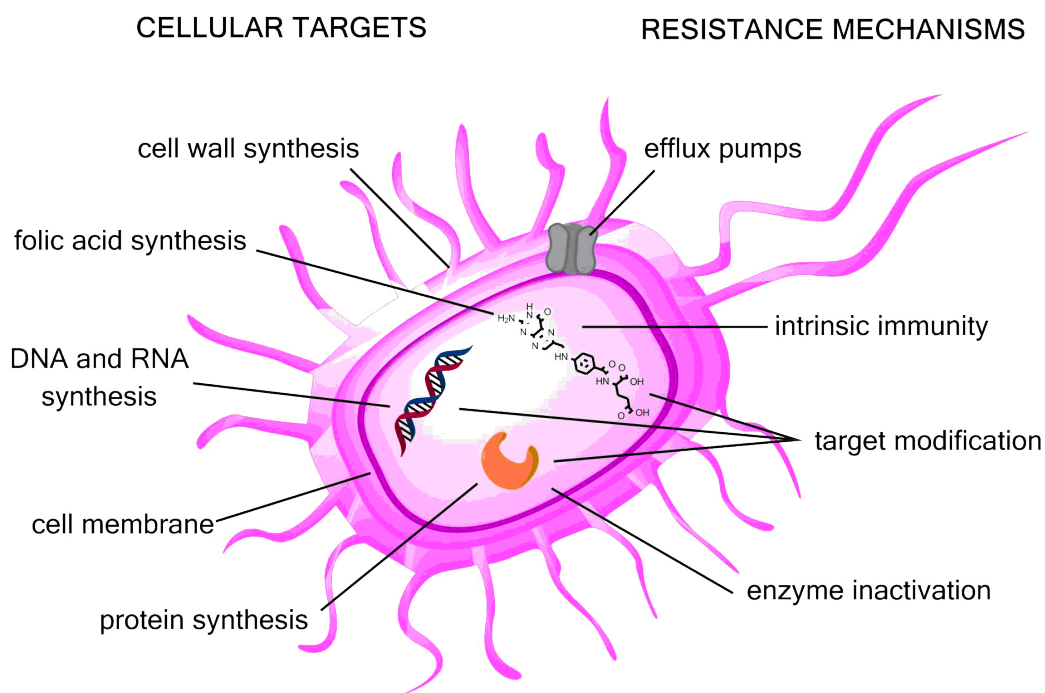


Figure 6 - Common bacterial cellular targets of bacteria shown on the left hand side; common resistance mechanisms found to be employed by bacteria shown on the right.

The first reported case of Methicillin-resistant *Staphylococcus aureus* (MRSA), perhaps the most well-known of resistant bacteria, was in France in 1962, and since then methicillin-resistant infections have become increasingly prevalent across the globe, particularly in hospital settings. MRSA is one of the most common antimicrobial resistance threats, accounting for around half of all deaths attributed to resistant bacteria.³² Patients that contract MRSA infections generally have poor prognoses, with around 11,300 deaths each year in the US being caused by this pathogen.³³ The resistance acquired by MRSA is the result of two primary adaptations. The resistant staphylococci express the enzyme PC1 β -lactamase, which is able to hydrolyse the amide functionality in the cyclic core of β -lactam antibiotics such as penicillin **1** and amoxicillin **3**.³⁴

In addition, the bacteria may acquire a gene encoding a modified penicillin-binding protein (PBP 2a). In concentrations of β -lactam antibiotics that would inhibit endogenous PBP, the modified enzyme protein is still able to remain active to continue to promote the synthesis of the cell wall, and in turn bacterial propagation and growth.³⁴

Vancomycin-resistant *Enterococci* (VRE) are infections that typically affect hospital patients, and can cause a number of different diseases, such as wound and urinary tract infections.³⁵ As vancomycin is often used as a last-line of treatment, there are few therapeutic options available for the treatment of VRE.

Carbapenem-resistant *Enterobacteriaceae* (CRE), drug-resistant *Neisseria gonorrhoeae*, and *Clostridium difficile* are the three bacteria designated as “urgent” threats in a recent Centre for Disease Control (CDC) report. This is the category of highest severity, reserved for bacteria that are resistant to all or almost all known antibiotic therapeutic options, and have a high risk of transmission between patients.³²

1.1.4 Structure and origins of bacteria

Bacteria are one of the most established and abundant forms of life on earth, and make up one of the three domains of life alongside archaea and eukaryotes. These organisms are indispensable for a multitude of biological processes, particularly for their participation in numerous nutrient cycles, such as the fixation of nitrogen from the atmosphere, the putrefaction of dead plants and animals, and the conversion of compounds like hydrogen sulphide and methane (that are toxic to most eukaryotes) into energy. There are an estimated $4-6 \times 10^{30}$ bacterial cells on earth,³⁶ inhabiting a diverse range of habitats and conditions. The human gut itself is host to an average of 10^{13} bacterial cells, which is ten times more than the total number of human cells across the whole body.³⁷

As prokaryotes, bacterial cells are significantly different to plant and animal cells (Table 1). Bacterial cells tend to be much smaller in size (1 -10 μm compared to 10 -100 μm), and lack organelles such as mitochondria and the endoplasmic reticulum. Most notable however, is the lack of an intracellular nucleus containing genetic material. Instead, DNA is contained throughout the cytoplasm. Rather than packaged around histones as chromatin in eukaryotic cells, the bulk of the genetic information of the cell exists as a single chromosome; a circular, double stranded piece of DNA. This chromosome may exist as one or multiple copies within a region of the cell called the nucleoid. The nucleoid also contains some

proteins and RNA, which are mostly transcription factors and mRNA involved in the regulation of the genome. The lack of introns and non-coding regions of the genome contribute to the efficiency of storage of genetic material within the cell (as opposed to eukaryotic DNA, which is only around 5% exons), with the DNA folded and condensed by architectural proteins into a supercoiled form.

	Prokaryotes	Eukaryotes
Evolution	3.5 billion years	1.5 billion years
Cell	Unicellular	Multicellular
Size of cells	1 – 10 μm	100 – 1000 μm
Genome	Nucleoid; plasmids	Nucleus
Organelles	None	Present
DNA	Circular: one chromosome	➤ 1 chromosome
Reproduction	Asexual	Sexual
O₂	Anaerobic	Aerobic

Table 1 - Cellular and structural difference between prokaryotic (bacteria) and eukaryotic cells.

Other pieces of genetic material are also present as plasmids: circular, double-stranded DNA molecules that exist outside of the nucleoid. Plasmid DNA encodes for additional genes that are not required for the general functioning of the cell, but may be of use under certain conditions or as a response to stress inducing stimuli.

The bacterial cell wall exists just outside the plasma membrane, and is integral to cell viability for a multitude of reasons: the maintenance of cell shape and structure, protection from osmotic lysis and toxins, and in some species also contributes to pathogenicity. The ubiquitous and vital nature of the cell wall, in addition to the fact it is absent in mammalian cells, makes this an attractive target for antibiotics.

The cell walls of Gram-positive bacteria are made up of a homogeneous layer of peptidoglycan, ranging from 20 nm to 80 nm in depth, which lies directly

outside the membrane. On the other hand, Gram-negative bacteria have much thinner cell walls: usually 2 to 7 nm of peptidoglycan layered by an outer membrane of 7 to 8 nm, and separated from the plasma membrane by the periplasmic space (Figure 7).

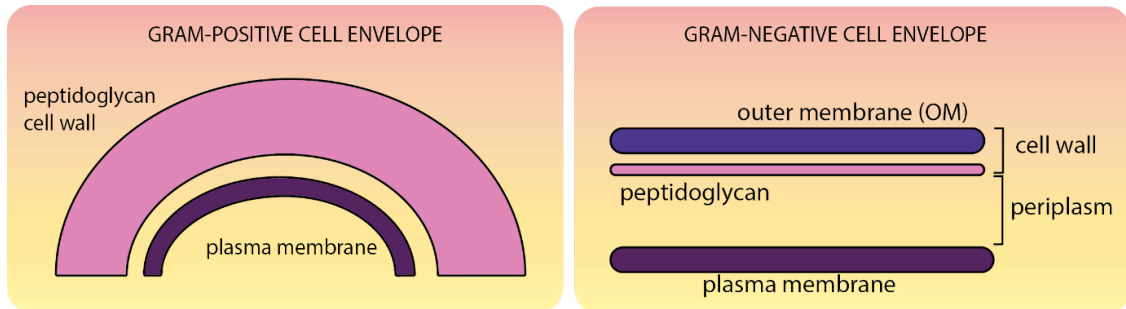
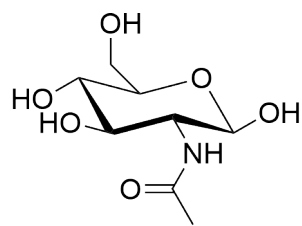


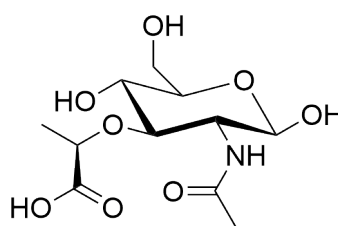
Figure 7 - Structures of the bacterial cell wall of Gram-positive and Gram-negative bacteria. Gram-positive bacteria have a thicker peptidoglycan layer compared to Gram negative, which have an additional outer membrane.

1.1.5 Peptidoglycan biosynthesis and lipid II

Peptidoglycan, the main component of the cell wall, is a polymer made up of alternating residues of β -(1,4) linked *N*-acetylglucosamine (NAG) **11** and *N*-acetylmuramic acid (NAM) **12** (Figure 8). The latter is bound to a short peptide of 4 to 5 amino acid residues, consisting of L-Ala, D-Glu, L-Lys, D-Ala and *meso*-DAP **13**, the exact structure of which varies between bacterial species. The peptides of separate linear, helical sugar chains are linked by the enzyme DD-transpeptidase to form the final, three-dimensional structure. Peptidoglycan is strong and dense, but also flexible, and can contract and expand in response to changes in osmotic pressure.



N-acetylglucosamine (NAG) **11**



N-acetylmuramic acid (NAM) **12**

Figure 8 - Structure of peptidoglycan monomers *N*-acetylglucosamine (NAG) **11** and *N*-acetylmuramic acid (NAM) **12**

Peptidoglycan synthesis begins in the cytoplasm, where enzymes MurA-G catalyse the formation of a pentapeptide linked to the nucleotide-sugar precursor UDP-*N*-acetylmuramyl (UDP-MurNAc) **14**. At the surface of the plasma membrane, MraY links this UDP-MurNAc-pentapeptide precursor **15** to undecaprenyl pyrophosphate **16**, a transport linker, to yield lipid I **17**. Addition of *N*-acetylglucosamine (GlcNAc) **18** from UDP-GlcNAc **19**, catalysed by MurG, produces lipid II **20**. A series of Fem enzymes catalyse formation of a peptide crossbridge (typically five glycine residues in Gram-positive bacteria) orthogonally from the third amino acid residue. This entity then flipped across the membrane into the periplasm through a flippase mechanism that has not been confirmed. A series of transglycosylations and transpeptidations result in polymerisation and the final peptidoglycan structure (Figure 9).³⁸

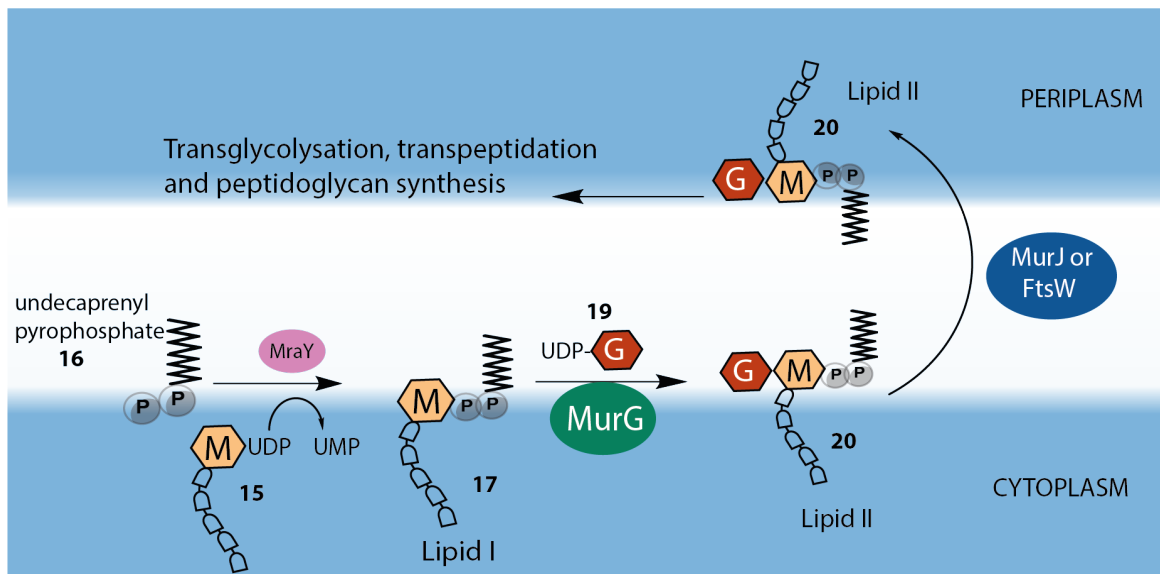
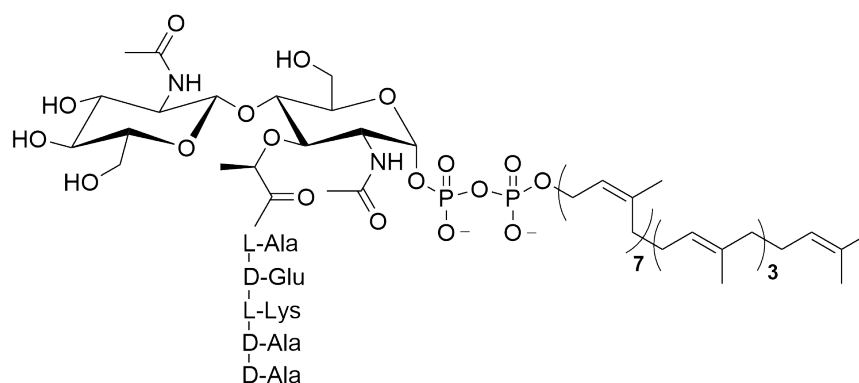


Figure 9 - Bacterial cell wall synthesis. *MraY* couples an undecaprenyl pyrophosphate **16** to UDP-MurNAc-pentapeptide **16** to form lipid I **17**; *MurG* adds GlcNAc from UDP-GlcNAc **19** to form lipid II **20**, which is subsequently flipped across the membrane to project into the periplasm.

Whilst there are a number of antibiotics, such as bacitracin **21** and turnicamycin **22**, that inhibit the synthesis of lipid I **17**, it is lipid II **20** (Figure 10) that is considered a highly attractive target for antimicrobials for a number of reasons. It is the central component of peptidoglycan synthesis, and highly conserved across eubacteria, providing lipid II-targeting antibiotic candidates with a higher probability of broad-spectrum activity, and the possibility of reduced toxicity due to the lack of homology in eukaryotic cells. Lipid II **20** is the rate-limiting step of peptidoglycan biosynthesis, due to the low number of undecaprenyl phosphate molecules in each cell at one time. Unlike other peptidoglycan precursors, lipid II **20** is more readily accessible due to its availability on the outer side of the bacterial plasma membrane, as opposed to existing solely within the cytoplasm.



Lipid II **20**

Figure 10 - Structure of lipid II **20**, comprised of disaccharide, pentapeptide, pyrophosphate and isoprenoid moieties.

1.1.6 β -lactam antibiotics

β -lactam antibiotics are one of the oldest validated antibiotic classes in clinical use, and are usually the principal course of treatment against a diverse range of bacterial infections, including pneumonia, meningitis, and gonorrhoea. Compounds in this group are linked by a common four-membered, β -lactam ring at the centre of their structures (Figure 11), usually connected to another cyclic component, except in the case of monobactams.

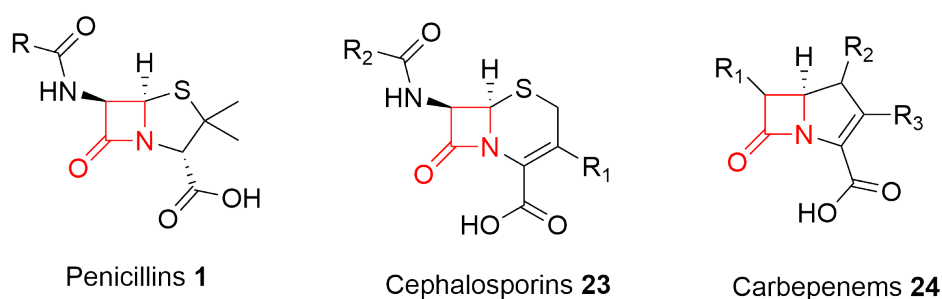
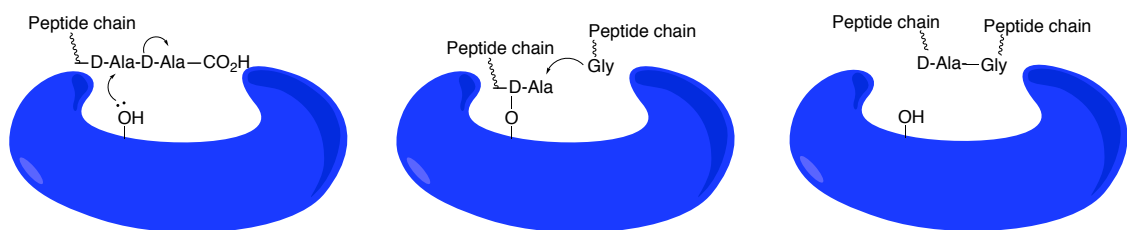


Figure 11 - General structures of three types of β -lactam antibiotics commonly used therapeutically.

β -lactam antibiotics' bactericidal activity is reached by interfering with cross-link formation between linear amino-sugar strands of peptidoglycan, which is

achieved by the inhibition of DD-transpeptidases; enzymes responsible for forming the covalent link between two peptides. Because of this vulnerability, these enzymes are also referred to as penicillin-binding proteins (PBPs). When employed, hydrolysis of peptidoglycan by other enzymes not only continues to take place, but actually increases due to the build-up of linear peptidoglycan precursors, resulting in an increase in osmotic pressure making the cell wall weaken, eventually leading to cytolysis.

Normal Mechanism:



Inhibited by Penicillin:

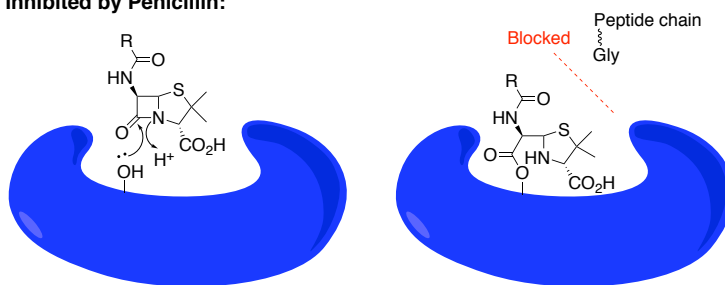


Figure 12 - Mechanism of β -lactam antibiotic activity by irreversible binding of the active compound to Ser403 of DD-transpeptidases.

β -lactam antibiotics are analogues of the two terminal amino acid residues of the peptide subunits of peptidoglycan monomers NAG **11** and NAM **12** (D-alanine-D-alanine), and the β -lactam core binds irreversibly to Ser403 residue of the active site of DD-transpeptidases (Figure 12).³⁹

1.1.7 Antimicrobial peptides

Antimicrobial peptides (AMPs) are a class of naturally occurring and synthetic peptides with a wide spectrum of targets (Table 2). AMPs are produced by all multicellular organisms, primarily as a first-line defence against pathogenic bacteria and viruses (but have also been implicated in activation against cancer cells)⁴⁰, and micro-organisms produce AMPs to defend from other hostile species in the surrounding environment. AMPs act through a number of different mechanisms: inhibition of proteins or DNA/RNA synthesis, and many are involved in the disruption of cell membranes, leading to cell death. Most AMPs have been found to be cationic, ranging from 10 to 50 amino acids in length, and are classified based on their structure as α -helical, β -sheet or extended.⁴¹

AMP	Mode of action	Active against
Defensins	Membrane binder, pore formation	Gram-positive bacteria
Glycopeptides	Peptidoglycan (D-Ala-D-Ala) binder	
Lantibiotics	Lipid II binder	
Daptomycin	Membrane pore formation	
Teixobactin	Lipid II binder	
Cecropins	Membrane formation	Gram-negative bacteria
Attacins	Unknown	
Polymyxins	Lipopolysaccharide binder, membrane disruption	
Diptericins	Unknown	
Metchnikowin	Unknown	Fungi
Drosomycin	Membrane pore formation	

Table 2 - Antimicrobial peptides (AMPs), classification of micro-organism they are biologically active against, and mechanism of action.

The bactericidal activity of AMPs is mainly attributed by their ability to interact with bacterial cell membranes and walls, and this is achieved through the combination of a net positive charge interacting with the negative exterior of phospholipids, and the presence of hydrophobic residues that can anchor into membranes or interact with lipidated regions of target structures. Fully

understanding the structure-activity relationship of AMPs is crucial for the creation of novel antibiotics with improved activities and spectrum of action.

A number of human AMPs display antibiotic activity and also have roles in the regulation of innate immunity. These vary in length from 5 to 149 amino acids, and the three major groups are defensins, cathelicidins and histatins.⁴² Mammalian defensins are cationic peptides containing cysteine residues that form intramolecular disulphide bridges, stabilising their β -sheet-based structure.⁴³ Cathelicidins are precursor proteins that produce C-terminal cleavage AMP products found in a number of mammalian species. To date, there is only one cathelicidin gene (CAMP) identified in humans, which encodes CAP18. Proteolytic cleavage yields the active peptide, LL-37 **25**, which varies its structure depending on the nature of its environment; in hydrophilic conditions LL-37 **25** exists as a random-coil, but folds into an α -helix when exposed to hydrophobic surroundings, such as lipid bilayer vesicles.⁴⁴ Histatins are short cationic peptides, named due to their high proportion of histidine residues. Similarly to cathelicidins, these form random-coils in aqueous media and α -helices in organic solvents and lipid bilayers.⁴⁵

Unlike human AMPs, those produced by microbes usually contain a number of structural features not observed in those originating from eukaryotic organisms, due to the fact they are often produced non-ribosomally. These peptides generally contain cyclic substructures with branched areas, and are made up of amino acids varying from the 20-naturally occurring forms found in animals. Most bacterial AMPs contain at least one D-amino acid; residues are often modified with *N*-methylation and *N*-formylation, glycosylation and acylation, or linked by unusual bonds such as thioethers (Figure 13). AMPs often contain non-proteinogenic amino acid residues; modified by enzymes following the main part of the synthesis. These unusual features offer a range of benefits; from improved binding to target molecules, to protection from protease degradation.

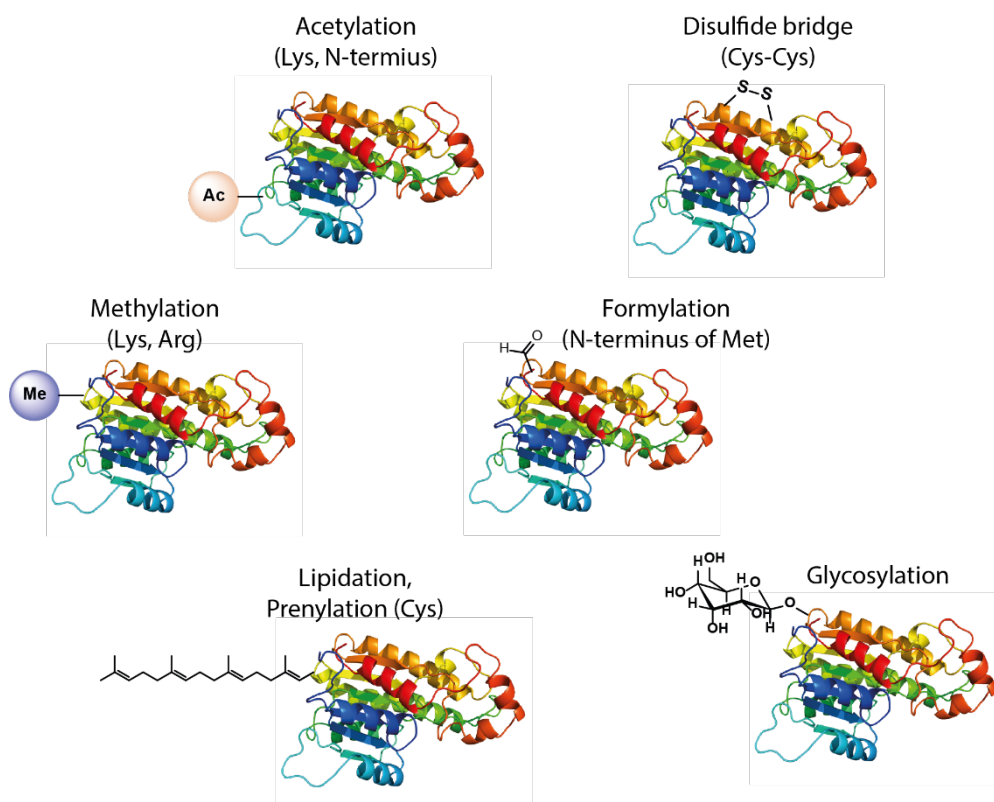


Figure 13 - Common modifications of bacterial peptides and proteins, and the amino acid residues or terminus they occur on.

The unique structural features of bacterial AMPs make them attractive as therapeutic candidates due to their improved stability and efficacy over their naturally-occurring, unmodified counterparts.⁴⁶ Unlike other antibiotics that target proteins and enzymes, the binding of AMPs to membranes represents an Achilles' heel of pathogenic bacteria, being highly conserved and structured in nature, and more difficult to effectively mutate. Typically, AMPs bactericidal activity is catalysed by membrane binding, which can be followed by membrane rupture, or inhibition of cell wall synthesis (Figure 14). Many current therapeutic options, including those targeting resistant bacteria, are bacterial natural products or derivatives of, and many fall into the subcategories of glycopeptides, lantibiotics and lipopeptides.

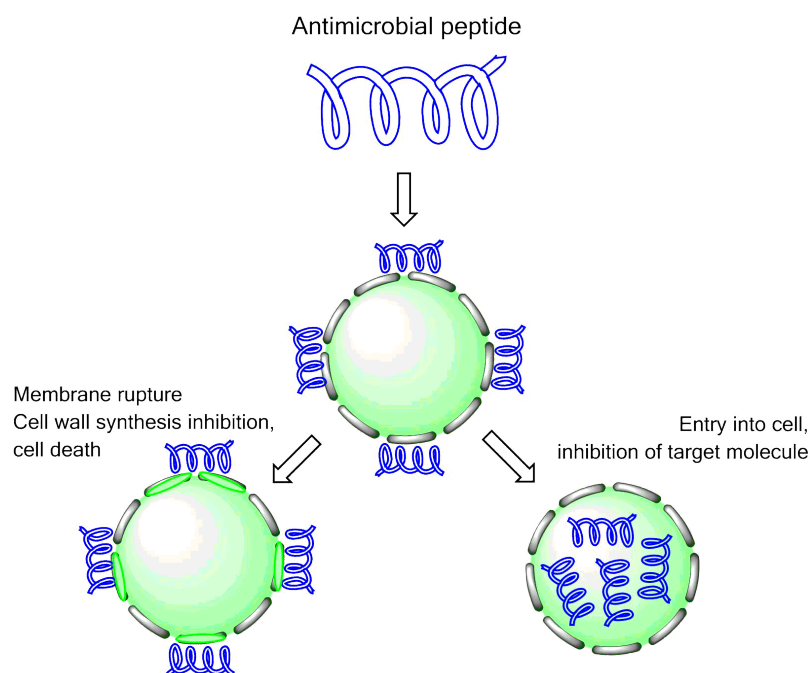


Figure 14 - Mechanisms of cationic antimicrobial peptide bactericidal activity. Binding of AMP to bacterial cell wall usually results in cell death either by cell wall synthesis inhibition, or inhibition of an intracellular target.

1.1.7.1 Glycopeptides

Glycopeptides are a class of actinomycetes-derived antibiotics characterised by a single or several glycosylation sites on cyclic peptides, which are used to treat Gram-positive bacterial infections. The first glycopeptide to be isolated in 1953 was vancomycin **10**, a drug that is still commonly prescribed, particularly in the treatment of MRSA and *Clostridium difficile*. Many of the newer-generation glycopeptides, such as teicoplanin **26** and telavancin **27**, also contain an additional lipid moiety, usually branched from a glycosylamine (Figure 15). These lipoglycopeptides have been found to display broader activity and improved pharmacokinetic properties,⁴⁷ however to date, no glycopeptide has been discovered that is able to combat Gram-negative species, as due to their relatively large size they are unable to traverse the significantly larger outer membrane, whose pores have an upper molecular weight limit of around 600 Da.⁴⁸

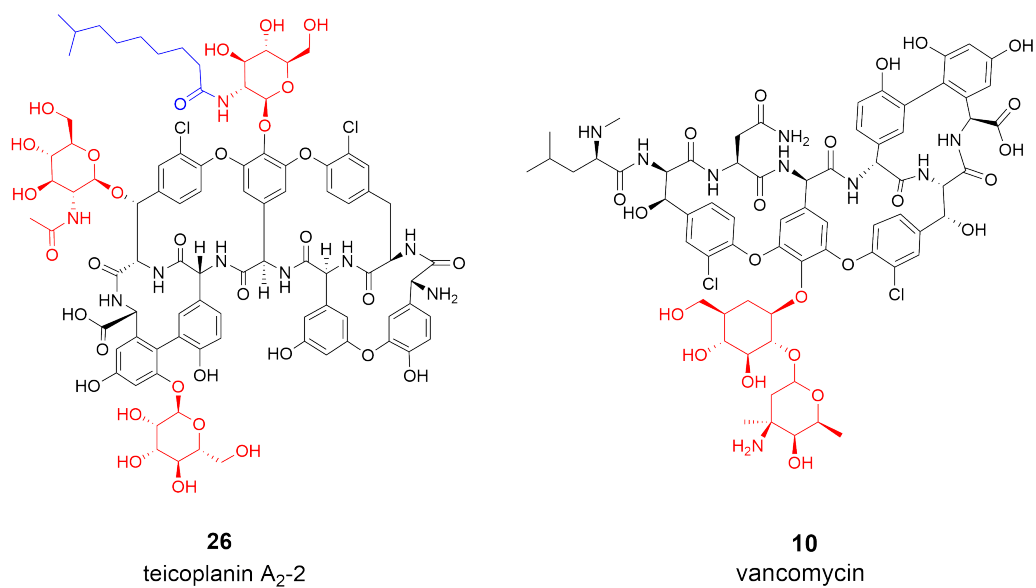


Figure 15 - Structure of glycopeptides teicoplanin **26** and vancomycin **10**, with sugars highlighted in red, and lipitation highlighted in blue.

Glycopeptide antibiotics target the D-Ala-D-Ala residues at the *N*-terminus of cell wall precursors such as lipid II **20** (Figure 16).⁴⁹ These drugs adopt a cradle-like structure that sequesters this moiety, and therefore prevents polymerisation by transglycosylases and transpeptidases, leading to cell hydrolysis and death.⁵⁰

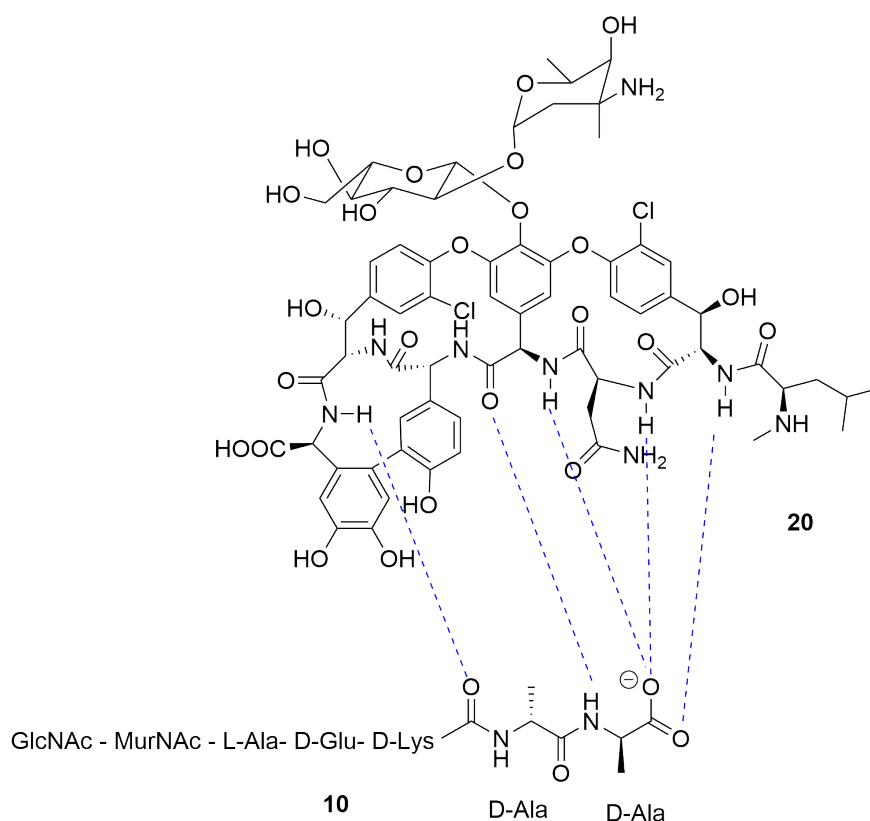


Figure 16 - Hydrogen bonding interactions and binding between vancomycin **10** and D-Ala-D-Ala of mutated lipid II **20**

Vancomycin **10** was originally considered to be “resistance-immune” due to this mechanism of action, and the inability of bacteria to successfully induce viable mutations to the structure of lipid II. However, after an increase in use during the 1980s, resistance was observed in *Enterococcus faecium*.⁵¹ This resistance mechanism was found to be the replacement of the terminal D-alanine residues with the depsipeptide D-Alanine-L-Lactate, reducing the binding affinity of vancomycin one-thousand fold.⁵² Resistant *E. faecium* achieved this through the action of two enzymes; VanH – which reduces pyruvate to D-lactate, and VanA which forms the ester bond of the depsipeptide. To date, six unique phenotypes – VanA, VanB, VanC, VanD, VanE and Van-G – have been found in *Enterococci*, differing in terminal residue mutation, levels of resistance observed, and whether the resistance is induced by drug exposure or already from a constitutive metabolic pathway.⁵³ All phenotypes mutate the terminal D-Alanine residue to either a D-Lactate or D-Serine. For D-Lactate mutations, loss of vancomycin **10** activity is attributed to the loss of a hydrogen bonding interaction in complex

formation (and in turn an increase in electrostatic repulsion) whereas resistance caused by D-Ser mutation is thought to be due to hydroxyl-mediated steric hindrance.⁵⁴

Phenotype	Peptidoglycan				
	N-terminus residues	Resistance	Source	Induction	Organisms
VanA	D-Ala-D-Lac	Vancomycin 10 Teicoplanin 26	Acquired	Inducible	<i>E. faecium</i> <i>E. faecalis</i>
VanB	D-Ala-D-Lac	Vancomycin 10	Acquired	Inducible	<i>E. faecium</i> <i>E. faecalis</i>
VanC	D-Ala-D-Ser	Vancomycin 10	Intrinsic	Intrinsic, inducible	<i>E. gallinarum</i>
VanD	D-Ala-D-Lac	Vancomycin 10 Teicoplanin 26	Intrinsic	Intrinsic	<i>E. faecium</i>
VanE	D-Ala-D-Lac	Vancomycin 10	Acquired	Inducible	<i>E. faecalis</i>
VanG	D-Ala-D-Ser	Vancomycin 10	Unknown	Unknown	<i>E. faecalis</i>

Table 3 - Phenotypes of and characteristics of vancomycin resistance.⁵³

As a result of these resistant phenotypes, many groups have sought to develop semisynthetic approaches towards vancomycin analogues and novel glycopeptides that retain potency even against mutated strains.⁵⁵ Three such compounds with comparatively lower MIC values and increased half-lives are telavancin **27**, dalbavancin **28** and oritavancin **29** (Figure 17)

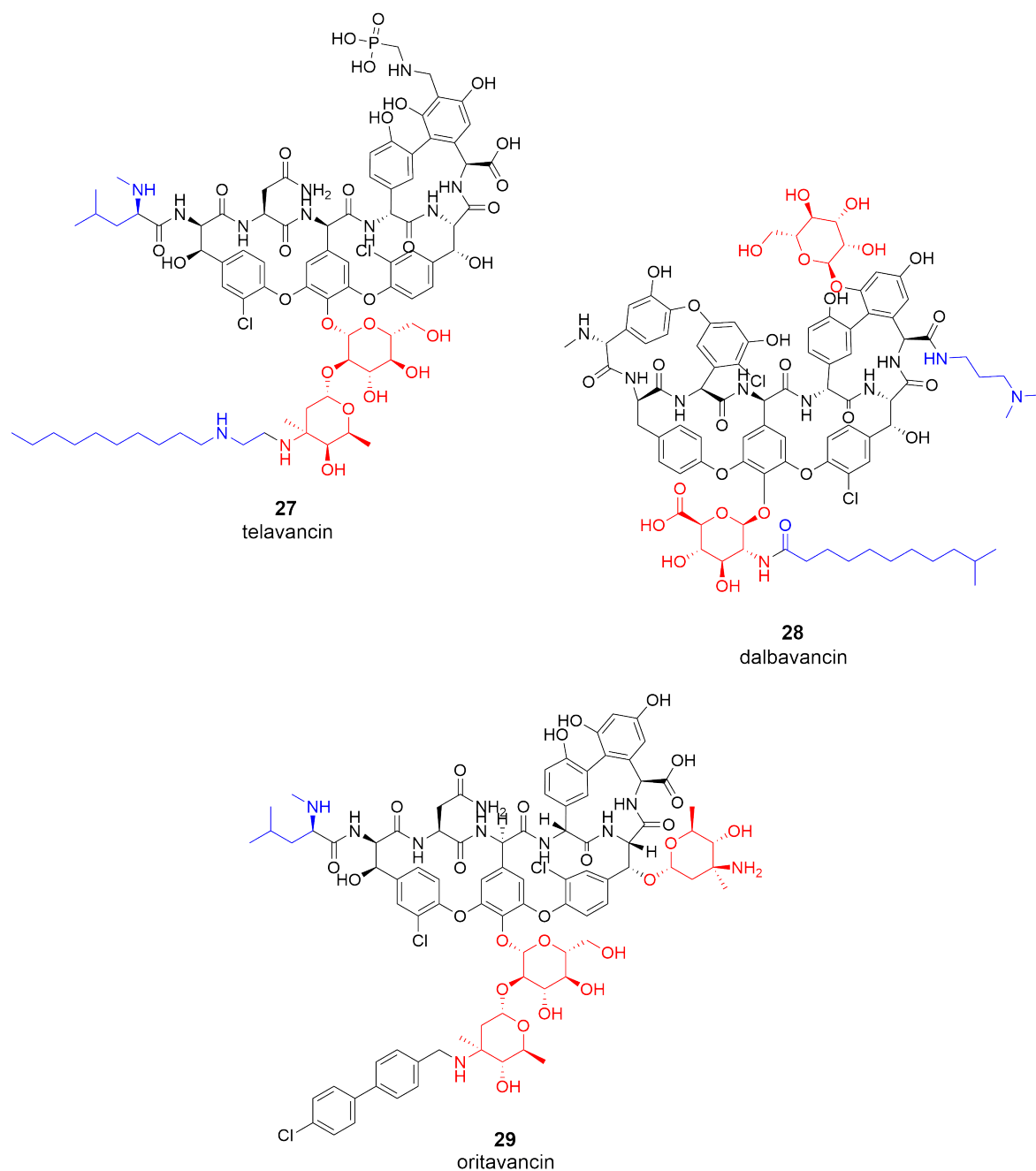
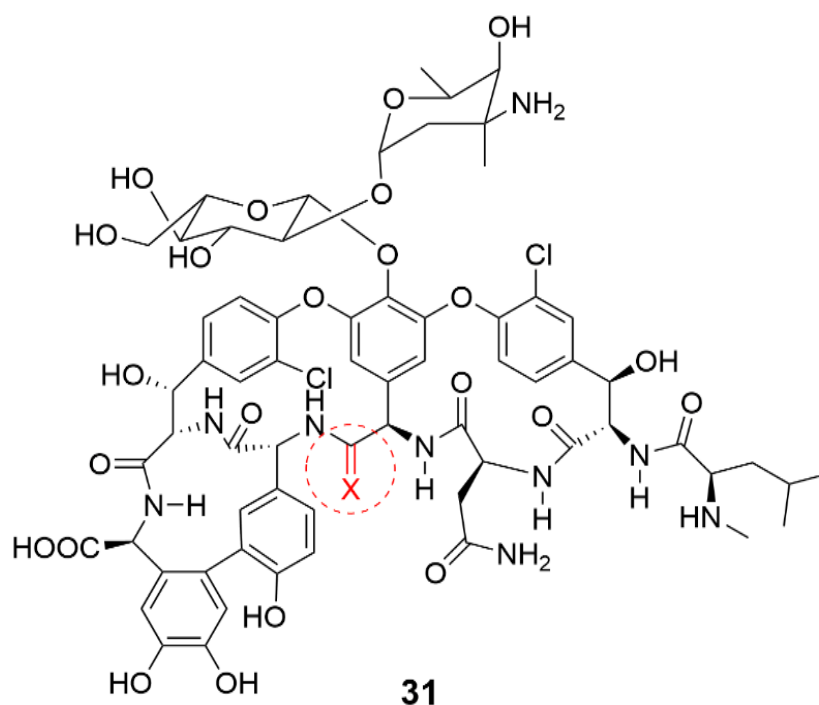


Figure 17 - Structures of second generation glycopeptides telavancin **27**, dalbavancin **28** and oritavancin **29**, with sugars highlighted in red and hydrophobic regions highlighted in blue

Dalbavancin **28** is derived from a natural product antibiotic produced by actinomycete *Nonomuria*, and modified from this compound in a three-step synthesis. Compared to vancomycin **10** and teicoplanin **26**, dalbavancin **28** exhibits increased *in vitro* bactericidal activity against resistant Gram-positive pathogens such as MRSA, VISA, and non-VanA strains of VRE (MBC of 1 µg/mL

against *S. epidermidis* strain L537, compared to vancomycin **10** MBC 16 µg/mL; teicoplanin **26** which did not exhibit bactericidal activity.^{56, 57} Whilst its mode of action is like other glycopeptides in that it binds to the two terminal amino acid residues of lipid II, dalbavancin **28** is also able to anchor into the bacterial membrane by dimerising. This action helps increase affinity for lipid II by enhancing the stability of the complex.⁵⁸ Oritavancin **29** is derived from the naturally occurring glycopeptide chloroeremomycin **30**, and contains a unique *N*-alkyl-*p*-chlorophenylbenzyl substituent on its disaccharide component. It is this alteration that confers improved activity against a number of enterococci, including resistant strains. Similarly to dalbavancin **28**, this modified component anchors into the bacterial plasma membrane, resulting in dimerisation and activity even against D-Ala-D-Lac phenotypes. Telavancin **27** is a semisynthetic vancomycin derivative that varies from these two lipoglycopeptides by the presence of a modified hydrophilic region in addition to a lipidated disaccharide. This polar phosphomethyl moiety exists on one of the five aromatic rings of the molecule, and improves the bactericidal activity *in vivo* by increasing distribution into host tissues. It has also been found to reduce nephrotoxic side effects of the drug by promoting clearance.⁵⁹

Recently the Boger group took inspiration from these lipoglycopeptide antibiotics with enhanced activity against Gram-positive species and resistant strains to investigate the effect of vancomycin derivatives **31** with variations at three main sites in the structure.⁶⁰ Initial studies in the group focused on alteration of a key single-atom site within the binding pocket. This particular carbonyl is attributed to the reduced binding affinity and antimicrobial activity that is induced when vancomycin resistant strains mutate their terminal lipid II amino acid residue from D-Ala to D-Lac, due to the electrostatic repulsion that occurs between it and the depsipeptide ester. The group rationally designed a series of single-atom variations at this point; varying the carbonyl O atoms with S, NH and H₂, and investigated the binding against two model ligands (Figure 18),⁶¹ and later the antibiotic activity against sensitive *S. aureus*, MRSA, and three strains of *Enterococci* exhibiting varying Van phenotypes.⁶⁰



Compound	X =	Ligand K_a (M^{-1})
31a	O	1.7×10^5
31b	NH	7.3×10^4
31c	H ₂	4.8×10^3
31d	S	1.7×10^2

Figure 18 - Site of the carbonyl mutation on vancomycin analogues made by the Boger group,⁶⁰ where X=O **31a**, X=NH **31b**, X=H₂ **31c**, X=S **31d**, with binding data against native Lipid II **20** shown.

Mutation to the thiocarbonyl displayed considerably reduced binding affinity and a heavily reduced MIC against all strains tested, compared to the native structure. This is attributed to the increased bond length and the larger van der Waals radii of sulfur compared to oxygen resulting in weakening of a key H-bond.

A minimal decrease in binding to the D-Ala-D-Ala ligand analogue ($K_a = 7.3 \times 10^4$ compared to 1.7×10^5 for native vancomycin **10**) suggested that the amidine mutation still functions as an H-bond acceptor for the amide NH in the target residue. Most notably, both binding affinity and MIC (0.5 $\mu\text{g}/\text{mL}$) were maintained towards the D-Lac variants. Given the basic nature of the amidine, this could be due to H-bond donation to the depsipeptide ester oxygen D-Ala-D-Lac, or

alternatively the formation of an electrostatic interaction between the protonated form of the amidine and the ester oxygen lone pairs, resulting in enhanced stabilisation compared to electrostatic repulsion thought to be the case as in native vancomycin **10**.

Okano *et al.* subsequently sought to increase the binding affinity and antibiotic activity further by adding an additional modification; derivatisation of the disaccharide with the (4-chlorobiphenyl) methyl (CBP) group found on the lipoglycopeptide oritavancin **29**. This hydrophobic component significantly enhanced activity against both sensitive and resistant strains between 10 - 100 fold (Figure 19).

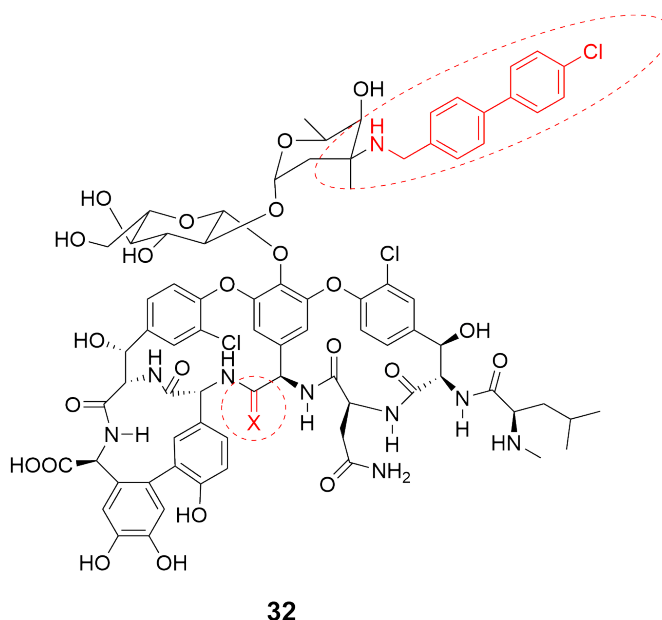


Figure 19 - Vancomycin derivatives **32** produced by the Boger group with both carbonyl mutation and addition of CBP group to disaccharide, where X= S, NH, O, H₂.⁶⁰

Finally, a third, C-terminal peripheral modification was added, introducing a quaternary ammonium salt to the structure, which have been found to increase cell permeation and induce membrane depolarisation, thus increasing the antibiotic activity (Figure 20).⁶² The derivatisation of the amines tested varied in length, including terminal tertiary dimethylamine, a five-membered cyclic quaternary salt, and the replacement of a methyl with a longer, linear tetradecyl

chain. Without exception each analogue displayed improved activity against VanA VRE, and generally followed a trend of increased activity with increased hydrophobicity. The analogue with a terminal quaternary ammonium salt at this position was the exception; exhibiting MIC values of 0.25 µg/ mL and 0.5 µg/ mL against *E. faecalis* and *E. faecium* respectively. Interestingly, this compound contains the native carbonyl rather than the amidine mutation found to induce activity against resistant strains of *Enterococci*, showing that the CBP and quaternary salt mutations are sufficient alone to combat the D-Ala-D-Lac mutation found in these bacteria. Ultimately, this study is an excellent example of how a natural product antibiotic can be rationally modified at a number of different locations to not just improve the antibiotic activity, but to combat the mechanisms developed by bacteria resulting in the surmounting of resistance as well.

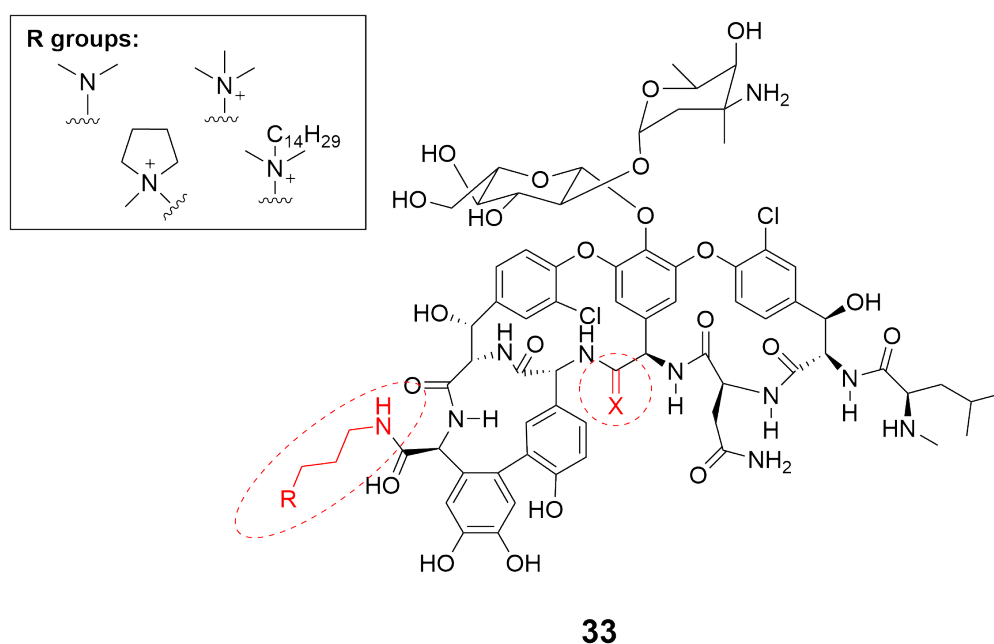


Figure 20 - Vancomycin derivatives **33** produced by the Boger group with both carbonyl mutation and addition of hydrophobic group, where $X = O, H_2$.⁶⁰

1.1.7.2 Lantibiotics

Lantibiotics (lanthionine-containing antibiotics) are a group of ribosomally synthesised peptides produced by a number of Gram-positive lactic acid bacteria

(LAB). They undergo considerable post-translational modifications to reach their biologically active forms, usually composed of a number of cyclic components, linked by thioether bonds. The unnatural amino acid lanthionine **34** itself is composed of two alanine residues, joined by a monosulfide on their respective β -carbons. Lantibiotics often contain the amino acids dehydroalanine (Dha, **35**) and (Z)-dehydrobutyrine (Dhb, **36**), which are formed via the NisB-catalysed dehydration of serine and threonine residues respectively (Figure 21). The macrocycles present in lantibiotics are the result of sulfhydryl cysteine additions to dehydrated residues, catalysed by NisC.⁶³

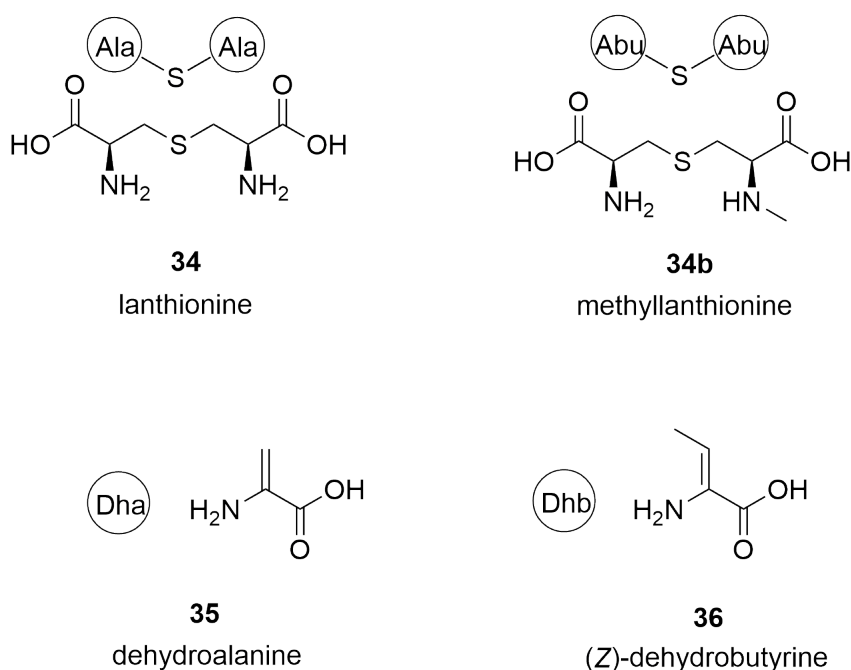


Figure 21 -Structures of the thioether linked amino acids lanthionine **34** and methyllanthionine **34b**, and unnatural dehydroalanine (Dha) **35** and dehydrobutyrine (Dhb) **36**, which appear in many naturally occurring lantibiotics.

Around 40 unique lantibiotics have been identified to date, and these can be divided into two categories based on biological activity and topology: type A are typically 20 to 34 residues in length, amphipathic in character with an overall positive charge, and adopting a screw-shaped structure, whereas type B are more compact in structure; either neutral or with a net negative charge. Nisin (**37**) is a 34-residue lantibiotic peptide produced by the bacteria *Lactococcus lactis*, containing five lanthionine rings and three dehydrated amino acids (Figure 22).

Nisin **37** has a dual antibiotic mode of action; binding to the pyrophosphate moiety of lipid II **20** resulting in both inhibition as peptidoglycan synthesis, as well as the formation of pores traversing the bacterial membrane that result in cell death.⁶⁴

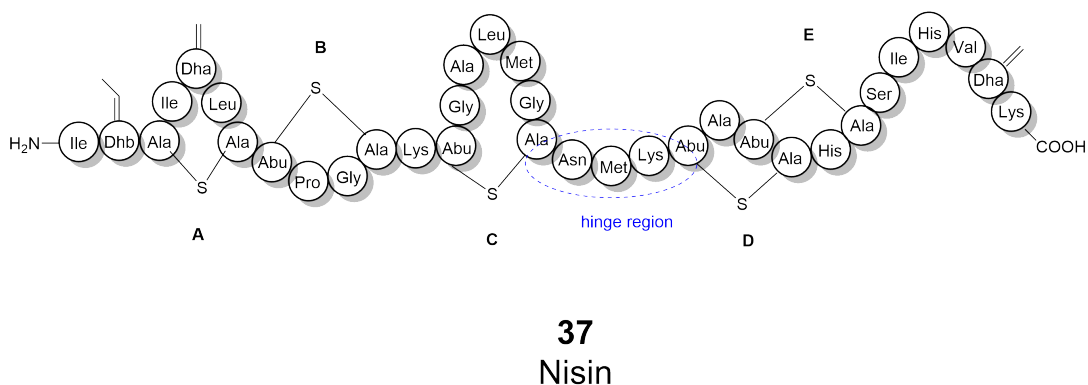


Figure 22 - Structure of nisin **37**, with dehydrated amino acids, hinge region and regions A-E indicated

At the interface of the phospholipid bilayer, a number of nisin **37** and lipid II **20** complexes form and associate, before the C-terminal linear tails of nisin **37** inserts into the membrane. This formation of pores is achieved by the alignment of nisin **37** molecules through the bilayer, at an angle perpendicular to the membrane surface, with lipid II acting as a surface anchor.⁶⁵ Solution-phase NMR of nisin **37** with a lipid II analogue containing a truncated isoprenoid (3LII, **38**) revealed the formation of a pyrophosphate cage, suggesting a different binding mechanism to that of other lipid II targeting drugs like vancomycin **10** (Figure 23).

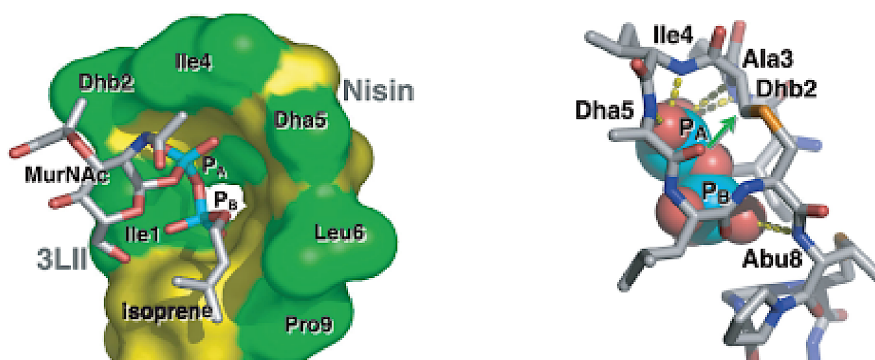


Figure 23 - Structure derived from NMR showing the pyrophosphate cage formed by nisin **37** around the lipid II analogue 3LII **38**, and the key interacting residues. Adapted from Hsu *et al.*⁶⁶

As a result of its excellent antibiotic activity (typically <10 µg/mL against a range of Gram-positive bacteria)⁶⁷ and low toxicity to mammals, nisin **37** has commonly been used as a food preservative since the 1960s. Its unique dual mode of action makes it an attractive template for drug design, but the compound has little potential in its current form as a therapeutic due to high susceptibility to protease degradation.⁶⁴

The total synthesis of nisin **37** was first reported by Fukase *et al.* in 1988, by fragment condensation of each lanthionine peptide segment, consisting of four rings and the C-terminal linear chain, using Boc solid phase peptide synthesis (SPPS).⁶⁸ Since then, a number of studies have attempted to fully elucidate the mechanism of action and binding of nisin **37** to lipid II **20**, in part to support the design and generation of stable, active analogues. Early attempts explored mutations in the amino-acid sequence but found no significant discoveries.⁶⁹ Much research has investigated a three-residue (Asn-Met-Lys) “hinge” region, located between loops C and D, thought to be essential for successful pore formation by providing conformational flexibility.⁷⁰ It was initially found that two mutants with hinge residue alterations (N20K and M21K) displayed improved activity against three genii of Gram-negative pathogens.⁷¹ Other alterations, such as N20P and M21V, resulted in better activity against Gram-positive pathogens,⁷² with the former also providing activity against drug-resistant species.

A library of nisin containing hinge derivatives was synthesised using simultaneous, indiscriminate site-saturation mutagenesis of each residue. Of

12,000 variants, structures of the active hits suggested a preference for small, chiral amino acids; leading to rationally designed AAA and SAA hinge regions which possessed 1.6 times higher activity than their native counterpart.⁷³

1.1.7.3 Lipopeptides

Peptides containing one or more lipids are referred to as lipopeptides. They are expressed by bacteria, and have been found to possess antibacterial, antifungal and haemolytic activity,⁷⁴ and are subcategorised based on amino acid sequence and length of lipid moiety.⁷⁵

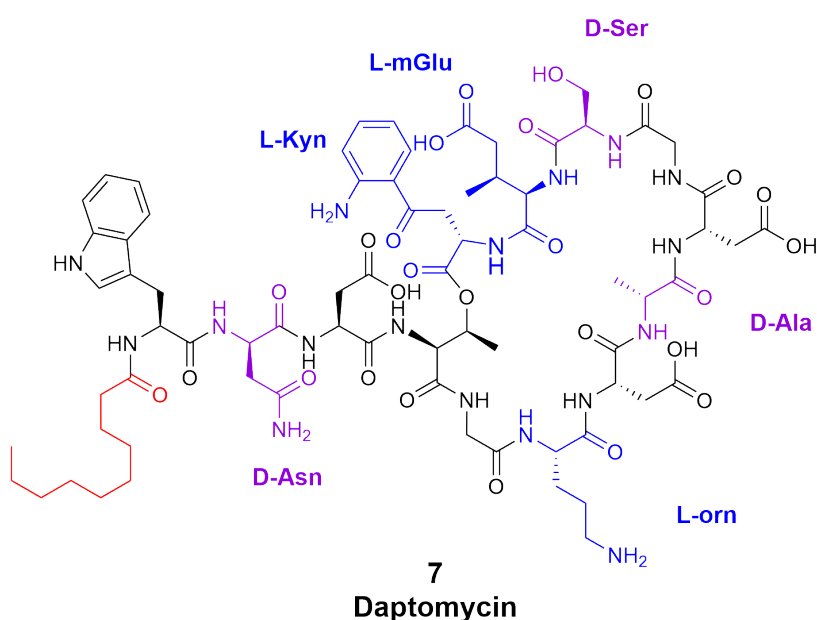
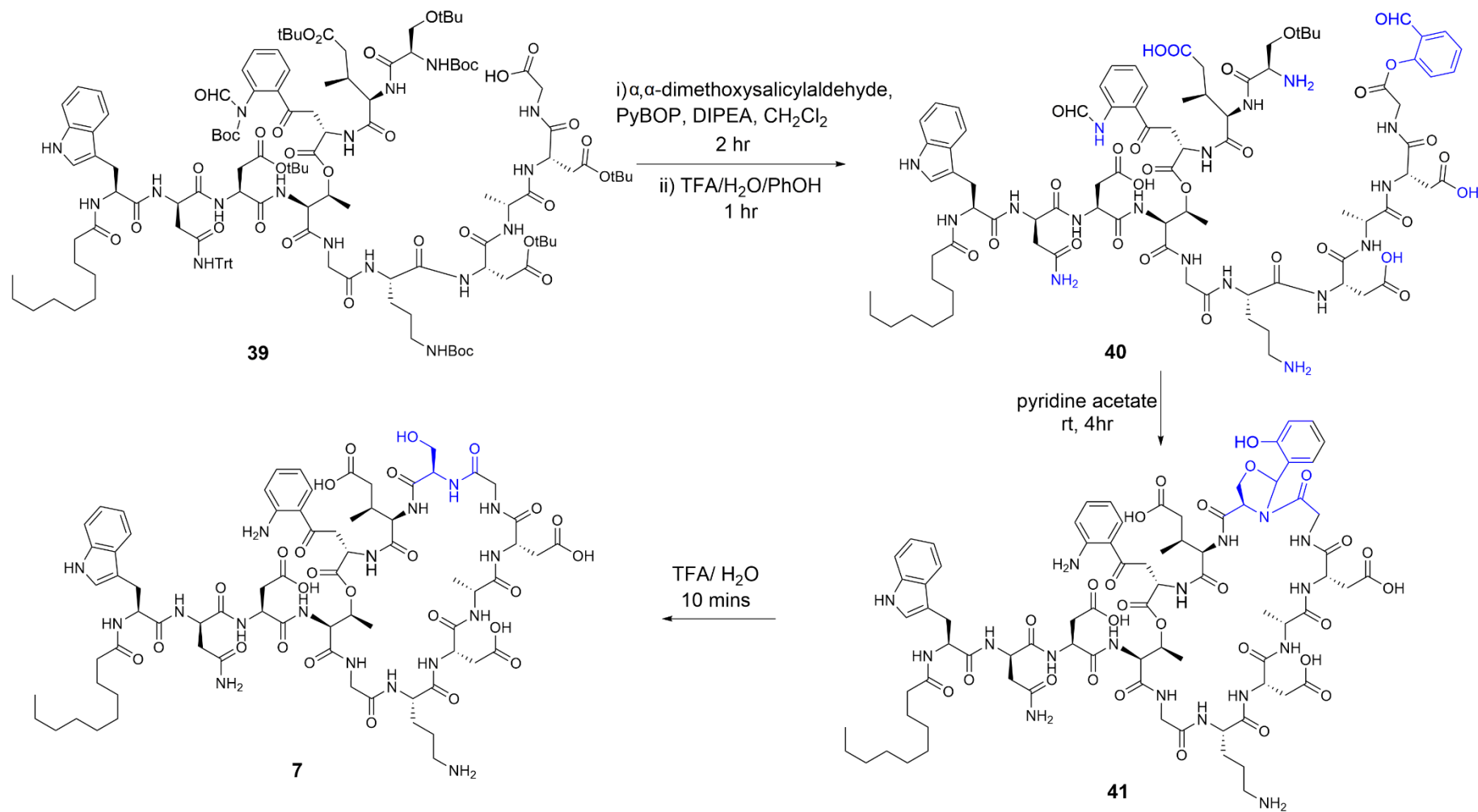


Figure 24 - Structure of daptomycin **7** with D-amino acids shown in purple, non-proteinogenic amino acids shown in blue, and decanoyl tail in red

Daptomycin **7** (Figure 24) is a 13-residue cyclic lipopeptide isolated from *S. roseosporus*, approved for treatment against several Gram-positive bacterial infections, including MRSA.⁷⁶ It contains three non-proteinogenic amino acids; L-ornithine (L-Orn), (2S, 3R)-methylglutamic acid (MeGlu) and L-kynurenine (L-Kyn); three D-amino acids, and a decanoyl tail is branched from the N-terminus through an amide bond. Unlike most antimicrobial peptides, it has an overall negative charge, but still interacts with the cell wall precursors at the interface of

the bacterial cell membrane, by interaction with calcium ions.⁷⁷ Bactericidal activity has been proposed to take place via the insertion of the hydrophobic decanoyl chain into the cell membrane, triggering potassium ions to flow out of the cell, thus resulting in depolarisation, loss of membrane potential and cell death.

The first total chemical synthesis of daptomycin **7** was reported in 2013, as a convergent peptide synthesis with cyclisation achieved by a chemoselective serine ligation (Scheme 1).⁷⁸



Scheme 1 - Final steps of the synthesis of adaptomycin **7** using a serine ligation with a reactive salicylaldehyde **40**, as described by Lam et al.⁷⁸

This provided a route to the synthesis of new daptomycin **7** analogues, to investigate SAR and find other compounds with improved antibiotic activity and lesser resistance susceptibility. Analogues mainly focused on the mutation of the MeGlu residue; as an unnatural residue with two chiral centres, the synthesis of enantiomerically pure (2*S*, 3*R*)-Fmoc-3-MeGlu(tBu)-OH is a difficult, expensive and time-consuming process. Replacement at this point with structurally similar glutamate resulted in a significant loss of activity (MIC against *S. aureus* increased to 8 µg/mL, compared to 0.1 µg/mL observed with native daptomycin **7**).⁷⁹ Replacement with the stereoisomer (2*S*, 3*S*)-MeGlu led to a further decrease in activity; 10 times less than the Glu mutant and 40 times less than native daptomycin **7**. To date, no daptomycin analogues produced by chemical syntheses have resulted in increased antibiotic activity.

1.1.7.4 AMP analogue design

The discovery of new antibiotic compounds to combat growing levels of bacterial resistance is an ever-mounting necessity. The synthesis of glycopeptide, lantibiotic and lipopeptide analogues, amongst others, has cemented the knowledge that in the majority of cases, a specific amino acid sequence is not dependent for activity; instead the retention and optimisation of key physicochemical properties are crucial for antibiotic function. These are mainly focused around structure: overall and local charge, hydrogen bond formation, and hydrophobic regions. Naturally occurring AMPs can present problems as potential therapeutics, due to instability and susceptibility to proteolytic degradation, as well as the inclusion of nonproteinogenic and synthetically challenging components, which rational analogue design can potentially overcome. As well as providing new drug candidates, AMP analogues assist in understanding the complex structure-activity relationship that exists between a natural product and its cellular target.

1.2 Teixobactin (42)

1.2.1 Discovery of teixobactin (42)

The main pitfall of the Waksman platform, and the major reason for the collapse of the golden age of antibiotic discovery, was the rarity of bacterial strains that are readily cultivable in a laboratory setting. In fact, less than one percent of all bacteria are accessible for investigation by this approach, leaving a vast quantity of “missing” microbial diversity. Together, the Lewis and Epstein groups initially began development of diffusion growth chambers, which unlike agar plates, mimicked micro-organisms’ natural environment.⁸⁰ Intertidal marine segment was used as a source of microorganisms, which mostly contains uncultivated aerobic heterotrophs – these were separated from the medium and mixed with agar and seawater. This culture was sandwiched between two membranes in the diffusion chamber, restricting the movement of cells whilst permitting the influx and efflux of chemicals and nutrients. Using this technique, several previously uncultivated bacterial species were discovered and isolated. The groups found that whilst MSC1, a newly identified species, could not easily be grown after transfer between petri dishes, MSC1 generally grew sustainably whilst on plates in the presence of other micro-organisms; suggesting that pheromone signalling is required from “neighbours” to activate growth. This provides evidence as to why so few species may be grown as colonies in isolation.

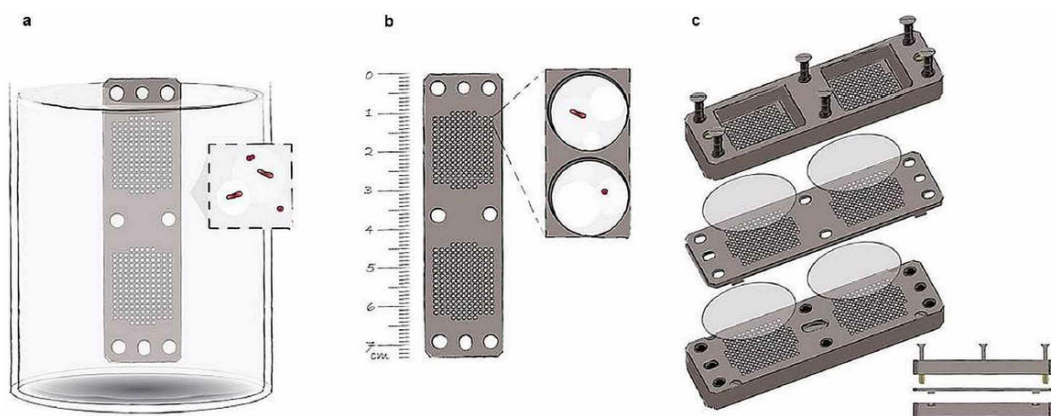


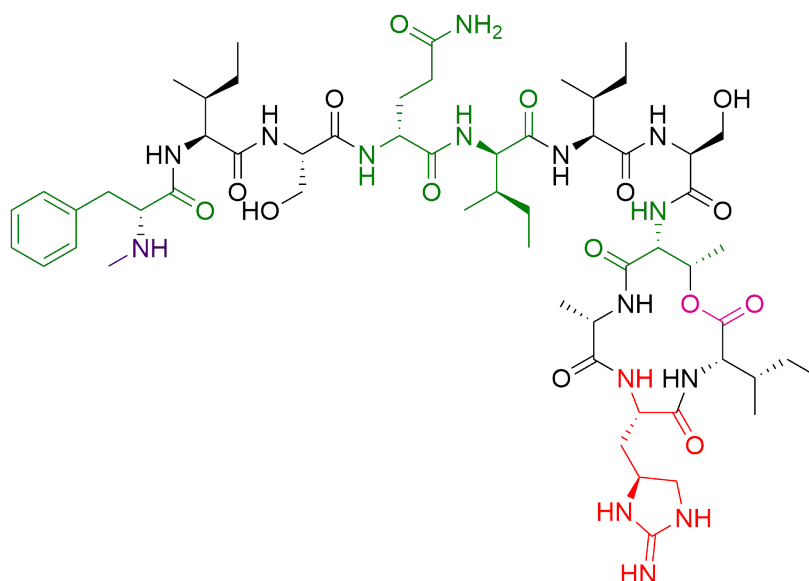
Figure 25 - Structure of the diffusion growth chamber iChip^{81, 82}

Using this basis, the groups went on to develop a more elegant device to provide the same method of bacterial cultivation within the host's endogenous environment. A novel method of high-throughput *in situ* cultivation using a device called an isolate chip, or "iChip" (Figure 25).⁸² With this instrument, Lewis and Epstein were able to dilute soil samples and trap one bacterial cell between two semi-permeable membranes, isolating bacteria and permitting influx of nutrients and growth factors from their native environment.² This method gave a growth recovery of approximately 50% of bacterial species, compared to 1% which will grow in a nutrient Petri dish.³ From one colony, a number of uncultured isolates were grown *in vitro*. Extracts from these samples were spotted onto a lawn of *S. aureus* growing on agar plates and incubated for 20 hours at 37 °C, and examined for visible clearing zones indicating antibacterial activity.

One of the extracts producing a substantial clearing zone was sequenced and submitted to the RAST genome, which analyses genomic DNA from unknown strains to identify close relatives. This extract was found to contain a previously unidentified β -proteobacteria, which was subsequently named *Eletheria terrae*, and was found to produce a compound with excellent activity against *Staphylococcus aureus*. The compound, determined by mass spectrometry, NMR and Marfey's analysis, was named teixobactin **42**.

1.2.2 Structure and biosynthesis

Teixobactin **42** (Figure 26) is a cyclic depsipeptide consisting of 11 amino acids. 4 of these are D-amino acids, and one amino acid is the post-translationally modified nonproteinogenic residue L-*allo*-enduracididine **43**. The compound is made up of a 7-residue hydrophobic linear "tail", which is coupled to a 13-membered macrocycle made up of four amino acids,



42
Teixobactin

Figure 26 - Structure of teixobactin **42**, with D-amino acids highlighted in green, N-methylation shown in purple, depsipeptide bond in pink and nonproteinogenic L-allo-enduracididine **43** in red

Teixobactin **42** is encoded by the genes *txo1* and *txo2*, which each produce a non-ribosomal peptide synthetase (NRPS). *Txo1* encodes the first 6 amino acids, and *txo2* the remaining five.⁸¹ Each amino acid residue is encoded by a module consisting of an adenylation domain, a thiolation carrier from which the amino acid is branched, a condensation domain that catalyses amide bond formation, and in the case of phenylalanine a methyltransferase as well. Macrocyclic formation, between Ile11 and Thr8, occurs at the same time as off-loading; this is catalysed by two thioesterases to give the complete structure in its active form.

1.2.3 Mechanism of action and therapeutic potential

The first indication that teixobactin **42** had a unique mechanism of action was the inability of bacteria to develop resistance against it. Usually, exposure of low doses of an antibiotic to bacteria induces mutations that cause an exponential rise in MIC over time. However, over the course of 27 days, no change in MIC occurred with *S. aureus* presented with 4x MIC levels of teixobactin **42**. This can

be due to non-specific toxicity, but human HepG2 cells presented with teixobactin **42** showed no signs of cell disruption, death or haemolytic activity, even at doses as high as 100mg/ mL, indicating that instead this is due to the target not being a protein.

Cells treated with teixobactin **42** resulted in higher levels of UDP-MurNAc-pentapeptide **15**, the cell wall precursor, suggesting inhibition at one or more stages in the synthesis of peptidoglycan synthesis. The addition of purified lipid II to these cells re-established peptidoglycan synthesis; showing that lipid II is at least one cellular target of teixobactin **42**. The ability of teixobactin **42** to bind to cell wall precursors was observed in TLC experiments, which showed that both lipid I and lipid II form stable 1:2 complexes with the antibiotic. One of the most significant discoveries made during this series of m experiments was that teixobactin **42** retained activity against vancomycin-resistant enterococci; despite vancomycin **10** having the same cellular targets (Table 4). Binding experiments with three forms of purified lipid II; one native (D-Ala-D-Ala) **20** and two with established common mutations (D-Ala-D-Lac and D-Ala-D-Ser) showed that teixobactin **42** indeed bound to all indiscriminately. To explore the possibility of an alternative binding site, teixobactin **42** was tested against various truncated forms of lipid I and II. It was able to bind undecaprenyl-pyrophosphate **16**, but not the same structure with just one phosphate; indicating the pyrophosphate moiety as a target site. Binding to the neighbouring sugar moiety was also shown by antagonisation assays that showed a tenfold higher concentration of undecaprenyl-pyrophosphate **16** was required to regain activity compared to lipid II **20**.

Binding target	Teixobactin	Vancomycin
Lipid I	✓	✓
Lipid II	✓	✓
Lipid III	✓	x
UDP-MurNAc-pentapeptide	x	nd
UDP-GlcNAc	x	nd
C₅₅-P	x	x
C₅₅-PP	✓	x
C₁₅-PP	✓	nd

Table 4 - Comparative antibiotic activity of teixobactin and vancomycin against cell wall precursors and derivatives thereof. P = phosphate, nd = not determined

Teixobactin **42** was also found to interact with lipid III **44**, a wall teichoic acid (WTA) precursor composed of undecaprenyl pyrophosphate **16** bound to GlcNAc **18**, with no peptide component. WTAs rigidify the cell wall by attracting stabilising metal cations, but are not considered essential for cell viability.⁸³ However, the inhibition of WTA precursors such as lipid III **44** can still be toxic for cells due to over-accumulation resulting in the dispersion of autolysins. The dual nature of targeting both lipid II **20** and lipid III **44** therefore may help to explain the excellent antibacterial activity of teixobactin **42**.

To test the therapeutic potential of teixobactin **42**, mice were infected with a dose of MRSA that would lead to death in 90% of cases. Teixobactin **42** was then administered intravenously one hour after exposure, in doses from 1-20 mg/ kg, and this was sufficient to prevent fatalities in all cases. The PD₅₀ was found to be 0.2 mg, significantly lower than vancomycin (2.75 mg).⁸¹

1.2.4 Enduracididine (43) and enduracidin (45)

The non-proteinogenic amino acid L-*allo*-enduracididine **43**, a cyclised form of RNA-encoded arginine, is an unusual structural feature of teixobactin **42**. It is most chemically and structurally similar to genetically encoded arginine. This residue was first discovered in 1968,⁸⁴ as a component of the depsipeptide antibiotic enduracidin **45**,⁸⁵ and exists in a number of isomeric forms (Figure 27).

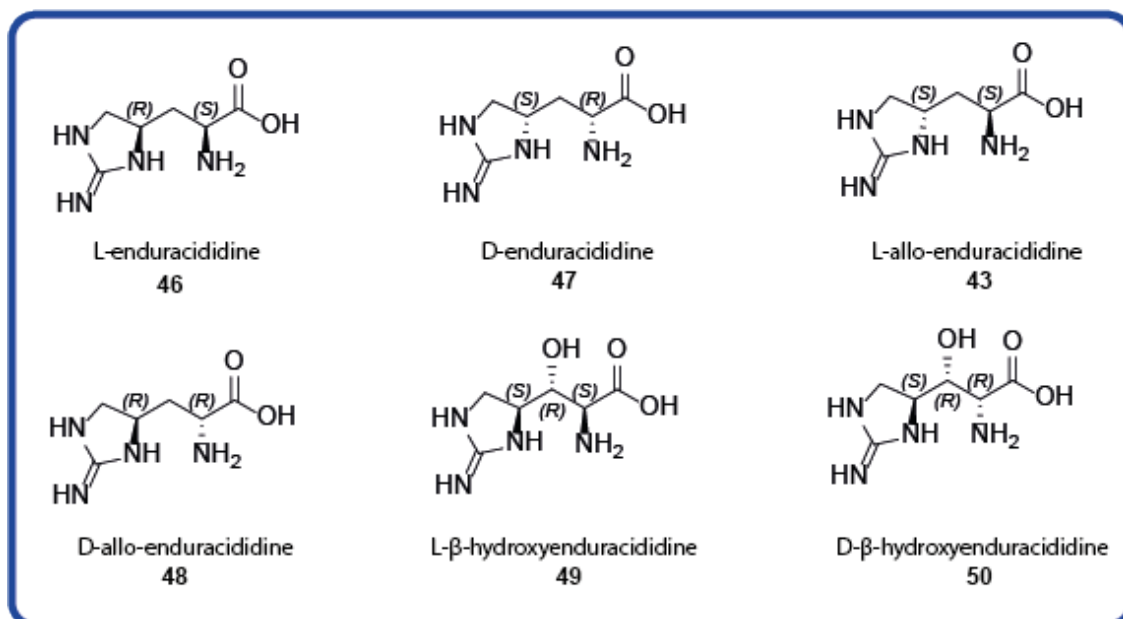


Figure 27- Stereoisomers and naturally occurring derivatives of enduracididine.

This compound **45**, isolated from the soil bacteria *Streptomyces fungicidicus*, displayed excellent antibiotic activity against Gram-positive bacteria (MIC of 0.1 – 2 $\mu\text{g}/\text{mL}$), and no cross-resistance with other antibiotics. The authors found that antimicrobial activity increased slightly in basic media; suggesting the importance of the basic enduracididine residues in the mechanism of action. Subsequently this compound was also extracted from other *Streptomyces* species^{86, 87} and determined to exist as two variants; enduracidin A **45a** and enduracidin B **45b** (Figure 28).

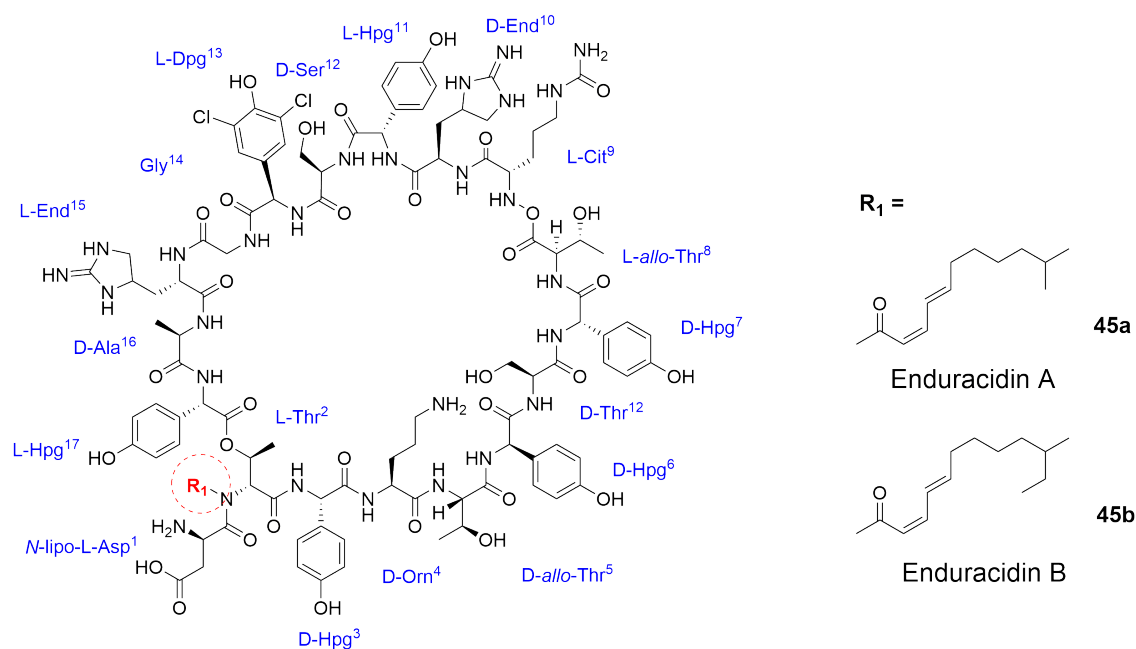


Figure 28 - General structure of enduracidin, with R groups shown for enduracidin A **45a** and enduracidin B **45b**.

Both forms of enduracidin **45** are 17-amino acid residue depsipeptides, of which 16 residues form the cyclic core. The remaining residue is an *N*-lipidated aspartic acid residue; enduracidin B **45b** differs from A **45a** by an additional CH₂ in this hydrophobic tail. Like teixobactin **42** and vancomycin **10**, these compounds also inhibit cell wall synthesis through the prevention of transglycosylation.⁸⁸ The enduracidins are highly homologous to the antibiotic ramoplanin family; although in these compounds the two enduracididine residues are mutated to L-leucine and glycosylated D-ornithine at the 15 and 10 position respectively. This group of glycolipodepsipeptides, produced by *Actinoplanes* ATCC 33076, are highly active against Gram-positive bacteria, including resistant strains such as MRSA and VRE.⁸⁹

1.2.4.1 Ramoplanin (51)

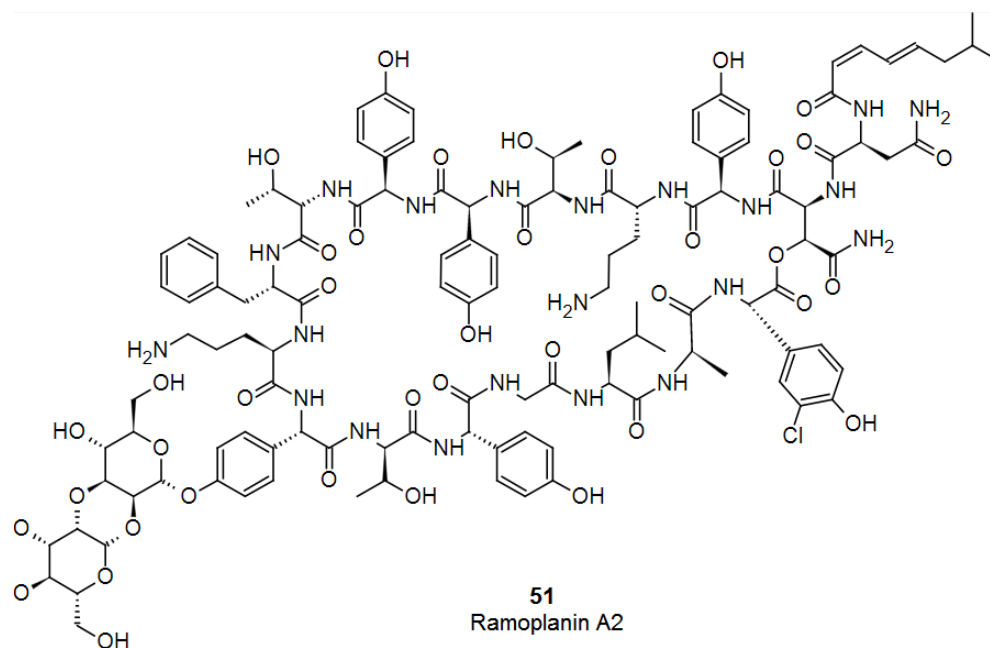


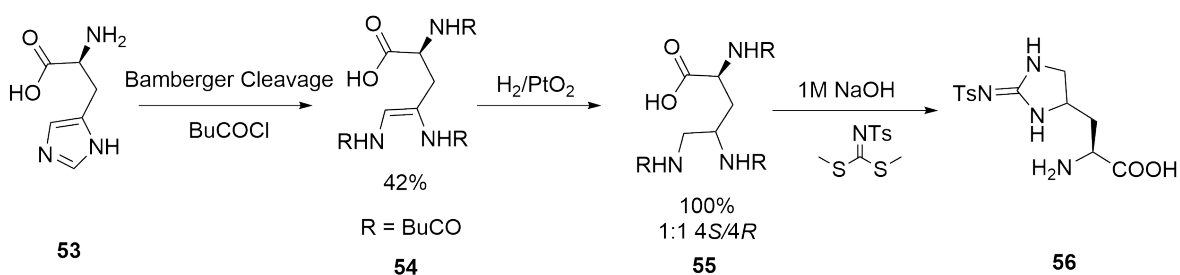
Figure 29 - Structure of ramoplanin A2 **51**, a glycolipodepsipeptide antibiotic drug.

Ramoplanin **51** is an actinomycetes-derived glycolipodepsipeptide antibiotic drug (Figure 29). Initially the mechanism of action of ramoplanin **51** was investigated by the incorporation of radiolabelled precursors into permeabilised bacterial cells. In both *S. aureus* and *B. megaterium*, UDP-MurNAc-pentapeptides **15** accumulated at concentrations close to the MIC and it was proposed that ramoplanin **51** inhibited the conversion of lipid I **17** to lipid II **20**.⁹⁰ The Walker group determined that in addition to lipid I, ramoplanin **51** undergoes a ligand-induced polymerisation in the presence of a water soluble lipid II analogue (with a ten-carbon unit as opposed to the native 55 carbon chain), assembling into viscous fibrils,⁹¹ and so is also an inhibitor of the transglycosylation step of cell wall synthesis. Using a similar method, Cudic *et al.* demonstrated that preparation of homogenous equimolar solutions of enduracidin **45** and citronellyl-lipid I **52** (a more soluble analogue with a shorter isoprenoid) resulted in immediate amorphous precipitation, thus indicating the same mode of action.⁹² The structural similarities of ramoplanin **51** and enduracidin **45** were investigated by this group, who sought to confirm that the inhibition of peptidoglycan synthesis

by these compounds was achieved by a similar mechanism of action. They proposed that ornithines 4 and 10, as the only charged residues of ramoplanin **51**, interacted with the anionic pyrophosphate and/or peptidyl carboxylates of lipid I **17** and lipid II **20**. To probe this theory, the side-chain primary amines of Orn4 and 10 were mutated to guanidine, secondary amine and acetamide groups.⁹³ Remarkably, the diguanidylated analogue displayed enhanced antibiotic activity, with an MIC of 0.25 µg/mL, an 8-fold increase from the wild-type, and also exhibited a ligand-induced aggregation. Alkylated analogue, which at these positions maintained the positive charge but contained increased steric bulk with isovaleryl groups, showed a significantly reduced MIC of 4 µg/ mL, 133 times lower than native ramoplanin **51**. Removal of the charge altogether by acetylation of each amine resulted in very poor antibiotic activity; 16 µg/ mL, 533-fold lower than the wild-type, and furthermore no detectable precipitate formed on addition of ligand. These results highlighted the importance of positive charge at positions 4 and 10 for the retention of activity, and supported the hypothesis that these residues are involved in interactions with negatively charged moieties of cell wall precursors, with the general order of activity being 1° amine > guanidine > 2° amine. Based on these results, the authors proposed that the two guanidine-containing enduracididine residues in enduracidin **45** exist to function in a similar manner.

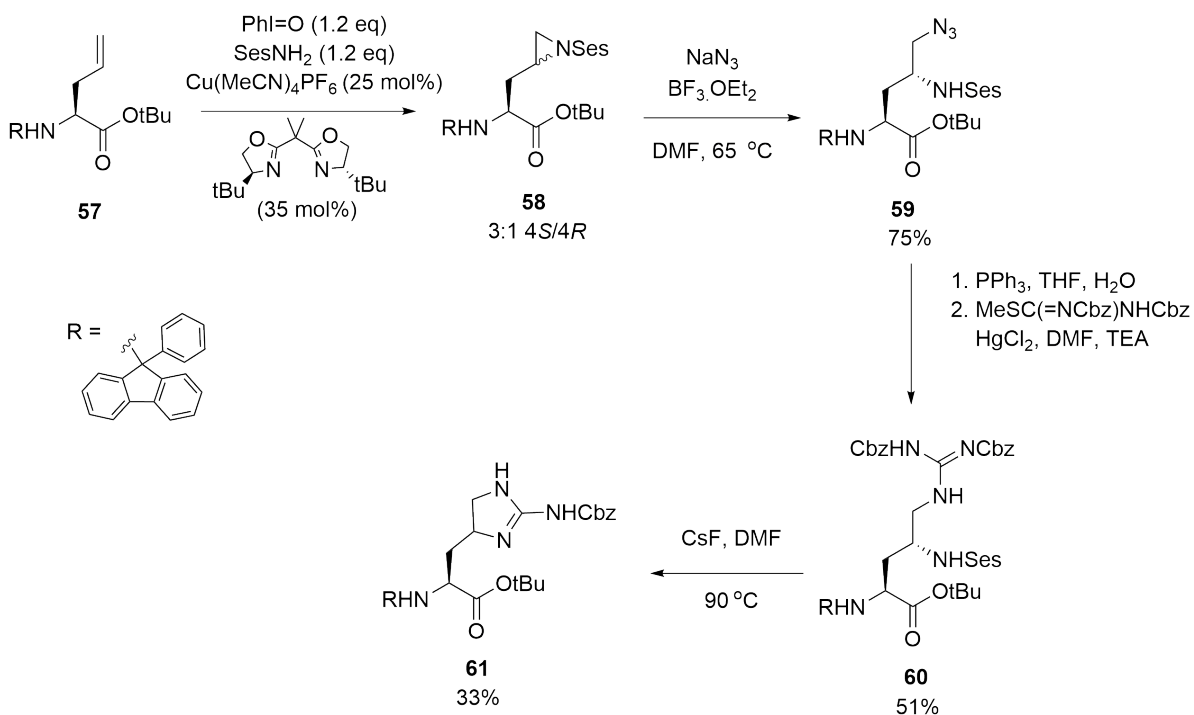
1.2.4.2 Enduracididine synthesis

Unfortunately, the potential of these compounds for therapeutic use as novel antibiotic drugs are hindered by the presence of non-proteinogenic enduracididine. The complexity of this amino acid is increased by the incidence of two chiral centres. As interest in lipid II-targeting antibiotics piqued, numerous attempts have been made to devise a straightforward and inexpensive synthesis of enduracididine from readily available starting materials. The first synthesis reported employed a Bamberger cleavage of methyl-L-histidinate **53**, followed by hydrogenation, to give an enduracididine skeleton as a 1:1 mixture at C4 (2*S*,4*R* and 2*S*, 4*S* diastereomers) (Scheme 2).⁹⁴



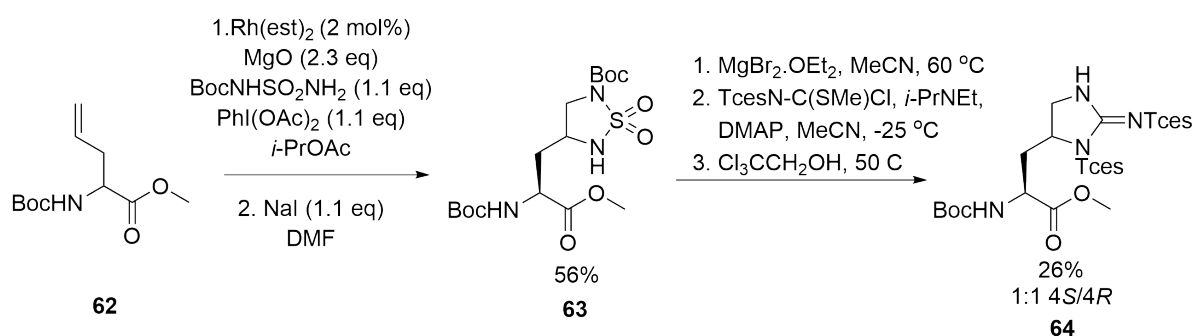
Scheme 2 - Synthesis of a protected form of enduracididine **56** via Bamberger cleavage and catalytic hydrogenation, starting from methyl-L-histidinate **53**.⁹⁴

More recently, Sanière *et al.* described the synthesis of a protected form of enduracididine: a protected α -allylglycine derivative **57** was reacted using a one-pot aziridination, mediated by copper-catalysed iminoiodane, the product **58** of which underwent azotisation, substitution and finally CsF catalysed cyclisation (Scheme 3).⁹⁵ However, this method was plagued by poor yields in numerous steps, particularly the aziridination which typically generated <30% of **58**, thus resulting in a very low yield, and the final derivative contained unusual protecting groups incompatible with standard peptide synthesis.



Scheme 3 – Synthesis of a protected form of enduracididine by a one-pot aziridination method designed by Sanière *et al.*⁹⁵

More recently, in 2014, Olson and co-workers also used a protected allylglycine derivative starting material **62**, reacted with $\text{H}_2\text{NS(O)}_2\text{NH Boc}$ to form a cyclic *N*-Boc sulfamide **63** (Scheme 4).⁹⁶ Compound **63** was then treated with $\text{MgBr}_2 \cdot \text{OEt}_2$ to cleave Boc from the sulfamide selectively (retaining Boc protection on the amine). The syn- and anti- diastereomers were then separated before conversion to a Tces-protected guanidine, before a global deprotection with LiOH ester hydrolysis and Pd/C catalysed hydrogenation to yield product **64**. Overall, the synthesis required only four steps and was a marked improvement on the previous synthesis, but was still racemic; requiring separation mid-synthesis for enantiomerically pure material.

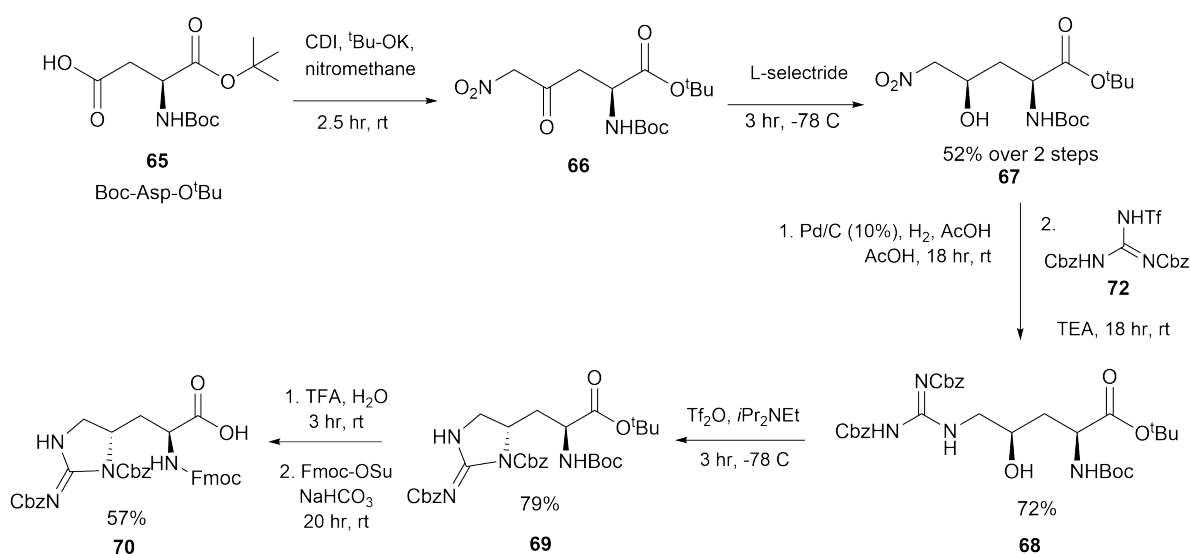


Scheme 4 – Synthetic route to enduracididine designed by Olson et al., by formation of a cyclic *N*-Boc sulfamide **63** intermediate starting from an allylglycine derivative **62**.⁹⁶

1.2.5 Total synthesis of teixobactin (**42**)

A year after the initial publication of teixobactin **42**, two total syntheses were reported.^{97, 98} A major portion of each of these involved an efficient synthesis of *L*-allo-enduracididine **43**. The synthetic route towards an *N*-Fmoc-protected derivative of unproteinogetic residue **70** by the Payne group began using a method previously published for (2*S*, 4*R*)-4-hydroxyornithine **71** (Scheme 5).⁹⁹ The commercially available Boc-L-Asp-OtBu **65** (protected at the C-terminus rather than the acid side chain) was used to acylate nitromethane to provide the corresponding nitroketone **66**. Stereoselective reduction of the ketone was then performed with L-Selectride, resulting in a 5:1 diastereomeric mix of (2*S*, 4*R*) and (2*S*, 4*S*) isomers **67**. After flash column purification, hydrogenation converted the

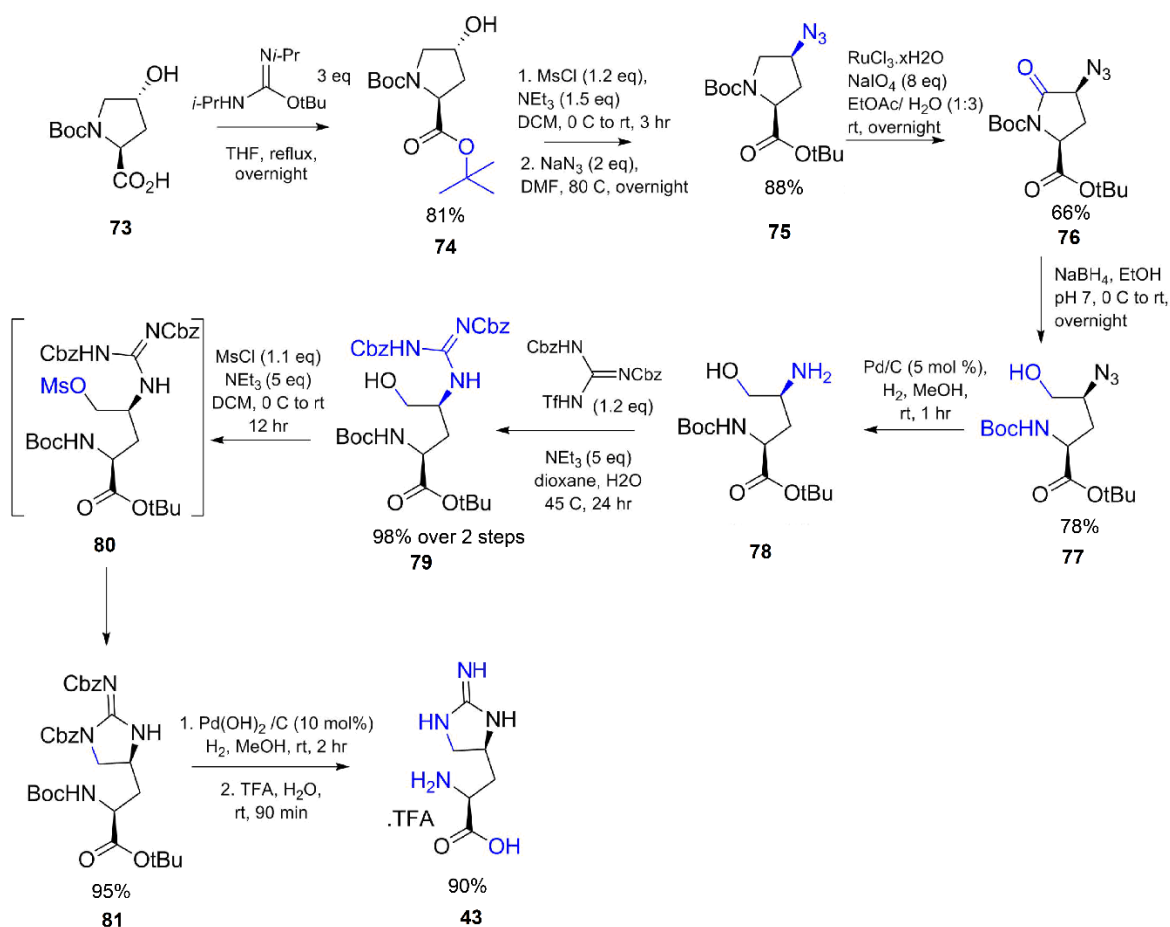
nitro group a primary amine, which was then guanidinylated using a bis-Cbz protected derivative of Goodman's reagent **72**. Cyclisation to form the protected form of the enduracididine side chain **69** was achieved by triflation of the hydroxyl in basic conditions. Finally, Boc and tBu protecting groups were removed with TFA, and the N-terminus reprotected using Fmoc-OSu to give the final form of the amino acid required for synthesis; Fmoc-End(Cbz)₂-OH **70**.



Scheme 5 - Synthetic route employed by the Payne group⁹⁶ for the synthesis of a protected L-allo-enduracididine building block **70** suitable for Fmoc-SPPS, based on synthesis by Rudolph et al.⁹⁹

In comparison, Jin *et. al.* applied a synthetic route published by their own research group the previous year, starting from Boc-*trans*-hydroxyproline **73** and forming L-*allo*-enduracididine **43** over 10 steps, with greater than 50:1 diastereoselectivity and an overall 31% yield (Scheme 6).¹⁰⁰ Initially, Boc-*trans*-Hyp-OH **73** was reacted with iodomethane with base to afford the methyl ester **74**, which was then converted to the corresponding mesylate; this was subsequently reacted with NaN₃ to form an azido group and simultaneously invert the stereochemistry at this position (**75**). After oxidation with RuCl₃.xH₂O and NaIO₄ to form the lactone **76**, the L-enduracididine skeleton **77** was formed via a reductive ring opening with NaBH₄. Catalytic hydrogenation with Pd/C converted

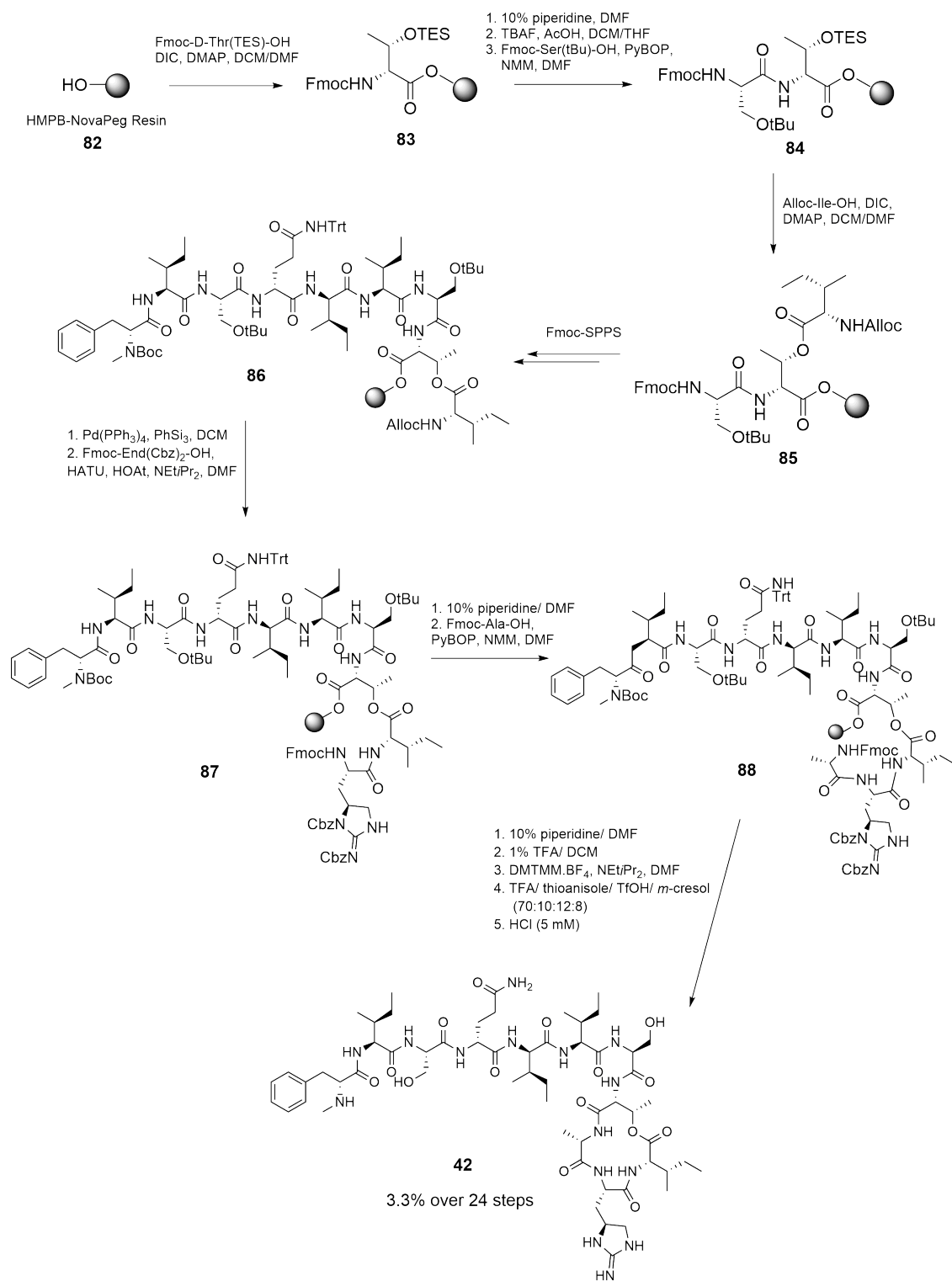
the azide to amine **78**, and the compound was guanidinylated **79**. Cyclisation was achieved with methanesulfonyl chloride in basic conditions to afford the final, protected enduracididine derivative **80**.



Scheme 6 - Enduracididine synthesis reported by the Yuan group, using Boc-*trans*-hydroxyproline **73** as a starting material and forming the TFA salt of *L*-allo-enduracididine **43** over 10 steps.^{98, 100}

With *L*-*allo*-End building blocks in hand, the total synthesis of teixobactin **42** was now accessible. The Payne group focused on using a largely Fmoc-SPPS based approach (Scheme 7). Initially, Fmoc-D-Thr(TEs)-OH was loaded to 2-chlorotriptyl chloride resin, followed by coupling of Fmoc-Ser(*t*Bu)-OH. Esterification of the threonine hydroxyl was attempted with Alloc-Ile-OH in various conditions; none of these yielded satisfactory conversion to the branched product. This was attributed to the large steric bulk of the resin linker adjacent to the reaction site; when the reaction was repeated using the more compact HMPB functionalised

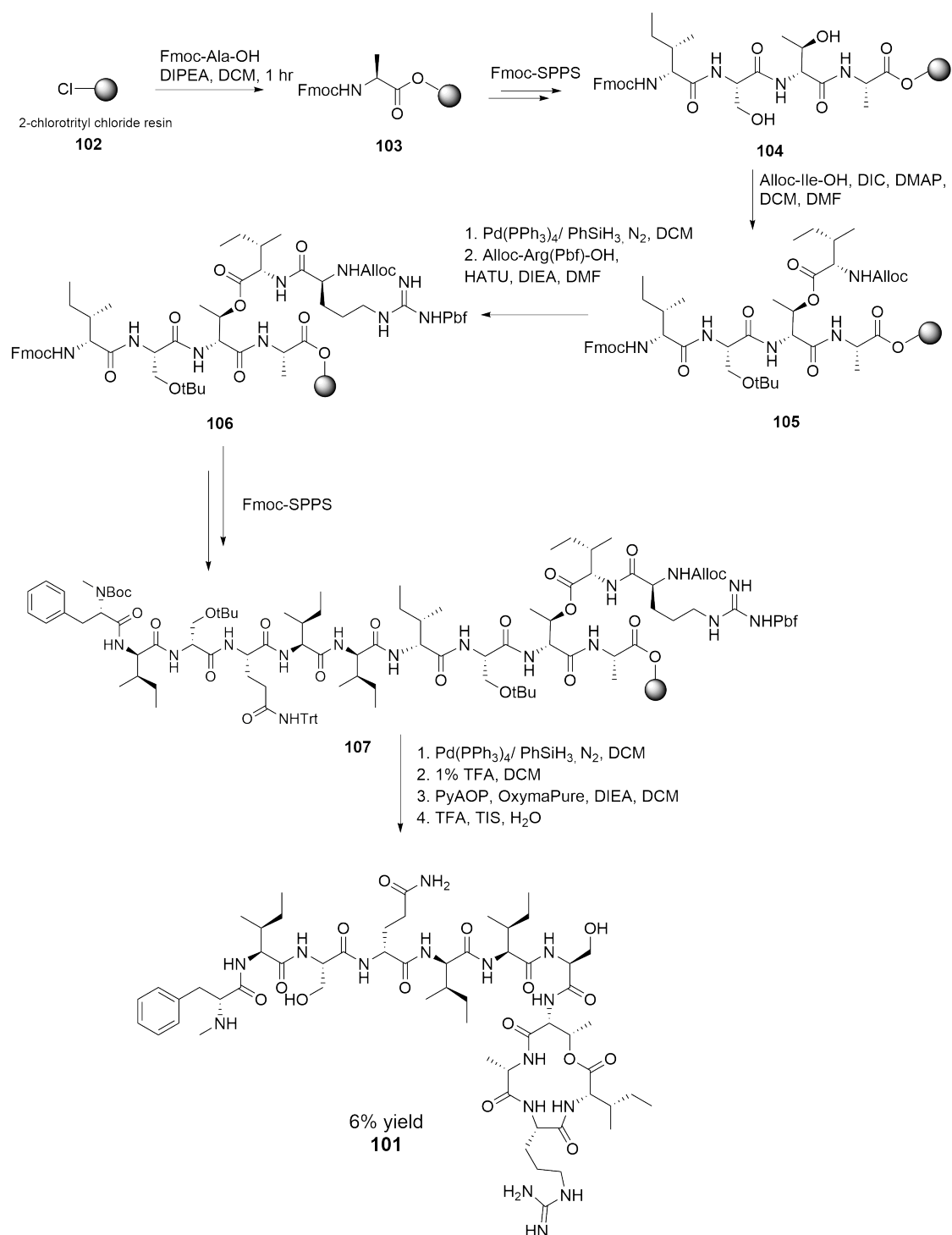
PEG-based resin **82** (which in addition has improved swelling capabilities), the esterification progressed to completion using DIC and DMAP after 16 hours at room temperature.¹⁰¹ Residues 1-6 of the linear portion were then coupled using standard Fmoc-SPPS, with *N*-Boc-Me-D-Phe-OH as the final coupling reaction. This N-terminal protection permitted the further synthesis from the orthogonal branch following Alloc deprotection of Ile with Pd(PPh₃)₄ and PhSiH₃ in DCM, with the final three residues coupled. Prior to Fmoc-Ala coupling, some diketopiperazine (DKP) formation was observed; this was avoided by reducing exposure to 10% piperidine/ DMF to 30 seconds (rather than 2 x 3 minutes). After the final Fmoc-deprotection, the peptide **88** was cleaved from resin using 1% TFA in DCM; a concentration low enough to permit reaction completion whilst ensuring all side chain protecting groups remained bound. Macrolactamisation was accomplished using 4-(4, 6-dimethoxy-1, 3, 5-triazin-2-yl)-4-methylmorpholinium tetrafluoroborate (DMTMM.BF₄) and DIPEA in DMF, before a final global deprotection step with TFA, trifluoromethanesulfonic acid (TfOH), thioanisole, and *meta*-cresol (70:12:10:8 v/v/v/v). Lyophilisation in 5 mM HCl yielded teixobactin **42** as a bis-HCl salt (as opposed to the potentially toxic TFA salt form). Overall, this route gave teixobactin **42** in 3.3% yield over 24 steps, following the initial resin loading. This synthetic form displayed consistent activity with the naturally extracted form reported by Ling *et. al.*⁸¹



Scheme 7 - Total synthesis of teixobactin **42** as described by the Payne group, reported in 3.3 % yield over 24 steps.⁶

Jin *et al.* reached teixobactin **42** using a different synthetic strategy that the group had previously used successfully in the total synthesis of daptomycin **7**;⁷⁸ the

convergent Ser/Thr ligation of two peptide fragments (Scheme 8).⁹⁸ The linear hexapeptide fragment **99** was prepared through standard Boc-SPPS, on aminosalicylaldehyde linked resin. After all six residues were coupled, protecting groups were removed a mixture of TFA/TMSOTf/thioanisole (8.5:1:0.5, v/v/v), before cleavage from the resin using ozonolysis for 5 minutes at -78 °C in acidic conditions. For the pentapeptide fragment **97**, the synthetic route as designed to allow the macrocyclisation to occur at the least sterically congested site (Thr8 – Ala9). The depsipeptide bond was first formed between Alloc-D-Thr-OH and Fmoc-Ile-OH in solution using PMB protection of the C-terminus, before being immobilised onto 2-chlorotritylchloride resin via the deprotected carboxylate. Removal of Alloc protection with standard conditions (Pd(PPh₃)₄/PhSiH₃) permitted the coupling of Boc-Ser(OtBu)-OH. Coupling of Fmoc-End(Cbz)₂-OH with DIC and HOBt progressed very slowly; requiring three 10 hour reactions to reach completion, most likely due to the very large steric bulk and rigidity of the side chain. After coupling of Fmoc-Ala-OH, cleavage from the resin with TFE, AcOH and DCM provided the linear, side-chain protected pentapeptide **96**. Similarly to Payne *et al.*, no DKP formation was observed at this point. Formation of the 13-membered macrocycle progressed to completion over 24 hours, using HATU, HOAt and OxymaPure in DCM at sub-millimolar concentration. The final form of teixobactin **42** was yielded by removal of all remaining protecting groups, using TFA and hydrogenation in the presence of Pd(OH)₂.



Scheme 9 - Synthesis of Arg¹⁰ teixobactin analogue **101** reported by Jad *et al.*, obtained in 6% overall yield.¹⁰²

101 was tested for its antibacterial activity versus four strains of bacteria; Gram-positive *S. aureus* and *B. subtilis*, and the Gram-negative species *E. coli* and *P. aeruginosa*. Like teixobactin **42**, a high concentration (51 µg/ mL) was required for inhibition of growth of the Gram-negative species, but was found to possess

good antibiotic activity against the Gram-positive species. However, the potency of **101** was considerably less than native teixobactin **42**, revealing an MIC value of 1.6 $\mu\text{g}/\text{mL}$ (compared to 0.2, an eightfold reduction) for *S. aureus* and 0.4 $\mu\text{g}/\text{mL}$ (compared to 0.016 $\mu\text{g}/\text{mL}$, a 25 fold reduction) for *B. subtilis*. Clearly, despite the structural similarity of this compound to teixobactin **42**, the loss of the cyclic guanidine side-chain of residue 10 gives rise to a considerable decline in antibiotic activity.

Shortly after, Parmar *et al.* also described the synthesis of **101** using the same synthetic method.¹⁰³ They also reported the biological activity of an additional analogue **108**; for which the four native D-amino acids had been mutated to their L- counterparts. **108** was also acetylated, rather than methylated, at the N-terminus, thus losing the positive charge at this position (Figure 31).

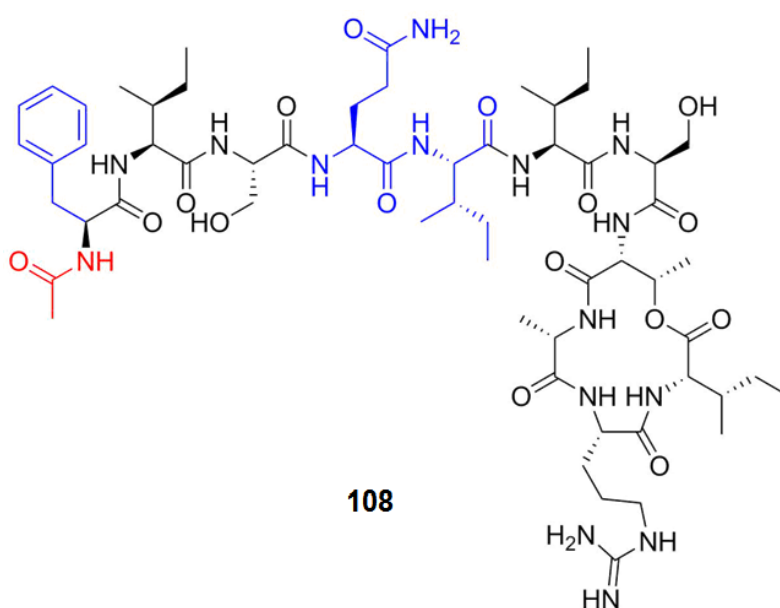


Figure 31 - Teixobactin analogue **108** synthesised by Parmar *et al.* with acetylated N-terminus (red) and three D-amino acids mutated to L-amino acids (blue).¹⁰³

108 was found to have no activity against Gram-negative *E. coli*, and minimal activity (MIC of 128 $\mu\text{g}/\text{mL}$) against Gram-positive bacteria *S. aureus*. It could not be determined for **108**, however, which of the two mutations (or both) had resulted in the significant decrease in activity. It is plausible that one mutation

without the other may not have resulted in such a drastic change in antibiotic activity in comparison to native teixobactin **42**.

Following the work by Parmer *et al.*, this hypothesis was investigated by Monaim *et al.*, who mutated L- to D- amino acids independently of tail acetylation in three distinct analogues (Figure 32).¹⁰⁴ It was found that the analogue **109** with the sole mutation of D- to L- amino acids had absolutely no antibiotic activity. The analogue that retained the stereochemistry of all amino acid residues but had an acetylated N-terminus **110** was found to have more or less no activity, with an MIC of 256 $\mu\text{g}/\text{mL}$ for *B. subtilis*, highlighting the possible importance of the terminal positive charge. Finally, the compound with both L-amino acids and the acetyl cap in conjunction had a high MIC of 128 $\mu\text{g}/\text{mL}$ against *S. aureus*. These results do not offer conclusive reasons for the presence of these unusual moieties. It is possible that D-amino acids are utilised by the host bacteria to prevent protease degradation, or alternatively may be related to conformation and the orientation of teixobactin **42** against the target. A positively charged N-terminus may be necessary to traverse the membrane and anchor the drug in place, or instead may provide some essential hydrophilicity in a compound that is otherwise markedly hydrophobic and likely water insoluble.

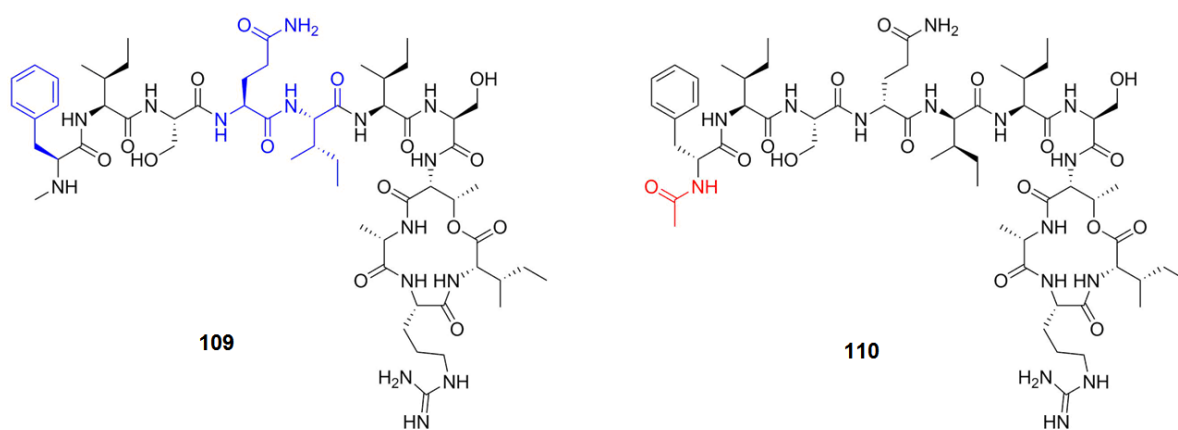


Figure 32 - Teixobactin analogues **109** and **110** synthesised by Monaim *et al.*, **109** with D- to L- variations (left hand side, blue) and **110** with an acetylated N-terminus retaining native stereochemistry (right hand side, red)

The significance of variation in structure was probed more extensively by the Nowick group, who synthesised eight different compounds with several alterations (Figure 33).¹⁰⁵ In particular, these mutations focused on investigating the roles of the guanidinium group at position 10; the stereochemistry of the macrolactone ring; and the composition of the “tail” (residues 1-5). The synthetic routes for these compounds did not involve the use of Alloc protection; instead residues 9 to 2 were introduced by standard Fmoc SPPS onto the resin, and Boc-protected *N*-Me phenylalanine was applied in place of Fmoc-Phe-OH for residue 1. This facilitated the esterification of the threonine side chain to proceed without resorting to using the less labile Alloc- protecting group. Using this same synthetic strategy, Yang *et al.* created the Arg10 analogue **101**; the Lys10 analogue **111**; the L-Thr8 analogue **112**; the D-*allo*-Ile11 analogue **113**; the *seco*-Arg10 analogue (removal of the depsipeptide bond) **114**; the *ent*-Arg10 analogue (stereochemistry of all amino acid residues reversed) **115**; “short”-Arg10 (truncated to remove residues 1-5) **116** and “lipobactin 1” **117** which replaced tail residues 1-5 with a dodecanoyl group (Figure 32). Variation of three of these resulted in complete loss of antibiotic activity (these being the *seco*- **114**, the short **116**, and the L-Thr8 **112** analogues).

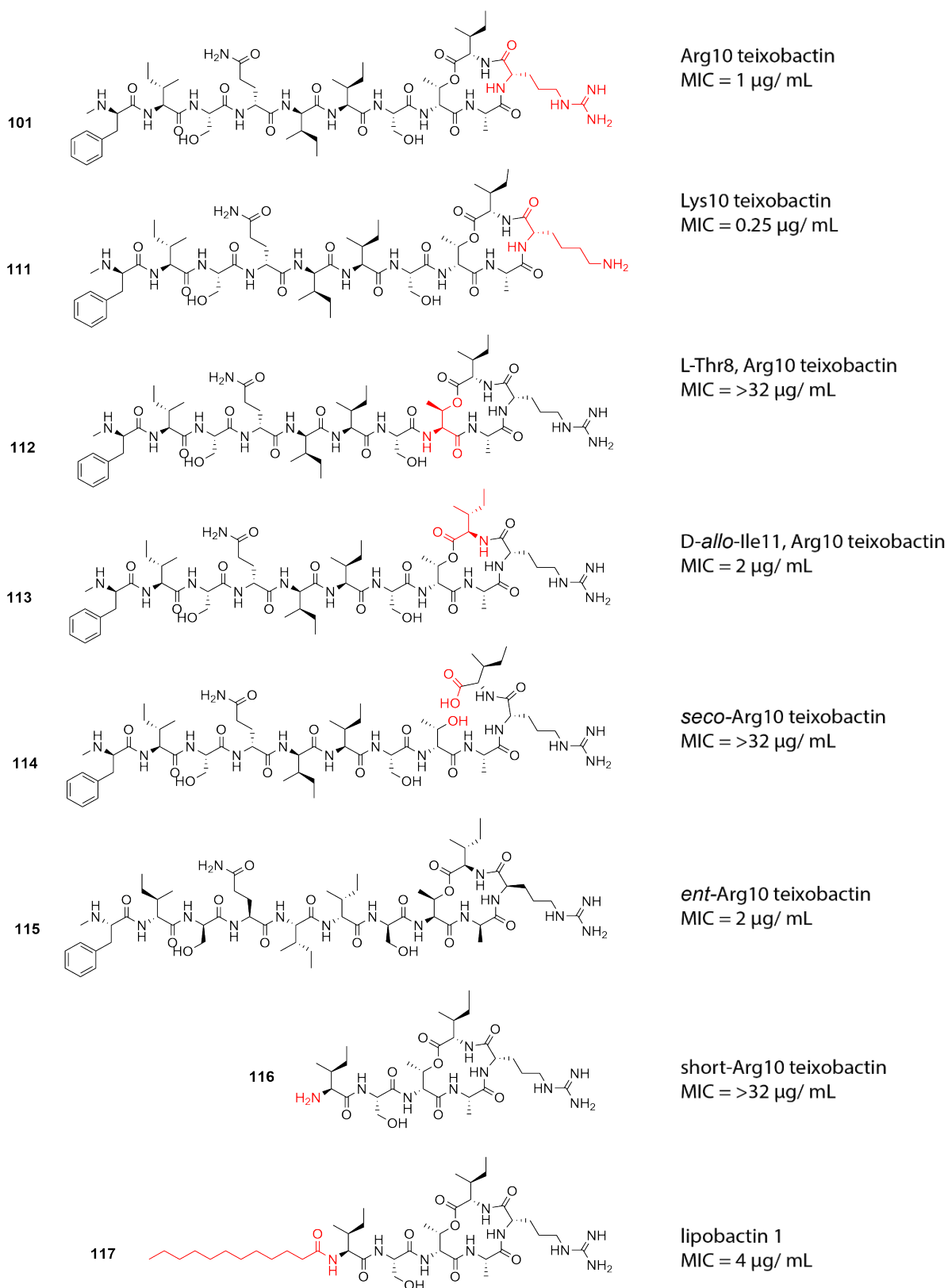


Figure 33 - Teixobactin analogues synthesised by the Nowick group.¹⁰⁵ MIC values against *B. subtilis* for each compound shown.

These results strongly supported the importance of retaining the structural integrity of the macrocycle, and also the necessity of the linear tail portion of the molecule. The comparable activity of the *ent*- analogue **115** supports the idea that the macrocycle forms a “cage” around the pyrophosphate group of lipid II **20** through hydrogen bonding, due to retention of the conformation. Lipobactin 1 **117** was found to have an MIC of 4 µg/ mL against *S. epidermis*, supporting the idea that these terminal residues act as a membrane anchor, or at least in some form of hydrophobic interaction. However, the fairly significant drop in activity showed that further optimisation of the structure and length of this lipid replacement is necessary. Possibly the most interesting result, however, was for the Lysine10 analogue **111**, which not only had comparable activity, but in fact *increased* activity in comparison with the more structurally similar Arginine10 analogue **101**. This was a significant increase from 1 µg/mL for Arg10 **101** to 0.25 µg/mL for Lys10 **111**, which suggests the use of the nonproteinogenic *allo*-enduracididine **43** is more for the purpose of resistance to proteolysis rather than specifically for its interaction with lipid II **20**. Given that the lysine analogue **111** possesses greater activity than native **42**, it is quite possible that the basicity of the residue at this position has the greatest influence on potency, and that more strongly basic residues are able to interact more strongly with the negatively charged pyrophosphate group.

Whilst these results illuminated many interesting results, it must be noted that the assays were performed against *S. epidermis* rather than the more clinically relevant *S. aureus*. Teixobactin **42** has a greater efficacy against *S. epidermis* than other species of the *Staphylococcus* genus, so at a glance these results may seem illusorily superior without additional testing against *S. aureus*. Furthermore, given the increased activity of Lys10 **111** compared to Arg10 **101** it would have been beneficial to vary enduracididine to each of these residues for all analogues to find the most potent active compounds, and for comparison to each other.

Monaim and Albericio *et al.* somewhat expanded on the unprecedented raised activity of the Lys10 analogue **111** by performing a lysine scan on all other residues of teixobactin, except those at the 1-, 8- and 10- positions which previous research had already established as essential in their current form.¹⁰⁶

They found that mutation to any isoleucine residues in the linear tail resulted in a total loss of antibacterial activity. However, mutations at the 3-, 4-, 7- and 9-positions retained weaker activity, strongly supporting the requisite for hydrophobicity in the tail of teixobactin and any analogous compounds.

Towards the beginning of 2017, Parmer and Singh *et al.* published an additional article on the synthesis of several teixobactin analogues; this time investigating the relevance of the stereochemistry of what they described as “key” residues – these being the four D-amino acids of teixobactin **42**.¹⁰⁷ It has been demonstrated that the D-threonine residue of the macrocycle is integral for both activity and depsipeptide formation, but there has been no conclusive evidence that mutations of the other three D-amino acids will always result in the loss of activity; only that the tail must be relatively hydrophobic and contain D-amino acids at some point. Parmer and co-workers produced seven teixobactin analogues (with an Arg10 mutation) that varied the stereochemistry of these three D-amino acids. With reference to the 1-, 4-, 5- and 8- positions, the LLLL **109**, DDDL **118**, DLDD **119** and LLDD **120** analogues showed no antibiotic activity at all. The LLLD **121** and LDDD **122** analogues had weak activity with MIC values of 128 µg/ mL and 32-64 µg/mL respectively against Gram-positive bacteria. The original DDDD analogue **101**, as expected, had an MIC value of 2 µg/ mL against the same strain. To probe these results further, the authors performed molecular dynamic simulations using NOE values from NMR. These suggested that the analogues which possessed good activity had less structural rigidity; the compound with all L-amino acids folded back onto itself into a hairpin structure. It was proposed therefore that rather than for protease resistance, teixobactin **42** contains D-amino acids to prevent “packing,” and that the increased stability gained through packing decreases the antibiotic activity of these compounds. It was proposed that increased solvent exposure to Arg10 resulted in the anomalous result for LLLD **121**.

Compound number	Code	N-Me-Phe1	Gln4	Ile5	Thr8	MIC $\mu\text{g/mL}$ (<i>S. aureus</i>)
101	DDDD	D	D	D	D	2
109	LLLL	L	L	L	L	GAW ^a
118	DDLD	D	D	L	D	GAW
119	DLDD	D	L	D	D	GAW
120	LDDD	L	D	D	D	32-64
121	LLDD	L	L	D	D	GAW
122	LLLD	L	L	L	D	128

Table 5 - Arg10–teixobactin analogues synthesised by varying D-residues.
^a Growth in all wells

1.3 Aims of the project

The discovery of teixobactin **42**, the first of a new class of antimicrobial peptide, provides new avenues towards the design and synthesis of novel compounds that have the potential to be immune, or at least less susceptible, to the development of antibiotic resistance. Teixobactin **42** itself has potential as a therapeutic, but the synthesis is relatively expensive and laborious; mainly due to the presence of the non-proteinogenic amino acid L-*allo*-enduracididine **43**, which has been proven difficult to provide in satisfactory yield in its enantiomerically pure form. The initial aim of this research was to design a new and efficient route to the total synthesis of teixobactin; the main novelty lying in the use of a nickel (II) Schiff base complex for the asymmetric synthesis of L-*allo*-enduracididine **43**. We aimed to use this route to produce all four stereoisomers to enduracididine to investigate the structure-activity relationship of the relative stereochemistry.

This research also sought to design and synthesise new teixobactin analogues that retain similar antibiotic activity to the native compound, that could be made via a more economical and efficient route. Replacement of the L-*allo*-enduracididine **43** with a DNA encoded variant was attempted, to remove a laborious part of the total synthesis. Truncation and replacement of the

hydrophobic linear peptide region of the molecule were investigated, to reduce the number of overall steps, and remove three unnatural and costly D-amino acids.

The macrocyclisation of teixobactin had been achieved in solution, but generally over long reaction times. Cyclisations performed in solution can typically be accompanied by numerous problems, such as low yield, oligomerisation and side product formation. This research aimed to investigate the use of safety-catch linked resins to design a new synthesis, forming the 13-membered ring simultaneously with cleavage from the resin in a single step. Solution-phase cyclisation was also targeted to be optimised by fully proving several different methods, including solution phase method depsipeptide formation and amide bond formation in a range of different conditions.

Finally, synthetic teixobactin analogues were to be screened for their antibiotic activity; determining their MIC against Gram-positive and Gram-negative bacteria, with active hits aiding the design and synthesis of further compounds, and providing further evidence for the mechanism of action of teixobactin **42**.

2. Towards a novel synthesis of L-*allo*-enduracididine (43)

2.1 Introduction

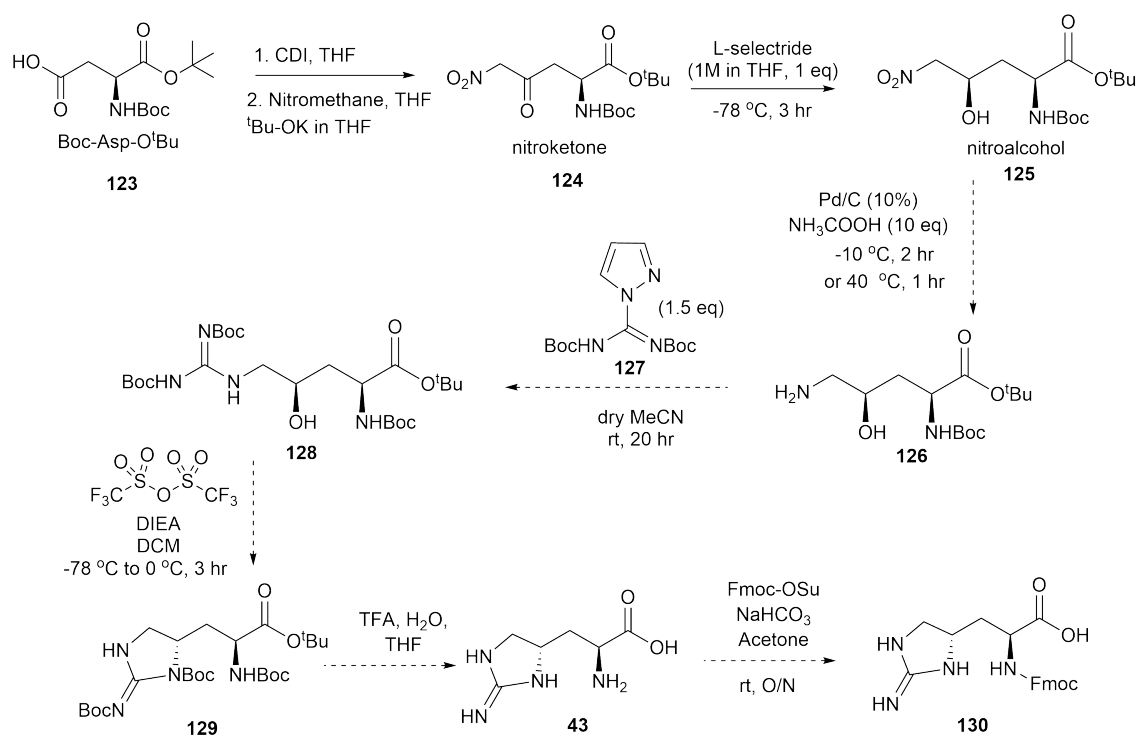
One of the unusual features of teixobactin **42** is the presence of the nonproteinogenic amino acid L-*allo*-enduracididine **43**, a cyclised form of RNA-encoded arginine containing two chiral centres, derived by post-translational modification of this residue *in vivo*.¹⁰⁸ Prior to 2015, a limited number of methods to synthesise this residue had been published; typically low yielding, involving a large number of steps and with low diastereoselectivity.⁹⁴⁻⁹⁶ In order to produce an efficient total synthesis of teixobactin, a new route to L-*allo*-enduracididine **43** would be required.

Given that binding to the cellular target lipid II **20** primarily relies on the interaction of teixobactin **42** with the pyrophosphate moiety, the presence of L-*allo*-enduracididine **43**, the sole basic residue, has been proposed to be highly important for effective binding of the compound.⁸¹ As the nature of this interaction has not been fully established, the result of variation of L-*allo*-enduracididine **43** to the other three stereoisomers on the antibacterial activity of the compound would give valuable information about the structure-activity relationship of this residue.

2.2 Aims of the chapter

Following the publication of the structure of teixobactin **42**,⁸¹ this project initially aimed to develop a total synthesis of the compound. Given the unique and unusual structure of teixobactin, one most challenging points of the synthesis is that of the nonproteinogenic amino acid L-*allo*-enduracididine **43**, which is not commercially available. This work aimed to develop an alternative, more efficient route that could be used in the total synthesis of teixobactin **42**, and structurally similar analogues, by the design and synthesis of an electrophilic compound that could be used in complexation with a Ni(II) Schiff base complex to provide a simpler, more economical approach with fewer steps.

Our initial synthetic route towards L-*allo*-enduracididine **43** was based on a synthesis of (2*S*,4*R*)-4-hydroxyornithine **71** reported by Rudolph *et al.* (Scheme 10).⁹⁹ It was aimed to take this *N*-Boc,*O*-*t*Bu-protected non-proteinogenic amino acid **71** and form a bis-Boc protected form of L-*allo*-enduracididine **129** using *N,N'*-Bis(Boc)-1*H*-pyrazole-1-carboxamide **127**, followed by intramolecular cyclisation with trifluoromethanesulfonic anhydride. From here **43**, protecting groups could be removed with TFA, and the N-terminal amine reprotected with Fmoc to give the final amino acid in a form compatible with standard solid phase peptide synthesis (**130**).



Scheme 10 - Initial synthesis design for *N*-Fmoc-L-*allo*-enduracididine **130**, with Boc-Asp-*Ot*Bu **123** as starting material, based on method by Rudolph *et al.*⁹⁹

However, soon after designing and commencing this synthetic route, a very similar method was published by Payne *et al.* in their total synthesis of teixobactin. This work also began with the synthesis of (2*S*,4*R*)-4-hydroxyornithine **71** using the same conditions, and varied significantly only in forming the bis-Cbz protected guanidine form of L-*allo*-enduracididine (as

opposed to Boc). Therefore, due to the lack of novelty, this method was discontinued.

Instead, the focus of this work shifted to a novel synthesis of L-*allo*-enduracididine **43** and its three stereoisomers **46**, **47**, **48**, through use of a Ni(II) Schiff base complex that had been designed by the Jamieson group in previous work.¹⁰⁹ These enduracididine stereoisomers could be incorporated into teixobactin analogues to probe the structure-activity relationship of stereochemical variations of this residue.

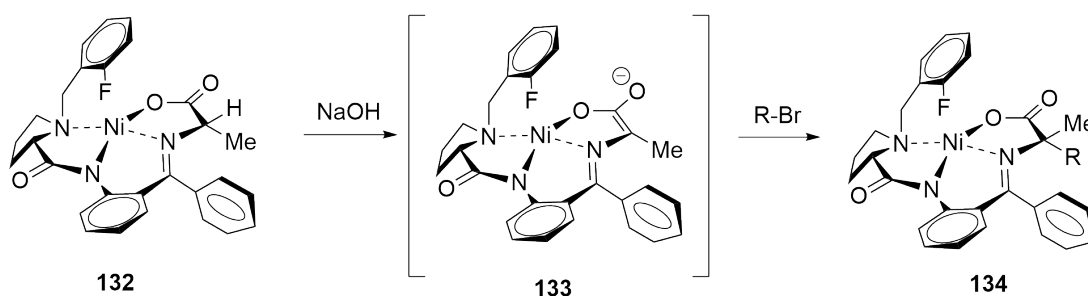
2.3 Synthesis design with a nickel (II) glycine Schiff base complex

Non-proteinogenic alpha-amino acids are classically obtained through chemical and enzymatic resolutions, isolation from natural sources, and through asymmetric synthesis.¹¹⁰ The latter of these techniques has been achieved by enantioselective introduction of the α -hydrogen,¹¹¹ α -amino group,¹¹² the α -side chain¹¹³ and the carboxyl group.¹¹⁴ Whilst catalytic enantioselective methods, such as hydrogenation and phase transfer catalysis (PTC) of racemic alpha-amino esters have been widely employed in recent years, the diastereoselective synthesis of alpha-amino acids using chiral templates derived from glycine, alanine and other amino acids have proven to be simple, cheap and robust.

Chiral Schiff bases were one of the first ligands used for asymmetric catalysis. In 2001, Ryouji Noyori was awarded the Nobel Prize in Chemistry for his development of a Cu(II) Schiff base complex used in the metal-carbenoid cyclopropanation of styrene, which he pioneered in 1968.¹¹⁵ This was followed by work by the Schollkopf group, who developed method for efficient asymmetric synthesis of α -amino acids using metalated chiral bis-lactim ethers of 2,3-diketopiperazines.¹¹⁶ In this work, a high level of diastereoselectivity was achieved by attack of the alkylating electrophile being forced to take place *trans*-to the inducing chiral centre, but the method was marred by expensive reagents, multi-stage syntheses and limitations in scale-up. However, this foundation of diastereoselectivity achieved by the arrangement of a rigid chiral inducing centre with prochiral groups led Belokon and co-workers to develop the use of transition

metal based complexes of glycine and alanine to create similar alpha-substituted amino acid products.¹¹⁷ In comparison to the work by Schollkopf, the use of transition metals resulted in simplified recovery of alpha-amino acid products, and improved yields, due to the increased acidity of the α -proton of the amino acid fragment resulting in the use of milder alkylation conditions. As a result, nickel(II) Schiff base complexes have been widely used for the asymmetric synthesis of α -carbon substituted unnatural amino acids.¹¹⁸

The Jamieson group has previously reported the use of Ni(II) Schiff base complexes derived from a 2-fluorobenzyl ligand **131** for the synthesis of unnatural mono- and α,α -disubstituted amino acids.¹⁰⁹ The introduction of a fluorine substituted ligand **131** was found to give an increased level of diastereoselectivity (>95:5 dr). X-ray crystal structures revealed the 2-F-benzyl moiety to exist across the *re*-face of the complex, sterically restricting access to the electrophile, and forcing alkylation to take place from the *si*-face instead, resulting in solely 2S configuration of the final amino acid product (Scheme 11). The improved diastereoselectivity resulting from the 2-F modified ligand was proposed to be due to the presence of the fluorine atom inducing a partial positive charge on the benzyl group, which could interact with the adjacent proline amide oxygen, thus promoting the π - π -stacking interaction that exists between the two cyclic components. In addition, the presence of a fluoride moiety facilitated analysis of reaction progression by the use of ¹⁹F NMR.

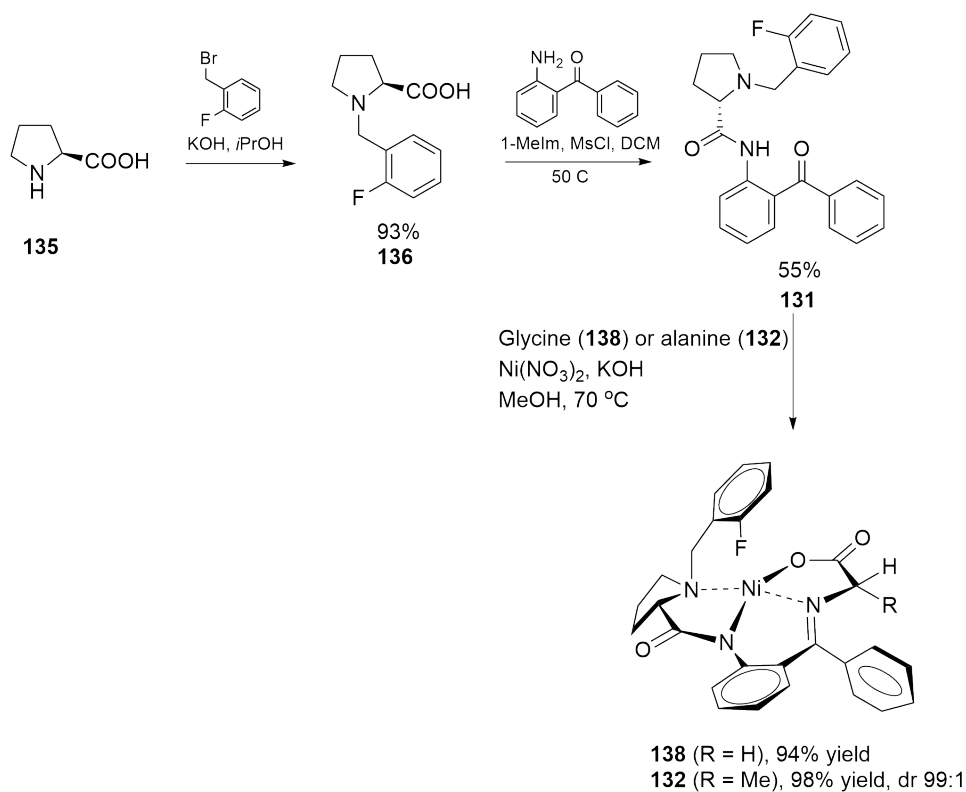


Scheme 11 - Deprotonation and alkylation pathway of the Ni(II) alanine Schiff complex (S)-Ni-Ala-2FBPB **132**, with alkylation solely from the *si*-face, directed sterically by the fluorobenzyl moiety.

In the work by Aillard *et al.*, this method was used successfully in the synthesis of aliphatic amino acids with side chains bearing terminal alkenes, for use in

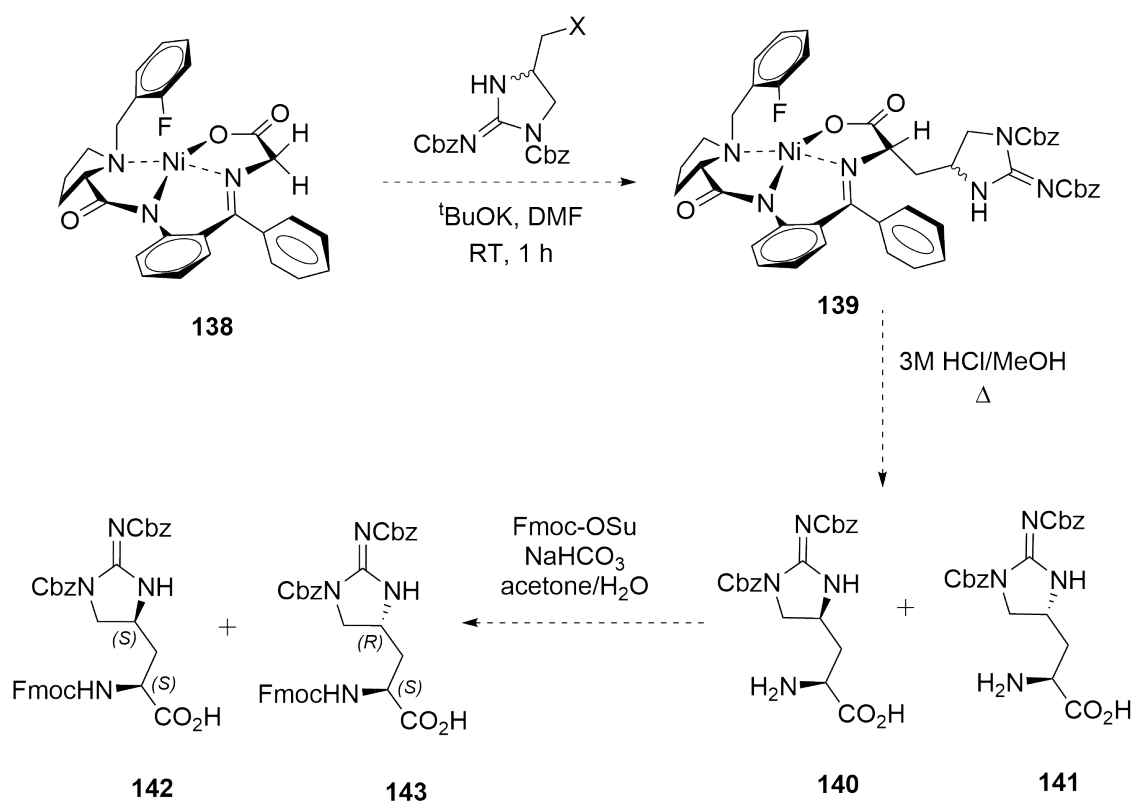
peptide “stapling.” This is where side-chain to side-chain cyclisation of a peptide is achieved through Grubb’s ring closing metathesis of these unnatural residues, typically situated in *i*, *i*+4 positions to induce α -helix formation.¹⁰⁹

The chiral ligand can be synthesised in six steps starting from L-proline **135**, which is *N*-alkylated using 2-fluorobenzyl bromide to yield the tertiary amine derivative **136**, which subsequently undergoes a condensation reaction with 2-aminobenzophenone by use of methanesulfonyl chloride and 1-Melm to yield the chiral auxiliary (*S*)-*N*-(2-benzoylphenyl)-1-(2-fluorobenzyl)-pyrrolidine-2-carboxamide (2-FBPB) **131**. This is subsequently purified to >99% enantiomeric excess by slow recrystallisation. Complexation of glycine or L-alanine with nickel nitrate under basic conditions gave a diastereomeric mix of the final nickel Schiff base complexes **138** (Gly) and **132** (Ala) in excellent yield (94% and 98% respectively, Scheme 12). The use of glycine results in a complex that can be used for the synthesis of α -monosubstituted amino acids. The complexation of L-alanine results in an unnatural amino acid with a methyl substitution at the α -carbon, in addition to the side chain which is coupled by electrophile alkylation in subsequent reactions. Ni(II) Gly **138** and Ni(II) Ala **132** complexes used in this work were synthesised by Boris Aillard of the Jamieson group.



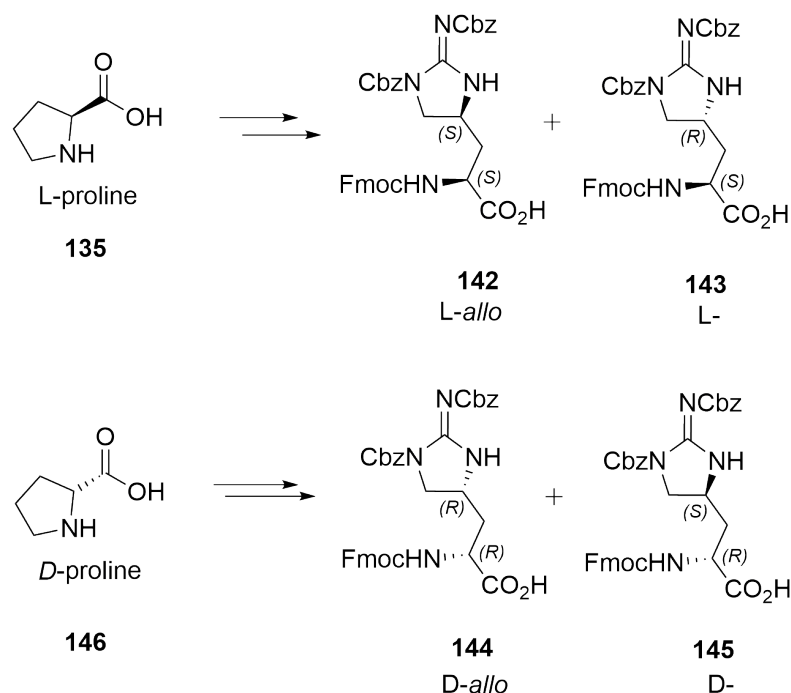
Scheme 12 - Synthetic route to Ni(II) glycine **138** and alanine **132** Schiff base complexes, starting from L-proline to create the (2-FBPB) ligand **131**. Synthesis completed by Boris Aillard at the University of Leicester.

Therefore, it was proposed that the synthesis of Fmoc-L-*allo*-enduracididine **130** could be achieved by diastereoselective mono-alkylation of the Ni(II) glycine Schiff complex (S)-Ni-Gly-2FBPB **138** with a suitable cyclic guanidine electrophile (Scheme 13). Whilst these complexes result in high enantioselectivity at the α -carbon, this reaction would produce a mix of diastereomers at the 3-position of enduracididine.



Scheme 13 - Proposed synthesis of a Fmoc, Cbz-protected form of L-allo-enduracididine (2S, 3S) **142** concurrently with the (2S, 3R)-isomer **143**, using Ni(II) glycine complex (S)-Ni-Gly-2FBPB **138** and a Cbz-protected cyclic haloguanidine electrophile.

Whilst this method significantly lowers the final yield of protected L-allo-enduracididine **142** due to the formation of diastereomers, it was deemed to be useful for insights into the structure-activity relationship of this amino acid in the binding of teixobactin **42** to lipid II **20** by determining the effect of variations in stereochemistry of this residue. It was envisaged the diastereomers **142** and **143** could be purified relatively simply by flash chromatography either prior to or following decomplexation. Finally, these enduracididine diastereomers could be prepared for use in solid phase-peptide synthesis by N-Fmoc-protection. To prepare the other two enduracididine isomers (D-allo **144** and D- **145**), the synthesis could be repeated using D-proline **146** as the starting material of the Ni(II) Gly Schiff complex to yield (R)-Ni-Gly-2FBPB **147**, in order to fully probe the significance of the relative stereochemistry at the 2- and 3- positions, resulting in an efficient method to access all forms of the nonproteinogenic amino acid (Scheme 14).



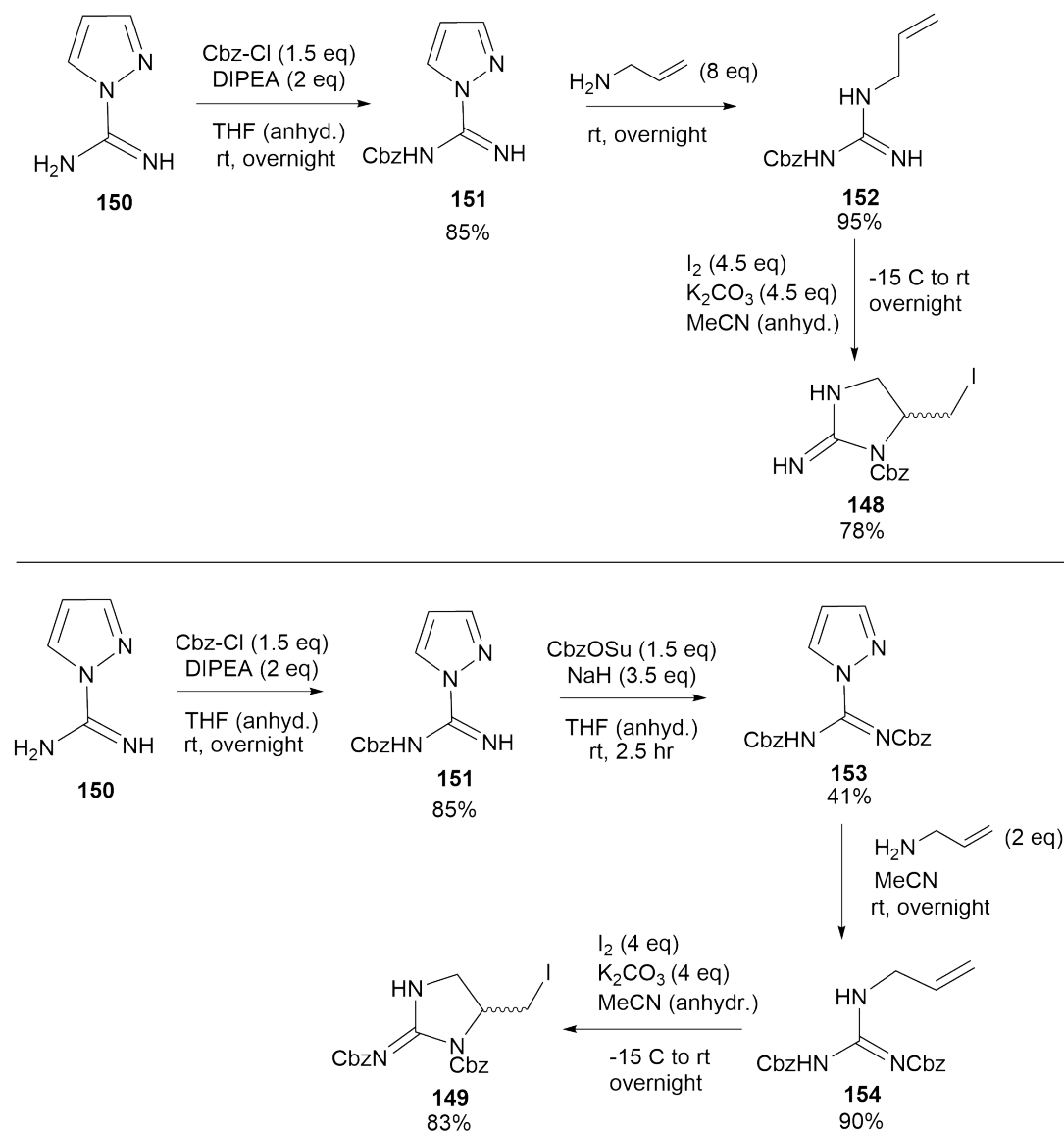
Scheme 14 - Proposed route to all four diastereomers of enduracididine (**142-145**) by use of L-proline **135** and D-proline **146** starting materials to synthesise enantio-specific Ni(II) glycine based complexes.

2.4. Initial alkylation reactions and electrophile optimisation

Synthesis of L-*allo*-enduracididine **43** using a Ni(II) Schiff base complex requires a halogenated form of the cyclic guanidine. A literature search revealed a published synthesis of the required iodinated electrophile with Boc or Cbz protection of the guanidine by the Rowles group.¹¹⁹ In this work, the authors reported the use of iodocyclisation reactions of Boc- and Cbz- protected *N*-allylguanidines to synthesise a number of mono- and bis-protected five- and six-membered guanidine heterocycles. Using these methods, both the mono-Cbz **148** and bis-Cbz **149** forms of the cyclic iodoguanidine were synthesised initially (Scheme 15).

Starting from 1-H-pyrazole carboxamide hydrochloride **150**, benzyl chloroformate in DIPEA was used to yield the mono-Cbz protected pyrazole **151**; stronger conditions are required in order to achieve a second protection (compound **153**); with NaH required for deprotonation, and the use of *N*-

(benzyloxycarbonyloxy) succinimide (CbzOSu) as electrophile. From **151** and **153**, allylamine is used to substitute the pyrazole ring to form **152** and **154** respectively. Cyclisation is then achieved through addition of iodine and potassium carbonate in acetonitrile to form the final Cbz-protected cyclic iodoguanidine electrophiles (mono-Cbz **148**, bis-Cbz **149**).

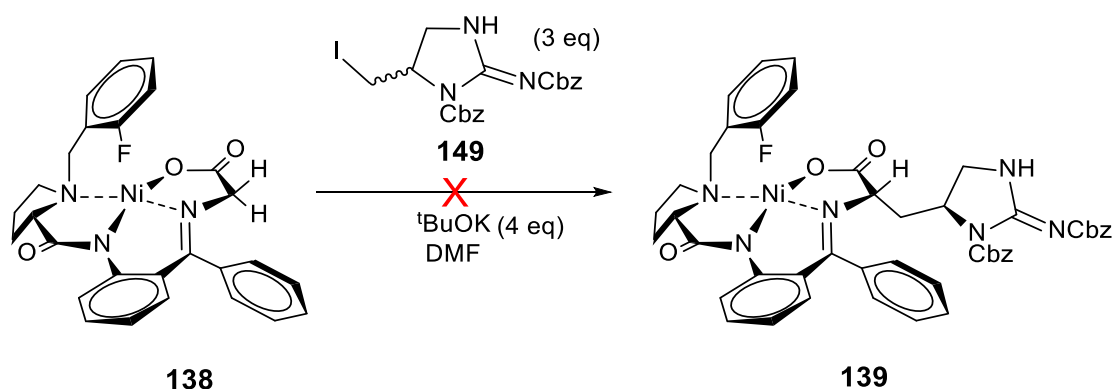


Scheme 15 - Synthesis of mono-Cbz and bis-Cbz cyclic iodoguanidine electrophiles **148** and **149**, both starting from 1-H-pyrazole carboxamide hydrochloride **150**.

Mostly these reactions did not require significant alteration from the published route;¹⁹ although it was found that the recrystallisation steps were difficult to

repeat with the provided methods, and these were optimised with variation of solvent and/or temperatures, resulting in improved yields compared to published values.

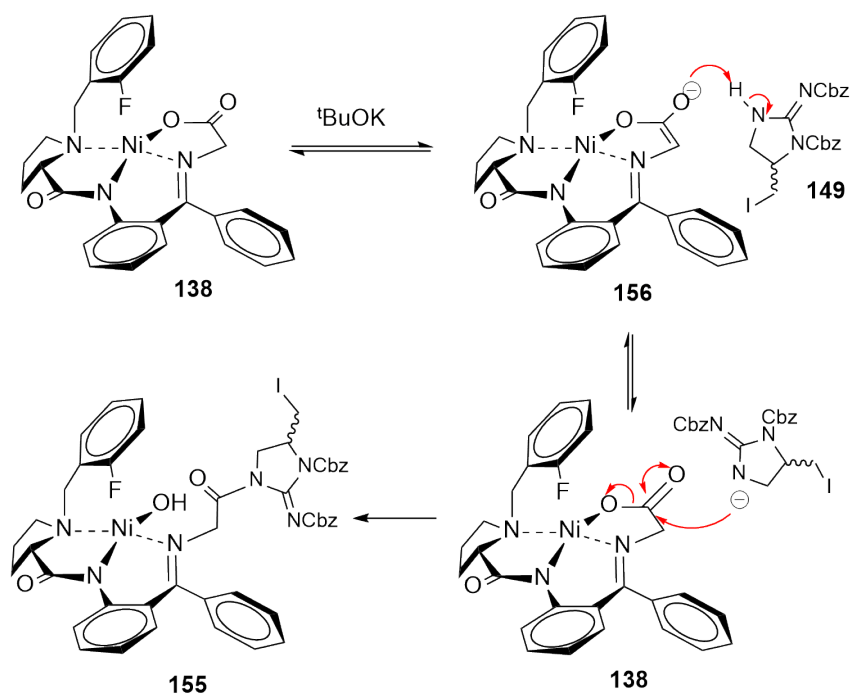
Initial asymmetric alkylation reactions with bis-protected Boc- and Cbz-derivatives of the iodoguanidine electrophile were attempted by other members of the group in unpublished work, employing similar conditions to those used successfully for complexation of 5-bromo-pentene and 8-bromo-octene for the formation of unnatural amino acids used in peptide stapling.¹⁰⁹ Alkylation of (S)-Ni-Gly-2FBPB **138** was firstly attempted with potassium *tert*-butoxide and the bis-Cbz cyclic iodoguanidine electrophile **149**, with variations in reaction temperature and timescales (Scheme 16).



Scheme 16 - Initial attempts at Ni(II) glycine complex **138** alkylation reactions with Bis-Cbz cyclic iodoguanidine electrophile **149**.

None of the reactions that were undertaken provided any determinable conversion to the desired product, but numerous side products were noted by TLC and mass spectrometry. Unfortunately due to the decomposition of the complex in silica during flash chromatography, isolation of these compounds proved difficult, and limited characterisation of these unknown entities was able to be achieved. Attempts to overcome the activation barrier by elevation of the temperature to 75 °C resulted in complete decomposition of the complex **138** to the 2-FBPB ligand **131**. Based on ESI MS data, these degraded side-products were reported as a hydrolysed form of the electrophile, and the formation of a

Ni(II) complex **155** with a molecular mass of 1008 Da. It was proposed that this 1008 Da species **155** may be a result of nucleophilic attack of the unprotected nitrogen of the guanidine **149** (Scheme 17). Whilst not strongly nucleophilic in its neutral state, deprotonation of the guanidine nitrogen by potassium *tert*-butoxide in the reaction may have resulted in the formation of a reactive anion **156**. This may also be formed following base-induced enolate formation; rather than attacking through the alkene moiety, the negatively charged oxygen may simply deprotonate the guanidine proton to induce the guanidinate anion, which subsequently attacks the carbonyl, resulting in amido-substitution onto the Ni(II) glycine complex (**155**).

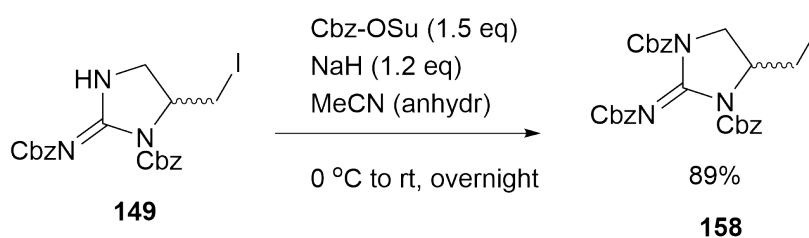


Scheme 17 – Proposed mechanism of side-product **155** formation caused by deprotonation of guanidine, resulting in nucleophilic substitution of the cyclic iodoguanidine onto the Ni(II) Gly complex **138**

In order to reduce the potential for deprotonation of the unprotected guanidine nitrogen, conditions were altered. One equivalent of KOtBu was added to the (S)-Ni-Gly-2FBPB complex **138** prior to addition of the electrophile **149** in order to allow complete consumption of the base prior to alkylation, thus eliminating any possible side reactions by the previously described mechanism. In these

reactions, whilst no degradation of the electrophile **149** were observed, no desired product was formed either.

Based on these results it was deemed essential to protect all three guanidine nitrogens prior to alkylation of Ni(II) glycine complex **138**. The bis-Cbz protected cyclic iodoguanidine **149** was reacted with benzyl *N*-succinimidyl carbonate, to yield the fully protected, tri-Cbz iodoguanidine **158** (Scheme 18).

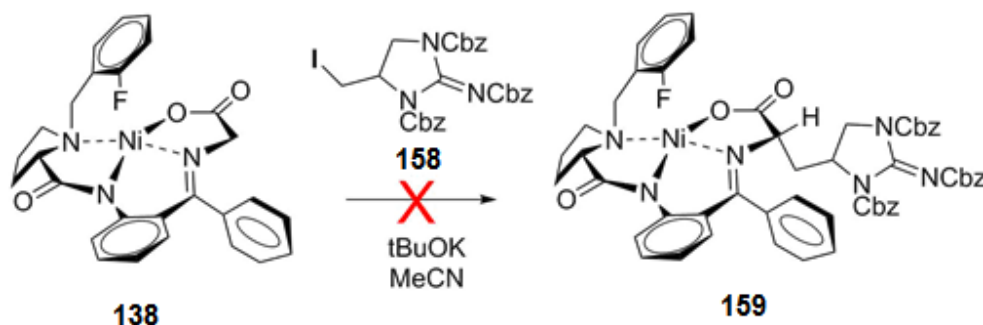


Scheme 18 — Synthesis of Tri-Cbz cyclic iodoguanidine **158** from Bis-Cbz form **149**

2.5. Reactions of (*S*)-Ni-Gly-2FBPB (**138**) with tri-Cbz protected cyclic iodoguanidine (**158**)

With the synthesis of the tri-Cbz protected cyclic iodoguanidine **158** completed, a preliminary alkylation reaction with (*S*)-Ni-Gly-2FBPB **138** was attempted. Potassium *tert*-butoxide (2 eq) was dissolved in anhydrous MeCN and cooled to 0 °C, before the Ni(II) glycine complex **138** was added. After this was stirred for 10 minutes, the electrophile **158** (3 eq) was added dropwise, and this resulting solution heated to 50 °C for 30 minutes. At this point the reaction was quenched with water, and analysed by TLC and mass spectrometry, both of which signalled the removal of electrophile **158** from the reaction. Whilst the TLC suggested some form of Ni(II) complex based-product formation (which results in the formation of a characteristic deep-red spot), a peak corresponding to that of the desired alkylated product could not be observed by mass spectrometry (Scheme 19). Given the complete guanidine protection of this electrophile, the previously

proposed nucleophilic attack of the guanidinium anion on the Ni(II) complex **138** ester to form **155** was ruled out .



Scheme 19 – Unsuccessful alkylation of (S)-Ni-Gly-2FBPB **138** using Tri-Cbz iodoguanidine electrophile **158**.

Previous work by the group had suggested the hydrolysis of the electrophile; however, in the anhydrous environment employed this should not occur. To determine whether the alkylation reactions had failed due to some other form of electrophile degradation, rather than polymerisation of the complex **138**, the tri-Cbz electrophile **158** was exposed to the same reaction conditions as previously described but in the absence of (S)-Ni-Gly-2FBPB **138**.

Under exposure to potassium *tert*-butoxide in DMF for 1.5 hours, the electrophile **158** degraded to numerous different compounds, as visualised by TLC. Analysis of the reaction solution by LCMS revealed a number of new compounds with lower molecular weights. These were determined to be the products of two separate side reactions occurring on the electrophile: the removal of carboxybenzyl protection, in addition to β -elimination of the iodide (Table 6).

Based on integration of LCMS product peaks, the major product formed under these conditions was the mono-Cbz β -eliminated electrophile **160** (from **148**). Another compound with the same m/z eluted later at 1.89 minutes, but with a considerably smaller peak; suggesting preferential retention of Cbz-protection on one particular site of the guanidine. The next two most abundant side-products were the β -eliminated forms of Bis-Cbz (**161** from **149**) and Tri-Cbz (**162** from **158**). This, in addition to a minor peak with m/z corresponding to the fully-

protected β -eliminated form retaining all three carboxybenzyl protecting groups, suggests that the β -elimination reaction occurs preferentially to the removal of the protecting groups.

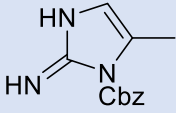
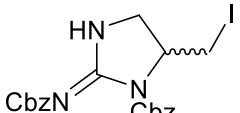
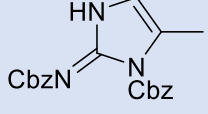
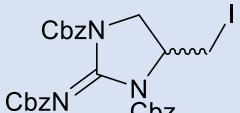
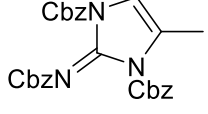
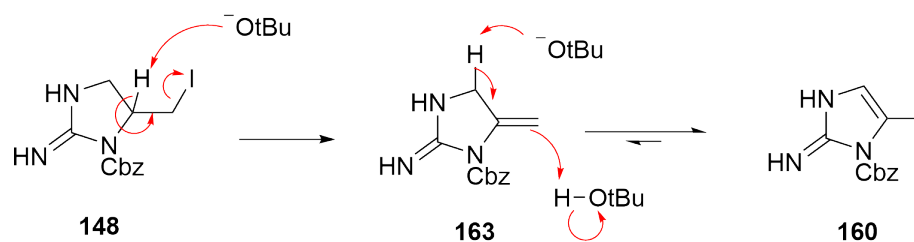
Entry	T_R	m/z	Structure	
1	1.22	232.11	Mono-Cbz, β -eliminated 160	
2	1.94	494.06	Bis-Cbz 149	
3	2.03	366.15	Bis-Cbz, β -eliminated 161	
4	2.38	545.24	nd	
5	2.43	500.18	Tri-Cbz 158	
6	2.43	628.10	Tri-Cbz β -eliminated 162	

Table 6 – Degradation products observed following exposure of tri-Cbz electrophile **158** to $KOtBu$ over 1.5 hours at room temperature, determined by ESI m/z peaks. nd = not determined, T_R = retention time in LC-MS.

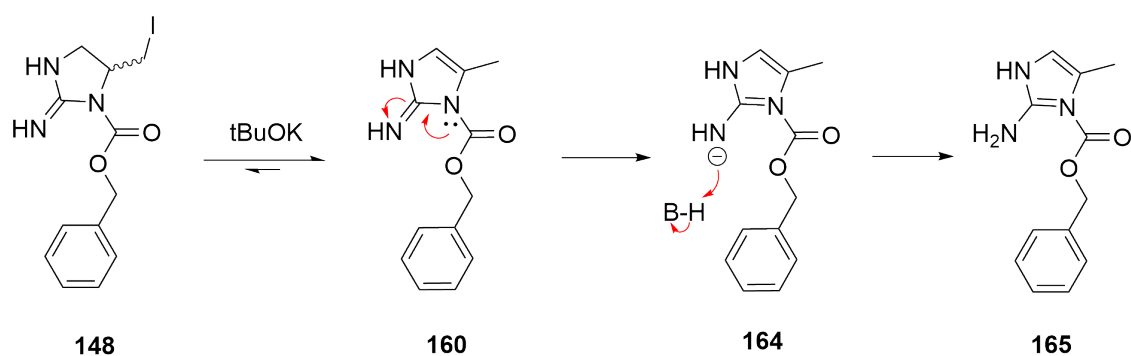
It was considered that in the strongly basic conditions employed in the complexation reactions, the cyclic guanidine electrophile **158** underwent a base-catalysed β -elimination to form a more thermodynamically stable product. The iodide is eliminated following removal of the proton on the tertiary carbon, and the resulting product is stabilised by the formation of a small conjugated system (Scheme 20). Finally, it was predicted that tautomerisation of the double bond would take place to produce the *endo*- form as the final product, based on Zaitsev's rule that the alkene exists preferentially as the form with the fewest hydrogen substituents.



Scheme 20 – Preliminary proposed mechanism of electrophile base-catalysed beta-elimination of iodide to form **163**, followed by tautomerisation to the more stable product **160**.

Potassium tert-butoxide has previously been found to catalyse anti-eliminations in dihalides under reflux¹²⁰ and at room temperature,¹²¹ but this side-reaction had not been previously observed in the complexation reactions of aliphatic alkyl bromides (5-Br-pentene and 8-Br-octene) used by the group for the formation of alkenyl amino acids.

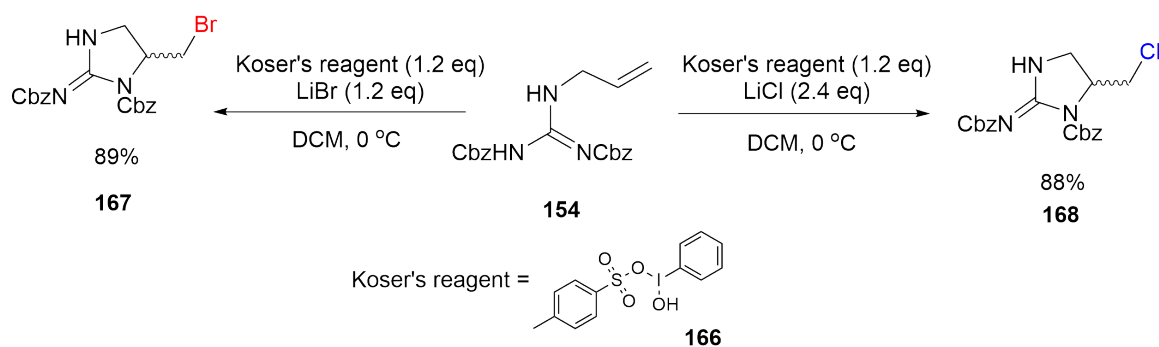
In order to isolate the unusual major byproduct with mass of 232 Da, this degradation reaction was repeated with the bis-Cbz electrophile **149**, with the aim of producing fewer products and simplifying purification. Briefly, the bis-Cbz protected electrophile **149** was dissolved in anhydrous DMF and added dropwise to a stirred solution of potassium *tert*-butoxide, before warming to room temperature and stirring for a further 1.5 hours. Following reaction quenching with water and extraction with DCM, the reaction was concentrated and analysed. TLC analysis indicated formation of similar degradation products to the previous reaction, as well as some retention of the starting material. As before, LCMS analysis showed the most abundant entity to have a m/z ratio of 232.11. This major product was purified with RP-HPLC and analysed by NMR, and was proposed to be benzyl 2-amino-5-methyl-1H-imidazole-1-carboxylate **72**, undergoing a further reaction following formation of compound **71** (Scheme 21).



Scheme 21 - Further reaction of beta-eliminated electrophile **164** yields the more stable aromatic imidazole **165**

This additional step was suggested given the considerably downshifted position of what had previously been concluded to be the alkenyl proton. The chemical shift of 6.54 ppm suggested that this proton may in fact exist on an aromatic imidazole based ring. Given this thermodynamically favourable side reaction, it is highly possible that the Ni(II) glycine complex alkylation is unable to take place prior to the base catalysed electrophile degradation, which could not be prevented by alteration of the guanidine protection strategy.

In order to prevent iodide elimination, we considered employing the synthesis of a different electrophile, containing the bromide or chloride as the halide leaving group. The synthesis of variants containing these halides has recently been reported from the same Bis-Cbz-allylguanididine **154** used in the routes to the iodo-derivatives **153** and **162** employed in these experiments (Scheme 22).¹²² In this method, the chloro- and bromo- forms of the Bis-Cbz electrophile **153** were produced using [hydroxy-(tosyloxy)iodo]benzene (Koser's reagent) **166** with the appropriate lithium halide in DCM at 0 °C, resulting in good overall yields of 88% and 89% respectively. However, these compounds would also risk the same β -elimination reaction as electrophiles **153** and **162**; and if they proved stable enough to avoid degradation, it would be unlikely for them to be substantially electrophilic to act as effective alkylating agents.



Scheme 22 - Reported synthesis of brominated and chlorinated cyclic guanidine electrophiles **167** and **168** from *N*-Allyl-*N'*,*N''*-bis-Cbz-guanidine **154** using Koser's reagent **166** undertaken by the Dodd group.¹²²

This was considered in conjunction with the undesired carboxybenzyl protecting group removal, which is usually achieved through *in situ* preparation of a Pd/C catalyst in the presence of an applied hydrogen atmosphere or with hydrogen generated with NaBH₄,¹²³ but can also be base-catalysed. We therefore deemed the most appropriate course of action to optimise the reaction conditions and attempt alkylation with a weaker base.

2.6. Alkylation of (S)-Ni-Gly-2FBPB (**138**) under optimised conditions

In order to avoid Cbz deprotection and β-elimination in subsequent alkylation reactions, the conditions were adjusted accordingly. The α-proton of the amino acid moiety of the Ni(II) glycine complex **138** has an approximate pK_a of 11, and following an initial alkylation at this position, the remaining α-proton is proposed to have a pK_a of 15.¹⁰⁹ Therefore, the use of a somewhat weaker base should not only promote the reaction by prevention of electrophile degradation, but also be unable to catalyse a second, undesired alkylation from taking place. Potassium *tert*-butoxide with a pK_{aH} of ~17 was altered to slightly less basic NaOH (pK_{aH} ~15.7) to see if this was sufficient to prevent both the β-elimination of the iodide, and also the removal of Cbz-protection. We were pleased to find that substitution of potassium *tert*-butoxide with sodium hydroxide under the same conditions resulted in neither detrimental side reaction being observed.

Whilst applying these new conditions to a reaction with (S)-Ni-Gly-2FBPB **138** did not result in product formation, the lack of side-reactions was promising and we subsequently screened conditions to try and promote alkylation of the complex (Table 7). Alkylation reactions were repeated as previously; briefly, NaOH was dissolved in anhydrous solvent and stirred at 0 °C, before addition of (S)-Ni-Gly-2FBPB **138**, with further stirring for 10 minutes to stimulate enolate formation. At this point, the tri-Cbz cyclic iodoguanidine electrophile **158** was added dropwise, and typically reactions were stirred for one hour before quenching with water and analysis by TLC and ESI MS.

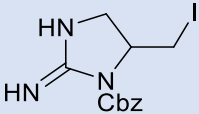
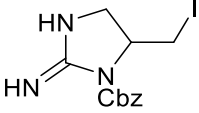
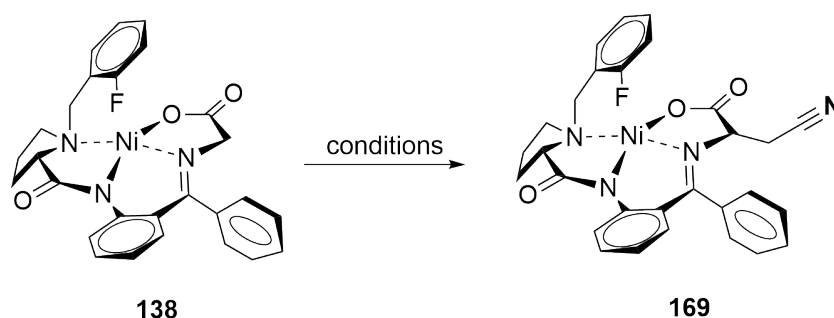
Entry	NaOH eq	Anhydrous solvent	Temperature	Product formation
1	4	DMF	rt	No reaction
2	2	DMF	rt	No reaction
3	2	DMF	50 °C	Major byproduct 148 
4	2	MeCN/DMF (1:1)	50 °C	Major byproduct 148 

Table 7 – Attempted alkylation of (S)-Ni-Gly-2FBPB **138** with varying equivalents of NaOH, solvent, and temperatures

Unfortunately, these reactions did not result in any visible alkylation, and in addition, heating of the reaction solutions to attempt to overcome the activation barrier resulted in similar unwanted degradation of the electrophile that had been previously observed, with removal of one Cbz-group resulting in the major side product **148**, and with β -elimination products also apparent (although under these conditions, some starting material was also retained). It was therefore determined that a considerably weaker base would be required to retain the integrity of the

electrophile if elevated temperatures were to be considered, which appeared to be necessary to overcome the activation barrier.

Enolate formation usually requires relatively strong base to deprotonate the proton α - to the carbonyl. In order to determine if a weaker base could be used in place of KOtBu or NaOH, complexation reactions were carried out with iodoacetonitrile, a known aliphatic, reactive, halogenated electrophile (Scheme 23).



Scheme 23 – Model alkylation of (S)-Ni-Gly-2FBPB **138** with iodoacetonitrile, to form complex **169**

As anticipated, DIPEA and triethylamine (TEA), with pK_{aH} values of 10.75 and 11 respectively, did not show any detectable conversion to the product **169** when exposed to iodoacetonitrile in DMF over an hour as previously described. We then considered if this reaction could be promoted by use of a mild co-ordinating agent to stimulate the induction of enolate formation in the Ni(II) Gly complex **138**, in a similar mechanism to that of LDA induced enolate formation. The reactions were repeated as previously with the addition of LiCl (2 eq), which was added to the Ni(II) Gly complex **138** prior to addition of base and electrophile. We were pleased to find that both TLC and mass spectra showed considerable formation of the desired product, appearing as the major peak in each spectra (Table 8).

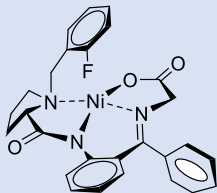
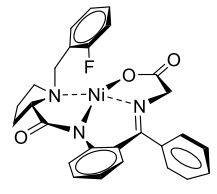
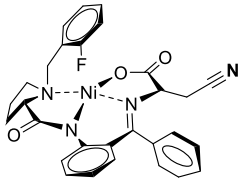
Entry	Base	Co-ordination	ESI MS (m/z)	Major product
1	DIPEA	-	$m/z = 516, 1054: M^{+H}, M^{+Na}$	138 
2	TEA	-	$m/z = 516, M^{+H}$	138 
3	DIPEA	LiCl	$m/z = 555, 577: t M^{+H}, M^{+Na}$	169 
4	TEA	LiCl	a)554, 595: t M^{+H}, M^{+K} b)1039, 1554:	a) 169  b) Undetermined polymerisation

Table 8 – Reactions of (S)-Ni-Gly-2FBPB **138** with iodoacetonitrile to form the alkylated product complex **169**

This optimised LiCl/ DIPEA reaction system was then applied to the tri-Cbz electrophile **158** with the Ni(II) Gly complex **138** (Table 9). Reactions in both DMF and MeCN did not yield any conversion to the product complex; but also did not result in any degradation of the electrophile **158** either, as indicated by both TLC

and ESI MS. LiCl appeared to have a low solubility in acetonitrile, so the reaction was repeated with excess (10 eq), with no change in results. In order to try and compromise solubility of all reagents involved, Ni(II) Gly complex **138** and LiCl were dissolved in DMF initially, with the electrophile dissolved in MeCN prior to addition. This time TLC indicated the consumption of (S)-Ni-Gly-2FBPB **138**, and revealed the formation of some new form of Ni(II) based complex with a lower polarity than that of the starting material, which could be determined by the characteristic red spot typical of Ni(II) complexes. ESI MS analysis indicated the presence of a major product with m/z of 1262. This peak had an ionisation pattern indicating at +1 charge, but a possible structure could not be identified. Similarly, in the reaction 5 where the solvent was replaced with THF to try and further improve solubility, multiple new complexes were formed, as visualised by TLC. Unlike the previous reaction, three complexes appeared to have formed with higher polarities and lower R_f values. Major m/z in the ESI spectrum were 1262, 1128, 1035, and 666, the latter being the $(M+K)^+$ of the unreacted tri-Cbz electrophile **158**, which also appeared to be intact by TLC.

Entry	Base	LiCl eq	Solvent	ESI MS / TLC
1	DIPEA (4 eq)	2	DMF	Starting materials only (138 , 158)
2	DIPEA (4 eq)	2	MeCN	Starting materials only (138 , 158)
3	DIPEA (4 eq)	10	MeCN	Starting materials only (138 , 158)
4	DIPEA (4 eq)	10	DMF/ MeCN	Undetermined complexes $m/z = 1262, 1150, 1039$ TriCbz electrophile 158 $m/z = 666 (M^{+K})$
5	DIPEA (4 eq)	10	THF	Undetermined complexes $m/z = 1262, 1128, 1035, 993$ TriCbz electrophile 158 $m/z = 666 (M^{+K})$

Table 9 - Reactions of (S)-Ni-Gly-2FBPB **138** with tri-Cbz cyclic iodoguanidine **158** resulting in no alkylation or undetermined complex formation.

A number of possible side reactions were considered when trying to determine the character of these complexes. We proposed that dimerisation/ trimerisation of the complex **138** could be taking place, with the formed enolate **156** substituting onto the carbonyl of another molecule; however this seemed unlikely given the substantial steric bulk involved in more than complex reaction with another.

In previous experiments the deprotonation of a free guanidine nitrogen was considered, and given the Cbz removal that was observed, this would also be possible where the Tri-Cbz protected form **158** was used. However, in the LiCl/ DIPEA reactions absolutely no degradation of this electrophile could be observed, indicating that the undesired side reactions were not a result of the guanidine acting as a nucleophile.

It was possible that some β -elimination was still occurring, given that this side-reaction is still possible even with three protecting groups. However, particularly given the high level of stability gained by the formation of an aromatic in compound **160**, it does not appear to be vulnerable to nucleophilic attack by the enolate.

At this point we determined that the complexation would not be possible with the tri-Cbz electrophile **158**, but given the reduced basicity and increased stability of the electrophile, some success could be possible with less-substituted forms.

2.7 Complexation of less substituted electrophiles in optimised conditions

Although reactions with the Bis- and mono-Cbz (**149** and **148**) and Boc electrophiles had been previously attempted unsuccessfully by other members of the research group in unpublished work, and despite the fact these partially unprotected cyclic guanidines **148** and **149** give rise to a higher risk of side reactions due to the presence of a free (albeit weak) nucleophilic site, these reactions were attempted with the optimised DIPEA/LiCl conditions (Table 10).

Despite the significant issues with side reactions, final reactions were carried out with a bis-Cbz and mono-Cbz cyclic iodoguanidines **149** and **148** to determine if issues with alkylation could be overcome by a reduction in steric hindrance and removal of side-reaction (Cbz deprotection) sites. However, with these compounds too, no alkylation was detectable.

Entry	Electrophile	Reaction conditions	Major products
1	Bis-Cbz 149 (3 eq)	LiCl (2 eq), DIPEA (4 eq), DMF/MeCN	Unknown complex, $m/z = 994, 1010$ ([M+Na] ⁺ , [M+K] ⁺) Electrophile 149
2	Mono-Cbz 148 (3 eq)	LiCl (2 eq), DIPEA (4 eq), DMF/MeCN	Unknown complex, $m/z = 860, 882$ (M+H ⁺ , M+Na ⁺) Electrophile 148

Table 10 – Attempted alkylation of (S)-Ni-Gly-2FBPB **138** with bis-Cbz and mono-Cbz cyclic iodoguanidines **149** and **148** under optimised conditions, resulting in undetermined complex formation but no detectable electrophile degradation by ESI MS.

Similarly to the reaction with tri-Cbz electrophile **158** new complexes were formed that did not match the molecular weight of the desired product. Given that the major m/z peaks get smaller as less protected electrophiles **148** and **149** are employed, and that these new products appear as red spots on TLC, it appears there is some form of reaction between the Ni(II) glycine complex **138** and the electrophile, rather than polymerisation of one of the species with itself. However, the products of these unwanted side reactions could not be determined, and ultimately the cyclic iodoguanidine in any protected or unprotected form was deemed incompatible with this method of asymmetric amino acid synthesis.

2.8 Conclusions

This chapter aimed to develop a novel route towards the total synthesis of teixobactin, with particular attention paid to the unproteinogenic amino acid L-*allo*-enduracididine **43**. Prior to the commencement of this research, the most stereoselective and scalable synthesis had been reported by Craig *et al.*, forming the unprotected form of this residue over 10 steps, with 31% yield and with 50:1 diastereoselectivity.¹⁰⁰ We sought to use a Nickel (II) Schiff base complex **138** that had previously been synthesised in house to provide a novel route to the *N*-Fmoc-protected, Cbz- or Boc-side chain protected form of the amino acid. A number of different electrophilic compounds were designed and synthesised

based on a previously published route, and reactions attempted with the Ni(II) Schiff base complex **138**. Unfortunately none of these yielded the desired complexed form of the amino acid, and so this method was discontinued. The results suggested that these reactions failed based on two major factors; firstly the large steric bulk of the electrophiles employed, particularly with mono- and bis Boc- and Cbz- protection of the guanidine functionality. Secondly, these electrophiles were found to be unstable in the strong basic conditions required from complexation; resulting in β -elimination to a more stable conjugated product when exposed to base. Aside from this, the conditions resulted in the removal of the guanidine side chain protection. Therefore, the Ni(II) Schiff base method may not be suitable for similar cyclic electrophiles; and is likely more suited to linear, aliphatic substrates which do not contain nucleophilic functionalities requiring orthogonal protection. However, where sensitive electrophiles are required, the use of a weaker base such as DIPEA in combination with LiCl may result in improved levels of product formation.

3. Synthesis of teixobactin analogues using on-resin cyclisation

3.1 Introduction

Interest in cyclic peptides has grown particularly over recent years. Compared to their linear counterparts, macrocyclic peptides offer a number of advantages. They usually display heightened resistance to exo- and endoproteases, making them attractive as stable therapeutics.¹²⁴ Unlike flexible linear peptides, which usually require some form of stapling to interact with large target molecules, the increased rigidity of macrocycles can make them effective binders of typically difficult targets, such as protein-protein interactions, and are often used to mimic surface-based loops. Cyclic peptides can be prepared in four different ways: head-to-tail, head-to-side-chain, tail-to-side-chain or side-chain-to-side-chain (Figure 34). The method selected is usually highly depending on the amino acid sequence of the peptide.

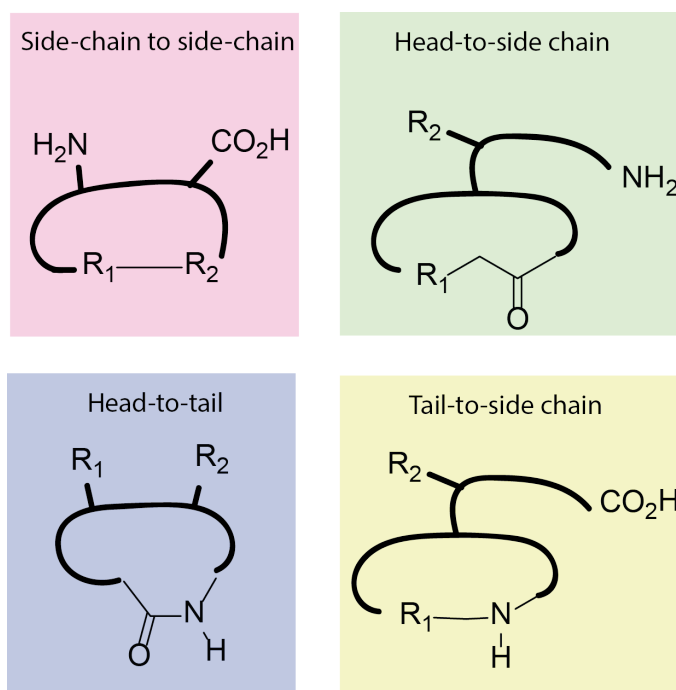


Figure 34 - Four methods of peptide macrocyclisation; employing one or both terminus, or up to two reactive side chains

These peptide cyclisation reactions are usually completed via the formation of an amide (lactamisation), ester (lactonisation) or disulfide bridge, and are typically required to be performed in solution. Solution-phase cyclisations usually require high dilutions of reagents to promote intramolecular reactions and prevent oligomerisation and other side reactions from occurring. Favourable results have been found when using a dual syringe pump system to simultaneously add linear peptide and coupling reagent to a stirred solution of DIPEA in DMF.¹²⁵

However, in many cases cyclisations have proved notoriously difficult to complete, particularly in constrained rings of 13-members or less. A number of novel methods to promote conversion to the cyclic product have been developed in recent years. Pseudoprolines are unnatural heterocyclic amino acids derived from serine, threonine and cysteine, bearing gem-dimethyl substituents (Ψ Me, Mepro), originally introduced to prevent aggregation and improve yields in SPPS. These turn-inducers have been shown to aid cyclisation through conformational constraint.¹²⁶ Macrocyclisation can also be promoted through the use of metal ion scaffolds. This has been demonstrated by Ag⁺ ions co-ordinating to a C-terminal thioester and N-terminal amine, entropically activating the linear peptide to catalyse amide bond formation.¹²⁷ The metal-mediated synthesis of 12- to 18- membered cyclic tetrapeptides has been achieved using dipeptide ester precursors.¹²⁸ In the presence of NaOMe, these form dianionic complexes with various metal anions such as Ni(II) and Pd(II), which yield the cyclic product upon decomplexation. Hydrocarbon “stapling” is a popular method in peptide chemistry of inducing secondary structure in an otherwise randomly coiled peptide through the formation of an unsaturated bond between two unnatural amino acid residue side chain, typically *i*, *i*+3, with ring closing metathesis between two alkenes accomplished by ruthenium-based catalysts. This method has then been applied to promote macrocyclisation, using the alkene bridge to constrain the peptide in a way that brings the two reactive entities within a smaller space, in the synthesis of the antimalarial peptide mahafacyclin B.¹²⁹

Reactive functional groups can be used to achieve macrocyclisation within peptides, rather than the use of a template or structural constraint. “Click” chemistry has become increasingly popular in peptide synthesis, with 1,3-dipolar cycloadditions between amino acids bearing azide- and alkyne groups to form

triazoles.¹³⁰ A 1,4-disubstituted triazole has also been developed by using a Copper(I) catalyst.¹³¹ This can be achieved through unnatural amino acids bearing these functional groups on their side chains; or through derivatised C- and N-terminus. This has been found to have the added benefit of increasing conformation rigidity, which has been found to be favourable in binding to targets, particularly proteins.

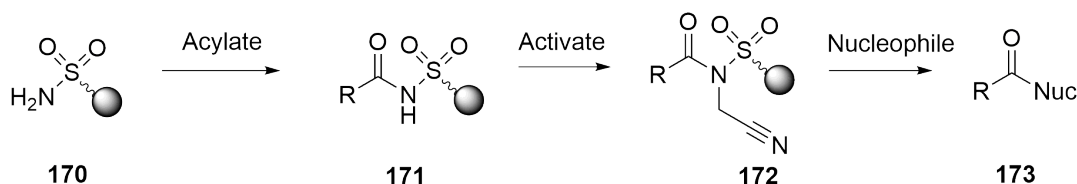
Cyclisation on a solid support can be advantageous over solution-based approaches. Intramolecular reaction on resin are subject to a pseudodilution effect, leading to reduced rates of intermolecular reactions and oligomerisation. This enables reactions to be performed with excess reagents, at high concentrations, thus increasing the rate and yield of the reaction. Purification is achieved simply through the washing of the solid support, rather than by chromatographic means.

Drawing inspiration from naturally occurring cyclic peptides produced non-ribosomally by bacteria, isolated thioesterases domains have been used to catalyse macrocyclisation of linear peptides on-resin.¹³² Thioesterases are activated by transacylation to an active-site serine, which is then vulnerable to substitution by a nucleophilic amino acid side-chain, or the amine N-terminus.

A synthesis of the cyclic depsipeptide sansavamide A, a natural product isolated from a marine fungus that displays high cancer cell cytotoxicity with an average IC₅₀ value of 27 µg/ mL against a panel of 60 cell-lines, was developed using a solid support with a side chain tethered phenylalanine residue, with Boc-protection on the amine and a methyl ester C-terminus.¹³³ Using this method, the natural product was produced in 67% yield over 10 steps. The phenylalanine derived linker allows the N-terminus residues and C-terminus residues to be coupled independently; and allows derivatisation and/or orthogonal protection strategies at both the C- terminus and N-terminus, facilitating cyclisation. Cyclisation achieved with standard coupling reagents (HBTU, DIPEA in NMP) over 16 hr at room temperature. As the peptide is still on resin at the point of cyclisation, the reaction can be performed without dilute conditions and without the risk of polymer by-product formation. The final cyclised depsipeptide can be gained by cleavage from the resin and linker with 50% TFA in DCM over 36

hours. Limited by the fact the C-terminus side must be coupled as a peptide, N-terminus can be coupled as usual with individual Fmoc-protected amino acids. A similar method has been employed, using histidine as the resin-bound amino acid residue.¹³⁴

The safety-catch principle described the use of the resin-linker that would remain unreactive throughout the standard acidic and basic conditions involved in solid phase peptide synthesis, before undergoing cleavage when submitted to mild conditions as a result of some form of chemical activation. The original “safety-catch” resin was designed by Kenner in 1971,¹³⁵ and applied an acylsulfonamide-linked resin for the attachment of the first amino acid.¹³⁵ Following peptide synthesis, the acylsulfonamide linker was labilised by *N*-methylation with diazomethane. The linear peptide could then be derivatised at the C-terminus dependent on the selection of cleavage conditions used; these included saponification to yield a carboxylic acid, aminolysis to yield a C-terminal amide and hydrazinolysis for hydrazine derivatives (Scheme 24).



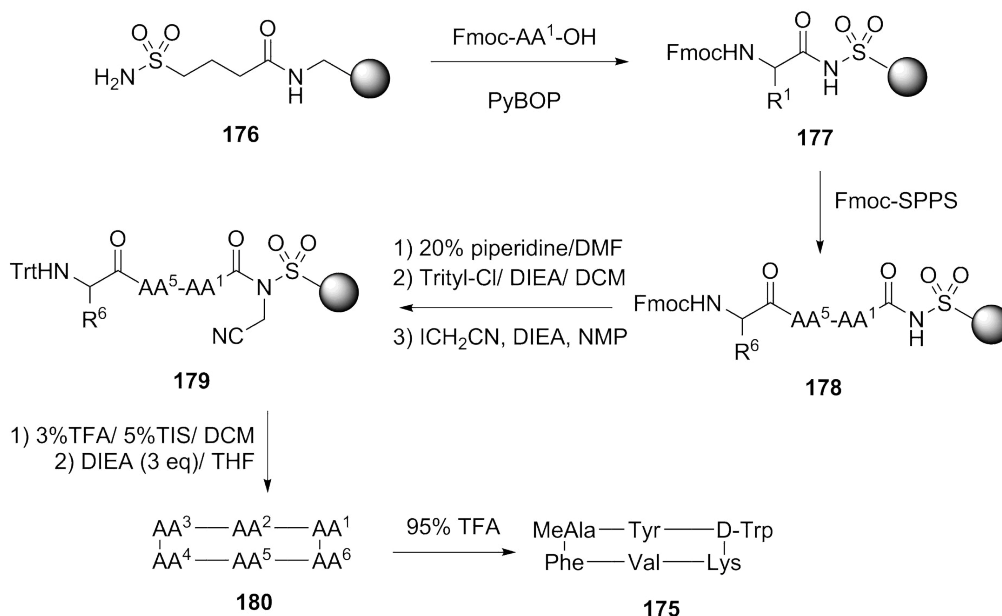
Scheme 24 – Mechanism of safety-catch resin. Resin-bound sulfonamide **170** is acylated with amino acid or peptide to form **171**. Once linear sequence is complete, sulfonamide is activated by alkylation (**172**) before displacement of the linker and solid-support by a nucleophile (**173**).

This idea was optimised by Backes and Ellman in 1999, who addressed some of the major issues with Kenner’s method, particularly the poor loading efficiency, high levels of racemisation during loading of the initial amino acid residue and the poor reactivity of the supposedly labile activated linker.¹³⁶ To probe the most effective loading strategy, numerous coupling agents, bases and solvents were examined; the most effective was determined to a double coupling of Boc-protected amino acid (5 eq), PyBOP (5 eq), *i*-Pr₂EtN (10 eq) in DCM at -20 °C, which gave a 90% yield with less than 0.5% racemisation to the D-isomer when

performed with Boc-Phe-OH **174**. The yield was not reported for these exact conditions at room temperature; but similar experiments in different solvents generally resulted in much poorer yields (DMF, less than 30% for THF, less than 50%), as well as reactions employing the use of additives HOBt and HOAt in DMF (both <10% yield respectively). Activation of the linker had previously been optimised by conversion of the arenesulfonamide to a more nucleophilic alkanesulfonamide functionality (pK_a 16 and 17.5 respectively), providing higher levels of *N*-alkylation, which was improved by using haloacetonitriles as activation agents.¹³⁷ Cleavage efficiencies from iodoacetonitrile activated sulfonamides were examined with amines and amino acid methyl esters, and amino acid coumarins.

Since its inception and optimisation, safety-catch sulfonamide-linked resins have been employed in the synthesis of fully protected methyl thioesters as protease substrate mimics,¹³⁸ C-terminal benzyl thioester for use in a selenosulfide ligation reaction,¹³⁹ and glycosylated peptides for the study of carbohydrate-lectin interactions.¹⁴⁰ The linker has also been reversed in order to yield C-terminus *N*-alkyl sulfonamide peptides upon cleavage from the resin.¹⁴¹

Aside from linear C-terminal derivatised peptides, sulfonamide safety catch resins have been involved in on-resin cyclisations. The first described example of this was the synthesis of a cyclic peptide MK-678 **175** (Scheme 25).¹⁴² After loading of the first amino acid to the sulfonamide linker **176**, standard Fmoc-SPPS conditions were used to create the linear sequence on resin (**178**). Following trityl protection of the N-terminus, the *N*-alkylation and activation was achieved with iodoacetonitrile and DIPEA in NMP to form **179**. The trityl protection was subsequently removed, yielding the free N-terminus to act as a nucleophile and displace the labilised linker, thus forming the macrocycle **180**. Treatment with TFA yielded the final cyclic hexapeptide **175** in 52% yield and 79% purity (Scheme 25).

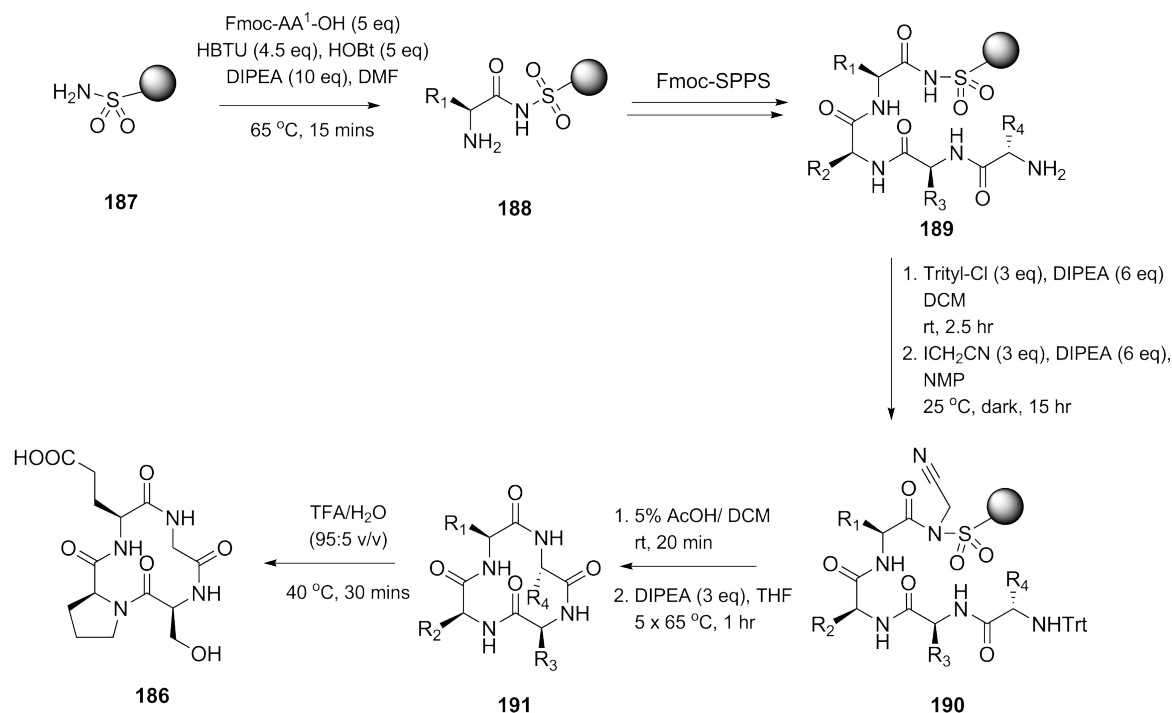


Scheme 25 – Synthesis of the cyclic peptide MK-678 **175** on a sulfonamide-linked safety-catch resin **176**.¹⁴²

The authors attempted the five other syntheses of the same peptide by changing the point at which the macrocyclisation occurred and by altering the linear sequence. The four successful experiments gave crude yields of 17-42%, with purities ranging from 44% to 74%. When the cyclisation was attempted from the linear sequence *N*MeAla-Tyr(*t*Bu)-D-Trp(Boc)-Lys(Boc)-Val-Phe-Resin **181**, however, the reaction was unsuccessful and gave no conversion to the cyclic product. This is interesting given that the methylated amine N-terminus should have been more reactive than the primary amine form in the other 5 experiments; however the increase in steric hindrance caused by the secondary amine may explain why this reaction did not work.

In terms of cyclic peptides, on-resin cyclisation using the safety-catch method has been used successfully in the synthesis of Integerrimide A **182**, a cyclic heptapeptide;¹⁴³ and the antimicrobial peptide Polymyxin B **183**, which contains a hexapeptide macrocycle core.¹⁴⁴ The syntheses of Tyrocidine A **184**, a cyclic decapeptide,¹⁴⁵ and a structurally related analogue with a glutamine to arginine mutation **185**¹⁴⁶ have also been achieved using this route. On-resin head-to-tail cyclisations are less commonly reported for peptides smaller than five residues

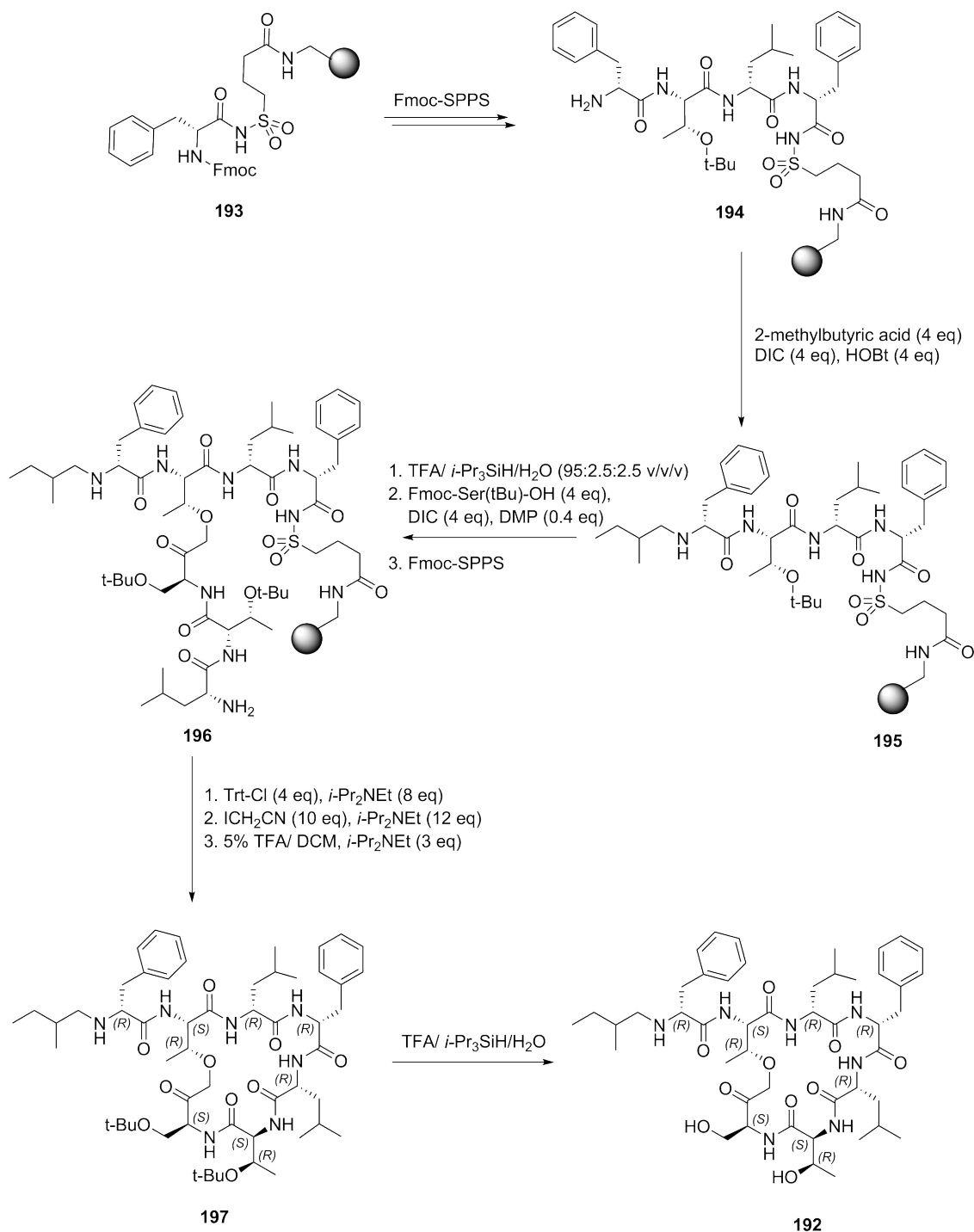
in size, but the sulfonamide resin has been successfully employed in the synthesis of 12-membered tetrapeptides with highly strained ring systems, such as the marine antimicrobial cyclic tetrapeptide Cyclo(GSPE) **186**, giving better yields in comparison to solution-based approaches using the same linear sequence under similar conditions (Scheme 26).¹⁴⁷



Scheme 26 - Synthesis of the 12-membered cyclic AMP Cyclo(GSPE) **186** using a sulfonamide safety-catch resin **187**.¹⁴⁷

One of the few cyclic depsipeptides to have been synthesised using the on-resin safety-catch approach is Kahalalide A **192**, isolated from a marine mollusc, with activity against Gram positive bacteria such as *M. tuberculosis*.¹⁴⁸ The synthesis employed the use of sulfonamide resin in a similar route to that of other reported peptides (Scheme 27). After coupling of the first four amino acid residues (**194**), the *N*-terminus was capped using 2-methylbutyric acid to form **195**, thus allowing selective depsipeptide formation between a threonine hydroxyl and the carboxylic acid of Fmoc-Ser(tBu)-OH, which was achieved using DIC and DMAP in THF, repeating the reaction in order to gain complete conversion to the ester

196. Following the remaining peptide extension, replacement of *N*-terminus protection from Fmoc to trityl, and linker activation with iodoacetonitrile, the cyclisation was performed in DCM with TFA and *i*-Pr₂NEt to give the crude product in 15-20% yield.



Scheme 27 – Synthesis of the antibacterial cyclic depsipeptide Kahalalide A **192** using sulfonamide-linked safety-catch resin.¹⁴⁸

Although the yield was fairly low, the overall crude purity of the peptide following cleavage and cyclisation was high (>90%), without significant peptide-based side products and impurities. This route was not optimised any further, but it was used to produce three more Kahalalide A analogues with lipid variations. Where the 2-methylbutyric acid was replaced with an acetyl cap, the compound lost all antibiotic activity against *Mycobacterium tuberculosis*. However, replacement with a longer hexanoyl functionality resulted in an improved MIC value from 64 µg/ mL to 32 µg/ mL.

Based on this previous work we proposed that a sulfonamide linked solid support could be used in order to achieve the on-resin cyclisation of teixobactin and related analogues, as an alternative to solution-phase cyclisation based approaches.

3.2 Aims of the chapter

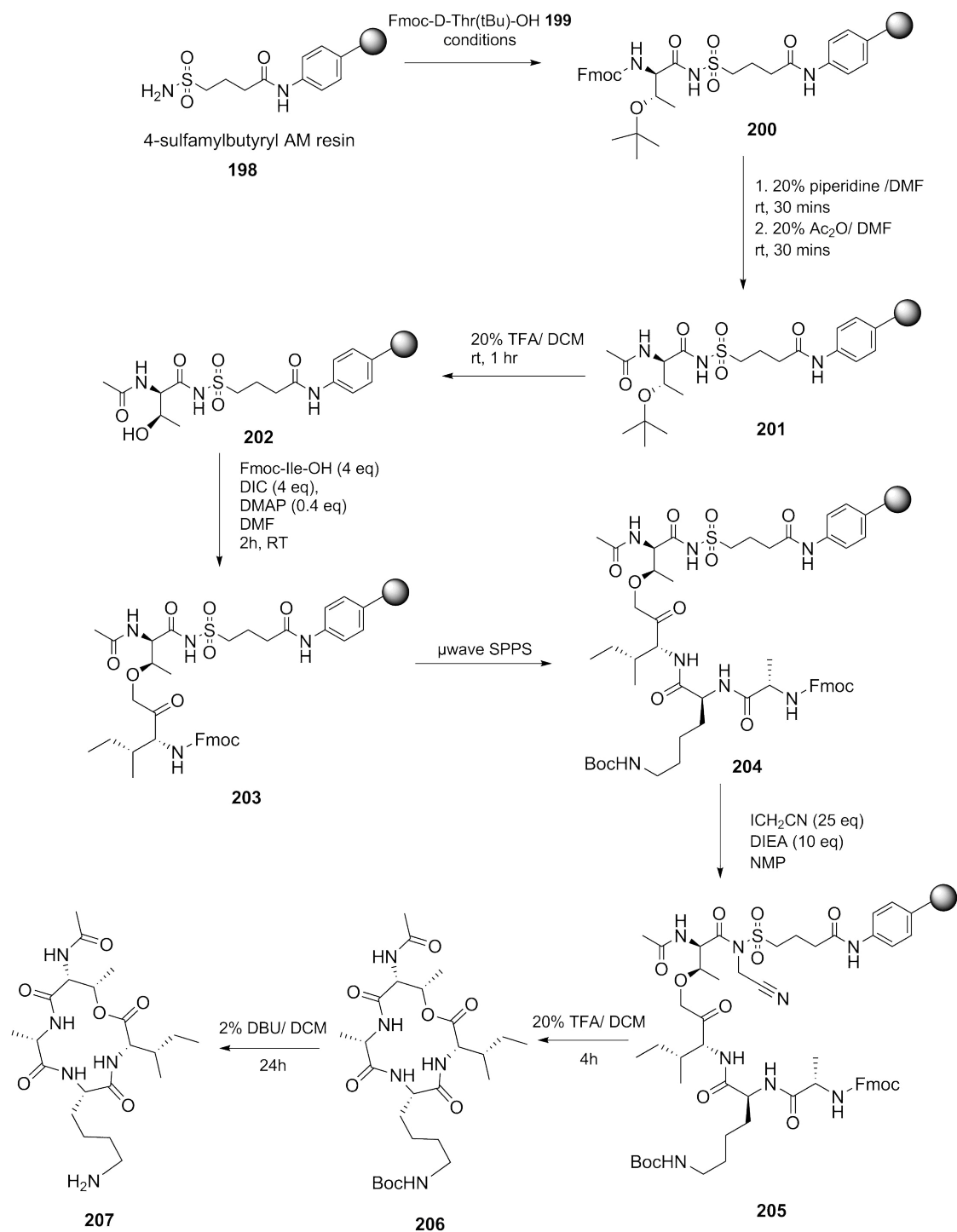
This chapter details the design of a synthetic route to teixobactin analogues using a “safety-catch” resin. These resins allow for cleavage from the resin and cyclisation to take place simultaneously and can offer a number of advantages over solution-based methods, particularly due to the pseudo-dilution effect allowing higher concentrations of reagents used in excess. Compared to previously published teixobactin **42** analogue syntheses, this would provide a novel route towards the antibiotic. By avoiding the use of an acid-labile resin, the use of a sulfonamide-linked solid support which is cleaved under different conditions also permitted a route to previously inaccessible analogues; containing highly acid-labile side chain protecting groups by which the standard cleavage conditions would promote the potential for side reactions.

The character of the safety-catch resin compatible with the synthesis was determined; and the difficult loading procedure optimised by screening different conditions and elucidating a potential reaction mechanism of the sulfonamide moiety with solid-phase synthesis based coupling reagents.

A number of different synthetic routes were designed employing the safety catch linker in order to produce a number of teixobactin **42** analogues and optimise the method to increase the final yield.

3.3 Loading of safety-catch resins

A synthetic route towards analogues of teixobactin **42** was designed using 4-sulfamylbutyryl resin **198** as the solid support (Scheme 28). This method coupled Fmoc-D-Thr(*t*Bu)-OH **199** as the first amino acid residue, before capping of the N-terminus by acetylation to form **201**. As this resin is stable until activated by a haloacetonitrile, 20% TFA is used to remove the *tert*-butyl protecting group and achieve depsipeptide bond formation using Steglich conditions (Fmoc-Ile-OH, DIC and catalytic DMAP in DMF), as previously described for Kahalalide A, to form **203**. The remaining two residues, including an *L-allo*-enduracididine variation for both analogues to create a model system for optimisation, could then be coupled by manual or microwave assisted peptide synthesis. Whilst most groups replace N-terminus Fmoc protection with a trityl group prior to activation, we wanted to determine if this was completely necessary, and so aimed to perform the iodoacetonitrile activation prior to N-terminus deprotection, to form **205**. With the sulfonamide activated, the use of non-nucleophilic base DBU was selected to simultaneously remove the final Fmoc-protection; induce cyclisation via the primary amine of the terminal alanine residue to form the 13 membered macrocycle **206**; and at the same time to cleave the peptide into solution; at which point all final side chain protecting groups could be removed to yield the final analogue structure **207**.



Scheme 28 - Initial synthesis design for cyclic Ac-tAKI **207**, using 4-sulfamylbutyryl resin **198**, with branching to form the depsipeptide bond and intermediate **203**, before continued Fmoc-SPPS and linker activation with iodoacetonitrile yielded **205** on resin.

The seminal studies by Backes and Ellman¹³⁶ and Kenner¹³⁵ each described a difficult initial loading, often resulting in high levels of racemisation. Therefore, in order to optimise the proposed synthetic route, the reaction of the sulfonamide

linker with the first amino acid to be coupled was probed initially in order to access greater yields further down the synthetic route (Table 11).

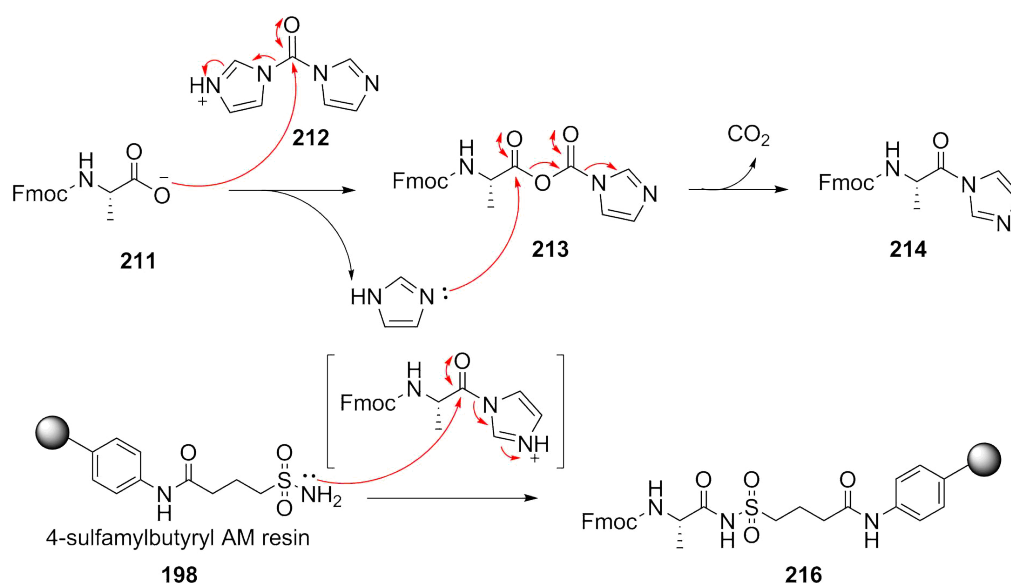
Entry	Fmoc-X loaded	Conditions	Temp (°C)	Loading (mmol/g)
1	D-Thr(Trt) 208	DIC (3 eq), 1-Melm (3 eq), DCM/DMF (4:1), 18 hr	rt	0.14, 0.17
2	D-Thr(Trt) 208	PyBOP (3 eq), DIPEA (5 eq), dry DCM, 8.5 hr	-20	0.20
3	D-Thr(Trt) 208	PyBOP (3 eq), DIPEA (5 eq), dry DCM, 8.5 hr	75	nl
4	D-Thr(Trt) 208	DIC (3 eq), 1-Melm (3 eq), HOBt (3 eq) DCM/DMF (4:1), 18 hr	rt	nl
5	L-Ala 209	PyBOP (3 eq), DIPEA (5 eq), CHCl ₃ , 8 hr	-20	0.50
6	D-Thr(Trt) 208	PyBOP (3 eq), DIPEA (5 eq), CHCl ₃ , 8 hr	-20	0.41
7	L-Thr(tBu) 210	DIC (3 eq), 1-Melm (3 eq), DCM/DMF (4:1), 18 hr	rt	0.50, 0.51
8	D-Thr(tBu) 198	DIC (3 eq), 1-Melm (3 eq), DCM/DMF (4:1), 18 hr	rt	0.45
9	D-Thr(Trt) 208	DIC (4 eq), 1-Melm (4 eq), DCM/DMF (4:1), 18 hr	rt	0.46

Table 11 – Conditions screened for 4-sulfamylbutyryl resin **80** loading, with Fmoc-amino acid coupled; reaction conditions, and loading (resin supplied as 0.73 mmol/g).

Loading of 4-sulfamylbutyl resin **198** was initially undertaken using two methods commonly employed in previous synthesis, with Fmoc-D-Thr(Trt)-OH **208** as the residue being coupled. Loading was determined by UV/Vis absorption of Fmoc-piperidine adduct on deprotection. DIC (3 eq), 1-methylimidazole (1-Melm, 3 eq) in DCM/DMF (4:1) overnight at room temperature resulted in a fairly poor loading of 0.14 and 0.17 mmol/ g (19% and 23% respectively). Similarly, the addition of HOBt to the DIC/1-Melm reaction solution resulted in a total loss of loading. The cold PyBOP reaction conditions were applied to a reaction with Fmoc-Ala-OH

209 instead, to see if the steric bulk of the threonine trityl protection could be influencing the poor yields, and a much greater loading of 0.50mmol/ g (68%) was achieved; suggesting the use of a less bulky orthogonal protection at this point may be essential. As this reaction was performed in chloroform rather than DCM, the conditions were repeated exactly using Fmoc-D-Thr(Trt)-OH **208**; which this time gave a much higher loading of 0.41 mmol/ g, suggesting that chloroform should be used with these reagents for maximal yields. The use of DIC/1-Melm conditions was investigated using a smaller *tert*-butyl threonine protection (**210**, **198**), which gave much higher percent conversion than for the same trityl protected amino acid. Finally, the coupling of trityl-protected threonine was improved by increasing the number of equivalents of both DIC and 1-Melm.

It was intriguing that standard methods used to increase reaction rates (temperature elevation, supplementation with reactive additive) resulted in a total lack of conversion to the Fmoc-amino acid coupled linker. Particularly, these unreactive solutions all contained a uranium based coupling agent. This is likely to be due to the fact that during the reaction with the Fmoc-protected amino acid, the HOBt ester formed is not active enough to be displaced by the sulfonamide nitrogen of the resin. This may explain why more reactive carbodiimides give at least some conversion to the product; except when spiked with HOBt, which reacts with the intermediate much faster than the sulfonamide is able to (Scheme 29).



Scheme 29 - Mechanism of carbodiimide (CDI) **212** based loading of 4-sulfamylbutyryl resin **198** with the reactive intermediate **214** formed.

The results from this loading screen elucidated effective protocols for both Fmoc-D-Thr(tBu)-OH **199** and Fmoc-D-Thr(Trt)-OH **208** which were then taken forward and applied to the rest of the synthetic route.

3.4 Initial synthesis of teixobactin macrocycle analogues

The preliminary method previously discussed was used to synthesise two cyclic tetrapeptides based on the macrocycle of teixobactin: cyclic Ac-thr-Ala-Lys-Ile (DLLL) **207** and cyclic Ac-Thr-Ala-Lys-Ile (LLLL) **217** (Figure 35).

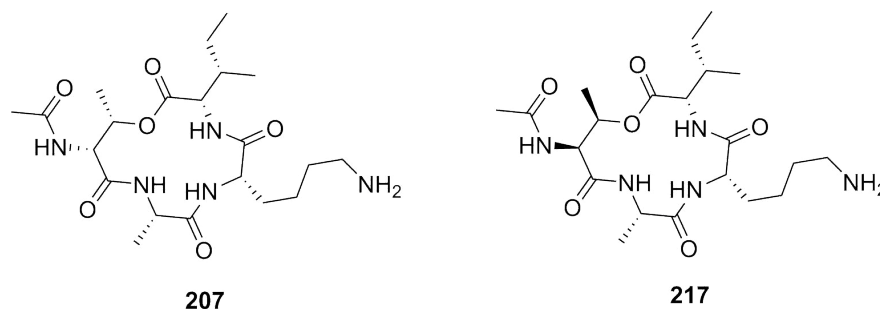
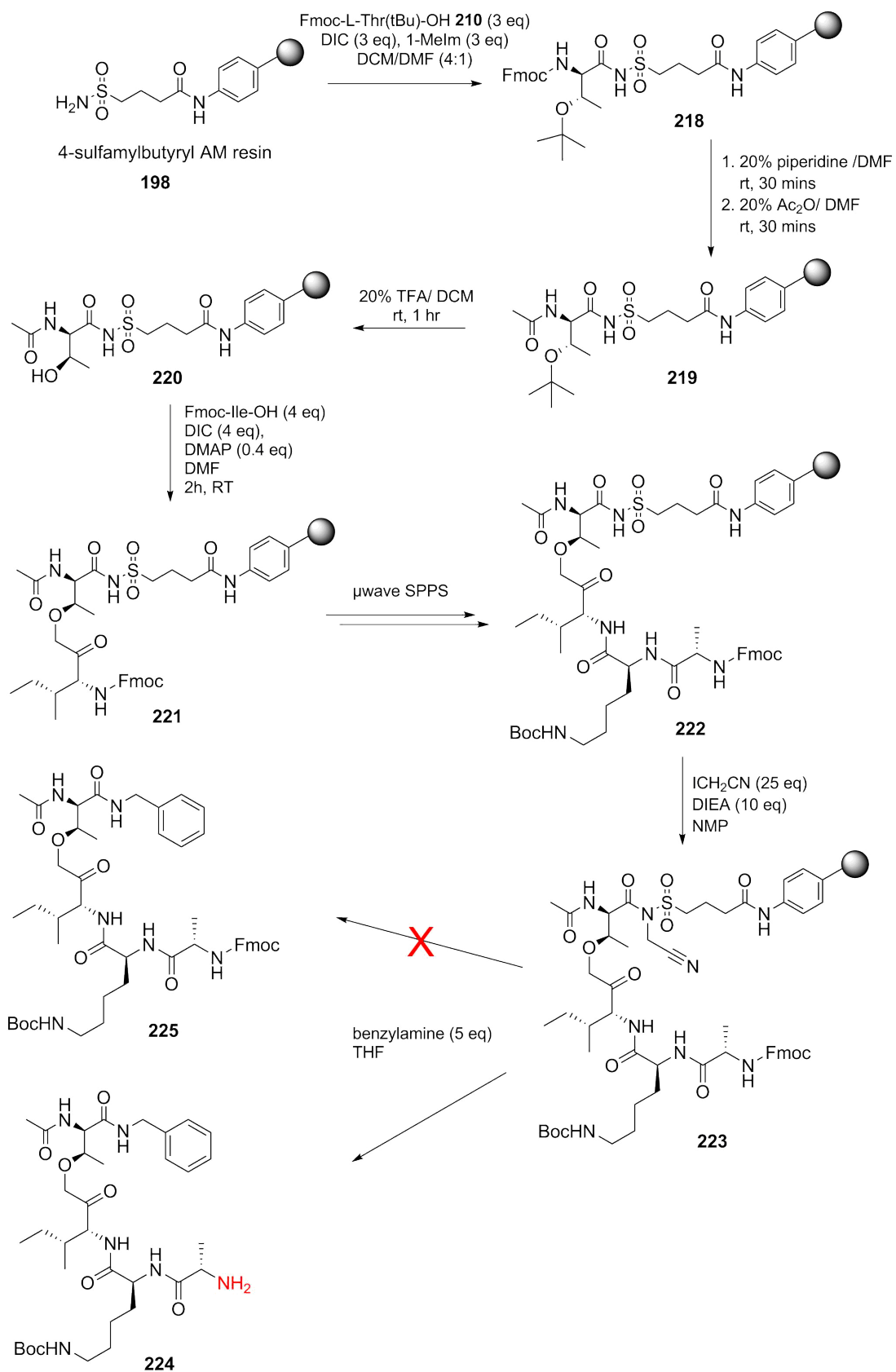


Figure 35 - Structures of cyclic tetrapeptides based on teixobactin **42** macrocycle: Ac-t(IK)A (DLLL, **207**) and Ac-T(IK)A (LLLL, **217**)

Initially the all L-isomer **217** was synthesised (Scheme 31). Good loading was achieved using one of the optimised procedures; before Fmoc-L-Thr(tBu) **210** was coupled, Fmoc-deprotected and acetyl capped at the N-terminus (**219**). The free threonine hydroxyl was exposed with 20% TFA/DCM, which then underwent an esterification with Fmoc-Ile-OH, DIC and DMAP in DMF to form **221**. As a sample of this resin could not be cleaved with acid to examine the percent conversion by mass spectrometry, this was determined spectroscopically by determining the level of piperidine adduct formation in the same way as for the initial loading, which revealed complete formation of the depsipeptide bond. After microwave synthesis to couple Fmoc-Lys(Boc)-OH and Fmoc-Ala-OH, the sulfonamide linker was activated with ICH₂CN (25 eq) and DIPEA (10 eq) in NMP to form **223**. To examine the character of the resin-bound peptide prior to attempting Fmoc removal and simultaneous cyclisation, a small quantity was reacted with benzylamine to yield the crude linear C-terminal derivatised product **225**.

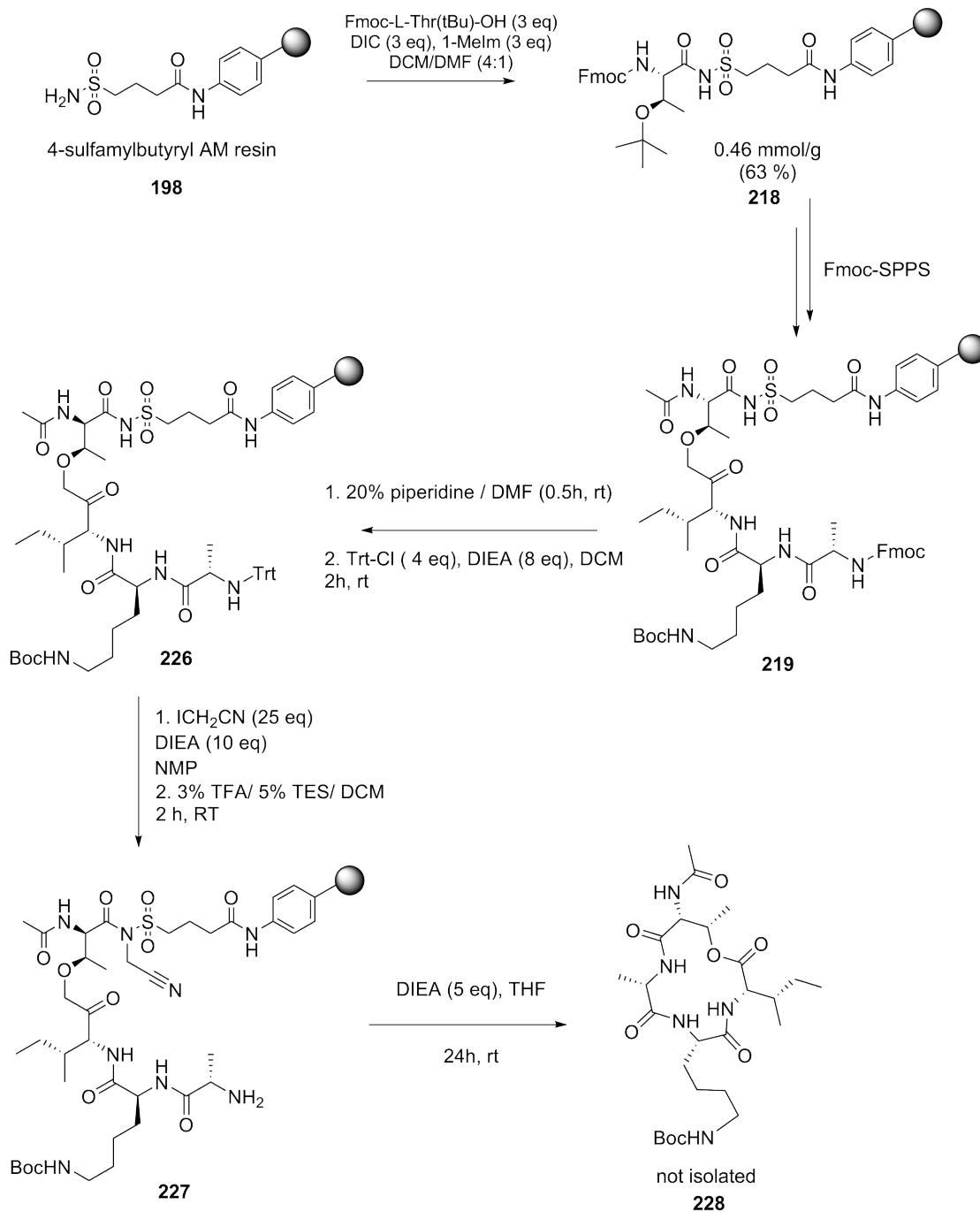


Scheme 30 - Initial synthesis of activated Ac-T(IKBoc-NH₂)A-resin **223** on 4-sulfamylbutyryl resin **198**, which upon cleavage with benzylamine resulted in the undesired peptide **224** lacking N-terminus Fmoc-protection as determined by ESI MS (*m/z* = 447).

Unfortunately, whilst this cleavage reaction worked well, clearly showing the benzylamine-derived linear tetrapeptide **224** in ESI MS, the major peaks revealed that almost complete Fmoc-deprotection has occurred during the activation step. It was considered that this may not be a problem further down the line, considering that the next step was the reaction of the free N-terminus primary amine with the activated linker; but until conditions for this cyclisation could be fully examined the route was altered to replace this Fmoc group with trityl protection prior to the haloacetonitrile labilisation step (Scheme 31).

After all four amino acid residues had been coupled to the resin **198** as previously to form **219**, 20% piperidine in DMF was used to yield a final Fmoc deprotection before re-protection with trityl chloride (4 eq) and DIPEA (8 eq) in DCM to form **226**. The progression of this reaction was monitored by ninhydrin staining, and was complete after two hours at room temperature. The on-resin cyclisation was attempted using DIPEA (5 eq) and THF at room temperature. After 24 hours, the solution was drained, and fresh DIPEA/THF added. This was reacted for a further 24 hours, and a similar addition at this point gave a third sample to collect any product **228** formed between 48 – 72 hours. After this point, benzylamine (5 eq) in THF was added to the resin in order to determine the reaction efficiency and to conclude if any activated peptide remained on resin after 72 hours in basic organic solvent.

Of the three solutions taken at 24 hour intervals, only the first contained any cyclised peptide **228** as visible in the mass spectrum; suggesting that either the reaction had gone to completion after this point, or after 24 hours any unreacted resin-bound peptide **227** had been deactivated at the linker. ESI MS showed a cyclised form of the tetrapeptide. However, the major peak ($m/z = 457$) corresponded to the Boc-deprotected form **217**. Given that Boc contains a carbamate functionality, similar to Fmoc, it is possible that these groups are not completely stable to iodoacetonitrile linker activation too.



Scheme 31 – Revised synthesis of cyclic tetrapeptide Ac-T(IK Boc)A **228**, employing an N-terminus Fmoc-deprotection and replacement with trityl to form intermediate **226** before subsequent linker activation to form the resin-bound linear precursor **227**, prior to macrolactamisation attempts.

Compared to Fmoc-deprotection, this is a much more serious problem, as it permits unwanted cyclisation via the lysine side chain primary amine, rather than the N-terminus. Macrocyclisation via the lysine amine appears to be the preferred mechanism; as this forms a 15-membered ring rather than the more constrained 13-membered native macrocycle. As the lysine amine exists at the end of an aliphatic chain, rather than adjacent to a methyl and in much close proximity to the core of the peptide, there is likely to be less steric hindrance, promoting this reaction where Boc-removal occurs to form compound **229** (Figure 36).

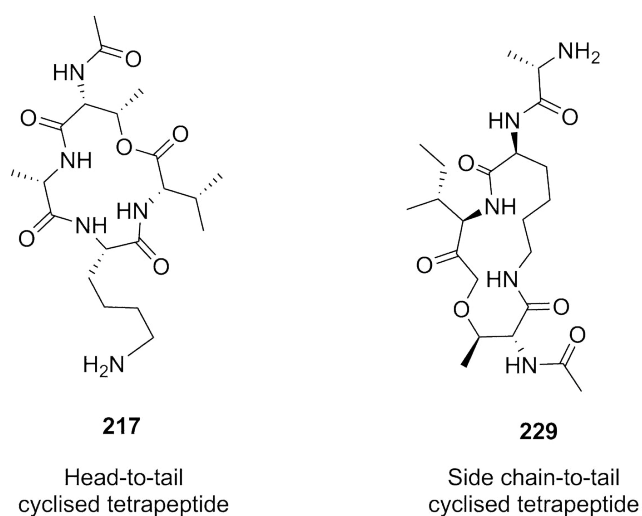


Figure 36 – Structure of the assumed, desired cyclic tetrapeptide Ac-T(IK)A **217** on the left hand side that is formed by head-to-tail macrolactamisation; actual structure of the cyclic tetrapeptide formed, **229**, resulting from side-chain-to-tail macrolactamisation. Compounds not isolated.

The formation of **217** or **229** would be determined more definitively using NMR spectroscopy, but unfortunately as the cyclisation reaction conditions had not yet been optimised, the crude yield was very poor (~1 mg) and did not allow for satisfactory analysis using this method.

It became apparent that in order to use a sulfonamide-based safety catch resin strategy to synthesise teixobactin analogues, no form of carbamate protection could remain on the peptide during the linker activation step. Therefore the synthesis was resigned to remove these protecting groups entirely.

3.5. Synthesis of teixobactin macrocycle with trityl-based side chain protection

3.5.1 Design of protection strategy

Initial experiments (Section 3.4) showed that carbamates are reactive during the sulfonamide activation process, therefore ruling out Boc as a protecting group for lysine, and also Fmoc as the protecting strategy for the *N*-terminus. The lability of the Boc group during activation leaves the amine side chain of lysine available to perform nucleophilic attack on the activated sulfonamide instead of the *N*-terminus amine during the cyclisation, leading to analogues with the same molecular weight but incorrect structures. Therefore, an alternative protecting strategy was created. This used trityl-based protecting groups that would remain stable during the resin activation.

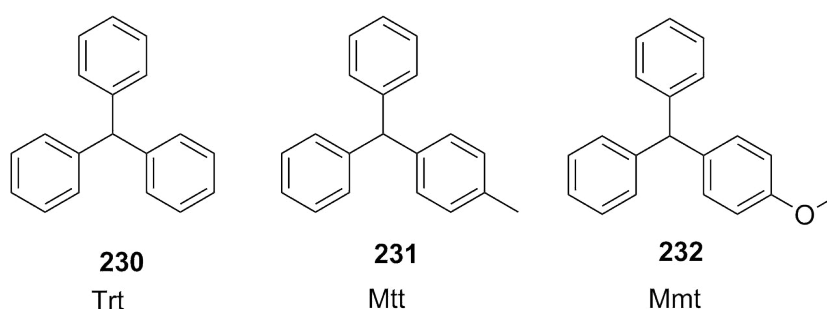


Figure 37 - Structures of trityl based protecting groups trityl **230** (Trt), 4-methyltrityl **231** (Mtt) and monomethoxytrityl **232** (Mmt) in order of ascending acid lability

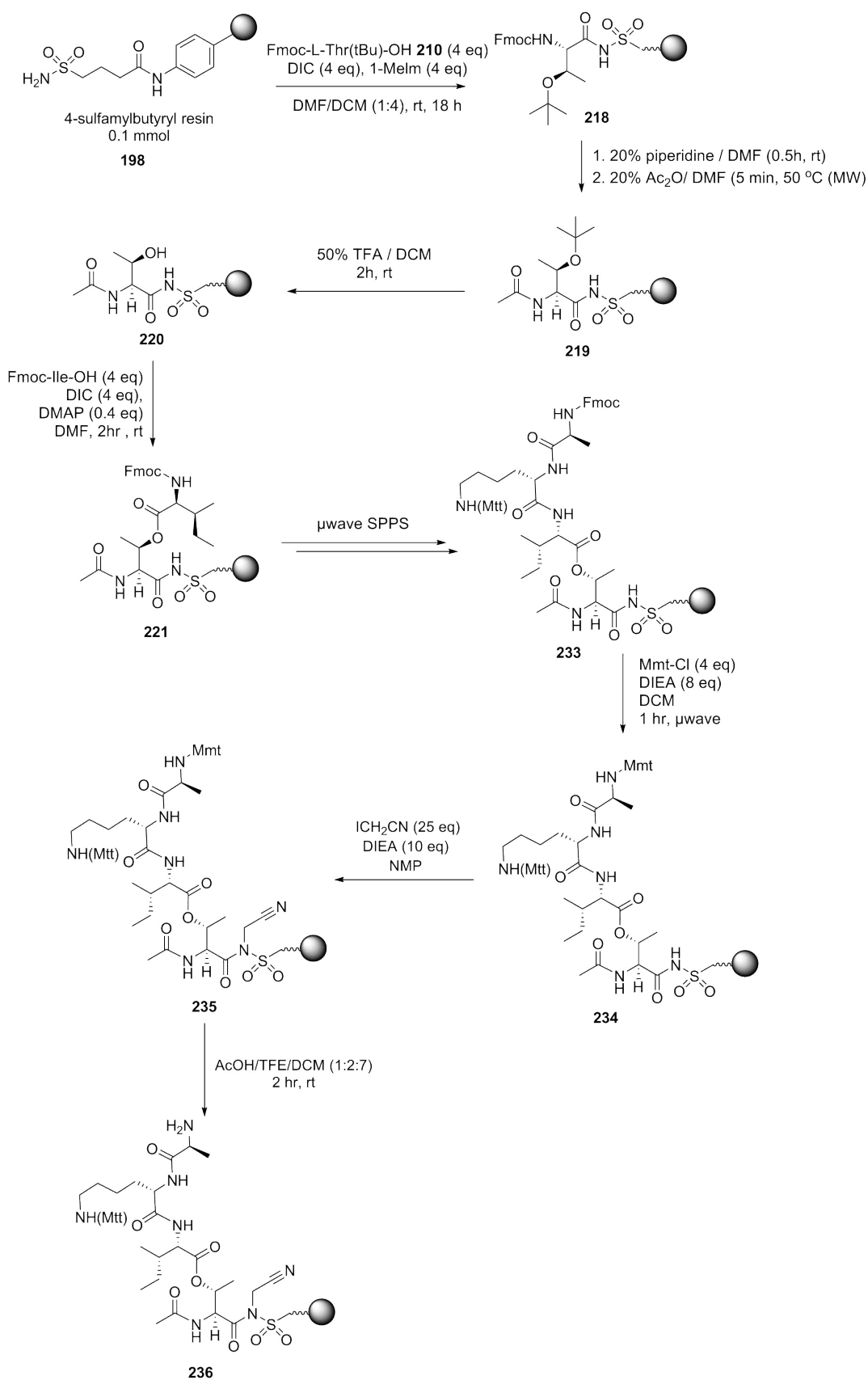
In order to selectively deprotect the *N*-terminus following activity, different trityl derivatives with varying labilities in acid were assigned to different parts of the structure. In this modified strategy, the lysine side chain Boc protection is replaced with a 4-methyltrityl (Mtt) **231** group. As opposed to trityl **230**, the terminal Fmoc group is cleaved and replaced with monomethoxytrityl (Mmt) **232** protection. Whilst these trityl based structures appear very similar, Mmt **232** is considerably more acid labile than Mtt **231** and can be selectively removed using milder acidic conditions, such as acetic acid, as opposed to TFA. Therefore

during synthesis, after reacting the sulfonamide linker with iodoacetonitrile to activate, the Mmt group **232** can selectively be removed using a solution of AcOH / TFE / DCM (1:2:7 v/v/v), leaving the Mtt **231** bound to the lysine side-chain amine.

3.5.2 Determination of trityl stability with linker activation conditions

The synthesis of acetylated teixobactin analogue macrocycles **207** and **217** was repeated, replacing Fmoc-Lys(Boc)-OH with Fmoc-Lys(Mtt)-OH, and the differential *N*-terminus protection achieved using Mmt-Cl with DIPEA in DCM, to form intermediate **234** (Scheme 32). Prior to Mmt removal and attempting cyclisation, a small sample of linker-activator resin-bound peptide **235** was cleaved with benzylamine at room temperature for two hours. ESI MS (+ve) showed a major peak with $m/z = 1092$, corresponding to the protonated fully protected linear sequence with benzylamine derivation, with no other obvious peaks for any form of deprotected form, showing that even the more labile trityl-based protecting groups were stable to the activation conditions overnight. Both Mmt **232** ($m/z = 273$) and Mtt **231** ($m/z = 257$) were also observed in the spectrum as fragmentation ions.

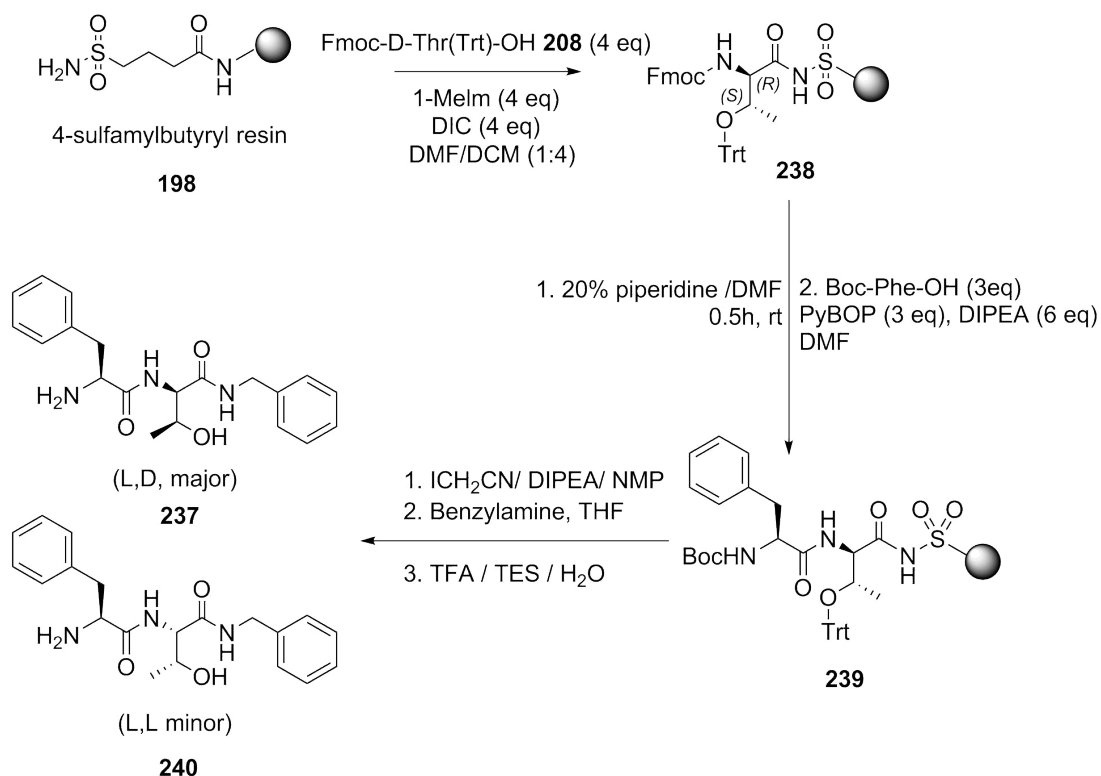
The addition of acetic acid with TFE and DCM (1:2:7 v/v/v) for two hours at room temperature resulted in complete removal of Mmt group, as determined by ninhydrin test. Once again, to ensure this had selectively removed this sole protecting group, a benzylamine cleavage test was applied to a small sample. Positive mode ESI MS showed a major peak ($m/z = 820$), the protonated linear peptide retaining lysine Mtt protection, as well as $m/z = 817$ (M-H⁻) and 931 (M+TFA-H⁻) in the negative mode. Whilst a large peak ($m/z = 257$, the molecular weight of Mtt), was indeed present in the positive mode, fragmentation of trityl in the mass spectrometer had previously been commonly observed, and only a negligible peak for peptide without the Mtt group ($m/z = 564$) could be seen. Therefore this multi-trityl protection strategy appeared to be fully compatible with this synthesis.



Scheme 32 - Revised synthesis of activated resin-bound linear tetrapeptide Ac-T(IKBoc-NH₂)A-resin **236**, via synthesis of *N*-Fmoc protected intermediate **233** containing Lys(Mtt), and later *N*-Mmt protected intermediate **234**.

3.5.3 Epimerisation study of loading to safety-catch resin

One of the major concerns with the use of safety-catch resins is the high possibility of epimerisation during loading due to the relatively harsh conditions that need to be applied. Compared to uranium based coupling agents, such as HBTU and HCTU, the use of carbodiimides often results in higher levels of racemisation. In order to determine the level of epimerisation of the first residue caused by the strong carbodiimide-based coupling, a model dipeptide, Phe-D-Thr-benzylamine **237** was designed and synthesised. This was formed by loading of Fmoc-D-Thr(Trt)-OH **208** onto 4-sulfamylbutyryl resin **198** using the optimised method (DIC/ 1-MeIm/ DMF/ DCM, Section 3.3), followed by Fmoc-deprotection and coupling of Boc-Phe-OH **174** using PyBOP and DIPEA (Scheme 33). This residue was chosen based on its side chain protection; the aromatic phenylalanine side chain absorbs more UV more strongly other aliphatic residues, and therefore is more suited to HPLC analysis. With this method, any epimerisation taken place during the loading of the resin is determinable by the formation of diastereomers that can be separated chromatographically. Following displacement from the linker and resin, the peptide solution was analysed by LCMS and analytical HPLC.



Scheme 33 – Synthesis of dipeptide diastereomers **237** and **240** to determine the level of epimerisation of the first amino acid residue loaded onto 4-sulfamylbutyryl resin **198**.

Product formation of **237** and **240** was initially assessed using LCMS, which indicated a product with the expected molecular mass ($m/z = 356$) eluting at T_R 1.08; this appeared to be one peak, although disturbance of the trace creating shoulders eluded to more than one compound. Analysis of the same sample with RP-HPLC revealed two compounds eluting at a similar point in the gradient; with relative integrations of 72:28 (Figure 38). This suggested that the loading of 4-sulfamylbutyryl resin **198** under these conditions results in a considerable level of epimerisation, and in turn a reduction in yield and purity of the final compounds.

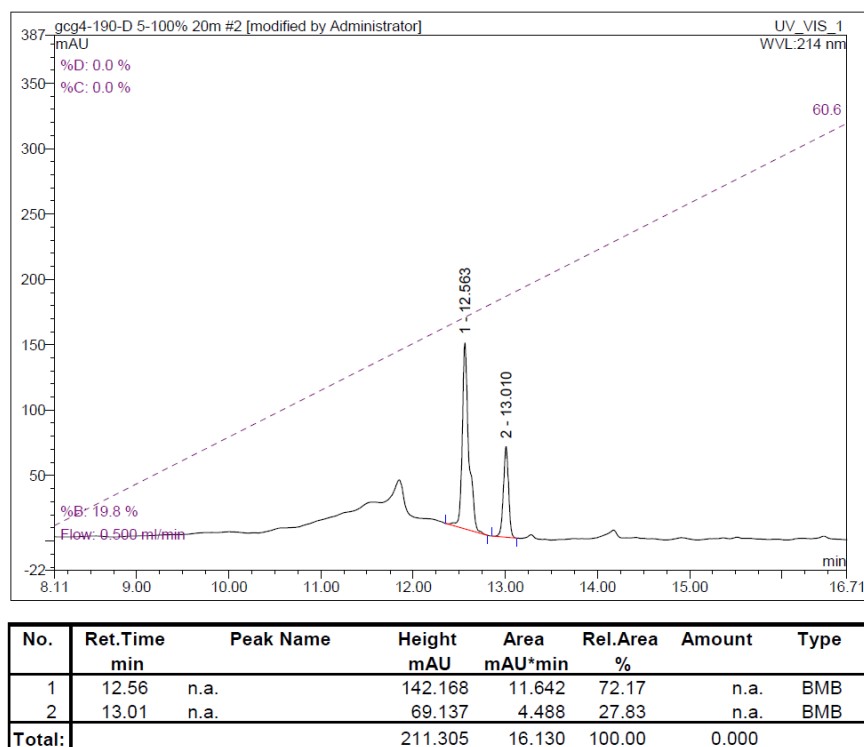


Figure 38 - Analytical HPLC trace showing two diastereoisomers **237** (72 %) and **240** (28%), eluting at similar retention times.

3.5.4 On-resin cyclisation reaction optimisation

In order to try and optimise conditions for macrolactamisation by displacement of the sulfonamide linker and resin by nucleophilic attack of the N-terminus amine on the carbonyl, the previously described activated resin-bound linear tetrapeptide Ac-T(IKMtt-NH₂)A-resin **236** was split into 3 equal portions, to which different cyclisation conditions were applied (Table 12).

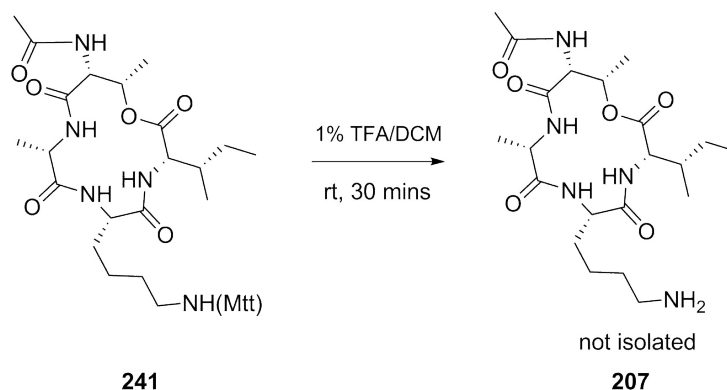
Entry	Cyclisation conditions
1	TEA (5 eq), THF, 4 hr, rt
2	TEA (10 eq), DMF, 2 hr, 85 °C (MW)
3	DIPEA (7 eq), DMF, 2 hr, 100 °C (MW)

Table 12 – Conditions employed in the attempted cyclisation of Ac-T(IKMtt-NH₂)A-resin **236**

The cyclisation of **236** was initially attempted by a reaction with triethylamine (TEA) in THF at room temperature (Table 12, Entry 1). A similar reaction with increased equivalents of TEA was then trialled by microwaving at 85 °C for 2 hours (Table 12, Entry 2). Due to the higher boiling point of DIPEA (127 °C), the third set of reaction conditions could be heated higher than TEA (bp= 89 °C) (Table 12, Entry 3). After the designated reaction time, the solution was concentrated *in vacuo* and the remaining precipitate analysed by mass spectrometry.

For each reaction, a very low quantity of precipitate was formed, particularly the room temperature reaction (Table 12, Entry 1), which showed minimal product formation by MS. A much better rate of conversion appeared to result from microwave heating, with clear MS peaks for the cyclised peptide. However, the LCMS traces for these reactions showed them to be exceptionally crude, with excessive side-product formation eluting at a similar gradient to that of the macrocycle. The reaction with DIPEA in DMF at 100 °C produced several more indeterminable side products than the previous reaction; suggesting that elevating the temperature too high is likely to be detrimental to the yield. This is plausible as peptides are notoriously susceptible to degradation at high temperatures when not bound to solid support; it is possible that high temperatures do increase the rate of cyclisation on resin but subsequently degrade the product once it is freely in the basic solution. Given the high boiling point of DIPEA, this was also more difficult to remove from solution post-reaction.

The precipitate formed following the reaction with TEA in DMF taken forward for the final Mtt-trityl deprotection to determine if any pure, cyclic peptide could be purified. 1% TFA in DCM was added to the sample and mixed for 30 minutes at room temperature (Scheme 34). At this point the solution was concentrated, and ice-cold diethyl ether added to remove free Mtt. The remaining solid was then diluted in water and acetonitrile to be purified by RP-HPLC.



Scheme 34 – Attempted Mtt deprotection from lysine residue of **241** from to form final acetylated cyclic tetrapeptide **207**. No product isolated.

It became apparent after the final deprotection that two product **207** isomers had been synthesised using this method; eluting at 1.07 and 1.15 minutes in the LCMS respectively ($m/z = 456, 457$). Purification by RP-HPLC was attempted but each resulted in a very low yield (<1 mg) making further characterisation difficult. Prior experiments had determined that a significant amount of epimerisation occurs during either the initial loading. It was also possible that racemisation was taking place during the esterification step, which also employs the same carbodiimidazole under similar conditions. Alternatively, at high temperatures this racemisation could take place during the final cyclisation step, resulting in the reduction of an already low yield.

The synthesis was repeated with D-thr(tBu) in place of the L-isomer used previously. This time for the cyclisation, the temperature of the microwave cyclisation reaction was reduced to 50 °C. This resulted in an improved level of peptide purity as seen in the HPLC spectrum, but at this point it was becoming clear that optimisation of yields with this method was going to be extremely limited.

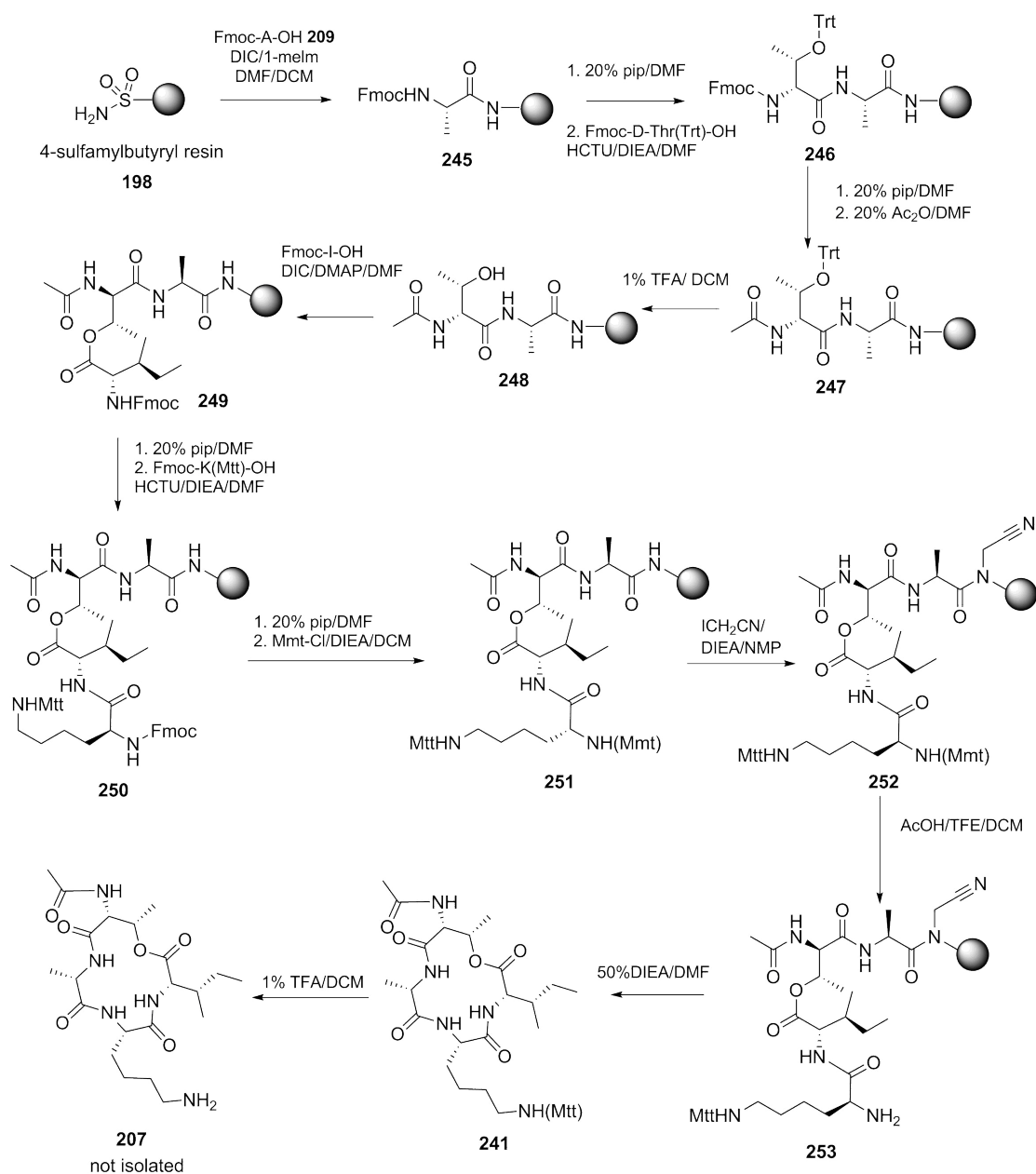
To ensure that this was not a sequence-specific error, the synthesis was applied to three other tetrapeptide sequences, with End10 replaced with L-Orn(Mtt) (**242**), L-His(Trt) (**243**) and L-alanine (**244**). The first two mutations were selected as they each have similar character to the native residue; ornithine is a basic residue with a shorter chain than lysine, and histidine contains an imidazole side chain which is also protonated at physiological pH. Both of these residues can each be

protected with Mtt and Trt respectively, making them compatible with the current synthesis. The alanine analogue **244** was selected as a control; and as its short methyl side chain does not require bulky trityl protection; thus probing if this is an issue with the previous experiments.

Cyclisations were attempted using TEA in DMF at 50 °C, and also with an excess of base at room temperature (DIPEA/DMF, 1:1 v/v). Each of these eight reactions produced very little material and multiple side products. Attempts were made to purify as isolate cyclised peptide, but with little success. The low yield of the Ala10 tetrapeptide suggests that the low level of cyclisation is not due to the steric bulk of the trityl groups, which had previously been considered. However, the high level of steric bulk around the site of cyclisation may still have been an issue. Therefore, before teixobactin analogue synthesis via the safety catch linker was abandoned, the synthesis was adjusted to try and remove this steric bulk and promote percent conversion.

3.6 Optimised synthesis of teixobactin macrocycle with Ala-loading

The previous synthetic route (Section 3.5.4) had resulted in very poor results. This appeared not to be due to side chain protection, as no improved conversion was observed by mutating the End10 to an alanine residue (**244**). However, the presence of the β -branched amino acid threonine, with peptide ester derivation at the hydroxyl, directly adjacent to the linker may have had a considerable effect on the level of cyclisation observed. Using an improved synthetic route, the synthesis of these cyclic teixobactin macrocycle peptides were reattempted; this method was similar to the full synthesis; but replaced the first residue to be loaded to the resin with alanine, rather than threonine (Scheme 35). Given that this residue is one of the smallest in size it is particularly suitable to be employed at this point, and also introduces an additional spacer region between the orthogonal ester branching and sulfonamide linker. In addition, Fmoc-Ala-OH **209** had been found to give superior resin loading when used in initial loading experiments (68% compared to 56% found for Fmoc-D-Thr(Trt)-OH **208** under the same conditions).



Scheme 35 - Revised synthesis of cyclic DLLL Ac-t(IK)A tetrapeptide **207**, with Fmoc-Ala-OH **209** as the initial coupling reaction to the sulfonamide resin **198**.

Loading of 4-sulfamylbutyryl resin **198** with Fmoc-Ala-OH **209** resulted in slightly lower conversion than previously observed (0.41 mmol/g as opposed to 0.50 mmol/g), but was still a satisfactory level nevertheless. The synthesis was carried out as previously; with coupling of Fmoc-D-Thr(Trt) **208**, acetyl capping of the N-terminus and branching from the threonine side chain to form the ester **249**. In comparison to the previous method, this synthetic route was more

appropriate for the synthesis of multiple analogues as the End10 mutation had become the last residue to be coupled; thus allowing the major part of the peptide to be synthesised in bulk and split at this later stage. After coupling of Fmoc-Lys(Mtt)-OH, the final Fmoc was removed and replaced with Mmt (**251**). Linker activation was achieved using the standard method with iodoacetonitrile and DIPEA in NMP, before on-resin cyclisation was attempted using 50% DIPEA in DMF. Initially this reaction was performed for 4 hours at room temperature. The filtrate was concentrated and analysed by MS and HPLC.

Unfortunately, this strategy did not appear to be an improvement on the previous method (Scheme 32). In addition, following attempted removal of Mtt from the crude product with 1% TFA/ DCM, a large peak appeared in the mass spectra corresponding to the hydrolysed form of the peptide ($m/z = 474.30$). It is possible that the TFA was not removed sufficiently prior to dissolution in water for analysis resulting in acid-catalysed hydrolysis of the ester. However this seems unusual, as no hydrolysed product had been observed in any other experiments.

The synthesis was repeated a final time, with slightly reduced excess of DIPEA (20%, reduced from 50%) and microwave conditions (50 °C over 2 hours). Whilst the MS appeared promising, the analytical-HPLC revealed an extremely crude sample, and further purification was not attempted.

3.7 Conclusions

A safety-catch resin, with a 4-sulfamylbutyryl linker bound to the solid support (**198**), was used to synthesise a series of teixobactin analogues (Scheme 34). The initial loading of the resin, previously found to be difficult to perform efficiently with high conversion to the product, was optimised by screen a range of coupling agents and conditions (Section 3.3). The results of this, which found elevated temperature and the addition of HOBt to be detrimental to yield, elucidated a possible mechanism for these reactions. Levels of epimerisation were determined to be low by C-terminus benzylamine derivation and subsequent LCMS and HPLC analysis.

The initial synthetic route used this resin resulted in removal of carbamate functionalities upon activation of the sulfonamide linker, making it unsuitable for the synthesis of teixobactin analogues containing basic amino acid residues with Boc protection (Scheme 30). Therefore, the synthesis was redesigned to incorporate trityl variants as protecting groups with three levels of acid lability in order to allow selective removal at various points in the synthetic route (Scheme 32).

Whilst this method has been employed successfully in the synthesis of other cyclic peptides and depsipeptides, these are mostly considerably less strained, with macrocycles composed of at least six amino acid residues. It is most likely that the formation of a 13-membered ring is simple too entropically unfavourable in such close proximity to a bulky polystyrene solid support. Therefore, for the synthesis of teixobactin analogues retaining the core macrocycle, this route is not suitable; however, the method used could certainly be applied to larger cyclic peptides, and for those where an acid or base labile resin is not compatible with the reagents required.

This synthetic route yielded some conversion to the cyclic product, but with very little material, even with the optimisation of cyclisation conditions. Therefore the synthesis was adjusted once more to alter the linker-bound amino acid from D-Thr(Trt) to L-Ala, with the idea of vastly reducing the level of steric hindrance around the reaction site. Whilst this appeared to give a slight increase in product formation based on UV absorption in LCMS and HPLC, the amount produced was too low to give an accurate yield determination or perform any extensive analysis. To scale up the reaction to a point enough material could be obtained for biological assays would not economically viable. However, this new loading method could be applied to other syntheses involving solution-based cyclisations.

4. Synthesis of teixobactin analogues using solution-phase cyclisation

4.1 Introduction

Solution-phase cyclisations can be synthetically challenging; in order to prevent intermolecular oligomerisation highly diluted solutions of reagents are required, and many factors such as peptide sequence, ring size and reaction conditions can have a substantial effect on reaction progression. The cyclisation of small rings (tetra- and pentapeptides) has been found to be particularly difficult, with considerably more dimerisation than is observed for larger rings.¹⁴⁹

This chapter discusses the synthesis of teixobactin analogues which employ a solution-phase cyclisation reaction for the formation of the 13-membered macrocycle. This was initially attempted by ester bond formation between the acid C-terminus and the threonine hydroxyl side chain, but was optimised by alteration to amide-bond formation through the N-terminus of the orthogonal side chain and the acid C-terminus.

4.2 Aims of the chapter

This chapter aimed to develop a highly efficient solution-phase cyclisation approach to access the 13-membered teixobactin **42** macrocycle by formation of its depsipeptide bond, or through amide bond formation. With access to the core macrocycle of teixobactin, syntheses were designed to probe the relevance of the hydrophobic linear tail of teixobactin. A series of truncated analogues - macrocyclic analogues with acetylated N-terminus - were synthesised and tested for antibiotic activity.

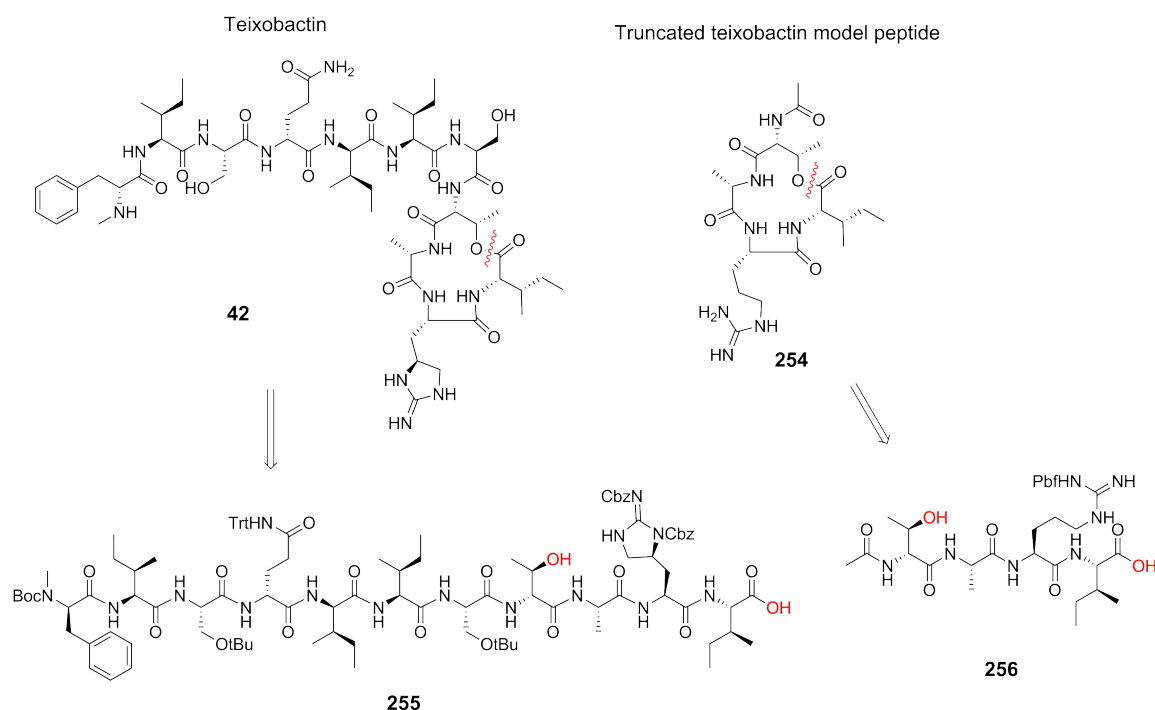
To investigate whether the linear portion of teixobactin **42** functions as a cellular membrane anchor, residues 1-7 were replaced by isoprenoids of two different lengths, in conjunction with seven L-*allo*-enduracididine **43** mutations.

This work also aimed to create fluorescent analogues of active compounds by attachment of fluorescein to the N-terminus, and to make minimal structures that may have potent activity against Gram-negative bacteria in addition to Gram-positive.

4.3 Solution-phase macrolactonisation

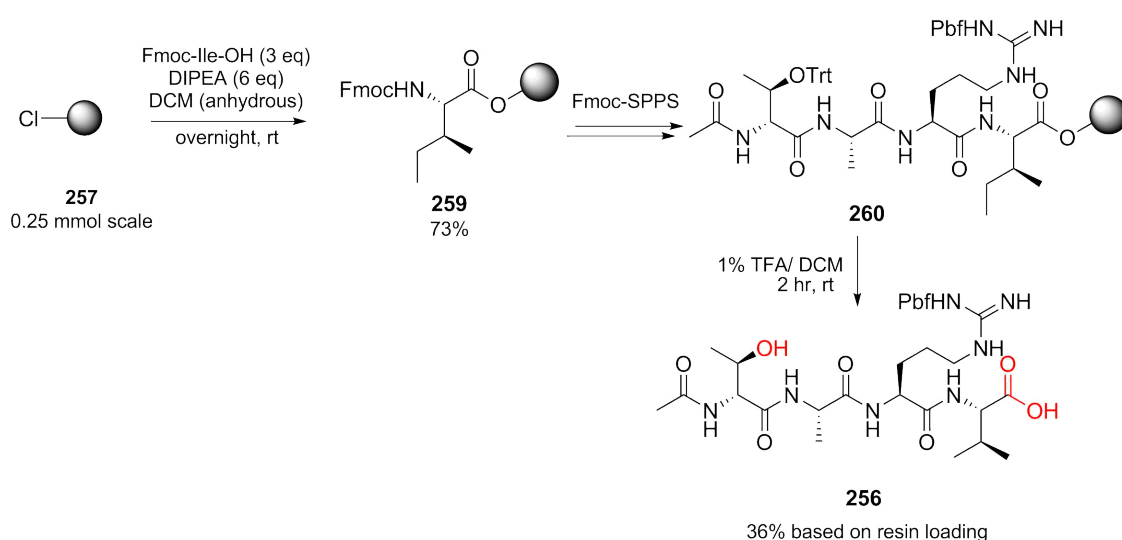
4.3.1 Studies on depsipeptide macrocyclisation

The macrocyclisation was first designed to be formed via the ester bond between the threonine hydroxyl and the C-terminus carboxylate of teixobactin **42** (Scheme 36). This route was attempted initially as optimisation of this reaction removes the requirement for branching to form the ester bond during the synthesis; this route creates an additional N-terminus that requires a third dimension of orthogonal protection to selectively deprotect.



Scheme 36 – Retrosynthesis of teixobactin **42** and teixobactin macrocycle analogue cyclic Ac-t(IR)A **254**, with reactive sites of linear peptide precursors **255** and **256** for depsipeptide formation shown in red.

A synthetic strategy was designed using a model peptide **254** mimicking the macrocycle of teixobactin **42**; composed of D- Thr, L-Ala, L-Ile, and with L-*allo*-enduracididine **43** modified to structurally similar L-arginine **100**, and the N-terminus capped with an acetyl group (Scheme 38). Synthesis of the linear peptide precursor **256** on 2-chlorotrityl chloride resin **257** allowed cleavage from the solid support whilst retaining orthogonal protection of arginine using weak acid (1% TFA in DCM for 10 minutes). Fmoc-D-Thr(Trt)-OH **208** was used instead of the more standard *tert*-butyl protection group in order to yield the free hydroxyl simultaneously with resin cleavage. Loading of 2-chlorotrityl chloride resin **257** was achieved using Fmoc-Ile-OH **258** and DIPEA in anhydrous DCM, with good loading of 1.1 mmol/g (73% conversion based on commercial value). With the Fmoc-Ile derived resin **259**, the other three amino acids were coupled using standard Fmoc-SPPS conditions, before a final acetylation using acetic anhydride to give the final linear sequence on resin. 1% TFA in DCM was used to cleave both the peptide from the solid-support and the hydroxyl trityl protection. This linear tetrapeptide **256** was purified by RP-HPLC and was obtained in reasonable yield and excellent purity (36% yield based on 0.175 mmol scale, >99% purity).

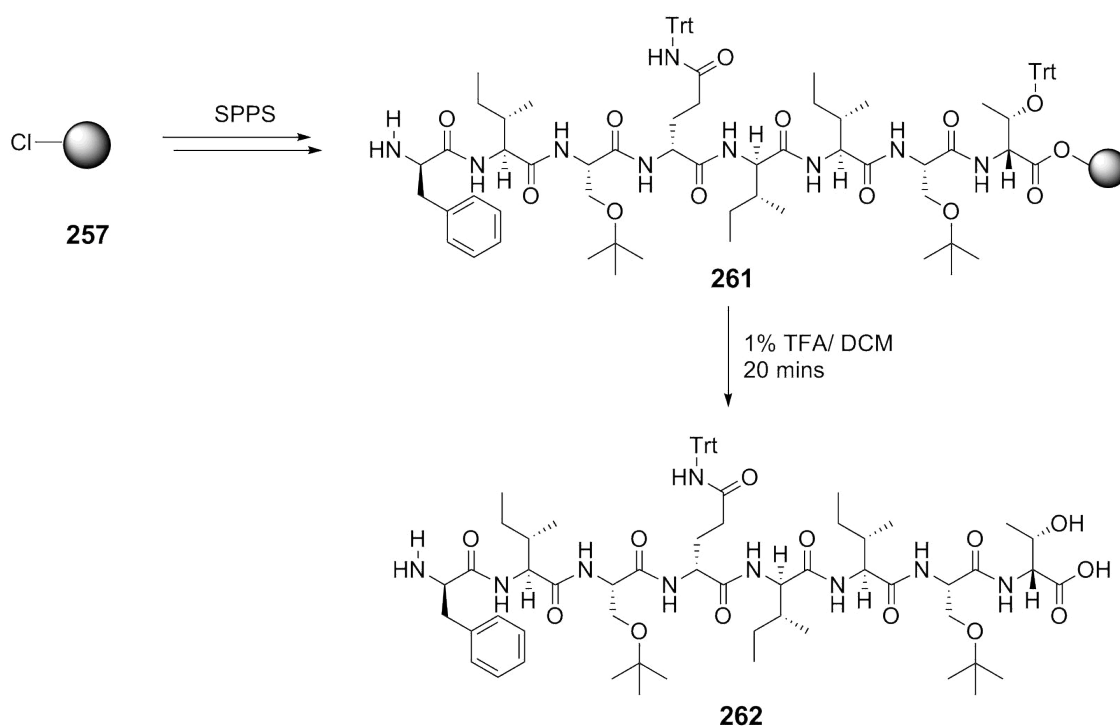


Scheme 37 – Synthesis of the linear peptide Ac-tAR(Pbf)I-OH **256** for depsipeptide formation macrolactamisation experiments

4.3.2 Determination of Gln(Trt) and Thr(Trt) protection lability

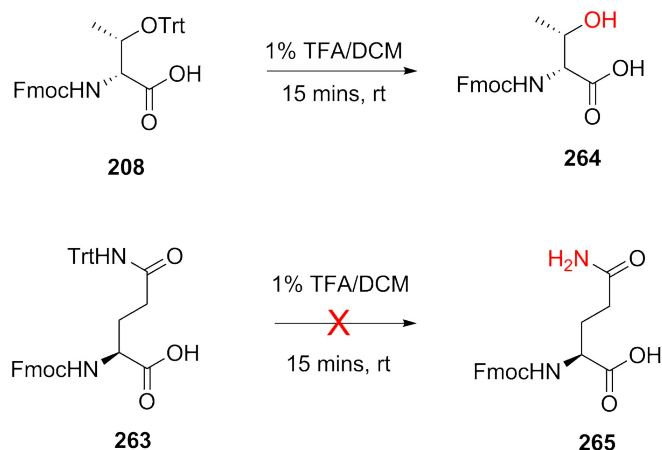
To apply this synthetic strategy to the larger teixobactin **42** analogues bearing more than four residues, the presence of other amino acids containing highly acid-labile side chain protection was also considered. Given the 1% TFA required to liberate the linear peptide from resin, undesired cyclisations between the C-terminus and other deprotected nucleophilic side chain functionalities could take place. The native structure of teixobactin **42** contains amino acids bearing reactive sites that require Cbz- or Boc protection (N-terminus, L-*allo*-enduracididine **43**) and *tert*-butyl protection (Ser7). These protecting groups are not labile in 1% TFA, but teixobactin **42** also contains D-Gln4 that requires trityl protection. In order to probe whether this synthesis could be applied to larger peptides such as the full teixobactin sequence, the deprotection of trityl protected threonine and glutamine were compared using 1% TFA, on both the resin-bound linear sequence of residues 1-8 **261**, and *N*-Fmoc protected free-acid forms of the two trityl protected amino acids.

Residues 1-8 of teixobactin (with D-Phe in place of Me-D-Phe) were coupled to solid support **257** using automated microwave-assisted peptide synthesis to give compound **261**, and this peptide was subsequently submitted to the same cleavage conditions (1% TFA/ DCM, 20 minutes at room temperature) employed previously for Ac-tAR(Pbf)I **260** on resin (Scheme 37). The resulting solution was analysed by ESI MS, which indicated the major product **262** to have a molecular weight corresponding to removal of only one trityl from the structure ($m/z = 1263$); analysis with LCMS revealed one distinct peak with this molecular weight, indicating selective trityl removal from one particular residue.



Scheme 38 – Synthesis of the linear peptide **261** H_2N -fISeqILS- on 2-chlorotrityl chloride resin **257**, and subsequent exposure to 1% TFA/DCM to yield the trityl-deprotected form **262**.

To further support the selective trityl removal was occurring at threonine rather than glutamine, Fmoc-D-Thr(Trt)-OH **208** and Fmoc-Gln(Trt)-OH **263** were used as models to determine the comparative lability between hydroxyl and amide side chain sites (Scheme 39). 1% TFA in DCM was added to each Fmoc-protected amino acid; notably there was an immediate colour change of the solution containing Fmoc-D-Thr(Trt)-OH **208** from clear to bright yellow. Only a slight colour change to pale yellow was observed with the Fmoc-Gln(Trt)-OH **263** solution over the 15 minutes of the reaction. After this point, the solvent was evaporated and each sample analysed by LC-MS. The chromatography trace for the glutamine sample showed only one constituent; with the molecular weight corresponding to the trityl-protected form of the Fmoc-amino acid (**263**, $m/z = 611$). On the other hand, the threonine test reaction showed more than one peak, corresponding to that of free trityl cation (243^+) and side-chain deprotected threonine (364.1178 , $[M+Na]^+$), **106**. In this latter sample, there was no trace of any starting material **105** whatsoever.



Scheme 39 – Exposure of Fmoc-D-Thr(Trt)-OH **208** and Fmoc-Gln(Trt)-OH **263** to 1% TFA/DCM over 15 minutes at room temperature results in of formation of **264**, but not **265**.

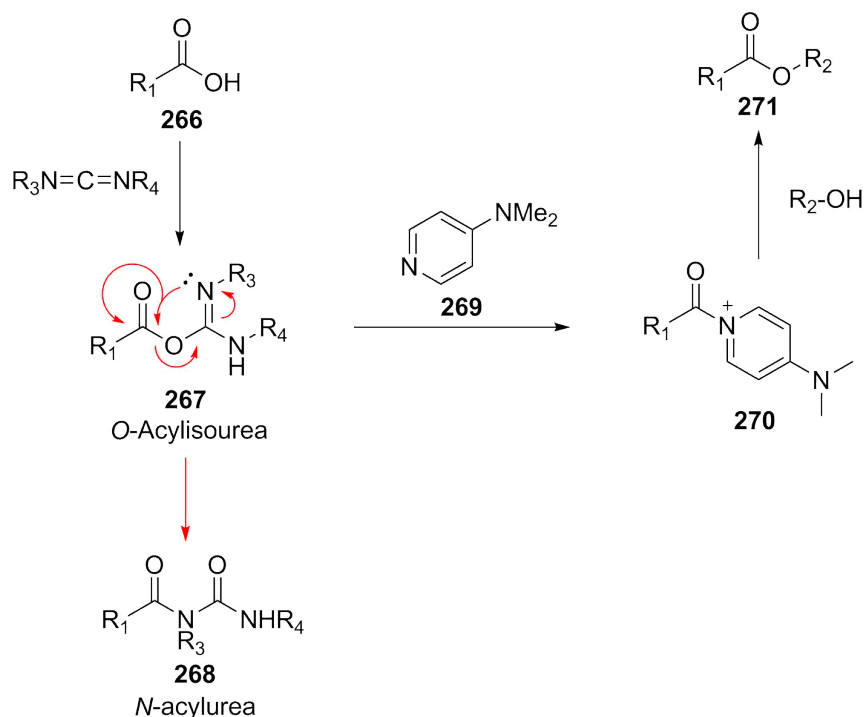
These results suggested that 1% TFA in DCM could be used effectively even in larger peptide analogues to selectively remove trityl protection from threonine residues, as opposed to amides where it is more commonly employed. This can be explained by the S_N1 removal of the trityl group being promoted by the increased susceptibility of hydroxyl groups to protonation in comparison to amides. The resonance of amides present in amino acids such as glutamine and asparagine delocalises the lone pair electrons on the nitrogen; thus becoming less nucleophilic and basic, and therefore less reactive in carefully controlled conditions.

4.3.3 Methods of depsipeptide formation

The most common method to synthesise esters in organic synthesis is through reaction of carboxylic acids and alcohols, under Fischer conditions. However, the harsh acidic conditions are not compatible with peptides due to backbone hydrolysis and removal acid-labile side-chain protecting groups. An alternative route is via conversion of the acid to the more reactive acyl chloride. This technique was employed in the first dipeptide synthesis in 1901 by Fischer and Fourneau.¹⁵⁰ This procedure is typically used for sterically hindered reactions for

which standard coupling reagents are too bulky. Reactions with acyl chlorides can result in undesired side reactions, such as carboxyanhydride formation via an oxazolonium ion intermediate¹⁵¹ – this tends to be with the Fmoc/Boc-protected reagents themselves, rather than the amino acid residue already incorporated into a peptide – therefore amino acid chloride reagents require sulfonyl protection at the N-terminus to avoid this side reaction. Acids are most commonly converted to chlorides with SOCl_2 , PCl_3 , or POCl_3 .¹⁵² , but these reactions give HCl as a by-product; so is not compatible with Fmoc-SPPS protecting groups. The addition of cyanuric chloride in triethylamine maintains basic conditions throughout, but ultimately this method is not efficient due to risk of hydrolysis, racemisation, cleavage of protecting groups and other side reactions. Acyl fluorides, on the other hand, are less reactive, but also less susceptible to hydrolysis and less prone to cause racemisation, and have been successfully employed in the synthesis of the cyclic lipodepsipeptide halipeptin A.¹⁵³

In recent years, the most common method used for peptide depsipeptide formation is the Steglich esterification, developed in 1978 (Scheme 40).¹⁵⁴ This is typically performed with DCC as a coupling reagent, and is adapted from a similar method used to form amides. For ester formation, DMAP **269** is also required as a catalyst due to the reduced nucleophilicity of hydroxyls in comparison to their amine counterparts. This method is much more compatible with orthogonally protected peptides due to the mild reaction conditions. However, DMAP **269** can trigger epimerisation in peptides, so this must be considered. Generally Steglich esterifications progress well, but for sterically hindered or otherwise slow reactions a rearrangement of the *O*-acyl intermediate **267** to the *N*-acylurea **268** is possible, which is no longer electrophilic. DMAP **269** is used to suppress this side reaction; acting as an acyl transfer reagent.



Scheme 40 - Mechanism of carbodiimide and DMAP **269** catalyzed ester **271** formation. DCC: R₃ and R₄ = cyclohexyl; DIC: R₃ and R₄ = *i*-propyl; EDC: R₃ = ethyl, R₄ = 3-dimethylaminopropyl

Depsipeptide formation using Steglich esterification has previously been achieved between a tyrosine phenol and Alloc-Ile with DIC, DMAP and DIPEA in DMF (2 x 24 hr, rt) to form phenyl ester,¹⁵⁵ and in the synthesis of the cyclic depsipeptide antibiotic Ramoplanin A2 **51**, Boger and co-workers used this reaction after having attempted a wide range of other methods unsuccessfully; acyl fluoride activation, mixed anhydride activation, Mitsunobu (triphenylphosphine catalyzed betaine formation from an azodicarboxylate, resulting in deprotonation of the carboxylic acid and subsequent ester formation), Yamaguchi (reaction of the alcohol with an anhydride, formed from the carboxylic acid and 2,4,6-trichlorobenzoyl chloride), and Corey-Nicolaou (catalysed by reaction of 2,2'-dipyridyldisulfide and triphenylphosphine) reactions.¹⁵⁶

4.3.3.1 Macrolactonisation of linear peptide Ac-tAR(Pbf)I-OH (256)

For the esterification of teixobactin **42** model macrocycle tetrapeptides, equipment was designed and set up to allow the slow controlled addition of peptide precursor in solution with base to a stirred dilute solution of coupling agent(s), adapted from a published method (Figure 39).¹²⁵ By maintaining a very dilute concentration of peptide precursor in the presence of other reagents, side reactions such as dimer- and trimerisation should be avoided.

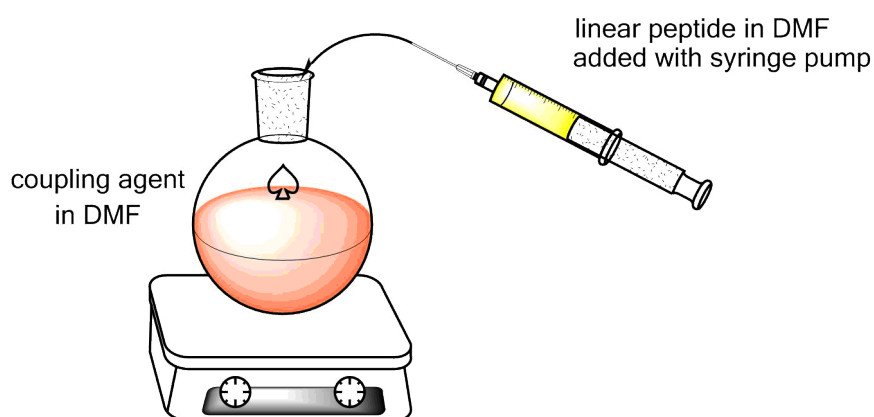
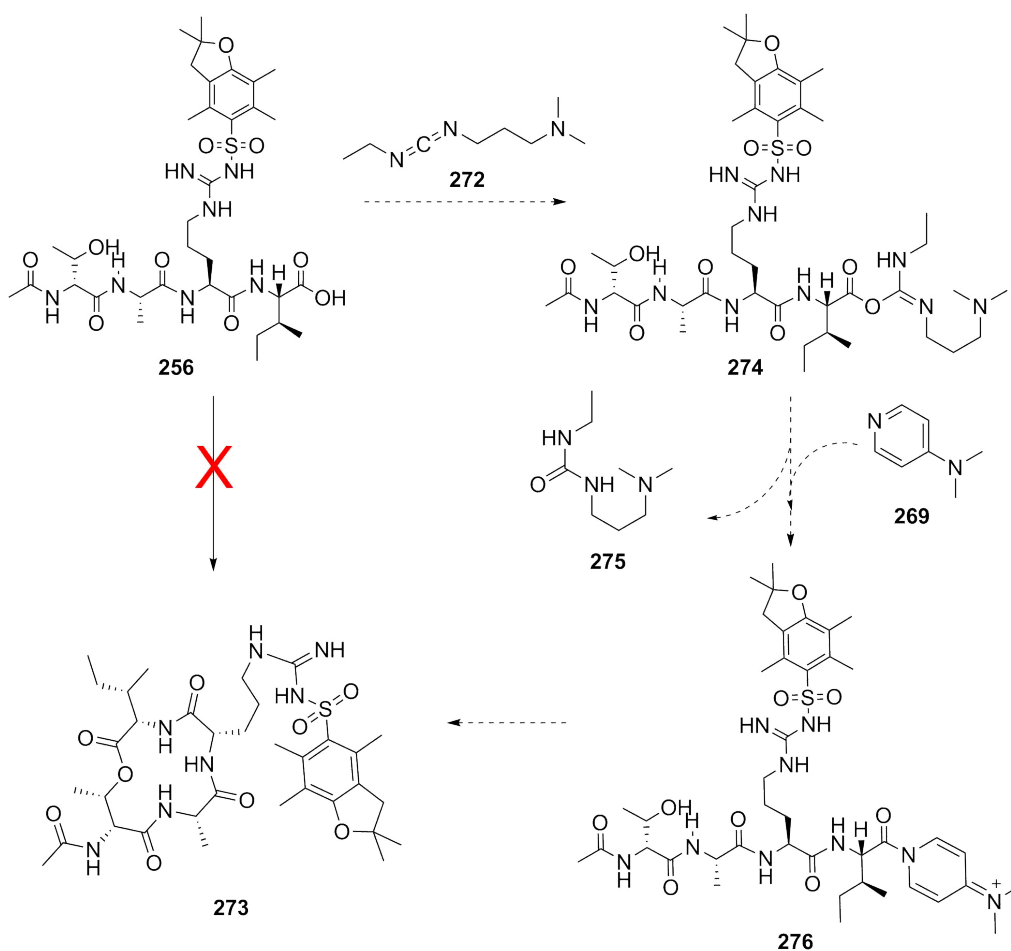


Figure 39 – Equipment set-up used for solution-phase tetrapeptide cyclisation reactions

Based on previously published peptide esterification reactions, standard Steglich esterification conditions were employed for the cyclisation of the linear peptide precursor Ac-tAR(Pbf)I-OH **256**, using (3-Dimethylaminopropyl)-*N*-ethylcarbodiimide hydrochloride (EDC, **272**) with DMAP **269** in dry DMF. These coupling reagents have previously been used together successfully in condensation reactions of dicarboxylic acids with diols.¹⁵⁷ Briefly, linear peptide **256** is added to via plastic syringe to a stirred solution of coupling agent plus a catalytic quantity of DMAP **269** in DMF at a rate of 0.12 mL/ hour (Scheme 42). After addition, the reaction is stirred for a further hour before analysis and purification. Unfortunately, LCMS and HPLC spectra showed very little conversion to the desired cyclic peptide product, with numerous side products formed; the major peak ($m/z = 754.39$) corresponds to the protonated form of the

linear peptide starting material. m/z peaks for cyclised product **273** were apparent ($m/z = 736.37$, $[M+H]^+$, 758.36 , $[M+Na]^+$), but based on integration in LC was much less abundant than the linear form (14:87).



Scheme 41 – Unsuccessful cyclisation reaction of linear peptide Ac-tAR(Pbf)-OH **256** with EDC **272** and DMAP **269** to form side-chain protected cyclic teixobactin macrocycle analogue peptide **273**, with the intended mechanism.

From here a series of reactions were carried out to determine if the cyclisation could be optimised using different reagents and reaction conditions (Table 13). These were carried out using the same peptide precursor **256**, and using the syringe pump addition method as before. Predominantly, reaction conditions generally used for amide couplings were investigated, to see if they could also prove to be effective in the formation of esters. This would allow the preliminary

deprotonation of the linear peptide precursor prior to addition of the coupling agent; which would potentially enhance the reaction progression.

Reactions with PyBOP **277** as coupling agent and DIPEA as base similarly did not yield any conversion to the cyclic product **273**, even when heated to 60 °C (although whilst high temperatures may promote reaction progression, this could also cause degradation or hydrolysis of the product if formed at all). The LCMS spectra did not contain any trace of the linear peptide; only DIPEA, unreacted PyBOP **277**, and 1,1',1''-phosphoryltrypyrrolidine **278** and HOBt **279** side products. These latter products **277** and **279** suggested that the derivation of the C-terminus to an activated ester had progressed to some degree; but the hydroxyl had not been sufficiently reactive to substitute at this position, and some form of degradation or polymerisation had then occurred. The use of the coupling reagent 1-[Bis(dimethylamino)methylene]-1H-1,2,3-triazolo[4,5-b]pyridinium 3-oxid hexafluorophosphate (HATU, **280**) did yield some conversion to the cyclised product, which could be observed by MS, but the HPLC trace revealed a crude spectrum with multiple side products all eluting in a similar region to that of the starting material and product. The depsipeptide formation reaction was finally attempted using EDC **272** in combination with triethylamine (TEA) and the additive HOBt **279** to try and promote reaction progression. This set of reaction conditions had been used previously in the cyclisation of small *N*-benzyl α -peptoids.¹⁵⁸ Once more the resultant HPLC spectrum showed a number of different unwanted side products; but the LCMS suggested slightly better conversion to the cyclic product **273**. This reaction was repeated, heating (MW) the final mixed solution at 50 °C for 45 minutes, improving the conversion slightly to 23%, but with no improvement on the purity. Due to poor reaction progression and the formation of multiple side products and/or degradation products, none of these reactions were further developed.

Entry	Coupling agent	Base	Additive	Solvent	Temperature	Linear : Cyclised ratio (LC)
1	EDC	DMAP	-	DMF	rt	86:14
2	PyBOP	DIPEA	-	DMF	rt	np
3	PyBOP	DIPEA	-	DMF	60 °C	np
4	HATU	DIPEA	-	DMF	rt	92:8
5	EDC	TEA	HOBt	DMF	rt	86:14
6	EDC	TEA	HOBt	DMF	rt addition, then μ wave at 50 °C, 45m	77:23

Table 13 – Conditions screened for the side-chain-to-tail cyclisation of linear Ac-tAR(Pbf)I-OH **256** to form the cyclic tetrapeptide **273**. Product ratio determined by peak integration in LCMS.

As the model tetrapeptide **256** used contained a somewhat bulky Pbf protecting group, the optimum esterification conditions from the screen were applied to a different linear model with less steric bulk to see if percent conversion could be improved. This was synthesised using the same method as previously (Scheme 37); with replacement of Arg(Pbf) with Lys(Boc). The linear precursor Ac-tAK(Boc)I-OH **281** (synthesised in 62% yield based on initial 0.06 mmol loading) was dissolved in DMF with TEA and added to a stirred solution of EDC **272** and HOBt **279** in DMF. The reaction was attempted solely at room temperature; and also with a latter microwaving step as previously performed (Table 13, Entry 6). These reactions progressed with the same issues observed as for Ac-tAR(Pbf)I-OH **256**; low conversion to the cyclic product **206** with multiple side-reactions, making purification difficult and low-yielding. Due to the poor results obtained,

and because this macrolactamisation strategy was limited to certain amino acid variations and protecting groups, an alternative cyclisation strategy involving amide bond formation was investigated to try and improve yields and purity.

4.4 Cyclisation via solution-phase macrolactamisation

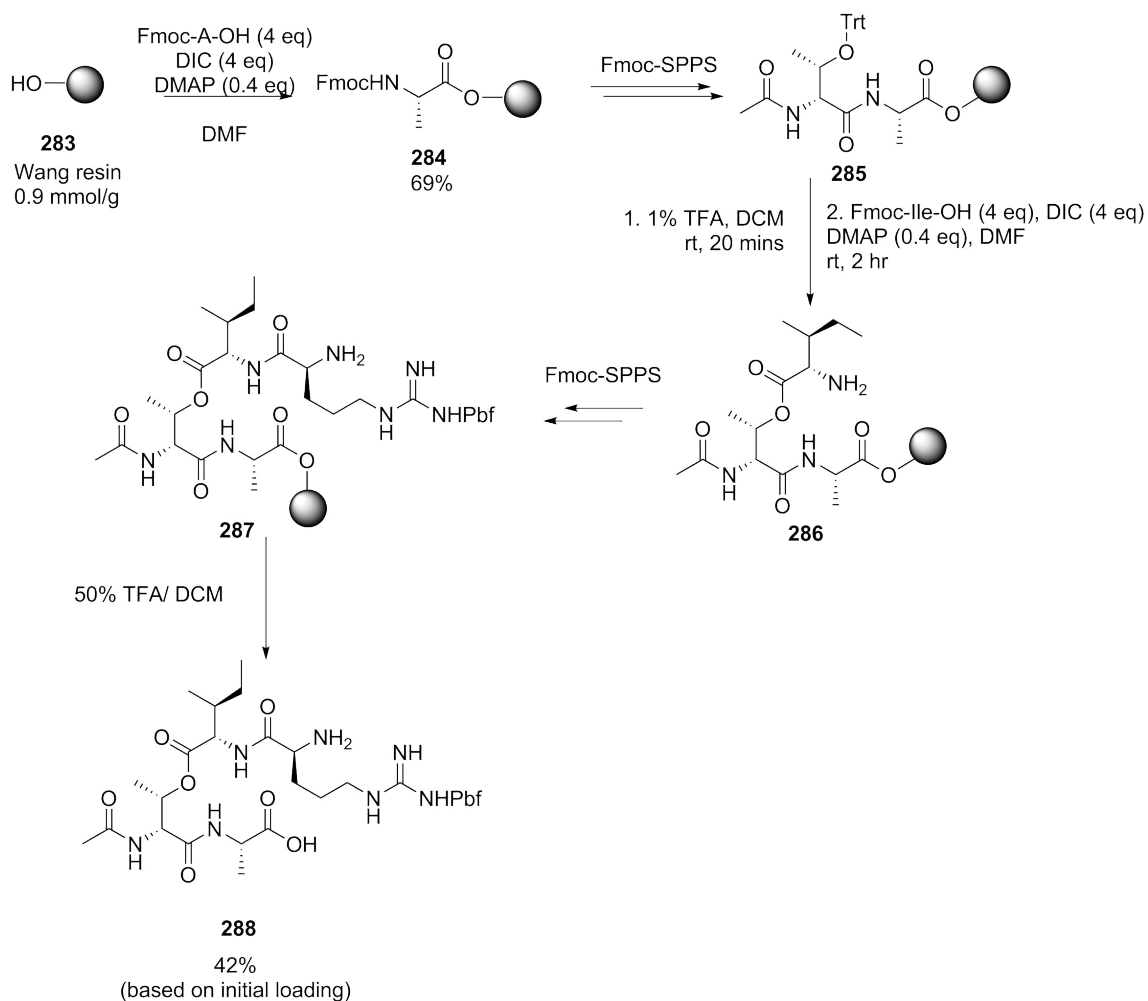
A new cyclisation strategy was required in place of macrolactamisation; due to low conversion, low overall yields and multiple side products, which could not successfully be overcome by optimisation of reagents and reaction conditions. Previous work had attempted cyclisation via amide-bond formation whilst on solid support using a safety-catch resin (Chapter 3). To apply this method to a solution-based approach, the synthesis of a similar peptide precursor could largely be translated straight from this work. In this synthesis, the depsipeptide bond between threonine and the carboxylate of Fmoc-Ile-OH was formed using DIC and DMAP in DMF. On sulfonamide resin, this reaction progressed efficiently; with 100% conversion over 2 hours, monitored using mass spectrometry and HPLC (Scheme 30).

Safety-catch resin-linked peptides were synthesised with both Ala or D-thr(tBu) as the first residue coupled to the solid support **198**. Loading of Fmoc-Ala-OH provided higher loading due to reduced steric hindrance – a significantly smaller side chain in addition to no protecting group. This strategy also has the advantage of making End10, or related residue 10 substitutions, the last residue to be coupled prior to cleavage, meaning that the other three residues of the macrocycle could be coupled in a bulk synthesis before splitting to screen the various mutations.

Initially, solution phase cyclisation was attempted using a model acetylated tetrapeptide with an Arg10 mutation, synthesised on Wang resin **283**. This mutation was selected initially owing to the lower probability of side reactions occurring from the arginine guanidine; Pbf one of the more acid stable protecting groups used in Fmoc-SPPS and the guanidine functionality should not be nucleophilic enough to cause side reactions in the event the selected reaction

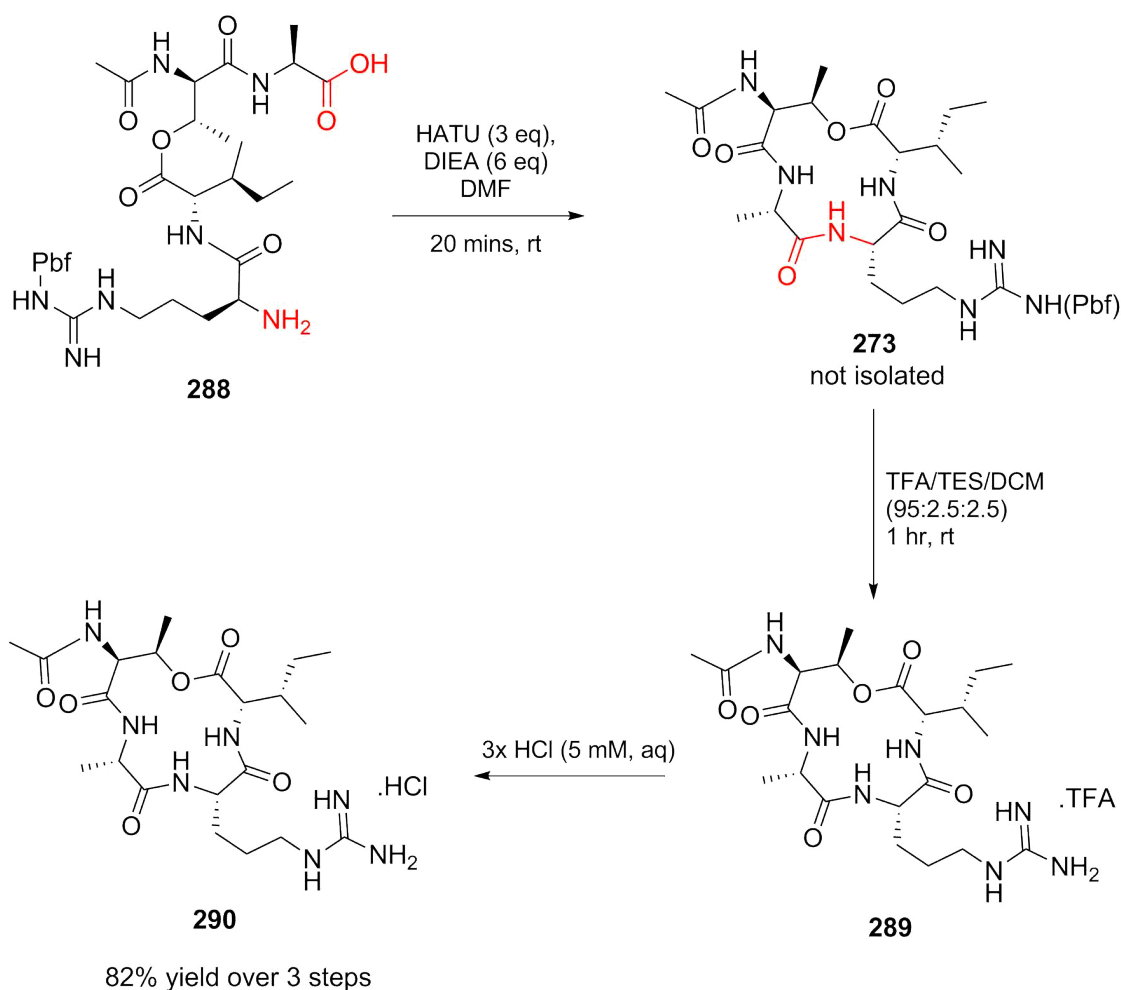
conditions resulted in its removal. Wang resin **283** is more stable to mild acidic (1% TFA) conditions compared to 2-chlorotrityl resin **257**.

Wang resin **283**, with a hydroxyl linker, requires reactions suitable for esterification to load the first amino acid. Fmoc-Ala-OH **209** was dissolved in DMF with catalytic DMAP **269** and added to the resin, before addition of DIC, and 63% conversion to **284** was achieved after 2 hours at room temperature (Scheme 42). Standard Fmoc-SPPS was used to give Ac-D-Thr(Trt)-A on resin (**285**), of which the trityl group was subsequently deprotected with 1% TFA/ DCM. Esterification was achieved with Fmoc-Ile-OH **258**, DIC and DMAP **269** in DMF; with 100% conversion to **286** over 2 hours at room temperature, similarly to peptide on sulfonamide resin **198** (Scheme 30). In comparison, one of the benefits of Wang resin **283** is that unlike the safety catch, it can easily be cleaved, allowing for facile analysis of reaction progression and peptide purity, rather than having to activate the linker and cleave by derivatisation with benzylamine. After all four amino acids were coupled, peptide was cleaved from Wang resin **283** to give the pure linear peptide **288** in 42% yield after purification by RP-HPLC. The crude purity (80%) was slightly lower than similar linear tetrapeptides; with the next most abundant product appearing to be an epimer; with racemisation most likely taking place during the initial loading of resin.



Scheme 42 – Synthesis of a branched tetrapeptide precursor *Ac-t(IR[Pbf])₂-NH₂-OH* **288** in 42% overall yield, for solution-phase cyclisation by macrolactamisation, as opposed to the macrolactonisation reactions attempted previously.

These macrolactamisation reactions were performed using the same method as for the depsipeptide formation previously attempted (Section 3.4, Scheme 31); linear peptide precursor **288** was dissolved in DMF and added dropwise via syringe to a stirred solution of coupling agent over 20 to 30 minutes, maintaining both solutions at very dilute concentrations (1- 10 mM) to avoid oligomerisation. In the initial reaction, HATU **280** (7.5 mM) was used as the coupling agent (Scheme 43). *Ac-tA[IR(Pbf)]₂-OH* **288** (10 mM) was dissolved with DIPEA (6 eq) and added over 20 minutes: once complete, the resultant solution continued to be stirred and was analysed by ESI MS and HPLC at t=0, t=1 hr and t=2 hr.



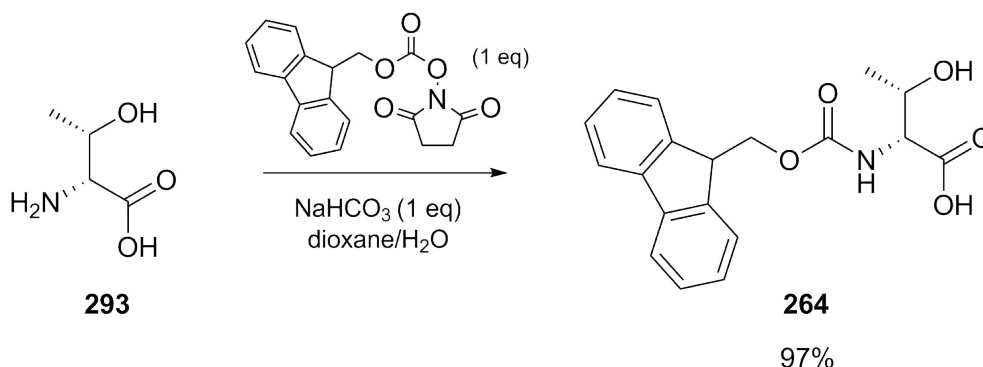
Scheme 43 – Cyclisation of the branched tetrapeptide Ac-t(IR[Pbf])-NH₂-OH **288** to form Arg-Pbf compound **273**, which was deprotected with 95% TFA to yield **289** as a TFA salt. This was replaced with an HCl salt using lyophilisation to yield the final teixobactin macrocycle analogue, cyclic Ac-t(IR)A.HCl **290**

Somewhat surprisingly, the cyclisation reaction to give **273** resulted in 100% conversion from the starting material **288**, with the peak corresponding to the linear peptide starting material not observed up to the limits of detection of HPLC; nor any reasonable peaks by MS. This was apparent even in the sample taken immediately after the last drop of peptide/base was added. After the solution was concentrated *in vacuo* and treated with TFA spiked with TES/DCM to remove Pbf protection from the arginine residue to yield the final acetylated cyclic peptide, MS analysis showed the cyclic (M+H)⁺ peak (*m/z* = 484) was the major peak with positive ionisation, and *m/z* = 596 (M+TFA-H)⁻ visible in negative mode. Given the absence of starting material **288** and one sole pure product peak **273**, it appears there is extremely fast conversion to the cyclised product. Following

HPLC purification, the TFA counter ion of **289** was replaced through three successive lyophilisations from 5 mM aqueous HCl, with ^{19}F NMR used to confirm the absence of fluorine. The cyclic peptide **290** was gained pure in 82% yield based on conversion from the linear precursor, and 11% yield based on the initial loading of Fmoc-Ala-OH to Wang resin.

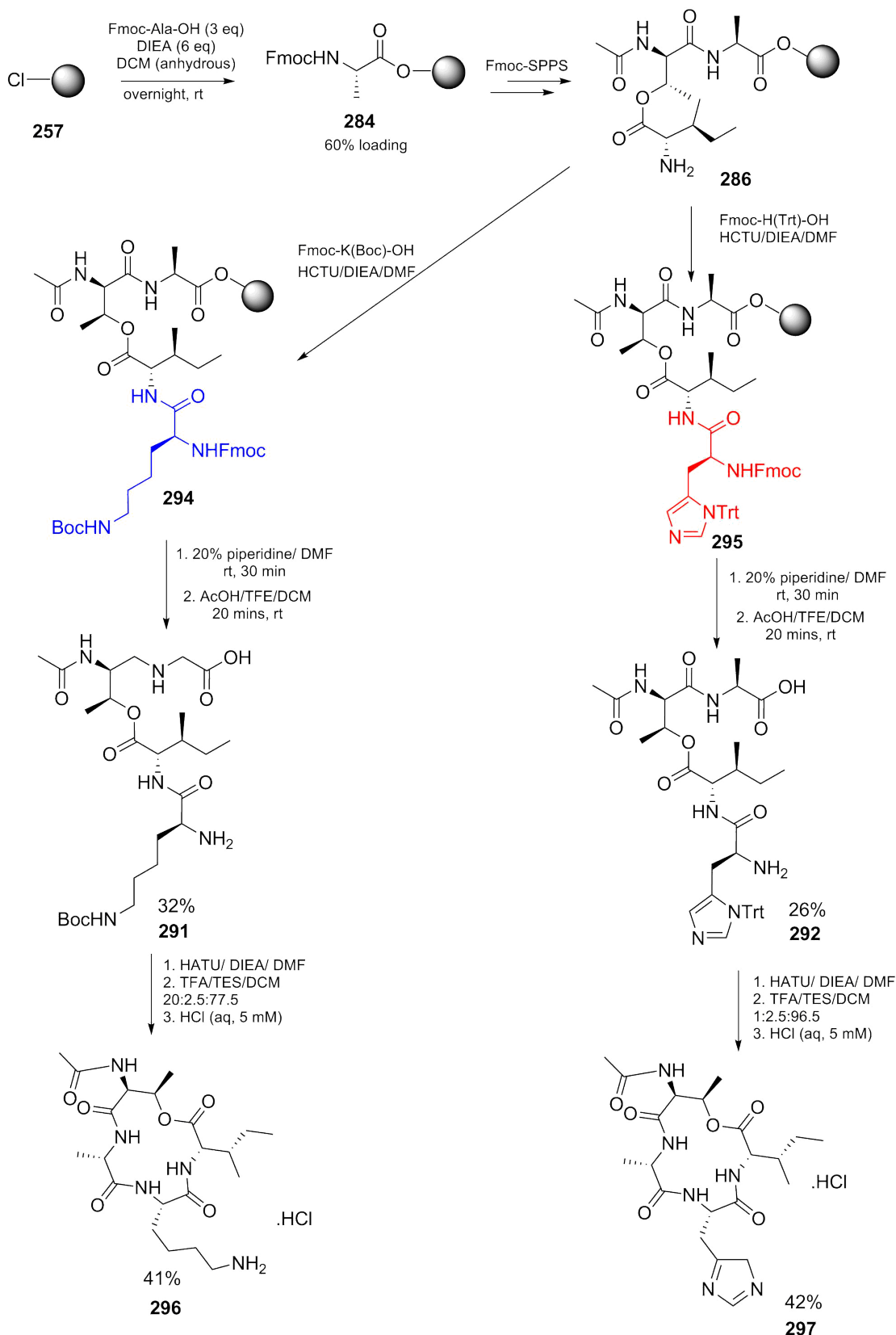
4.5 Synthesis of truncated, acetylated macrocyclic analogues

With this method in hand, two other truncated model peptides were synthesised to ensure the method could be translated to alternative resins. Wang resin **283** is unsuitable for any basic End10 mutations other than arginine, due to the high concentration of TFA required to cleave from the resin. Therefore, Ac-tAK(Boc)I-OH **291** and Ac-tAH(Trt)I-OH **292** were synthesised on 2-chlorotrityl chloride resin **257** using a similar method (to Scheme 42). As this resin **257** is cleaved with 1% TFA, Fmoc-D-Thr-OH **264** was required (without any hydroxyl protection, to allow for esterification). This was synthesised from D-threonine **293**, using Fmoc *N*-hydroxysuccinimide ester (FmocOSu) with NaHCO_3 in dioxane/ H_2O , using a published method (Scheme 44).¹⁵⁹ Use of unprotected threonine is usually avoided due to potential acylation of the hydroxyl group, which has been observed occurring during coupling reactions with active esters.¹⁶⁰ However, during these syntheses, no acylation at this position was observed by LCMS.



Scheme 44 – Synthesis of Fmoc-D-Threonine **264** from D-threonine **293**, used in synthesis of cyclic tetrapeptides.

The synthesis of each linear tetrapeptide **291** and **292** was carried out on the same batch of resin **257** initially, and split at the point immediately prior to the coupling of the final, mutated amino acid residue (Scheme 45). Cleavage from the resin was achieved with AcOH/TFE/DCM (1:2:7) over 20 minutes at room temperature. The reaction time was particularly crucial in the case of the His10 analogue **295**: cleavage tests were performed for differing lengths of time (20, 45 and 60 minutes). In the latter two reactions, significant quantities of Trt-deprotected peptide were observed in the mass and HPLC spectra. Whilst a small amount of trityl was cleaved after twenty minutes, this appeared to be a sufficient length of time to both maximise cleavage from the resin and minimise trityl deprotection. Due to the nucleophilicity of the unprotected and deprotonated histidine imidazole, reaction conditions were used that minimised trityl removal. Similarly to the arginine analogue **288**, the cyclisation for each of these two peptides **291** and **292** progressed efficiently over the course over 20 minutes, both showing 100% conversion by analytical HPLC. Final pure yields are reported after purification by RP-HPLC and conversion from the TFA to the HCl salt.



Scheme 45 – Synthesis of cyclic truncated peptides *Ac-t(IK)A.HCl* **296** and *Ac-t(IH)A.HCl* **297** from respective linear branched precursors *Ac-t(IK[Boc])-NH₂-OH* **291** and *Ac-t(IH[Trt])-NH₂-OH* **292**

With an extremely efficient cyclisation method now in hand, giving 100% conversion to the macrocycles **289**, **296** and **297** over 20 minutes, this could now be applied to more complex peptides, bearing more similarity to the full structure of teixobactin.

Based on the inactivity of a previously truncated analogue bearing an arginine mutation **116**,¹⁰⁵ it was considered unlikely that these analogues would be active against Gram-positive bacteria, but possible as these exact structures had not been made previously. It was also considered that mutation to another chemically and/or structurally similar amino acid in place of End10 may display antibacterial activity.

4.6 Synthesis of teixobactin lipopeptidomimetics

Previous experiments by a number of different research groups sought to explore the implications of variation of numerous structural and chemical features of teixobactin **42** (Section 1.4.6), mainly focusing on the relevance of the unproteinogenic L-*allo*-enduracididine **43**; the stereochemistry of each residue; and the function of residues 1-6 as a hydrophobic membrane anchor. In addition, acetylation of the N-terminus resulted in a significant loss of antimicrobial activity.^{103,104} In spite of this, little attention has been paid to the retention of a basic amine functionality at the terminus of analogous lipidated compounds. We sought to apply our efficient cyclisation strategy to the synthesis of novel lipidated analogues containing a unique hydrocarbon which had been rationally proposed to attempt to enhance the binding affinity of the compounds. In addition to lipidation, a series of End10 mutations were designed to fully probe the effect of mutations at this position, in conjunction with the lipid tail. At the time of writing, only one lipidated teixobactin analogue has since been published: lipobactin **117**, with residues 1-6 replaced with a dodecanoyl tail.¹⁰⁵ Lipobactin **117** bears an arginine at the 10 residue, but a Lys10 analogue had been found to have higher activity by the same group.

4.6.1 Prenylation of peptides and proteins

Prenylation is a naturally occurring post-translational modification event that takes place in eukaryotic cells. 3-Methyl-but-2-en-1-yl monomers make up isoprenoids, of which farnesyl (15-carbon) **298** and geranylgeranyl (20-carbon) **299** are involved in PTMs (Figure 38).¹⁶¹ Prenylated proteins are thought to have a variety of roles, and have particularly been implicated in cell signalling, and cell growth, differentiation and proliferation.¹⁶² Although there is a lack of direct evidence, isoprenoids are considered to act as protein anchors, facilitating attachment to cellular membranes. The prenylation of proteins *in vivo* involves transfer of a farnesyl **298** or geranylgeranyl **299** moiety to C-terminal proximate cysteine(s) by farnesyl transferase, geranylgeranyltransferase I and Caax protease.¹⁶² The CAAX box is a region at the C-terminus of particular proteins that directs the post-translational modification; where C = cysteine, A = any aliphatic residue, and X = determines which enzyme acts on the substrate. Where X = serine, methionine, alanine or glutamine, the protein becomes farnesylated; and where X = leucine or isoleucine, the modification is a geranylgeranyl group.¹⁶³ Such substrates are typically G-proteins, such as Ras and GTPases.

Aside from isoprenoids, S-palmitoylation and N-myristoylation are other commonly observed post-translational modifications resulting in lipidated proteins (Figure 40). Palmitoylated proteins contain a 16-carbon saturated fatty acyl **301** attached via a cysteine thioester. Unlike isoprenoids, this is not limited to the C-terminus, and can occur anywhere throughout the protein. The modification is reversible; allowing the protein to be “switched on and off”. N-myristoylation solely occurs at the N-terminus of a protein, and not on amino acids with nucleophilic side chains, such as lysine. The addition of myristoyl **300**, a 14-carbon saturated fatty acid, is catalysed by N-myristoyltransferase (NMT) at the N-terminus of glycine via amide bond formation.¹⁶⁴

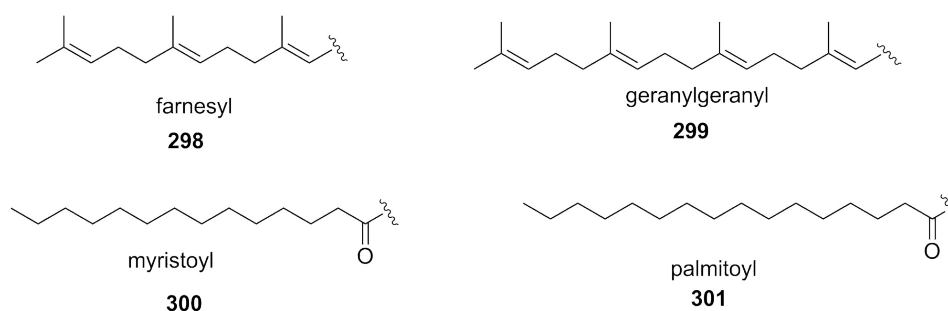


Figure 40 – Common lipid-derived post-translational modifications of peptide and proteins

Some strains of bacteria, such as the human pathogen *Legionella pneumophila*, have been observed to express CAAX motif proteins which hijacks host enzyme machinery in order to increase its own membrane binding and localisation, and subvert cellular processes within the host.¹⁶⁵ Bacteria also contain three native proteins that catalyse lipidation of proteins and peptides: Lgt, Lsp and Lnt.

Cationic antimicrobial peptides that bind to the bacterial cell wall precursors generally contain a lipid-like, hydrophobic moiety in at least one region of the molecule. This is true of teixobactin **42** and vancomycin **10**; bearing short saturated modifications at the N-terminus; teicoplanin **26** including 8-methylnonanoyl; and enduracidin **45** and ramoplanin **51** that contain lipids with both saturated and unsaturated regions (Figure 41). Derivation of peptides and peptoids with N-terminal lipidation has previously been found to increase antimicrobial activity.¹⁶⁶⁻¹⁶⁸ In addition to providing a cellular membrane anchor, lipidation can also improve protease-resistance and enhance bioavailability.

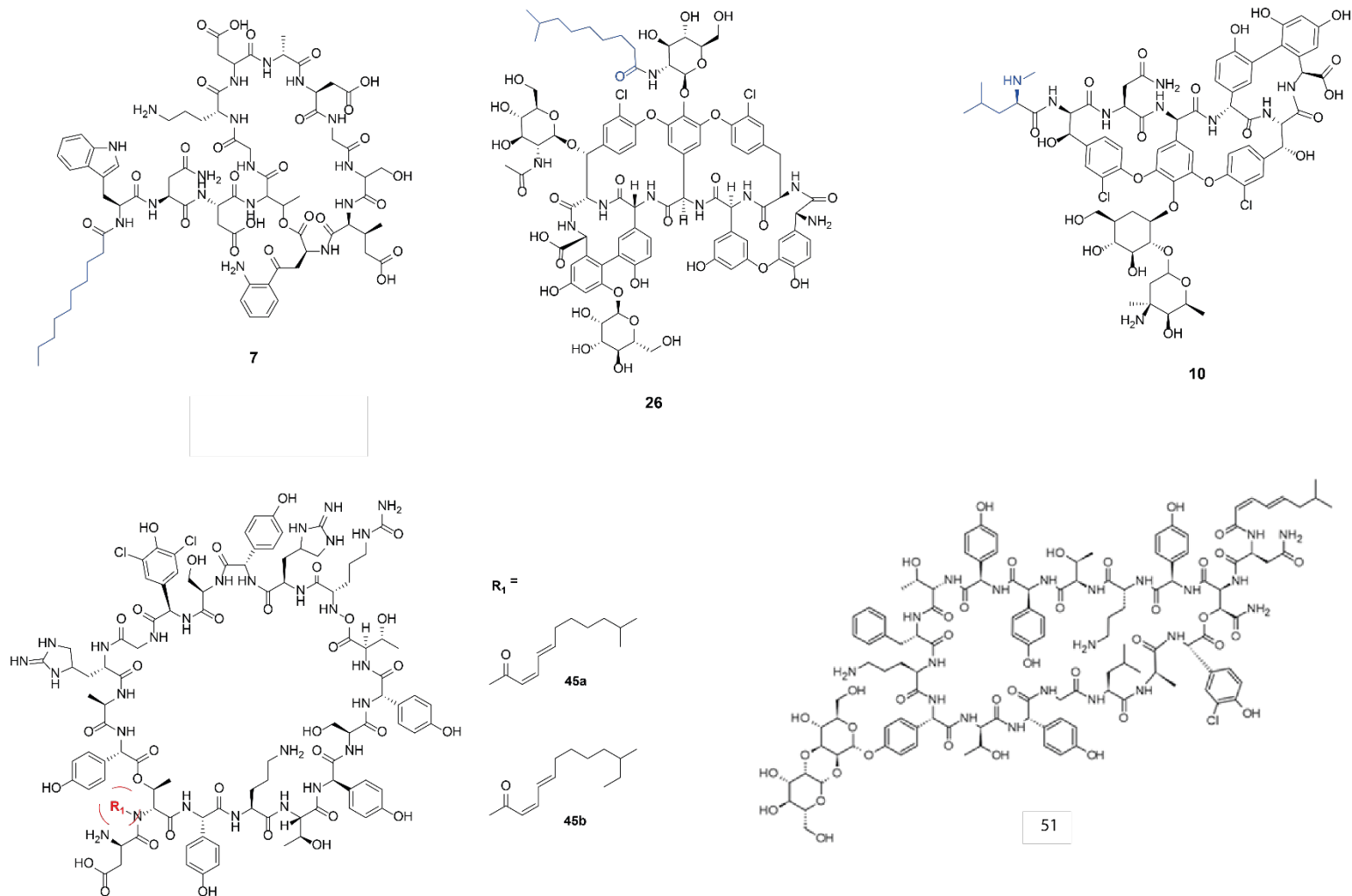


Figure 41 – Structures of naturally lipidated antibacterial compounds daptomycin **7**, teicoplanin A₂-2 **26**, vancomycin **10**, enduracidin A **45a** and B **45b**, and ramoplanin **51**.

Most previous lipidated peptidomimetics used simple saturated fatty acids to derivatise the N-terminus; but little attention has been paid to the fact many naturally occurring AMPs contain unsaturated regions. The cellular target itself, lipid II, contains a polyprenyl bound to the pyrophosphate moiety, and bacterial phospholipid membranes generally contain polyunsaturated and *trans*-unsaturated fatty acids. Reduction of saturated chains may be employed by Gram-negative bacteria to increase rigidity of antimicrobial products, and by more effectively anchoring the antibiotic into the membrane binding to the cellular target at another region of the AMP may be promoted. Therefore, it was hypothesised that replacement of the teixobactin **42** hydrophobic tail with an isoprenoid may induce better antibiotic activity compared to a saturated chain.

Concerning selection of the size of the isoprenoid derivatives, we aimed to achieve a balance between a chain long enough that would allow effective membrane anchorage, but also a short enough length to limit the overall hydrophobicity and retain water solubility of the teixobactin **42** analogues. Prenylation of large proteins involves farnesyl **298** and geranylgeranyl **299**, but these are unlikely to have a considerable effect on solubility; however of a 4-residue macrocycle of less than 500 Da these may have a more considerable influence. Therefore geranyl **302** (10 carbons) and farnesyl **298** (15 carbons) were selected for analogue lipidation, rather than longer isoprenoids like geranylgeranyl **299**. Chemically reactive derivatives of these isoprenoids were also much more commercially available.

Prenylation of synthetic peptides has previously been used for the investigation of mechanism of cellular uptake of fluorescent cell-penetrating peptides, such as CDC42 C-terminal mimics.^{169, 170} In these studies, peptides were synthesised on resin and after cleavage, cysteine thiols were prenylated using the isoprenoid bromide in solution with zinc acetate.

4.6.2 Synthesis of *N*-terminus prenylated teixobactin analogues

To produce prenylated teixobactin analogues, the ideal lipidation would take place directly on the *N*-terminus, replacing the acetyl group of the previously synthesised truncated compounds (Figure 42).

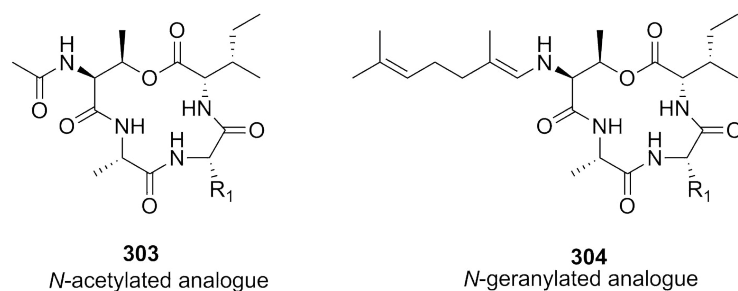
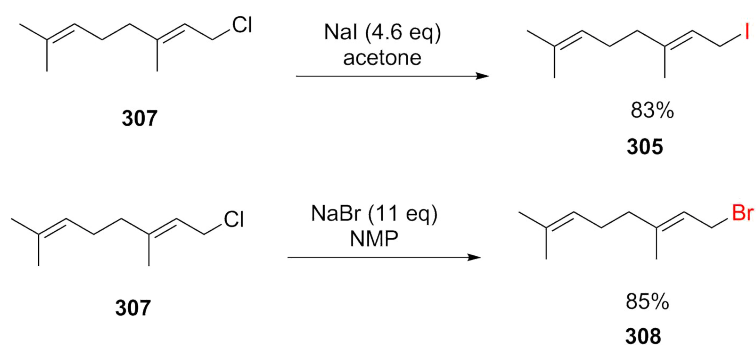


Figure 42 – General structures of *N*-acetylated analogues and *N*-geranylated analogues

Prenylation of amines and amides does not occur in eukaryotic cells, and few examples of bacterial *N*-prenylation have been reported.^{171, 172} Thiols are significantly more nucleophilic than amines, and amines require stronger base to be deprotonated; the pK_a of amines is significantly higher than that of thiols (35, compared to 10-11, or 8.2 in the case of cysteine thiols). However, as this would allow a simple adjustment of the previously employed synthetic route if successful, the potential of this method justified investigation.

Known to be reactive with cysteine thiols, isoprenoid halides were employed in attempted *N*-prenylation reactions.¹⁷⁰ Theoretically, the prenyl iodide should be the most electrophilic; followed by bromide and finally chloride. Initial test reactions were performed solely with geranyl derivatives **305**, **307** and **308** rather than farnesyl for ease of analysis. Geranyl iodide **305** and farnesyl iodide **306** are not commercially available, so the former was synthesised from geranyl chloride **307** using the Finkelstein reaction. This starting material was also used to synthesise the bromide derivative **308**.



Scheme 46 – Synthesis of Ger-I **305** and Ger-Br **308** from Ger-Cl **307** by Finkelstein reaction.

Unlike formation of geranyl bromide **308**, which resulted in a pale yellow transparent liquid, geranyl iodide **305** was isolated as a dark brown viscous oil. Despite the relatively clean reaction conditions and work up, the ^1H NMR showed the product to be fairly crude; suggesting that while the iodide **305** may have superior reactivity, it is also much more susceptible to spontaneous degradation, which is likely to be why it is not a commercially available reagent.

The geranyl halide derivatives **305** and **308** were confirmed by mass spectrometry, and by a consistent C1 shift in the ^1H NMR compared to Ger-Cl **307** starting material (Figure 43).

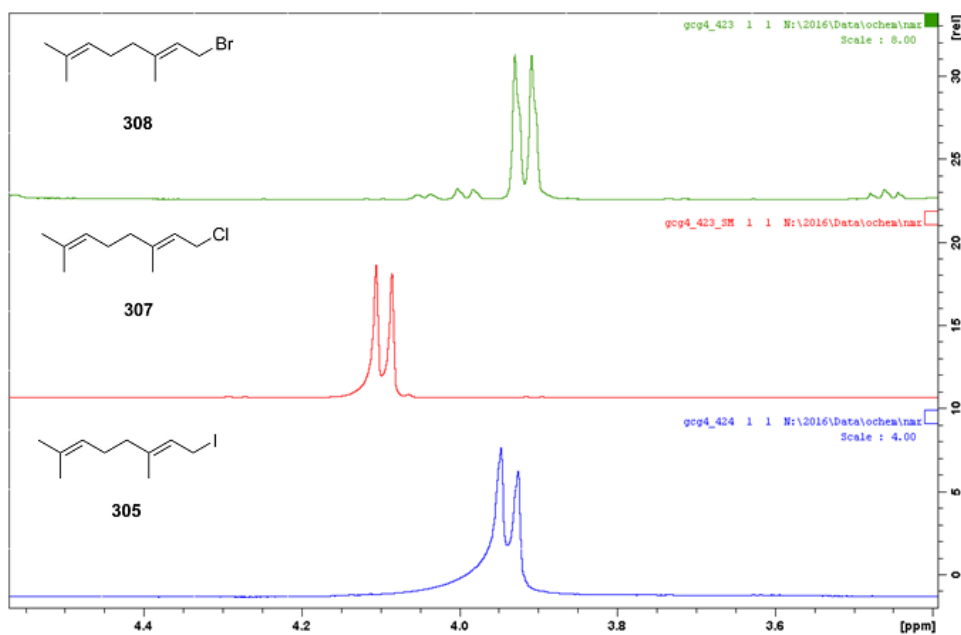
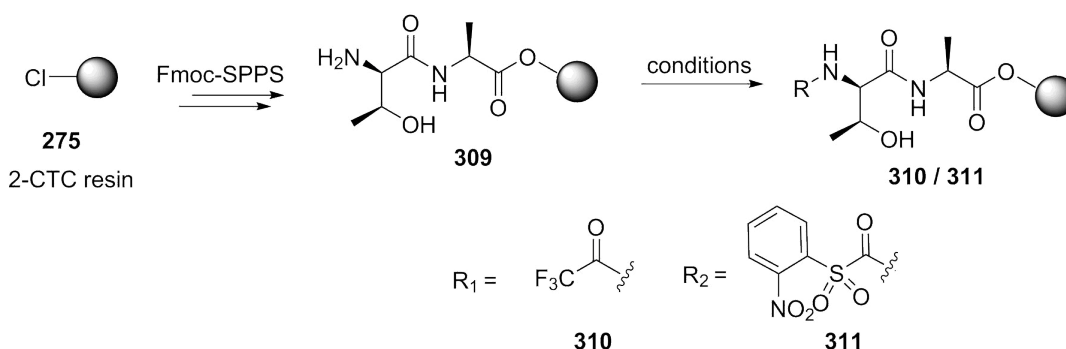


Figure 43 - ^1H NMR C1 shifts of Ger-Br **308** (top, green) and Ger-I **305** (bottom, blue) synthesised from Ger-Cl **307** (red, middle)

To achieve *N*-prenylation, deprotonation of the amine with a strong base could be attempted; however this would be incompatible with the rest of the peptide synthesis and would likely result in α -proton abstraction via oxazolone formation, leading to multiple epimers and isomers, resulting in a lower purity and yield of the final product. Prenylation reaction conditions were tested using a simple dipeptide bound to 2-chlorotrityl chloride resin (**309**). To prevent the possibility of bis-alkylation, *N*-terminus amine protection was carried out prior to prenylation.

The conditions employed were based on those found to be optimum for *N*-alkylation with saturated hydrocarbons.^{173, 174} Reactions were carried out on model peptides on resin, bearing either no *N*-terminus protection, TFA protection, or 2-nitrobenzenesulfonamide protection (Scheme 47), using geranyl bromide, geranyl iodide or geraniol (with a terminal hydroxyl group)



Scheme 47 - Protection of model peptide $\text{H}_2\text{N-tA}$ on resin. For TFA protection **310**, conditions = *ETFA* (10 eq), *DBU* (12 eq) in *DMF*, *rt* 1 hr. For 2-NBS protection **311**, conditions = 2-NBS-Cl (5 eq), *DIPEA* (5 eq) in *DMF*, *rt* 1 hr.

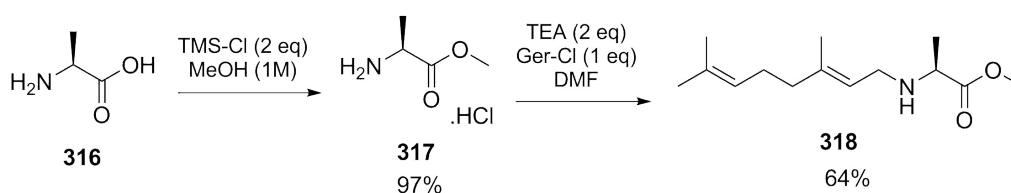
Prenylation of dipeptides **310** and **311** was attempted under a range of conditions (Table 14). *N*-trifluoroacetate protected peptide **310** displayed very poor conversion to geranylated product **313** in a range of reaction conditions; some product was observed using Ger-Br **308** and geraniol **312** at room temperature, but an increase in temperature did not increase product formation. Use of geranyl iodide **305** resulted in no visible conversion to the prenylated amide, possibly due to the low purity and high instability of the reagent. Where 2-NBS **311** was used as the protection strategy rather than TFA-protection **310**, a small amount of product **314** formation was observed at elevated temperature; although this was

difficult to quantify as multiple side products appeared to be produced in these reactions. None of the reactions attempted resulted in significant formation of any of the *N*-prenylated products. As the risk of bis-alkylation seemed minimal, and the protection resulted in conversion of the amine to the less reactive amide, the prenylation was attempted using the dipeptide without *N*-terminus protection (**309**); however this appeared to yield no determinable product conversion whatsoever. On-resin *N*-prenylation was therefore deemed to not be a viable option in analogue synthesis.

Entry	N-terminus protection	Isoprenoid	Base/Catalyst	Solvent	Temp	Product formation (ESI MS, HPLC)
1	TFA 310	Ger-Br 308	DBU	DMF/NMP	rt	np
2	TFA 310	Ger-Br 308	DIPEA	DMF	rt	Negligible
3	TFA 310	Ger-I	DIPEA	DMF	rt	np
4	TFA 310	Ger-Br 308	DIPEA	DMF	rt	np
5	TFA 310	Ger-Br 308	DIPEA	DMF	50 °C	np
6	TFA 310	Geraniol 312	PPh ₃ , DIAD	THF (anhy.)	rt	Low, multiple byproducts
7	2-NBS 311	Ger-Br 308	DIPEA	DMF	rt	np
8	2-NBS 311	Ger-Br 308	DIPEA	DMF	50 °C	Low, multiple byproducts
9	2-NBS 311	Ger-Br 308	DIPEA	DMF	75 °C	Low, multiple byproducts
10	None (H ₂ N-) 309	Ger-Br 308	DIPEA	DMF	rt	np
11	None (H ₂ N-) 309	Ger-I 305	DIPEA	DMF	rt	np

Table 14 – On resin *N*-geranylation reactions of H₂N-*t*A-resin without *N*-terminal protection (**309**) and with TFA (**310**) and NBS (**311**) protecting groups. np = no product formation. Any by-product formation was not characterised.

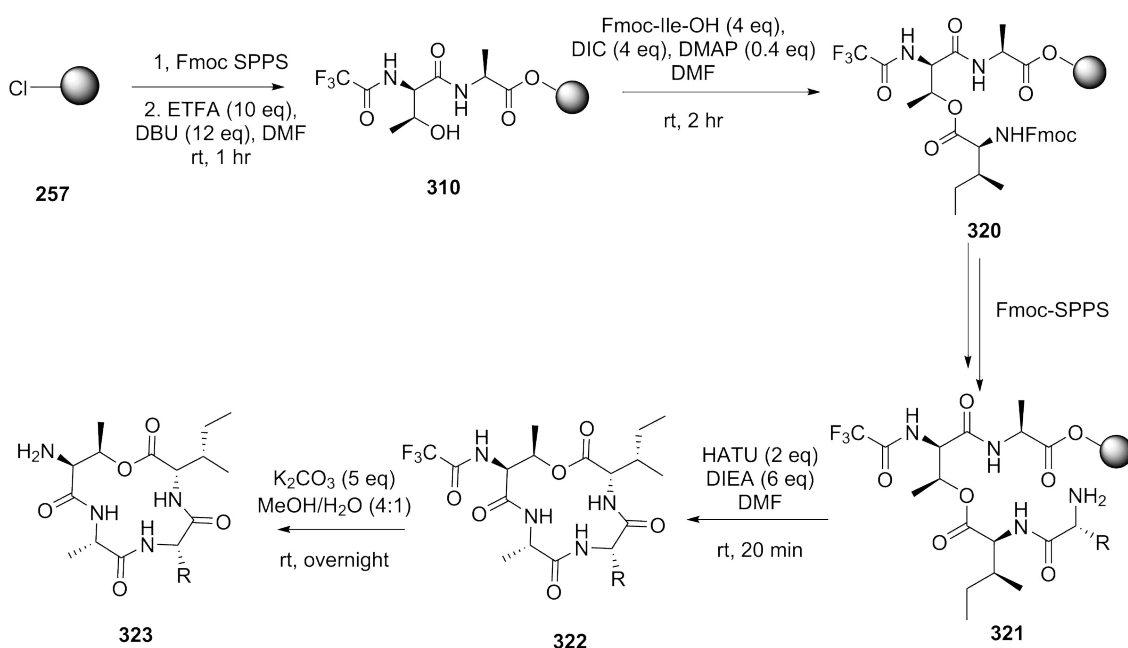
To examine whether *N*-prenylation would proceed off resin, the reaction conditions were applied to L-alanine methyl ester hydrochloride **317**, which was synthesised from L-alanine **316** in order to improve the solubility in DMF (Scheme 48).



Scheme 48 – Synthesis of *N*-geranyl alanine methyl ester **318** from *L*-alanine methyl ester hydrochloride **317**, synthesised from *L*-alanine with TMS-Cl in methanol.

Briefly, *L*-alanine methyl ester was dissolved in DMF with triethylamine and cooled to $-15\text{ }^{\circ}\text{C}$ before the addition of geranyl chloride (1 eq). The reaction was kept cold for 30 minutes before warming to room temperature. Analysis by TLC and mass spectrometry showed two major products in addition to leftover starting material; the mono- **318** and bis-geranylated **319** forms, with the mono-alkylated as the major product. The two products were isolated with flash chromatography. These results suggested that a better level of prenylation may be achieved by conducting the reactions off-resin, rather than while the peptide is still on the solid support, although the high level of bis-alkylation would result in a significant drop in yield, may elute at a similar time to a mono-alkylated cyclic peptide.

In order to investigate if *N*-prenylation was possible as the penultimate step of the total synthesis (prior to deprotection of amino acid side chain protection), a cyclic peptide with a free N-terminus amine was synthesised (**323**, Scheme 49). This was achieved by adapting the synthesis of the truncated analogues by replacing the acetyl cap with a protecting group that could be removed in mild conditions.



Scheme 49 – General synthetic route to cyclic tetrapeptides **323** with no N-terminal protection for N-prenylation reactions via N-TFA protected intermediate **322**

TFA as a protecting group had previously been used in model peptide reactions and is removed with weak aqueous base,¹⁷⁵ compatible with the peptide and side chain protection, in order to prevent premature deprotection and epimerisation. In practice, for both cyclic peptides synthesised for this experiment (Arg10 (**324**) and Lys10 (**325**) variations), total removal of the N-terminal TFA protection could not be achieved with mild heating, or even with heating under reflux. In the case of the Lys10 cyclic peptide **325**, an unusual product **326** was formed during the attempted deprotection; where the TFA protection had been removed, but the cyclic product had undergone some form of dimerisation. HRMS showed formation of a product **326** with a molecular mass of 1029 Da, as well as a small amount of the Boc-deprotected form **327** (929 Da), suggesting this was some form of peptide side product. This could possibly be a reaction of the free amine cyclic peptide **207** with a hydrolysed linear form **328**; but this resulted in a molecular mass of 1027, and hydrolysis of the depsipeptide had not been previously observed under any other conditions.

Before this dimerisation side-reaction was determined, this 1029 Da product **326** was thought to be the correct deprotected structure, with a peak of $m/z = 1052$ in the ESI spectrum corresponding to $(2M+Na)^+$, and so this was taken forward for

prenylation following RP-HPLC purification. This reaction was attempted using the conditions applied previously to L-alanine methyl ester **317**, with geranyl chloride **307** replaced with geranyl bromide **308**. The ESI mass spectrum of the reaction after 4 hours shows peaks for the mono- (+137), and more abundantly bis- (+273) geranylated forms of the unknown peptide **326**. This suggested that *N*-prenylation of the cyclic peptide in solution as the penultimate step, prior to global deprotection, is a viable strategy for formation of these analogues. However, due to the unknown character of the peptide starting material, and the large amount of bis-alkylation that had been observed for both reactions, this route would need further adaptation to give satisfactory yields of the desired cyclic peptides. Therefore, a different prenylation strategy was designed and pursued.

4.6.3 Synthesis of cysteine-prenylated teixobactin analogues

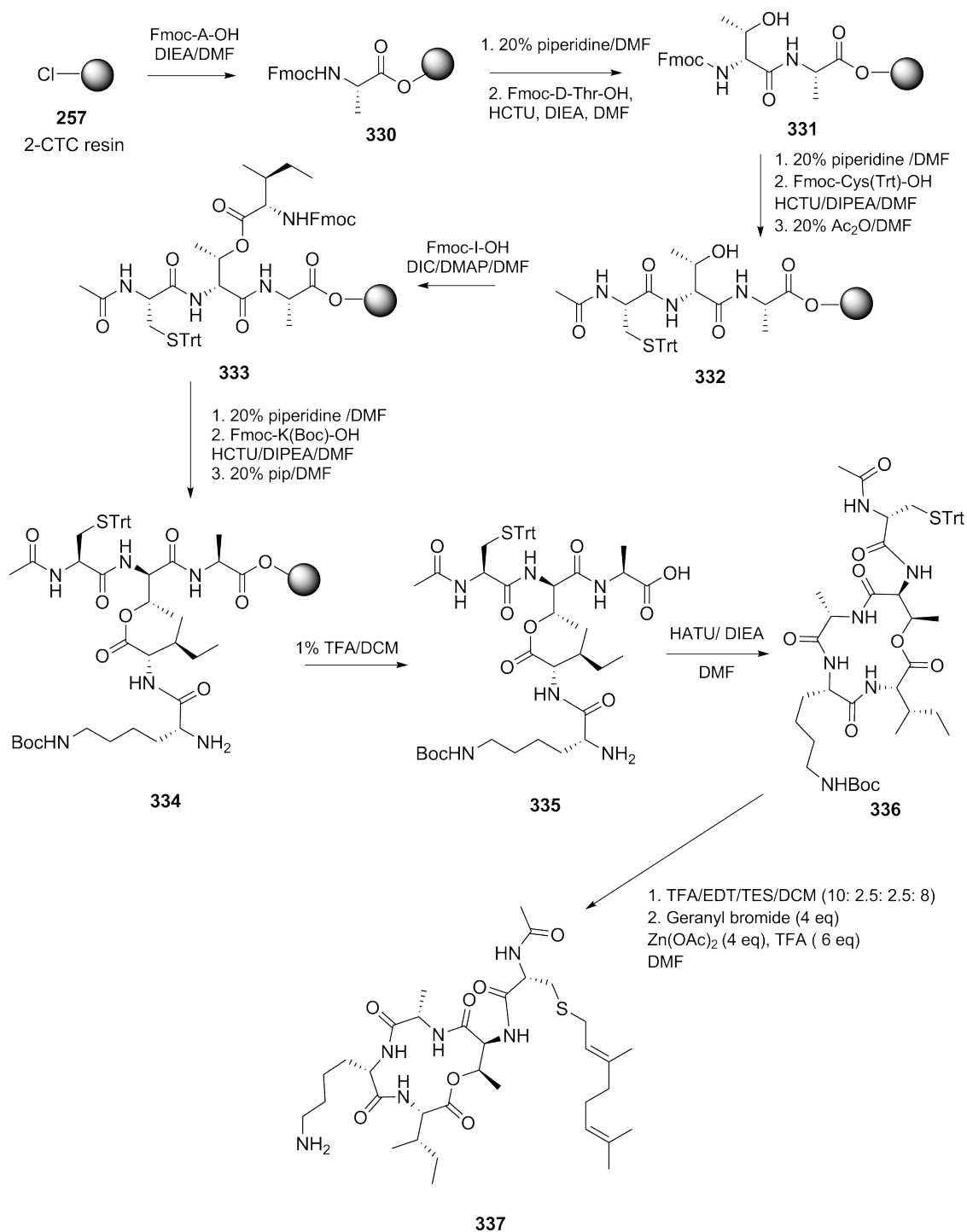
With *N*-prenylation proving difficult, attention was turned to an alternative strategy that could more closely mimic post-translational prenylation effects that occur in cells. Synthetic peptides with cysteine thiol prenylation are commonly reported in literature; generally achieved with zinc catalyst, prenyl bromide and TFA in a mix of aqueous and organic solvent.^{169,170} Mostly these cysteine prenylations were carried out on linear peptides; and with a cyclic depsipeptide in place there is potential for the hydrolysis of ester in aqueous media with strong acid.

Teixobactin **42** does not contain a cysteine residue. However, the next residue to the macrocycle is a serine. We proposed that replacement of serine to cysteine (mutation of hydroxyl to thiol) would not have a significant effect on the activity and binding of the compounds, as these residues are not too dissimilar structurally and chemically. By alkylating the cysteine thiol, this removes the increased nucleophilic character introduced at this position.

Adapting the synthetic route used for preparation of truncated analogues, Fmoc-Cys(Trt) **329** was introduced following D-Thr8, with *N*-terminal acetyl capping. As previously, this allowed orthogonal branching of residues 10 and 11, before resin cleavage and solution-phase cyclisation. After global deprotection of the cysteine

thiol trityl and any other remaining protecting groups, prenylation of thiol with an isoprenoid halide achieved the final structure.

Initially the prenylation was attempted with varying quantities of geranyl bromide **308** and zinc acetate, which were both suitably soluble in DMF, avoiding the need for aqueous conditions and the potential hydrolysis of the depsipeptide bond. However, under these reaction conditions no conversion to the desired product was detected. However, on addition of TFA to the reaction mixture, full conversion to the geranylated form **337** was observed after 45 minutes, as determined by LCMS (Scheme 50).



Scheme 50 – General scheme of cyclic cysteine thiol-prenylated peptide synthesis. The resin-bound linear branched precursor **334** is formed using standard SPPS and Steglich esterification. Cleavage from the resin with 1% TFA yields **335**, retaining Cys(Trt) protection. Cyclisation is achieved with HATU and DIPEA in DMF yields **336**; which is subsequently deprotected and prenylated to yield the final peptide **337**.

Given the high lability of the trityl group, orthogonal cysteine deprotection may be achieved in parallel with peptide cleavage from the resin using 1% TFA, however

we were pleased to find that in these conditions this was not a problem, and no trace of peptide **335** with free thiol was observed by LCMS. By repeating the reaction with 1% TFA/DCM spiked with EDT and TES, however, complete thiol deprotection was achieved to give **337**, demonstrating the necessity for these reagents in the removal of this protecting group.

With the synthesis of one prenylated teixobactin **42** analogue completed, our attention turned to other analogues with End10 substitutions to be prepared using this method (Figure 44). To fully investigate the significance of this residue, a number of different analogues were prepared, mainly focusing on chemically and structurally similar genetically encoded amino acids. In addition to the Lys10 analogue **337** that been synthesised with this method, this residue was varied to arginine **338**; the closest in character to *L-allo*-enduracididine (**43**). The effect of altering the native guanidine functionality to a urea was probed by introduction of citrulline **339** at the -10 position. Ornithine **341** analogues, a basic amino acid residue structurally similar to lysine **340** but with a slightly shorter (-CH₂) side chain, were also synthesised. His10 analogues, containing an imidazole ring **342**, were synthesised as another residue possessing a partial positive charge under physiological pH. As controls, and to further investigate whether a basic residue was entirely essential at this position, analogues containing alanine **316** (neutral, CH₃ side chain) and glutamic acid **343** (acidic) were also synthesised. Each of these seven analogues were synthesised with both geranyl **346** and farnesylation **347** at the cysteine thiol.

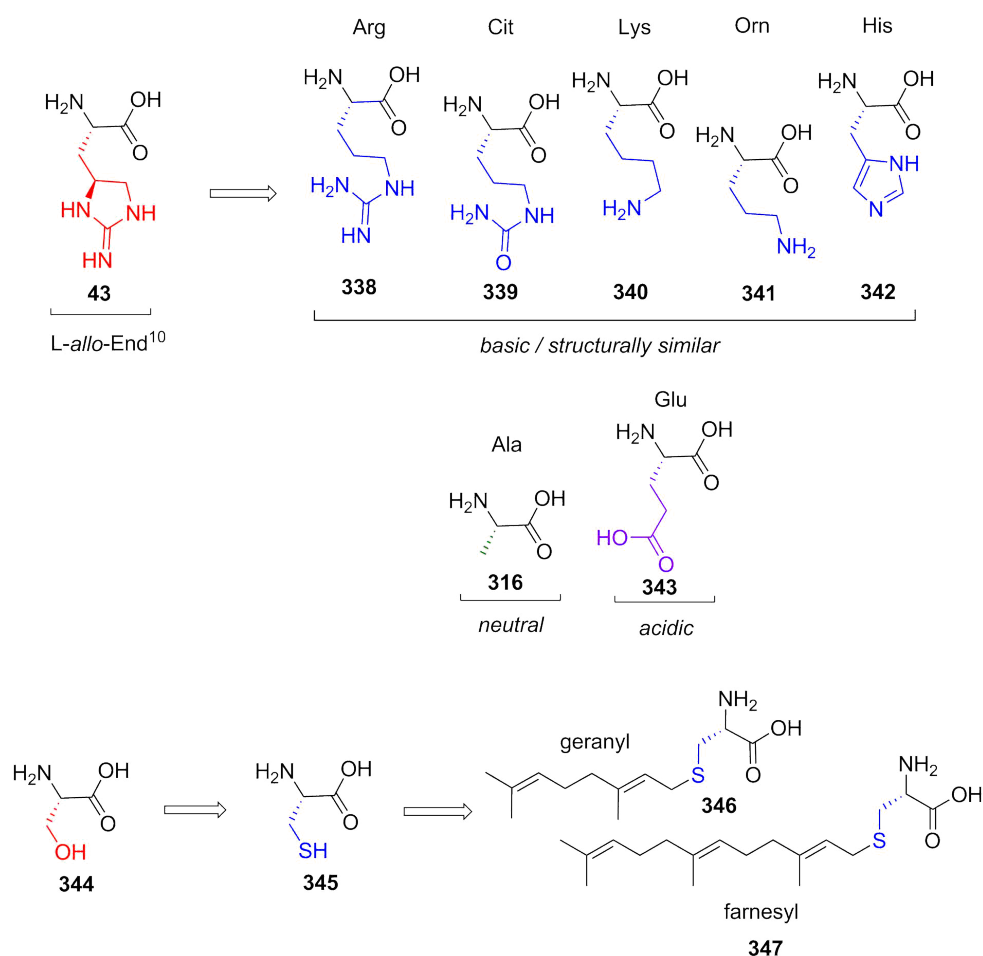


Figure 44 – Variations of residue 10, replacing the nonproteinogenic residue *L*-allo-enduracididine **43**, and variation of serine **344** to cysteine **345** to allow geranyl- and farnesylation.

The synthetic route is ideal for the synthesis of multiple *L*-allo-enduracididine **43** analogues, given that this residue is the final amino acid to be coupled prior to Fmoc-deprotection and cleavage from the resin. Therefore, the first nine steps up to that point can be performed on large scale (i.e. 1.5 mmol). In addition, the prenylation is the final step, providing ease of synthesis for compounds with varying length of isoprenoid. Previous attempts of *N*-alkylation have shown that with these reaction conditions there is little to no risk of any prenylation of any side chains other than the cysteine thiol.

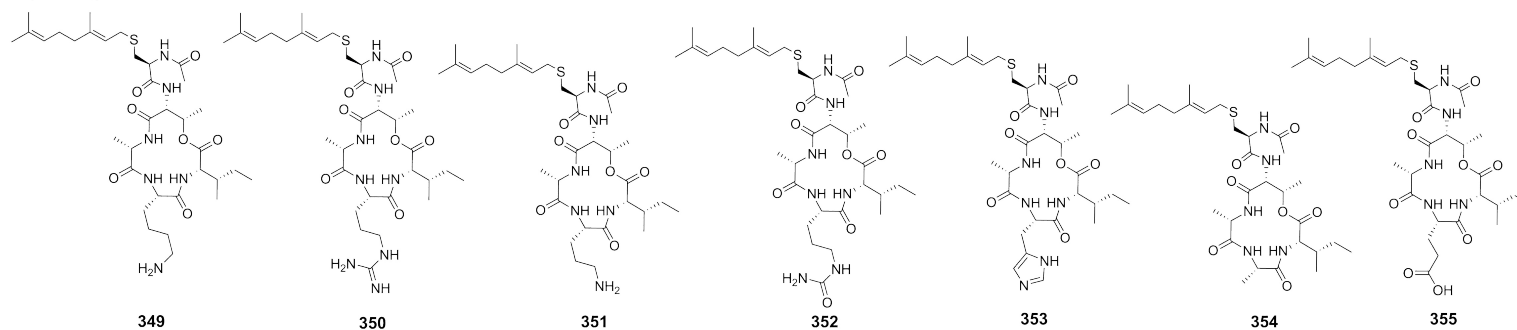
Due to the presence of trityl protection of histidine **342**, there was a possibility that the cleavage from resin could also result in the remove of trityl protection at this position, resulting in a site for potential side reactions to occur. However, we

were pleased to find that in 1% TFA/ DCM, no visible trityl removal was observed in MS or HPLC.

Crude prenylated cyclic peptides were all purified using RP-HPLC, and analysed using HPLC, HRMS, and NMR. Where possible, complete NMR assignment of these analogues was undertaken (see Experimental section 5.3.11). As previously, the final purified peptides were lyophilised with three cycles of 5 mM aqueous HCl for conversion from the TFA salt. Product mass and peptide content was determined using ^1H NMR spiked with a known quantity of *p*-nitrophenol. The antibacterial activities of these compounds are supplied at the end of this chapter, and yields and purities are located in the experimental section. To conclude, this synthesis allows the preparation of a variety of prenylated teixobactin analogues, even those with acid-labile side chain protecting groups.

A total of fourteen prenylated peptides were synthesised and purified as HCl salts (four *allo*-End10 variations, with two isoprenoids – geranyl **302** and farnesyl **298**) (Figure 45).

Geranyl analogues



Farnesyl analogues

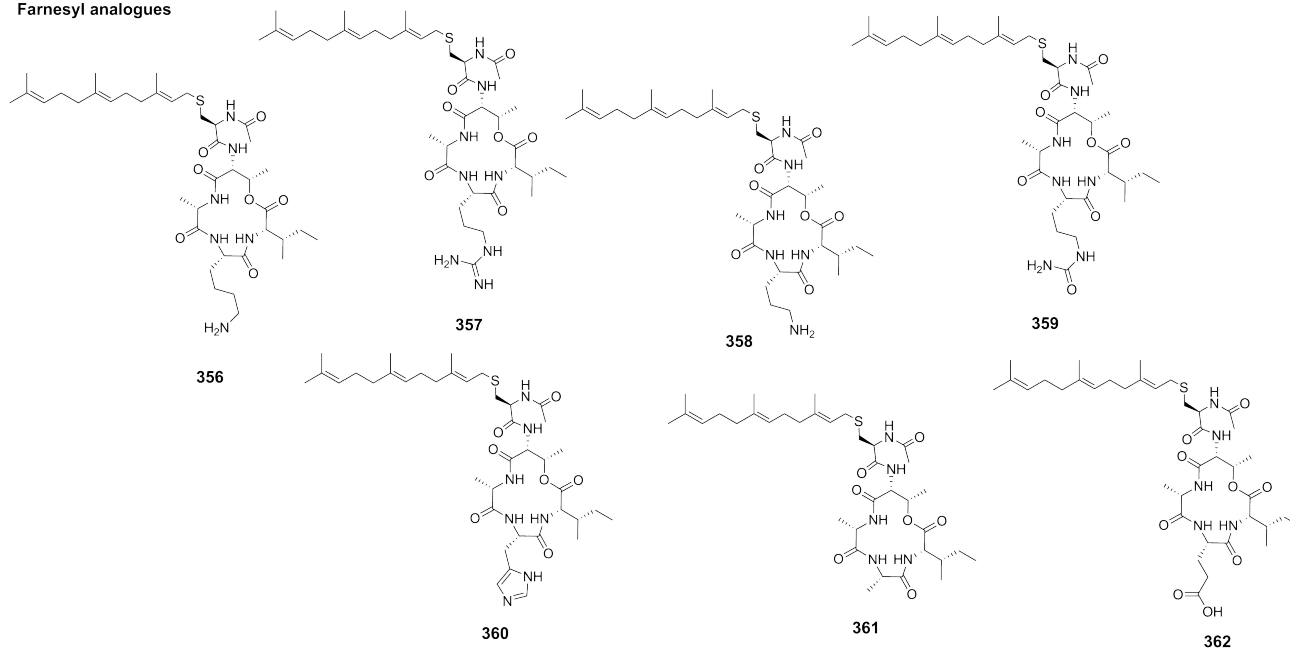


Figure 45 - Structures of all geranylated teixobactin analogues (**349 - 355**) and all farnesylated analogues (**356 - 362**) synthesised and purified as HCl salts

4.6.4 Synthesis of analogues with a positively-charged hydrocarbon tail

To date, little attention has been paid to the possible requirement of retention of a positive charge at the N-terminus of teixobactin **42**. Recent work by the Hergenrother group found that amines are commonly required for effective accumulation Gram-negative targeting antibiotics within target cells.¹⁷⁶ Some compounds, like teixobactin **42** also contained alkylated amines; although these were found to generally have reduced activity – maybe methylation is an evolutionary artefact, or possibly to prevent the action of deaminases.

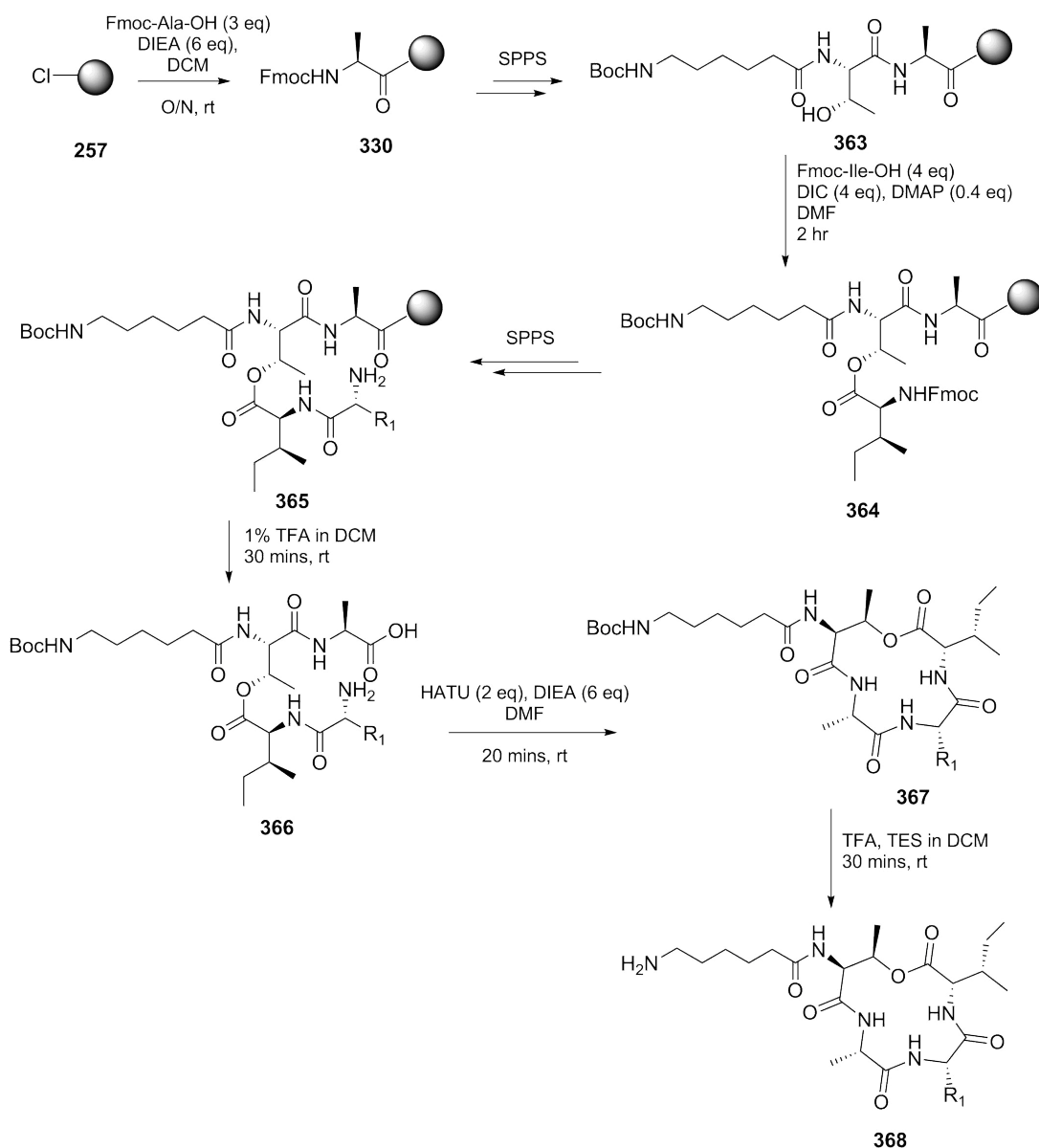
The study suggested polarity and molecular weight are key factors in the ability of compounds to traverse the outer membrane and accumulate within the cell.¹⁷⁶ Initially, they assessed a library of 100 diverse natural-product derived compounds. Most of the active compounds were found to contain an amine, be amphiphilic and rigid, and have low globularity. 12 of 41 positively charged compounds were found to accumulate within Gram-negative cells; whereas none of the neutral or acidic compounds were successful. All 12 accumulating compounds contained amines; of which 8 were primary. Conversion of these primary amines to other functional groups, such as acids, amide, esters, nitriles, azides and alcohols had deleterious effects on the levels of accumulation. Even conversion to respective secondary or tertiary amines had a significant impact on activity. Using this knowledge, the authors converted deoxynymycin, a natural product only active against Gram-positive bacteria, into one with diverse activity against a number of both positive (such as *S. aureus*) and negative (such as *E. coli* and *K. pneumoniae*) pathogens.

A basic functionality at the end of a hydrophobic region is a common component in many naturally occurring and synthetic antibiotic compounds, particularly glycopeptides and bacitracin. We propose that this positively charged entity may exist as a trans-membrane grapple: as the lipophilic portion traverses the lipid membrane, the positively charged terminus interacts with the negatively charged phosphate on the other side of the bi-layer, thus locking the antibiotic in place, and preventing removal, degradation or efflux.

We envisaged that by truncating the native structure of teixobactin to the core macrocycle and combining this with a hydrocarbon bearing a terminal amine, a series of compounds could be created that target Gram-negative bacteria as well as Gram-positive. Penicillin **1** converted to ampicillin **348** gave it broad spectrum activity¹⁷⁷ but there are few other successful cases of conversion of Gram-positive targeting antibiotics to Gram-negative as well.

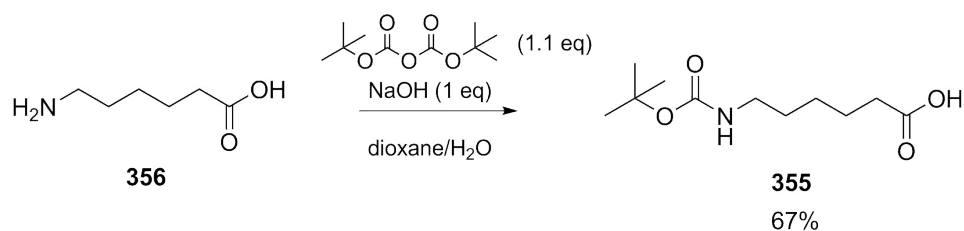
In order to enter Gram-negative cells compounds must be able to cross the larger outer membrane via pores that have an upper molecular weight limit of around 600 Da, too low for that of teixobactin **42** (1242 Da). However, with initial truncated analogues weighing around 460 Da, the addition of a short hydrocarbon may be sufficient to remain under this limit.

Lipobactin (**117**), created by Nowick *et al*, and the previously described prenylated compounds replace residues 1-6 with hydrocarbon chains, thus eliminating this terminal polarity.¹⁰⁵ Previous work by Parmar *et al* and Monaim *et al* had showed that removal of this terminal basicity by acetylation resulted in almost complete removal of antibiotic activity.^{103, 104} Therefore, a synthesis was designed to create lipidated variations that returned this amine functionality (Scheme 51).



Scheme 51 – Synthesis of teixobactin **42** analogues retaining positive charge at the hydrocarbon tail terminus, using previous route to truncated analogues, replacing reaction with acetic anhydride with 6-aminohexanoic acid **356** instead.

As previously, Fmoc-SPPS was carried out on 2-chlorotrityl resin **257**, with initial loading of Fmoc-Ala-OH **209**. Following subsequent deprotection, coupling of Fmoc-D-thr-OH, and deprotection steps, the N-terminus was coupled to a Boc-protected amino acid hydrocarbon. This Boc-protected amino acid Boc-Ahx-OH **369** was synthesised from 6-aminohexanoic acid **370** using a published protocol (Scheme 52).¹⁷⁸



Scheme 52 – Synthesis of *N*-(*tert*-Butyloxycarbonyl)aminohexanoic acid (*Boc*-6-Ahx-OH **369**) from 6-aminocaproic acid **370** with *Boc* anhydride.

Following esterification and Fmoc-deprotection, the material was split to allow the syntheses of two analogues (Arg10 **371** and Lys10 **372**, Figure 45). After these coupling reactions and a final Fmoc-deprotection, the linear peptide was cleaved from resin with 1% TFA in DCM, thus preserving Boc and Pbf protecting groups on both the side chain of residue 10 and the N-terminus. The crude peptide was cyclised as previously, before a final global deprotection with TFA spiked with 2% TES in DCM (Scheme 52). Cyclic deprotected peptides were purified by RP-HPLC and characterised with HPLC, HRMS, and NMR. HCl salt conversion and peptide content determination were performed as described previously (Section 4.4, Scheme 43).

Replacement of residues 1-7 with a saturated amino-hydrocarbon facilitated a much simpler synthesis, employing fewer steps, with higher yields and purities obtained. Monitored by HPLC and MS, the synthesis proceeded with a significantly pure excess to allow continuation with crude material throughout all steps; before one purification as the final step (as opposed to the isoprenoid analogues that required purification prior to cyclisation, and occasionally also prior to prenylation). The exclusion of the cysteine residue that was previously essential for prenylation allowed for these analogues to be produced without acetylation of the N-terminus, and the saturated nature of the hydrocarbons resulted in much more stable compounds that cannot isomerise over time or in solution in this region.

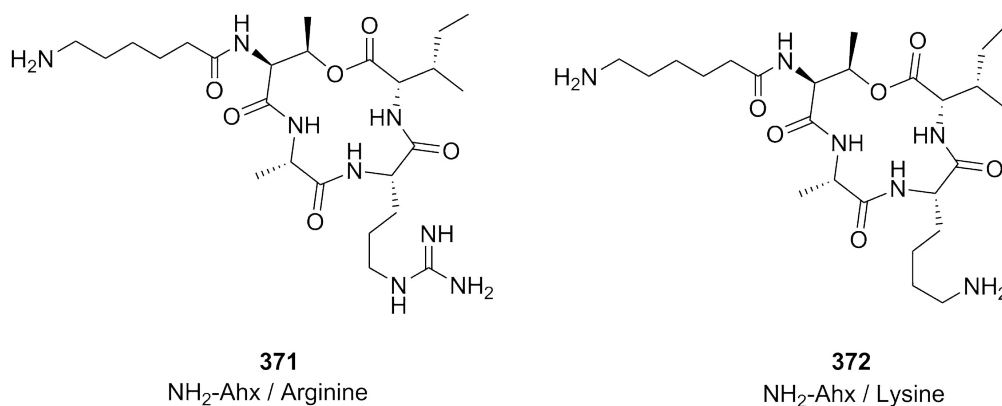


Figure 45 – Structure of the two teixobactin analogues synthesised retaining the positive charge at the terminus of the hydrophobic tail, with Arg10 **371** and Lys10 **372** variations.

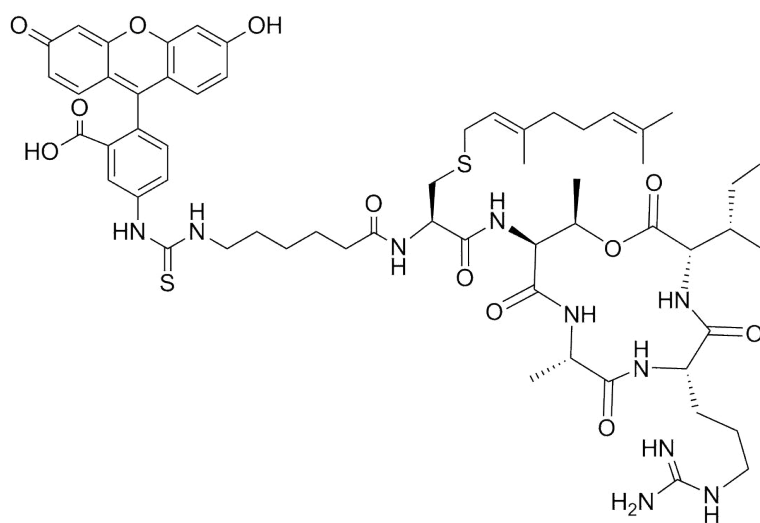
A possible problem with these compounds is the presence of a primary amine, as opposed to an alkylated one. The Hergenrother study suggested that primary amines have the highest levels of accumulation in Gram-negative bacterial cells, but for a significant portion of the compounds tested, the positive charge existed in close proximity to a cyclic or aromatic core. Where the authors increased the separation of the amine functionality from a sterically congested ring system, higher levels of accumulation were observed. Based on the two synthetic compounds having a primary amine rather than an alkylated derivative, and it existing a significant distance away from the central macrocycle of the compound, this should be advantageous to crossing the outer membrane of gram negative bacteria via pore channels. However, it is possible that there is a limit to exactly how far away the primary amine can be before the compound loses activity. The further away from a sterically hindered cyclic component the primary amine becomes, the more accessible it becomes to deaminases and chemical degradation. The other issue is that if the tail is truly necessary for membrane anchoring or binding to a lipophilic moiety of Lipid II **20**, then it is hard to maintain a balance between hydrocarbon length and an overly lipophilic compound that has reduced solubility in aqueous media. An extended tail also increases the molecular weight of the analogues; which may tip the balance for entry via pores in Gram-negative cells.

4.7 Attempted synthesis of fluorescent active teixobactin analogues

FITC-labelled peptides have a wide range of uses, including fluorescence microscopy, flow cytometry and immunofluorescence based assays.¹⁷⁹ Derivatisation of cell permeable peptides with a fluorescent moiety can be used to determine the cellular target of the peptide or region of localisation.

We proposed that this could be applied to teixobactin **42** analogues to see if they accrued in the cell membrane or elsewhere in the cell; and the distribution of analogues that were not active against Gram-positive bacteria.

In order to synthesise fluorescent derivatives of prenylated teixobactin analogues (Figure 46), the method had to be altered in order to replace acetyl with FITC. Derivation with FITC also require a 6-aminohexanoic acid linker to prevent fluorescein thiazolinone formation, a commonly observed side reaction that follows the Edman degradation pathway¹⁸⁰, by spacing from bioactive region.¹⁷⁹

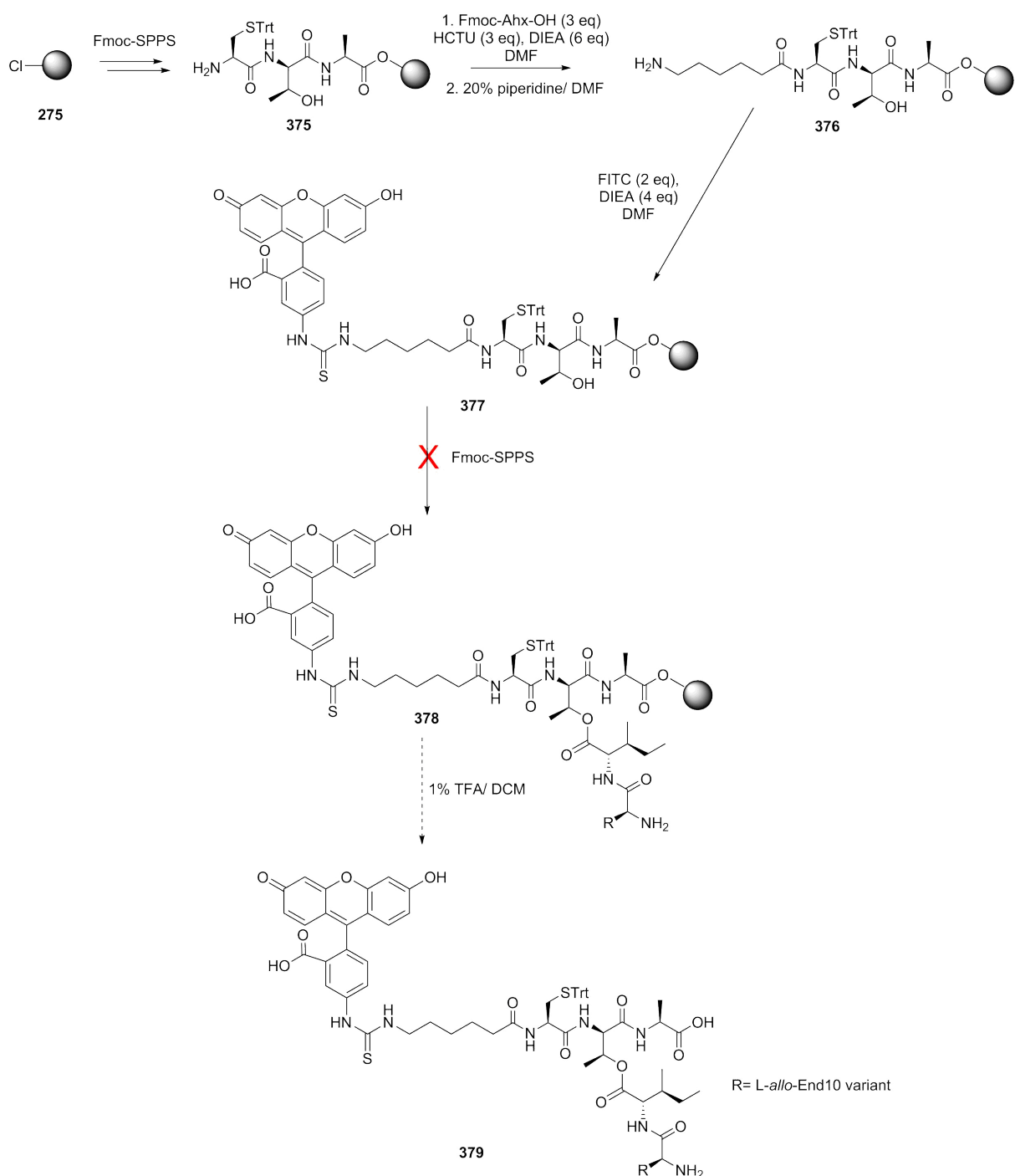


373

Figure 46 - Structure of proposed FITC-coupled teixobactin analogue with Arg10 variation and geranylation (**373**).

If successful, the easiest route towards these fluorescent analogues would be a simple adaptation of the current synthesis of the prenylated analogues by replacement of the acetyl capping step with the Fmoc-Ahx-OH **374** coupling and

subsequently reaction with FITC. However, these fluorescent reagents are notoriously susceptible to degradation by photobleaching, so in peptide syntheses are usually coupled as the final step.



Scheme 53 - Attempted synthesis of FITC-coupled geranylated teixobactin analogues 379.

The syntheses of four analogues (with Lys **380**, Arg **381**, Orn **382** and Ala **383** at the 10 position respectively) were attempted on 2-CTC resin **275**. Coupling of the fluorophore and all subsequent reactions were performed with shielding from light. However, it was quickly apparent that FITC was not stable to the reaction conditions required for Fmoc-SPPS without significant degradation of the peptide.

Given that it was apparent the synthesis would be difficult and require extensive alteration, fluorescent conjugates of the prenylated analogues were not pursued any further. This was considered in conjunction with the fact such a large fluorophore on such a small compound was likely to have a significant effect, and drastically change the molecular weight, lipophilicity, and potentially binding of the macrocycle. Given that previous alterations to residues 1-6 of teixobactin by other research groups have had quite significant effects on the antimicrobial activity of the drug, any observed accumulation of these analogues in cells may not be a true reflection of the acetylated, prenylated counterparts.

4.8 Antibiotic activity of truncated and lipidated teixobactin analogues

Synthetic teixobactin analogues were tested for antibiotic activity by titration against Gram-positive and clinically relevant methicillin-sensitive *Staphylococcus aureus*, in addition to Gram-negative *Escherichia coli* (Table 15). MIC assays were completed by Zaaima Al Jabri, and later repeated in triplicate by Megan De Ste Croix, both of the Department of Genetics, University of Leicester. Antibiotic activity was determined by serial-dilution of analogue compounds, which were then incubated with a strain of bacteria. Inhibition of bacterial growth was assessed after 18 hours.

Entry	Compound number	Variations	<i>S. aureus</i> ATCC 25923 ($\mu\text{g ml}^{-1}$)		<i>E. coli</i> ATCC 25922 ($\mu\text{g ml}^{-1}$)	
			MIC	MBC	MIC	MBC
1	290	Ac-tARI	>32 for all			
2	296	Ac-tAKI				
3	297	Ac-tAHI				
4	349	Lys / Ger				
5	350	Arg / Ger				
6	351	Orn / Ger				
7	352	Cit / Ger				
8	353	His/ Ger				
9	354	Ala/ Ger				
10	355	Glu/ Ger				
11	356	Lys / Farn	8	16	16	>32
12	357	Arg / Farn	16	>32	>32	>32
13	358	Orn / Farn	8	16	32	>32
14	359	Cit / Farn	>32	>32	>32	>32
15	360	His / Farn	>32	>32	>32	>32
16	361	Ala / Farn	>32	>32	>32	>32
17	362	Glu/ Farn	>32	>32	>32	>32
18	371	H ₂ N-Ahx Arg	>32	>32	>32	>32
19	372	H ₂ N-Ahx-Lys	>32	>32	>32	>32

Table 15 - Minimum inhibitory concentration (MIC) and minimum bactericidal concentration (MBC) of teixobactin analogues against Gram-positive *S. aureus* and Gram-negative *E. coli*

As expected, none of the truncated compounds (**290**, **296**, **297**) displayed any antibiotic activity. This supported findings by Nowick *et al.*, whose “short teixobactin” **116** with residues 1-6 removed was found to be inactive.

In addition, compounds **349** to **355**, with a shorter, geranylated thiol, were completely inactive against both species of bacteria. Compounds **349**, **351** and **351**, with Lys10, Arg10 and Orn10 mutations respectively, did not possess any antibiotic activity, unlike their geranylated counterparts. This would suggest that there is a minimum requirement for the length of hydrocarbon to sufficiently anchor in the Gram-positive bacterial membrane in order to bind to lipid II **20** and inhibit the synthesis of peptidoglycan. These results suggests that while the

macrocycle is integral for binding to the pyrophosphate region of lipid II **20**, the hydrophobic portion of the drug is also essential to mediate binding, whether as a membrane anchor or to another region of the target.

Of the farnesylated compounds, three of seven analogues were found to exhibit antibiotic activity against *S. aureus*. Each of these compounds contained an End10 mutation that retained the basic nature of the native amino acid; the amines lysine (**356**) and ornithine (**358**), and arginine (**357**) with a guanidine side-chain (Figure 47). None of the analogues that were not basic were able to inhibit Gram-positive nor Gram-negative bacteria, once again demonstrating the importance of the positive-charge at this position; providing evidence for interaction with the negatively charged pyrophosphate. The analogue in which End10 was replaced by citrulline (**359**), an amino acid similar in structure but chemically diverse to arginine, did not show any antibiotic activity, most likely due to the reduced polarity of the moiety.

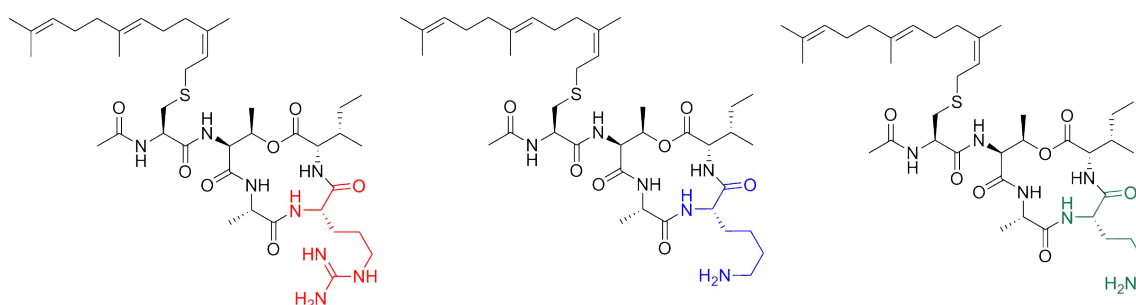


Figure 47 - Structure of three active farnesylated teixobactin analogues with Arg10 (**357**), Lys10 (**356**), and Orn10 (**358**) variations

The arginine and farnesyl-mutated analogue **357**, the most structurally and chemically similar compound to that of native teixobactin, displayed the weakest activity of 16 $\mu\text{g}/\text{ml}$ against *S. aureus*, despite being the most structurally similar to native teixobactin **42**.

Compound **358**, with ornithine and farnesyl mutations, displayed moderate activity, with an MIC of 8 $\mu\text{g}/\text{ml}$. This activity was retained by lengthening this side chain by an extra CH_2 and thus altering this residue to a lysine (compound

356). The increased activity of **358** and **356** over Arg10 **357** suggests that basicity at this position plays a significant role in the antibacterial strength of these analogues.

Most interestingly, these active farnesylated analogues also displayed antibiotic activity against Gram-negative *E. coli*, which has rarely been observed in previously documented teixobactin analogue antibiotic activity studies. The lysine and farnesyl-mutated analogue **349**, and the ornithine and farnesyl mutated analogue **351** both displayed moderate activity of 16 µg/ ml against *E. coli*. This is a significant finding, and an improvement on the antibiotic activity against Gram-negative bacteria displayed by the native compound **42**.

Name	Structure	Work	MIC <i>S. aureus</i> µg/ mL	MIC <i>E. coli</i> (µg/ mL)
Teixobactin 42	Me-flSqiISt*AEndI*	Lewis ⁸¹	0.25	25
Arg10- Teixobactin 101	Me-flSqiISt*ARI*	Albericio ¹⁰²	2	NI
Arg10- Teixobactin 101	Me-flSqiISt*ARI*	Singh ¹⁰³	2	64
All L-, Ac, Arg10- Teixobactin 108	Ac-FISQIIST*ARI*	Singh ¹⁰³	128	NI
All L-, Arg10- Teixobactin 109	Me-FISQIIST*ARI*	Albericio ¹⁰⁴	NI	NI
Ac-Arg10- Teixobactin 110	Ac-flSqiISt*ARI*	Albericio ¹⁰⁴	NI	NI
Arg10- Teixobactin 101	Me-flSqiISt*ARI*	Nowick ¹⁰⁵	1	NI
Lys10- Teixobactin 111	Me-flSqiISt*ARI*	Nowick ¹⁰⁵	0.25	NI
D-Ile, Arg10 teixobactin 113	Me-flSqiISt*ARI*	Nowick ¹⁰⁵	2	NI
Ent-Arg10- teixobactin 115	Me-FisQIisT*ari*	Nowick ¹⁰⁵	2	NI
Lipobactin 1 117	Dodecanoyl- ISt*ARI*	Nowick ¹⁰⁵	4	NI
Farnesyl- Lysbactin 356	Farn/ Lys	Girt	8	16
Farnesyl- Ornbactin 358	Farn/ Orn	Girt	8	32
Farnesyl- Argbactin 357	Farn/ Arg	Girt	16	NI

Table 16 - Table of antibiotic activity of selected published active teixobactin analogues. Mutations are shown in red; asterisks indicate point of cyclisation. NI = no inhibition.

Comparatively, other research groups have produced teixobactin analogues which also retain similar activity to teixobactin. The vast majority of these deviate only slightly from the original structure; are 11-residue depsipeptides that mutate the unproteinogetic L-*allo*-enduracididine at the 10 position; or contain residues that are stereoisomers of the natural compound: most notably, Arg10 analogue synthesised by Albericio *et al.* and Singh *et al.*, the Lys10 analogue by Nowick *et al.*. In terms of lipidated analogues, lipobactin, also designed and synthesised by the Nowick group, has good activity (4 µg/ml) against *S. epidermis*, but this is an 8-fold reduction from teixobactin – comparable to the three active farnesylated analogues **356-358**.

4.9 Conclusions

One of the key reactions in the synthesis of teixobactin **42** or any related analogues is the formation of the 13-membered macrocycle. Through a series of solution-phase cyclisation experiments, attempting both the formation of the depsipeptide bond and an amide bond, the cyclisation was optimised with conditions that provided 100% conversion over the course of 20 minutes at room temperature, an improvement on previously reported conditions that have been reported to take between one hour¹⁰³ to one day¹⁰² to complete.

With the cyclisation in hand, a number of lipidated teixobactin analogues were produced. These were truncated from residues 1 to 7. Three acetylated analogues were produced (**290**, **296**, **297**) that showed no antibiotic activity; revealing that whilst the macrocycle is involved in the binding to the pyrophosphate-sugar moiety of lipid II, some form of hydrophobic tail is also essential for activity.

Prenylation was selected as the form of lipidation as this is a commonly observed post-translational modification in eukaryotic cells with relevance in membrane anchorage, and many bacteria produce anti-microbial peptides with unsaturated lipids. We proposed that the areas of unsaturation may increase the rigidity of the anchor and therefore increase the activity of the analogues. Attempts at *N*-

prenylation yielded some product; but generally produced other side products and resulted in unwanted bis-alkylation. Therefore, the serine was rationally substituted to a cysteine residue to allow prenylation of the thiol. This was achieved with isoprenoid bromide with zinc catalyst and TFA in DMF. In total, 14 prenylated analogues were synthesised, with seven *L-allo*-enduracididine mutations and two isoprenoids; geranyl and farnesyl. Of these, three were found to be active; farnesyl compounds with Arg10 (**357**), Orn10 (**358**) and Lys10 (**356**) residues. This is a significant discovery given that Lipobactin **117** produced by the Nowick group and the three active farnesylated compounds all have activity in the region of 4-16 µg/ mL, demonstrating that replacement of the linear tail residues of teixobactin **42** can be achieved without significant detriment to activity. In addition, these three farnesylated analogues **356** – **358** displayed significant activity against Gram-negative *E. coli*, which has not been commonly observed with other documented teixobactin analogues. This could be attributed to the smaller size of these analogues (~750 Da) compared to native teixobactin **42** (1,242 g/ mol), potentially allowing them to traverse the pores of Gram-negative bacterial cell membranes.

If possible, *N*-prenylation of cyclic teixobactin macrocycle analogues could be attempted where the *N*-terminus had been protected with Alloc throughout the synthesis, the removal of which should not catalyse side-product formation. Whilst some bis-prenylation would be highly likely to occur, this product could actually provide illuminating results in terms of the effect on antimicrobial activity. An additional hydrophobic tail could provide additional anchorage into the bacterial membrane, or on the other hand may be detrimental to the binding.

Fluorescent derivatives of the active compounds were attempted (Section 4.7), but could not be produced with simple adjustment of the synthetic route. Fluorescent derivatives could be achieved by protecting the *N*-terminus with a third level of orthogonality using an Alloc protecting group. This would allow the synthesis to proceed as previously up to and including the thiol prenylation, at which point Pd(PPh₃) and PhSiH₃ could be used to catalyse Alloc deprotection and coupling FITC as the penultimate step, rather than midway through the synthesis. This would avoid exposure to coupling and Fmoc-deprotection reactions, but would still require a final deprotection of any amino acid side chain

protecting groups. Depending on the amino acid residue at the 10- position this requires varying levels of TFA; FITC derivation may not be suitable with arginine analogues that require a very high percentage (~95%) of TFA to remove the Pbf protection, but may be more compatible for trityl or Boc protected residues. Ultimately, fluorescein-conjugated teixobactin analogues are likely to yield significant results with larger compounds, rather than small analogues composed of four to five residues.

In addition to prenylated analogues, two cyclic teixobactin analogue peptides with lipids bearing terminal primary amines were synthesised in order to also target Gram-negative species as well as Gram-positive (**371**, **372**), but neither showed any antibiotic activity. The synthesis provides a method for further analogues with varying lengths of saturated hydrocarbons and the possibility of alkylation of the amine. Methylation of the N-terminus is a common occurrence in naturally occurring antibiotic peptides. The exact purpose of methylation in antibiotic compounds has not been confirmed; it is possible that this modification prevents deamination; increases hydrophobicity; has relevance in cell signalling; or a combination of these. To fully probe the importance of methylation at the N-terminus of teixobactin, further polarised tail peptide analogues were should be synthesised with methyl group at this site. In addition, the length of the hydrocarbon tail should be varied. It was originally proposed that there may be a minimum requirement of membrane anchor length, with teixobactin **42** and lipobactin **117** both having hydrophobic regions of 15 – 25 atoms in length, but the lysine/ geranyl analogue described previously contained a significantly shorter chain. It is therefore undetermined if there is a minimum requirement of hydrophobic tail length to provide sufficient membrane anchorage and antibiotic activity, particularly with the addition of the basic terminal moiety, as this may need to fully traverse the phospholipid bilayer.

5. Final conclusions and future work

This research aimed to develop routes to novel analogues of teixobactin **42**, in order to fully probe its mechanism of action of binding with lipid II **20**, and also in order to develop simpler, more affordable analogues with increased drug-like properties.

Initial work focused on a new and efficient route towards a synthesis of the nonproteinogenic amino acid L-*allo*-enduracididine to provide a route towards the total synthesis. A synthetic method employing a Ni(II) Glycine Schiff base complex **138** was proposed (Section 2.3, Scheme 13). Due to the enantioselectivity of this method at the 2-position of L-*allo*-enduracididine **43**, this route would also provide means to enduracididine stereoisomers: variation of the natively occurring L-*allo*-end **43** of teixobactin **42** with its stereoisomers was considered useful to probe the effect on antimicrobial activity.

Unfortunately, despite numerous attempts with various iodoguanidine electrophiles (**148**, **149**, **158**) even in optimised conditions (Section 2.6), no conversion to the desired complex could be obtained. This was proposed to be due to steric bulk of the electrophiles employed, compared to the aliphatic hydrocarbons commonly used in this type of Ni(II) Schiff base chemistry. Instead, focus was turned to the synthesis of simpler, truncated analogues of teixobactin **42** that would aim to provide comparable antibiotic activity with simpler syntheses and less costly reagents, particularly aiming to create a synthetic analogue replacing L-*allo*-enduracididine **43** with a DNA encoded variant, and without the three D-amino acids of teixobactin **42**'s linear chain.

Truncated analogues **207** and **217** consisting of the teixobactin **42** core macrocycle, capped by an acetyl functionality, were synthesised using an on-resin cyclisation approach, employing a sulfonamide-based safety-catch resin **198** (Section 3.6, Scheme 35). The linear sequence was synthesised on resin **198** with both Fmoc-D-Thr-OH (Section 3.5.2, Scheme 32) and Fmoc-Ala-OH (Section 3.6, Scheme 35) as the preliminary coupled amino acid. All syntheses formed the depsipeptide bond by nucleophilic substitution of the hydroxyl of D-threonine onto the acid C-terminal of Fmoc-Ile-OH **258** using DIC and DMAP

269. This reaction was found to progress efficiently over the course of two hours at room temperature, as monitored by ESI MS and HPLC. However, the final reaction involving the displacement of the activated sulfonamide linker with the *N*-terminus amine could not be optimised to a sufficient standard, and all reactions attempted resulted in poor yield and the formation of multiple side-products, and cyclic peptides **207** and **217** were not isolated. Safety-catch resins are often employed in the synthesis of larger macrocycles; to form the constrained 13-membered ring of these analogues may not have been sterically viable. The basis of this synthetic route was taken forward to be applied to a solution-phase cyclisation approach (Section 4).

Solution-phase macrolactonisation (Section 4.3) proved inefficient despite a number of conditions screened to improve the levels of cyclisation (Section 4.3.3.1, Table 13). Therefore, a synthetic route employing macrolactamisation was applied instead (Section 4.4, Scheme 43). Comparatively this proceeded extremely well, and was used to yield full conversion after 20 minutes to truncated teixobactin **42** macrocycle products **290**, **296**, and **297**, and also provided a cyclisation method for more complex analogues.

The linear sequence of teixobactin **42** (residues 1-7) is proposed to be a bacterial cell membrane anchor. In the design of simplified teixobactin **42** analogues, we rationalised that this could therefore be replaced entirely with a lipid to achieve the same mode of binding. Residues 1-6 of **42** were replaced with isoprenoids of two differing lengths in order to try and determine if this hypothesis was correct and if so, what the minimum length requirement is to gain sufficient membrane anchorage. To facilitate this modification, Serine7 was rationally substituted to a cysteine residue to allow thiol prenylation. These reactions proceeded well without significant side reactions or byproduct formation, and in addition, 1% TFA/DCM used to cleave linear peptide precursors from the resin did not remove cysteine trityl protection prematurely. This method was successfully used to synthesise fourteen novel teixobactin analogues, with 7 variants replacing *L*-*allo*-End10, in combination with two lengths of isoprenoid (geranyl **302** and farnesyl **298**).

All synthetic teixobactin analogues synthesised in this work were screened for their antibiotic activity, with MIC determined against Gram-positive and Gram-negative bacteria. Of the nineteen compounds analysed, three were found to possess antibiotic activity, all with replacement of residues 1-7 with a farnesyl tail and varying native L-*allo*-enduracididine **43** to DNA-encoded basic residues lysine, ornithine and arginine (**356**, **357**, **358**). The three analogues had reduced activity against Gram-positive *S. aureus* compared to teixobactin **42** (8-16 µg/mL, compared to 0.25 µg/mL for **42**), but considering this considerable alteration from the native structure **42**, this was a promising result. In addition, and unexpectedly, two of these compounds (**356**, Farn-Lys10bactin and **358**, Farn-Orn10bactin) also displayed antibiotic activity against the Gram-negative bacteria *E. coli*. This is potentially attributed to the vastly reduced size compared to the native compound **42**, allowing the analogues to travel through membrane pores, although this has yet to be fully determined.

In future work these active compounds **356**, **357** and **358** could be submitted for further MIC assays against a larger panel of both Gram-positive and Gram-negative pathogens. Solution-phase NMR or surface plasmon resonance (SPR) could be used with lipid II (**20**) mimetics in order to more effectively determine if their mode of action is indeed the same of teixobactin **42**. Ultimately, this work strongly suggests that a cyclic antimicrobial peptide such as teixobactin can be drastically altered to a simpler analogue and still retain a good level of antibiotic activity; and decreasing the size of these large cyclic peptide antibiotics may pave a new way to target Gram negative bacteria.

6. Experimental

6.1 General information

All chemicals used were purchased from commercial sources and used without further purification unless otherwise stated. Peptide-grade DMF and NMP were obtained from Rathburn (UK). Resins were purchased from NovaBioChem (Merck Millipore). Fmoc-protected amino acids and coupling agents were purchased from NovaBioChem (Merck Millipore) and Pepceuticals. Materials for MIC assays were purchased from Oxoid Ltd., Basingstoke, UK. All chemicals were stored under conditions outlined in the manufacturer's instructions. Anhydrous solvents were dried and stored under nitrogen, under pre-activated 4 Å molecular sieves. SPPS was carried out in fritted polypropylene solid phase extraction cartridges (0.05 – 0.2 mmol scales), or custom-made glass sintered reaction vessels (0.25 mmol scale and higher), created in-house. Solvent evaporation took place under low pressure on Buchi vacuum rotary evaporator, and a Labconco FreeZone 2.5 lyophiliser was used for the freeze-drying of peptides

Column chromatography was performed using a Biotage Isolera One automated flash purification device, typically with a solvent system of ethyl acetate in petroleum spirit, or methanol in DCM.

^1H , ^{13}C and ^{19}F NMR spectra were recorded on Bruker DPX 300 (^1H , 300 MHz, ^{13}C , 75 MHz, ^{19}F , 282 MHz), Bruker DPX 400 (^1H , 400 MHz, ^{13}C , 100 MHz, ^{19}F , 376 MHz), Bruker Avance III 500 (^1H , 500 MHz, ^{13}C , 125 MHz) spectrometer as indicated. Chemical shifts (δ) are quoted in ppm relative to residual non-deuterated solvent peaks). Coupling constants (J) are reported in Hz to the nearest 0.1 Hz.

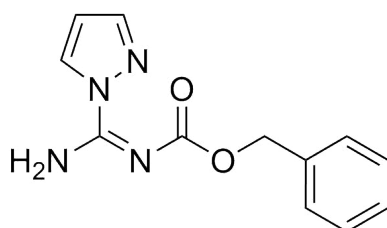
LC-MS was performed using a Xevo QToF mass spectrometer (Waters) coupled to an Acquity LC system (Waters), using an Acquity UPLC BEH C18 column (2.1 x 50 mm, Waters). Samples were ran at a flow rate of 0.6 mL/ min using a two-solvent system of 95% water + 0.1% formic acid (solvent A) / 5% acetonitrile +

0.1% formic acid (solvent B), which ran for 0.5 minutes before following a linear gradient over 2.1 minutes to 100% acetonitrile + 0.1% formic acid, which was then held continuously for a further minute. Typically, m/z data from 50 – 1500 Da was obtained, using an acquisition rate of 10 spectra per second, with ESI capillary voltage of 3 kV, cone voltage of 30 V and collision energy of 4 eV.

Analytical and semi-preparative HPLC were performed using HPLC-grade MeCN and deionised H₂O, and TFA buffer on the DIONEX UltiMate 3000; model 310 UV detector, 230 pumps with a gradient controller, and 410 autosampler). This utilised a Phenomenex Gemini-NX C-18 110 Å AXIA packed column, with dimensions of 250 x 21.20 mm and flow of 0.5 mL/min with injection volume of 20 µl for analytical HPLC, and dimensions of 150 x 4.60 mm and flow of 1.6 mL/min with a variable injection volume of up to 2 mL for semi-prep HPLC. A two-solvent system was used for the collection of data: H₂O with 0.1% TFA (Solvent A) and MeCN with 0.1% TFA (Solvent B). UV detection was measured across four channels of 214 nm, 260 nm, 310 nm and 330 nm for analytical HPLC, and solely 214 nm for semi-preparative HPLC. A typical gradient for the collection of pure peptide and for the analysis of crude and pure peptides was 5-100% MeCN over 30 minutes.

6.2 Chemical syntheses

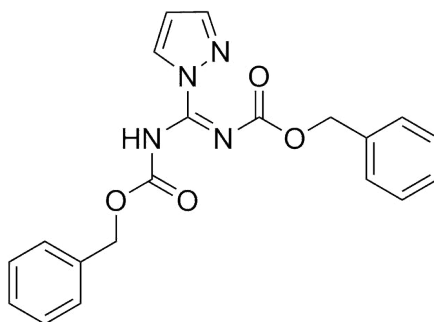
***N*-Benzyloxycarbonyl-1H-pyrazole-1-carboxamide (*N*-Cbz-1H-pyrazole-1-carboxamide) (**151**)**



1H-Pyrazole-1-carboxamide hydrochloride **150** (4.4 g, 30 mmol, 1 eq) was dissolved in THF (anhydrous, 25 mL) with benzyl chloroformate (6.42 mL, 45 mmol, 1 eq) with stirring. DIPEA (10.5 mL, 60 mmol, 2 eq) was added dropwise over the course of 10 minutes, and effervescence observed. Once added, the

reaction was stirred overnight at room temperature, forming a precipitate with gel-like consistency. H₂O (50 mL) was added to the mixture, which was then extracted with DCM (4 x 50 mL). Organic fractions were combined, washed with brine, dried over MgSO₄ and evaporated under reduced pressure. The precipitate was recrystallised in cold DCM to yield *N*-Cbz-1H-pyrazole-1-carboxamide **151** as a white crystalline solid (6.20 g, 85 % yield). R_f 0.35 (1:3 EtOAc / petroleum ether 40-60); ¹H NMR δ_H (400 MHz, CDCl₃) 5.22 (2H, s, CH₂), 6.42 (1H, s, CH), 7.45-7.26 (5H, m, Ph), 7.69 (2H, br s, NH and CH), 8.46 (1H, s, CH), 9.06 (1H, br s, NH). ¹³C NMR δ_C (100 MHz, CDCl₃) 67.6, 109.3, 128.1, 128.3, 128.5, 128.9, 136.3, 143.7. LC-HRMS(ES+) at T_R = 1.86 found 245.1047. C₁₂H₁₃O₂N₄ ([M+H]⁺) requires 245.1039. Δ MW (ppm) = 3.3 RP-HPLC: (UV 260 nm, 5-100% MeCN in H₂O, 0.1% TFA, 20 min gradient) and found to be >99% pure. Elution after 15.513 minutes of gradient.

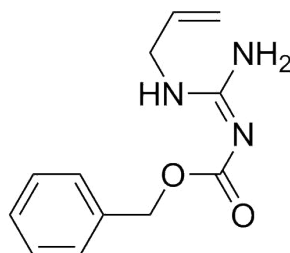
***N, N'*-Bis(carboxybenzyl)-1H-pyrazole-1-carboxamide (*N, N'*-Bis(Cbz)-1H-pyrazole-1-carboxamide) (153)**



N-Cbz-1H-pyrazole-carboxamide **151** (2.17 g, 8.9 mmol, 1 eq) was dissolved in dry THF (30 mL) and cooled to 0 °C. NaH (60% dispersed in mineral oil, 1.25 g, 31.15 mmol, 3.5 eq) was added portionwise over 10 minutes. Cbz-OSu (3.33 g, 13.35 mmol, 1.5 eq) was added and the reaction stirred to room temperature over 2.5 hours. TLC (30% EtOAc/ hexane) was used to monitor the reaction. After completion, brine (25 mL) was cautiously added to decompose excess NaH. The mixture was extracted with chloroform (3 x 30 mL) and organic fractions combined and washed with brine (3 x 20 mL). The organic fractions were dried

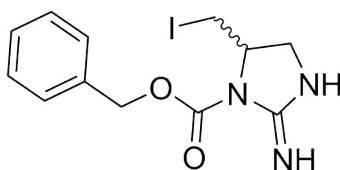
with MgSO₄ and concentrated *in vacuo*. The product was crystallised using diethyl ether to yield the white solid *N, N'*-Bis(Cbz)-1*H*-pyrazole-1-carboxamide **153** (1.37 g, 41% yield). R_f 0.28 (30% EtOAc / Hexane); ¹H NMR δ_H (300 MHz, CDCl₃) 5.22 (4H, d, *J* = 10.7, 2 x CH₂), 6.41 (1H, dd, *J* = 3.0, 1.8, CH), 7.37 (10H, m, 2 x Ph), 7.62 (1H, dd, *J* = 1.6, 0.7, CH), 8.30 (1H, dd, *J* = 2.8, 0.7, CH), 9.33 (1H, br. s, NH); ¹³C NMR δ_C (75.4 MHz, CDCl₃) 68.5, 68.7, 110.3, 128.2, 128.5, 128.6, 128.7, 128.9, 134.5, 135.8, 138.2, 143.0, 150.7, 158.2; LC-HRMS(ES+) at T_R = 2.22 found 401.1244. C₂₀H₁₈N₄O₄Na ([M+Na]⁺) requires 401.1226. RP-HPLC (UV 260 nm, 5-100% MeCN in H₂O, 0.1% TFA, 20 min gradient) and found to be >99% pure. Elution after 18.283 minutes of gradient.

***N*-carboxybenzyl-*N'*-allylguanidine (*N*-Cbz-*N'*-allylguanidine) (**152**)**



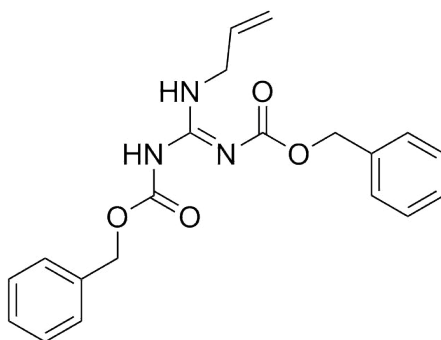
N-Cbz-1*H*-pyrazole-1-carboxamide **151** (2.57 g, 10.5 mmol, 1 eq) and allylamine (6.3 mL, 84 mmol, 8 eq) were heated under reflux for 3 hours. The reaction was then stirred at room temperature overnight and monitored by TLC (75% EtOAc/ petroleum ether 40-60). The solution was purified using column chromatography (18% - 100% EtOAc in DCM) to yield *N*-Cbz-*N'*-allylguanidine **152** as a white solid (2.32 g, 95% yield). R_f 0.27 (50:50 EtOAc / DCM); ¹H NMR δ_H (300 MHz, CDCl₃) 3.75 (2H, dt, *J* = 3.4, 1.7, CH₂), 5.09 (2H, s, CH₂), 5.27 (2H, m, 2 x CH), 6.32 (1H, m, CH), 7.35 (5H, m, Ph); ¹³C NMR δ_C (75.4 MHz, CDCl₃) 43.6, 66.2, 104.8, 116.8, 127.8, 127.9, 128.4, 133.5, 137.3, 162.4, 163.6; LC-HRMS(ES+) at T_R = 1.34 found 234.1248. C₁₂H₁₆O₂N₃ ([M+H]⁺) requires 234.1243.

2-Imino-4-(iodomethyl)imidazolidine-1-carboxylate (**148**)



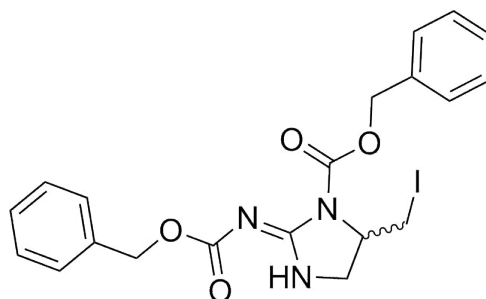
N-Cbz-*N'*-allylguanidine **152** (78.6 mg, 0.34 mmol, 1 eq) was dissolved in MeCN (anhydrous, 6.8 mL) with K₂CO₃ (anhydrous, 211.5 mg, 4.5 eq, 1.53 mmol) and cooled to -15 °C. Iodine (388 mg, 1.53 mmol, 4.5 eq) was added and stirred for a further hour at -15 °C. The reaction was then warmed to room temperature and stirred overnight, with monitoring by TLC (75% EtOAc / Petroleum Ether 40-60). Upon completion, sodium thiosulfate (10% in H₂O v/v) was added until total decolourisation occurred. The mixture was extracted with DCM (3 x 10 mL) and dried with MgSO₄, filtered and evaporated under reduced pressure, to yield benzyl-1-((benzyloxy)-carbonyl)-5-(iodomethyl)-imidazolidin-2-ylidene carbamate **148** as an off-white-to-yellow solid. (95.4 mg, 78 % yield). R_f 0.43 (10:90 MeOH/ CHCl₃); ¹H NMR δ_H (400 MHz, CDCl₃) 3.04 (1 H dd, *J* = 8.4, 9.6, CHNH), 3.13 (1H dd, *J* = 10.0, 4.50, CHNH) 3.33 (1H dd, *J* = 10.2, 5.9, ICH), 3.69 (1 H t, *J* = 9.8 ICH), 3.93-4.02 (1H m, CH), 5.06 (s, 2 H, CH₂Ph,), 7.32 - 7.39 (m, 5 H, Ph). ¹³C δ_C (100 MHz, CDCl₃) 8.8, 48.5, 54.7, 66.7, 128.0, 128.6, 136.9, 163.2, 164.8. LC-HRMS(ES+) at T_R = 1.41 found 360.0216. C₁₂H₁₅N₃O₂I ([M+H]⁺) requires 360.0209. Δ MW (ppm) = 1.9

N,N'-(2-propen-1-ylcarbonimidoyl)bis-, C,C'-bis(phenylmethyl) ester (*N*-allyl-*N',N'*-bis-Cbz-guanidine) (**154**)



N,N'-Bis(Cbz)-1H-pyrazole-1-carboxamide **153** (3.773 mg, 9.97 mmol, 1 eq) and allylamine (1.5 mL, 19.94 mmol, 2 eq) were dissolved in MeCN (10 ml). The reaction was stirred at room temperature for 16 hours and monitored by TLC (25% EtOAc / petroleum ether 40-60). The solvent was evaporated and purified by column chromatography on silica (2% to 20% EtOAc in petroleum ether 40-60) to yield *N*-Allyl-*N',N''*-bis-Cbz-guanidine **154** (3.19 g, 90%) as a crystalline white solid. R_f 0.44 (25% EtOAc/ PE 40-60); $^1\text{H NMR } \delta_{\text{H}}$ (300 MHz, CDCl_3) 4.05 – 4.11 (2H, m, NHCH_2), 5.13-5.26 (6H, m, 2 x CH , 2 x CH_2), 5.87 (1H, m, $\text{CH}=\text{CH}_2$), 7.34 (10H, m, 2 x Ph), 8.39 (1H, br. s, NH), 11.76 (1H, br. s, NH); $^{13}\text{C } \delta_{\text{C}}$ (100 MHz, CDCl_3) 43.5, 67.4, 68.4, 117.1, 128.1, 128.3, 128.6, 128.9, 129.0, 133.1, 134.8, 136.9; LC-HRMS(ES+) at $T_{\text{R}} = 2.43$ found 368.1617. $\text{C}_{20}\text{H}_{22}\text{O}_4\text{N}_3$ ($[\text{M}+\text{H}]^+$) requires 368.1610. RP-HPLC (UV 214 nm, 5-100% MeCN in H_2O , 0.1% TFA, 20 min gradient) and found to be >99% pure. Elution after 23.973 minutes of gradient.

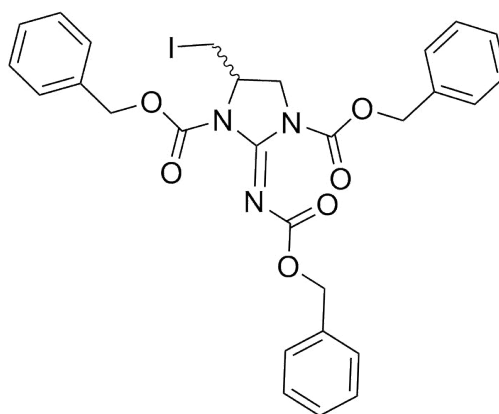
Benzyl-1-((benzyloxy)-carbonyl)-5-(iodomethyl)-imidazolidin-2-ylidene carbamate (149)



N-Allyl-*N',N''*-bis-Cbz-guanidine **154** (3.19 g, 8.68 mmol, 1 eq) was dissolved in MeCN (anhydrous, 200 mL) with potassium carbonate (anhydrous, 4.80 g, 347 mmol, 4 eq) and cooled to $-15\text{ }^\circ\text{C}$. Iodine (8.81 g, 34.7 mmol, 4 eq) was added, and the reaction warmed to room temperature and stirred overnight. Reaction progress was monitored by TLC (1:1 EtOAc/ PE 40-60). Once complete, sodium thiosulfate in H_2O (10% w/v, 100 mL) was added until complete decolourisation occurred. Aqueous was extracted with DCM (3 x 50 mL), and these organic fractions were combined and dried over MgSO_4 before being concentrated *in vacuo*. The crude pale solid was washed with cold methanol (3 x 10 mL) and cold

ethyl acetate (3 x 10 mL) to give benzyl-1-((benzyloxy)-carbonyl)-5-(iodomethyl)-imidazolidin-2-ylidene carbamate **149** as a slightly off-white solid powder (3.56 g, 83 %). $R_f = 0.25$ (1:1 EtOAc/ PE 40-60). $^1\text{H NMR } \delta$ H (400 MHz, CDCl_3) δ ppm 8.64 (1h br s, NH), 7.48-7.29 (10 H m, 2 x Ph), 5.33 (1H d, $J = 12$, PhCH), 5.26 (1H d, $J = 12$, PhCH), 5.16 (1H s, PhCH_2), 4.45-4.28 (1H m, CH), 3.87-3.80 (1H m, CH), 3.59 (1H dd, $J = 11.2, 2.4$, CH), 3.42 (1H dd, $J = 8.8, 2$, CH), 3.30 (1H dd, $J = 9.2, 9.6$, CH); $^{13}\text{C NMR}$ (100 MHz, CDCl_3) δ ppm 6.9, 31.0, 56.3, 67.6, 68.8, 128.1, 128.5, 128.8, 135.0, 206.9. LC-HRMS(ES+) at $T_R = 1.95$ found 494.0580. $\text{C}_{20}\text{H}_{21}\text{O}_4\text{N}_3\text{I}$ ($[\text{M}+\text{H}]^+$) requires 494.0577. Δ MW (ppm) = 0.6; RP-HPLC (UV 214 nm, 5-100% MeCN and 5-80% MeCN in H_2O , 0.1% TFA, 20 min gradient) and found to be >99% pure. Elution after 15.677 minutes (5-100%) and 18.133 minutes (5-80%) of gradient.

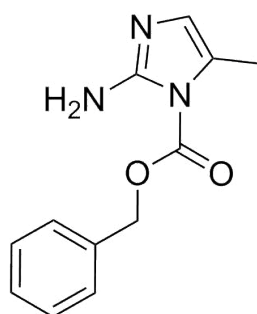
Dibenzyl (E)-2-(((benzyloxy)carbonyl)imino)-4-(iodomethyl)imidazolidine-1,3-dicarboxylate (158)



Benzyl-1-((benzyloxy)-carbonyl)-5-(iodomethyl)-imidazolidin-2-ylidene carbamate **149** (493 mg, 1 mmol, 1 eq) was dissolved in THF (anhydrous, 3.3 mL) and cooled to 0 °C. NaH (60% dispersion in oil, 48 mg, 1.2 mmol, 1.2 eq) was added under nitrogen. *N*-(Benzyloxycarbonyloxy) succinimide (374 mg, 1.5 mmol, 1.5 eq) was added and the reaction warmed to room temperature, before stirring overnight under nitrogen. Reaction was monitored by TLC (1:1 EtOAc/PE 40-60). Once complete, H_2O (3 mL) was added to decompose excess sodium hydride. The product was extracted with DCM (3 x 10 mL), and these organic fractions were combined, washed with brine (10 mL), dried over MgSO_4 and

concentrated under reduced pressure. The crude product was purified by column chromatography (12% to 100% EtOAc in PE 60-80). The pure product **158** was obtained via recrystallisation from PE 40-60. $R_f = 0.55$ (1:1 EtOAc/ PE 40-60); $^1\text{H NMR}$ δ H (400 MHz, CDCl_3) δ ppm 7.41-7.29 (15H m, 3 x Ph), 5.26 (1H d, $J = 12$, PhCH), 5.25 (1H d, $J = 12$, PhCH), 5.20 (1H d, $J = 12$, PhCH), 5.17 (1H d, $J = 12$, PhCH), 5.14 (1H d, $J = 12$, PhCH), 5.07 (1H d, $J = 12$, PhCH), 4.40-4.32 (1H m, CHN), 3.96-3.85 (2H m, NCH_2), 3.40 (1H dd, $J = 10$, 3.2, CH_2I), 3.28 (1H dd, $J = 10.0$, 8.4 CH_2I); $^{13}\text{C NMR}$ (100 MHz, CDCl_3) δ ppm 158.2, 150.9, 150.8, 141.7, 136.4, 134.9, 134.7, 129.4, 128.9, 128.8, 128/8, 128.5, 128.5, 128.4, 128.1, 72.9, 69.2, 69.0, 68.0, 54.5, 48.5, 6.1; IR (ν_{max} cm^{-1} , neat): 1785, 1733, 1685, 1645, 1456, 1393, 1314, 1258, 1226, 1178, 1162; LC-HRMS(ES+) at $T_R = 2.43$ found 628.0970. $\text{C}_{28}\text{H}_{27}\text{O}_6\text{N}_3\text{I}$ ($[\text{M}+\text{H}]^+$) requires 628.0945. Δ MW (ppm) = 4.0

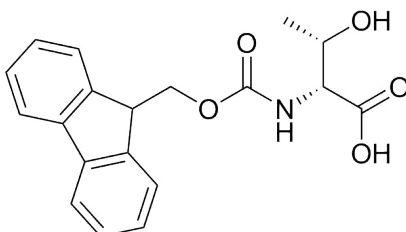
Benzyl 2-amino-5-methyl-1H-imidazole-1-carboxylate (**165**)



Potassium-*tert*-butoxide (29 mg, 0.26 mmol, 1.3 eq) was dissolved in dry DMF (325 μL) under an atmosphere of nitrogen. Benzyl-1-((benzyloxy)-carbonyl)-5-(iodomethyl)-imidazolidin-2-ylidene carbamate **149** (100 mg, 0.2 mmol, 1 eq) in DMF (anhydrous, 175 μL) was added dropwise, and on addition the colour changed from orange to deep red. The reaction was stirred for 1.5 hours at room temperature and monitored by TLC. Once complete, the reaction was quenched with H_2O (3 mL) and extracted with DCM (3 x 10 mL). These organic fractions were combined and washed with LiCl (5% v/v, aq, 3 x 10 mL) and brine (10 mL), before being dried over MgSO_4 and concentrated *in vacuo*. The product was purified using semi-preparative RP-HPLC, using a gradient of 5-100% acetonitrile in water over 30 minutes. Pure fractions were combined and

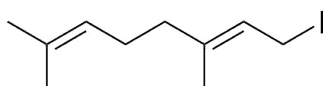
lyophilised to give benzyl (4-methyl-1H-imidazol-2-yl)carbamate **165** as a white crystalline solid (40 mg, 85%). $R_f = 0.76$ (1:1 EtOAc/ PE 40-60). $^1\text{H NMR}$ δ H (400 MHz, CDCl_3) δ ppm 7.43-7.25 (5H m, Ph), 6.54 (1H s, NCH), 5.28 (2H s, PhCH), 2.27 (3H s, CH_3) $^{13}\text{C NMR}$ (100 MHz, CDCl_3) δ ppm 10.2, 68.7, 109.6, 128.5, 128.7, 128.8, 134.9, 154.3. IR (ν_{max} cm^{-1} , neat): 1715, 1675, 1435, 1298, 1275, 1241, 1191, 1132. LC-HRMS(ES+) at $T_R = 1.223$ found 232.1089. $\text{C}_{12}\text{H}_{14}\text{O}_2\text{N}_3$ ($[\text{M}+\text{H}]^+$) requires 232.1086. Δ MW (ppm) = 1.3

Fmoc-D-Threonine-OH (**264**)



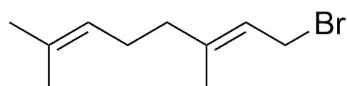
D-threonine **293** (2.5 g, 21 mmol, 1 eq) was dissolved with NaHCO_3 (1.77 g, 21 mmol, 1 eq) in dioxane/ H_2O (53 mL, 1:2.5 v/v) and cooled to 0 °C. Fmoc-OSu (7.09 g, 21 mmol, 1 eq) was dissolved separately in dioxane (73 mL) and added dropwise over 30 minutes, forming a white suspension that was stirred at room temperature overnight. The resultant clear solution was concentrated *in vacuo* and acidified with HCl (1M, aq) to form a suspension. The product was extracted with EtOAc (3 x 200 mL), the organic layers combined and washed with brine (250 mL) and dried over MgSO_4 , to yield the product Fmoc-D-Threonine-OH **264** (6.95g, 97%) as a white solid without further purification required. $R_f = 0.18$ (10% MeOH/ CHCl_3 + 0.1% AcOH). $^1\text{H NMR}$ δ H (400 MHz, CDCl_3) δ ppm 1.24 – 1.31 (m, 3H), 4.22 (t, 1H, $J = 6.85$), 4.37 (d, 1H, $J = 8.6$), 4.43 (br d, 2H, $J = 7.04$), 5.77 (br d, 1H, $J = 8.8$), 7.28 – 7.34 (m, 2H), 7.39 (t, 2H, $J = 7.34$), 7.56 – 7.64 (m, 2H), 7.76 (d, 2H, $J = 7.43$); $^{13}\text{C NMR}$ δ H (125 MHz, CD_3OD) δ ppm 20.5, 61.0, 68.2, 68.6, 121.0, 128.2, 128.8, 142.6, 145.1, 145.4, 159.0, 174.2. LC-HRMS(ES+) at $T_R = 1.86$ found 342.1346. $\text{C}_{19}\text{H}_{20}\text{O}_5\text{N}$ ($[\text{M}+\text{H}]^+$) requires 342.1341 Δ MW (ppm) = 1.5

Geranyl iodide (Ger-I) (305)



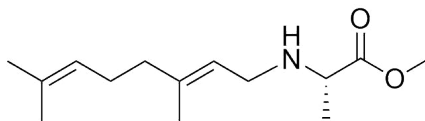
Sodium iodide (3.72 g, 24.8 mmol, 4.6 eq) was dissolved in acetone (15.5 mL). This solution was cooled to 0 °C and shielded from light. Geranyl chloride **307** (1 mL, 5.39 mmol, 1 eq) was then added, and the reaction stirred at room temperature for 3 hours. The solution was then diluted with water (60 mL), and extracted with hexane (3 x 50 mL). The organic fractions were combined and washed with Na₂S₂O₃ (10% aq, 2 x 50 mL) and then brine (50 mL). The organic extract was dried over MgSO₄ and concentrated *in vacuo* to yield geranyl iodide **305** as a dark brown oil (1.19 g, 83%) ¹H NMR (400 MHz, CDCl₃) δ ppm 1.60 (s, 3H), 1.64 (s, 3H) 1.68 (s, 3H), 2.00 – 2.15 (m, 4H), 3.94 (br d, 2H, *J* = 8.8 Hz, CH₂I), 5.03-5.12 (m, 1H), 5.50-5.60 (m, 1H). ¹³C NMR (125 MHz, CDCl₃) δ ppm 23.2, 24.1, 28.2, 29.8, 30.7, 38.1, 119.8, 126.25, 129.0, 141.8

Geranyl bromide (Ger-Br) (308)



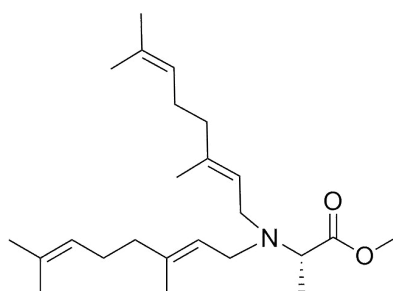
Geranyl chloride **307** (1 mL, 5.39 mmol, 1 eq) was dissolved in NMP (4.65 mL) with stirring at room temperature. Sodium bromide (6.10 g, 59.3 mmol, 11 eq) was then added to the solution. The reaction was stirred for a further 2 hours, before quenching with water (1 mL), and extracted with DCM (3 x 50 mL). The organic fractions were combined and washed with brine (50 mL). The organic extract was dried over MgSO₄ and concentrated *in vacuo* to yield geranyl bromide **308** as a pale yellow viscous liquid (0.99 g, 85%) ¹H NMR δ H (500 MHz, CDCl₃) δ ppm 1.60 (3H s, CH₃), 1.68 (3H s, CH₃), 1.72 (3H s, CH₃), 1.74 (3H s, CH₃), 2.01-2.14 (4H m), 4.01 (2H d, *J* = 8.34, CH₂Br), 5.03-5.12 (1H m, CH), 5.50-5.59 (1H m, CH). ¹³C NMR (125 MHz, CDCl₃) δ ppm 16.0, 17.7, 25.8, 26.2, 29.5, 34.3, 39.5, 120.6, 123.6, 131.9, 143.5

Methyl (E)-(3,7-dimethylocta-2,6-dien-1-yl)-L-alaninate (N-Ger-Ala-OMe) (318)



L-alanine methyl ester hydrochloride **317** (280 mg, 2 mmol, 1 eq) was dissolved in DMF (4 mL, 0.5 M) with stirring, and cooled to -15 °C. Triethylamine (560 μ L, 4 mmol, 2 eq) was then added, resulting in precipitate formation. Geranyl chloride **307** (370 μ L, 2 mmol, 1 eq) was added and the reaction maintained at -15 °C for a further 30 minutes, after which it was warmed to room temperature and stirred overnight, with progress monitored by TLC and MS. The solution was concentrated *in vacuo* and purified by column chromatography (2-20% MeOH in CHCl_3 + 0.1% AcOH) to yield the product **318** as an off-white solid (177 mg, 64%) $R_f = 0.57$ (10% MeOH/ CHCl_3 + 0.1% AcOH). $^1\text{H NMR}$ (500 MHz, CD_3OD) δ ppm 1.47 (3H br d, $J = 6.95$, CH_3), 1.62 (3H s, CH_3), 1.68 (3H s, CH_3), 1.76 (3H s, CH_3), 2.08 – 2.20 (4H m), 3.52 (1H q, $J = 7.15$, CH) 3.59 – 3.70 (2H m, CH_2), 4.84 (3H s, OCH_3), 5.08 – 5.14 (1H m, CH), 5.29 (1H br t, $J = 7.25$, CH). $^{13}\text{C NMR}$ (100 MHz, CD_3OD) δ ppm 16.4, 16.7, 17.8, 25.9, 27.2, 40.7, 44.7, 58.0, 115.3, 124.7, 133.0, 147.2, 174.3

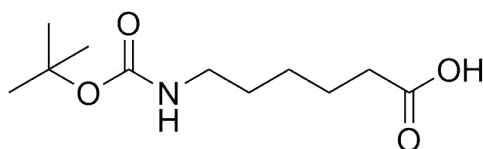
Bis((E)-3,7-dimethylocta-2,6-dien-1-yl)-L-alanine (N,N-Ger₂-Ala-OH) (319)



L-alanine methyl ester hydrochloride **317** (280 mg, 2 mmol, 1 eq) was dissolved in DMF (4 mL, 0.5 M) with stirring, and cooled to -15 °C. Triethylamine (560 μ L, 4 mmol, 2 eq) was then added, resulting in precipitate formation. Geranyl chloride (370 μ L, 2 mmol, 1 eq) was added and the reaction maintained at -15 °C for a further 30 minutes, after which it was warmed to room temperature and stirred

overnight, with progress monitored by TLC and MS. The solution was concentrated *in vacuo* and purified by column chromatography (2-20% MeOH in CHCl₃ + 0.1% AcOH) to yield the product **319** as an off-white solid (61 mg, 17%) R_f 0.84 (10% MeOH/ CHCl₃ + 0.1% AcOH). ¹H NMR (400 MHz, CDCl₃) δ ppm 1.28 (br d, 3H, *J*=7.24 Hz, 2x CH₃) 1.59 (s, 6H, 2x CH₃) 1.63 (6H s, 2x CH₃) 1.67 (6H s, 2x CH₃), 1.98 – 2.16 (9H, m), 3.18 (4H br s, *J* = 6.46), 3.69 (3H s, OCH₃), 5.01 - 5.12 (2H m), 5.23 (2H br t, *J*=6.46) ¹³C NMR (100 MHz, CDCl₃) δ ppm 14.3, 16.1, 17.6, 25.6, 26.4, 39.8, 48.0, 51.2, 57.1, 122.0, 124.1, 131.4, 138.5, 174.4. **LC-HRMS(ES+)** at T_R =2.17 found 376.3218. C₂₄H₄₂O₂N ([M+H]⁺) requires 376.3216 Δ MW (ppm) = 0.5

6-*N*-(*tert*-Butyloxycarbonyl)aminohexanoic acid (Boc-6-Ahx-OH, 369)



6-Aminocaproic acid **370** (1.31 g, 10 mmol, 1 eq) was dissolved in dioxane/ H₂O (2:1, 10 mL) and cooled to 0 °C. NaOH (1M, 10 mL, 10 mmol, 1 eq) was added, followed by di-*tert*-butyl dicarbonate (2.40 g, 11 mmol, 1.1 eq). The reaction was warmed to room temperature and stirred overnight. The solution was concentrated *in vacuo*, and extracted with ethyl acetate (30 mL). The aqueous layer was acidified with HCl (1M) to pH 1, and further extracted with ethyl acetate (3 x 30 mL). Organic fractions were combined, dried over MgSO₄ and concentrated *in vacuo* to yield Boc-6-Ahx-OH **369** (1.55 g, 67%) as a white crystalline solid, with no further purification required. R_f = 0.65 (EtOAc). ¹H NMR δ H (500 MHz, CDCl₃) δ ppm 1.29 - 1.40 (2 H, m) 1.43 (9 H, br s) 1.46 - 1.53 (2 H, m) 1.63 (2 H, quin, *J*=7.5 Hz) 2.15 - 2.28 (1 H, m) 2.33 (2 H, t, *J*=7.5 Hz) 3.11 (2 H, br d, *J*=6 Hz) 4.59 (1 H, br s, NH). ¹³C NMR (125 MHz, CDCl₃) δ C: 179.2, 156.1, 80.5, 40.4, 34.1, 29.7, 28.4, 26.2, 24.4. IR (*v*_{max} cm⁻¹, neat): 1682, 1515, 1364, 1274, 1246, 1162, 1137, 1096. **LC-HRMS(ES+)** at T_R = 1.67 found 254.1372. C₁₁H₂₁O₄NNa ([M+Na]⁺) requires 254.1368 Δ MW (ppm) = 1.6

6.3 Peptide syntheses

6.3.1 General procedure for automated peptide synthesis

All automated syntheses were carried out on a Biotage Alstra Initiator+ on a 0.1 mmol scale, using a 10 mL reaction vessel. Rink amide ChemMatrix resin (0.47 mmol/g, 1 eq) was swollen in DMF at room temperature for 20 minutes prior to synthesis. Fmoc-protected amino acids were each dissolved in DMF (3 eq, 0.2 M), HCTU dissolved in DMF (3 eq, 0.5 M), and DIPEA dissolved in NMP (6 eq, 0.5 M). 20% piperidine in DMF with OxymaPure (0.1 M) was prepared as Fmoc-deprotection solution. All Fmoc-amino acids were coupled for 5 minutes at 70 °C, apart from Fmoc-Arg(Pbf)-OH, which was coupled at room temperature for 25 minutes, before heating to 75 °C for a further 5 minutes, and Fmoc-D-amino acids, which were submitted to two separate coupling reactions. For each Fmoc-deprotection, two reactions were undertaken: first at 75 °C for 30 seconds, followed by 3 minutes at 75 °C.

6.3.2 General procedures for resin loading

6.3.2.1 Loading of 2-Chlorotrityl chloride resin

2-Chlorotrityl chloride resin (1.51 mmol/g, 1.32 g, 2 mmol, 1 eq) was added to an oven dried glass filtration vessel. Anhydrous DCM (10 mL) was added, and the resin allowed to swell for 20 minutes. Fmoc-Ala-OH (1.868 g, 6 mmol, 3 eq) was then added, forming a suspension. DIPEA (2.09 mL, 12 mmol, 6 eq) was then also added and the vessel flushed with nitrogen. The reaction was shaken overnight at room temperature. Following this, the vessel was drained and the resin washed with DMF (3 x 10 mL), MeOH (3 x 10 mL) and DCM (3 x 10 mL). An Fmoc-loading test was carried out by measuring UV absorption of the Fmoc-piperidine adduct at 300 nm, and found to be 0.75 mmol/ g (50% loading, 1 mmol).

6.3.2.2 Loading of Wang resin

Wang resin (0.90 mmol/ g, 222 mg, 0.2 mmol, 1 eq) was added to a sintered glass filtration vessel. A solution of Fmoc-Ala-OH (250 mg, 0.8 mmol, 4 eq) and DMAP (9.8 mg, 0.08 mmol, 0.4 eq) in DMF (1 mL) was then added, followed by DIC (125 μ L, 0.8 mmol, 4 eq). The vessel was shaken at rt for 2 hours, before being washed with DMF (3 x 10 mL), MeOH (3 x 10 mL) and DCM (3 x 10 mL). An Fmoc-loading test was carried out by measuring UV absorption of the Fmoc-piperidine adduct at 300 nm, and found to be 0.60 mmol/ g (67% loading, 0.14 mmol).

6.3.2.3 Loading of Rink amide resin

Rink amide ChemMatrix resin (0.47 mmol/ g, 213 mg, 0.1 mmol, 1 eq) was added to a sintered glass filtration vessel. A solution of Fmoc-Ala-OH (250 mg, 0.8 mmol, 4 eq) and DMAP (9.8 mg, 0.08 mmol, 0.4 eq) in DMF (1 mL) was then added, followed by DIC (125 μ L, 0.8 mmol, 4 eq). The vessel was shaken at rt for 2 hours, before being washed with DMF (3 x 10 mL), MeOH (3 x 10 mL) and DCM (3 x 10 mL). An Fmoc-loading test was carried out by measuring UV absorption of the Fmoc-piperidine adduct at 300 nm, and found to be 0.60 mmol/g (67% loading, 0.14 mmol).

6.3.2.4 Loading of safety-catch resins

Method A: 4-Sulfamylbutyryl Rink resin (0.45 mmol/ g , 555 mg, 0.25 mmol, 1 eq) was added to a plastic sintered SPE cartridge (6 mL) and swollen in DMF (3 mL) for 0.5 hours, before being drained. Separately, a solution of Fmoc-Ala-OH (311 mg, 1 mmol, 4 eq) and 1-Melm (80 μ L, 1 mmol, 4 eq) in DMF/ DCM (1:4, 3 mL) was prepared and added to the resin. The reaction was shaken at room temperature for 10 minutes, before DIC (157 μ L, 1 mmol, 4 eq) was also added. The reaction was sealed and shaken overnight at room temperature, before being washed with DMF (3 x 10 mL), MeOH (3 x 10 mL) and DCM (3 x 10 mL). The reaction was repeated once more as previously, washed and dried *in vacuo*. An Fmoc-loading test was carried out by measuring UV absorption of the Fmoc-

cleavage product at 300 nm, and found to be 0.50 mmol/ g (68% conversion, 0.14 mmol).

Method B: 4-Sulfamylbutyryl AM resin (0.73 mmol/g, 137 mg, 0.1 mmol, 1 eq) was added to a plastic sintered SPE cartridge (3 mL) and swollen in CHCl₃ (1 mL) for 0.5 hours before being drained. Separately, a solution of Fmoc-Ala-OH (93 mg, 0.3 mmol, 3 eq) and DIPEA (105 μL, 0.6 mmol, 6 eq) in CHCl₃ (1 mL) was prepared and added to the resin. The tube was cooled quickly in dry ice. PyBOP (156 mg, 0.3 mmol, 3 eq) was added then added dry, and the tube shaken, before being left at -20 °C overnight. After, the resin was washed with DMF (3 x 10 mL), MeOH (3 x 10 mL) and DCM (3 x 10 mL) and dried *in vacuo*. An Fmoc-loading test was carried out by measuring UV absorption of the Fmoc-cleavage product at 300 nm, and found to be 0.44 mmol/ g (60% loading, 0.06 mmol).

6.3.3 General procedures for Fmoc-SPPS

6.3.3.1 Fmoc deprotection

To the resin-bound peptide, 20% piperidine/ DMF (excess) was added. The vessel was sealed and shaken at room temperature for 20 minutes, after which the solution was drained. The resin was then washed with DMF (3 x 10 mL), MeOH (3 x 10 mL) and DCM (3 x 10 mL). Reaction completion was monitored by ninhydrin stain; producing blue beads for a positive result.

5.3.3.2 Fmoc-protected amino acid coupling

The resin-bound peptide was swollen with DMF for 15 minutes before being drained. In a vial, a solution of Fmoc-protected amino acid (3 eq), HCTU (3 eq) and DIPEA (6 eq) in DMF was prepared and added to the resin, and shaken at room temperature for one hour, after which the solution was drained, and washed with DMF (3 x 10 mL), MeOH (3 x 10 mL) and DCM (3 x 10 mL). Reaction

completion was monitored by ninhydrin stain, with a clear or yellow bead indicating reaction completion.

5.3.3.3. Acetyl capping of N-terminus

To the loaded resin, DMF was added, followed by acetic anhydride (1.2 eq). The vessel was shaken at room temperature for 30 minutes, before being drained and washed with DMF (3 x 10 mL), MeOH (3 x 10 mL) and DCM (3 x 10 mL). Reaction completion was monitored by ninhydrin stain, with a clear or yellow bead indicating reaction completion.

5.3.3.4 Esterification of threonine side chain hydroxyl

The peptide-bound resin (1 eq) was swollen in DMF for 15 minutes, then drained. Separately, Fmoc-Ile-OH (4 eq) or Fmoc-Aib-OH (4 eq) and DMAP (0.4 eq) were dissolved in DMF, and added to the resin. DIC (4 eq) was then added, and the reaction shaken at room temperature for 2 hours. Reaction completion was monitored by cleaving a small portion of resin with 1% TFA/ DCM, and analysing the filtrate with analytical RP-HPLC and LCMS.

6.3.4 Peptide cleavage from resin

6.3.4.1 Activation, cleavage testing and cyclisation with safety catch resins

Activation: Peptide on 4-sulfamylbutyryl AM resin (1 eq) was swollen in NMP (1 mL) for 1 hour at room temperature. Without draining, DIPEA (10 eq) was added to the mixture. ICH₂CN (25 eq) that had been filtered through a basic alumina plug was then also added, and the reaction shaken overnight at room temperature, before being washed with DMF (3 x 10 mL), MeOH (3 x 10 mL) and DCM (3 x 10 mL)

Mmt deprotection: To the resin-bound peptide, DCM (700 µL) was added, followed by TFE (200 µL) and finally AcOH (100 µL). The reaction was sealed

and shaken at room temperature for 0.5 hours before being washed as previously, followed by a subsequent DMF wash (3 x 10 mL).

Cleavage test: For 4-sulfamylbutyryl Rink amide AM resin, a small amount of resin (~ 5 mg) was taken, and TFA/ TES/ DCM (95: 2.5: 2.5, 200 μ L) added. This reaction was shaken at room temperature for 0.5 hours, before the filtrate was evaporated, and the remaining precipitate dissolved in H₂O / MeCN for analysis by LCMS and analytical HPLC.

For 4-sulfamylbutyryl resin, a small amount of resin (~ 5 mg) was taken, and benzylamine (5 eq) in THF (50 μ L) added. This reaction was shaken at room temperature for 2 hours, before the filtrate was evaporated, and the remaining precipitate dissolved in H₂O / MeCN for analysis by LCMS and analytical HPLC.

Cyclisation: To the activated resin-bound peptide, a solution of DIPEA/ DMF (1:1, 1 mL) was added. The mixture was microwaved at 75 °C for 20 minutes, before the solution was drained and evaporated to yield the crude cyclised peptide.

6.3.4.2 Cleavage conditions for 2-chlorotriyl chloride resins

After the completion of all Fmoc-amino acid couplings and the final Fmoc-deprotection, a solution of 1% TFA/ DCM (8 mL) was added to the resin. This reaction was shaken at room temperature for 20 mins, before the acidic peptide solution was filtered into a Falcon tube (30 mL). The resin was washed with further additions of DCM (3 x 8 mL), and evaporated under reduced pressure. The residual solution was diluted with H₂O/ MeCN (5 mL) and lyophilised to afford the TFA salt of the crude product as an off-white solid.

6.3.4.3 Cleavage conditions for Wang and Rink amide resins

After the completion of all Fmoc-amino acid couplings and the final Fmoc-deprotection, a solution of TFA/ TES/ DCM (5 mL, 95:2.5:2.5 v/v/v) was added to the resin. This reaction was shaken at room temperature for 2 hours, before the acidic peptide solution was filtered into a Falcon tube (30 mL). The resin was washed with further additions of DCM (3 x 8 mL), and evaporated under reduced

pressure. The residual solution was diluted with H₂O/ MeCN (5 mL) and lyophilised to afford the TFA salt of the crude product as an off-white solid.

6.3.5 Solution phase macrolactamisations

6.3.5.4 Solution-phase macrolactamisation (ester formation)

The linear branched peptide Ac-tAR(Pbf)I-OH (7.5 mg, 0.01 mmol, 1 eq) was dissolved in DMF (5 mM) with TEA (8.4 µL, 0.06 mmol, 6 eq) and added to a plastic syringe. Separately, in an RBF, EDC (5.75 mg, 0.03 mmol, 3 eq) and HOBt (4.6 mg, 0.03 mmol, 3 eq) were dissolved in DMF (3.75 mM) and stirred at room temperature. The peptide/base solution was added dropwise to the EDC/HOBt solution by syringe pump over 20 minutes. After addition, the reaction was heated (MW) at 50 °C for a further 45 minutes, before it was evaporated under reduced pressure. The concentrated crude solution was dissolved in MeCN/ H₂O, analysed by analytical RP-HPLC and LCMS, and purified attempted by semi-preparative RP-HPLC (5-100 % MeCN + 0.1% TFA in H₂O + 0.1 % TFA over a 30 minute gradient) without success.

6.3.5.5 Solution-phase macrolactamisation (amide formation)

The linear branched peptide Ac-t[IR(Pbf)-NH₂]AI-OH (7.5 mg, 0.01 mmol, 1 eq) was dissolved in DMF (10 mM) with DIPEA (8.4 µL, 0.06 mmol, 6 eq) and added to a plastic syringe. Separately, in an RBF, HATU (11.4 mg, 0.03 mmol, 3 eq) was dissolved in DMF (7.5 mM) and stirred at room temperature. The peptide/base solution was added dropwise to the HATU solution by syringe pump over 20 minutes. After addition, a sample was taken for analysis by analytical RP-HPLC and LCMS, and the reaction stirred for a further hour, before it was evaporated under reduced pressure. The concentrated crude solution was dissolved in MeCN/ H₂O, and purified by semi-preparative RP-HPLC (5-100 % MeCN + 0.1% TFA in H₂O + 0.1 % TFA over a 30 minute gradient) to yield the cyclic product (82% yield, >99% purity).

6.3.6 Modifications of cyclic peptides

6.3.6.1 Removal of cysteine trityl protection and subsequent prenylation

A freshly prepared solution of TFA/ EDT/ TES/ DCM (90: 2.5: 2.5: 5) was added to the cyclic peptide and the solution stirred at room temperature for 30 minutes. The solution was then concentrated, and the peptide precipitated with ice cold diethyl ether (10 mL).

A solution of $\text{Zn}(\text{OAc})_2 \cdot 2\text{H}_2\text{O}$ (4 eq) in DMF (40 mM) was prepared and added to the free-thiol containing crude cyclic peptide (1 eq). TFA (5 μL) was then added, and effervescence observed. Finally, geranyl bromide (4 eq) was added and the reaction shaken at room temperature for 30 minutes, after which the reaction was concentrated *in vacuo*, diluted with water and lyophilised to dryness. The prenylated cyclic peptide was purified by semi-preparative RP-HPLC (5-100 % MeCN + 0.1% TFA in H_2O + 0.1 % TFA over a 30 minute gradient), to give the final product as the TFA salt.

6.3.6.2 TFA to HCl salt conversion

Pure cyclic peptide was dissolved in HCl solution (5 mM, aqueous) and lyophilised to dryness. This was repeated a further two times. The product was analysed by ^{19}F NMR to the absence of peaks used determine the conversion of TFA to HCl salt.

6.3.7 Peptide content determination

6.3.7.1 Determination of peptide content by UV-Vis

Peptide content for sequences containing phenylalanine residues was determined by UV-Vis absorption at 257 nm. Phe-containing peptides were dissolved in 7.4 mL H_2O , from which 100 μL was taken and diluted to 600 μL with water. Concentration of the stock solution was determined by measurement of absorption at 257 nm applied to the equation

$$mg / mL = \frac{Abs \times DF \times MW}{\epsilon}$$

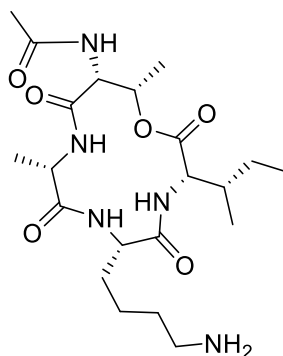
where abs = absorption at 257 nm, DF = dilution factor, MW = molecular weight, and ϵ = molar extinction coefficient, which is 200 M/ cm. From this, the quantity in mg of peptide can be calculated.

6.3.7.2 Determination of peptide content by ^1H NMR

For peptides lacking chromophores, peptide content was determined by ^1H NMR. A known volume of peptide in D_2O (or $\text{D}_2\text{O}/\text{MeCN}$ depending on solubility) was added to a known quantity of *para*-nitrophenol in D_2O . Peptide content was calculated by comparing relative integrations of distinct peaks in the ^1H NMR spectrum from peptide and *para*-nitrophenol respectively.

6.3.8 Syntheses of individual peptides

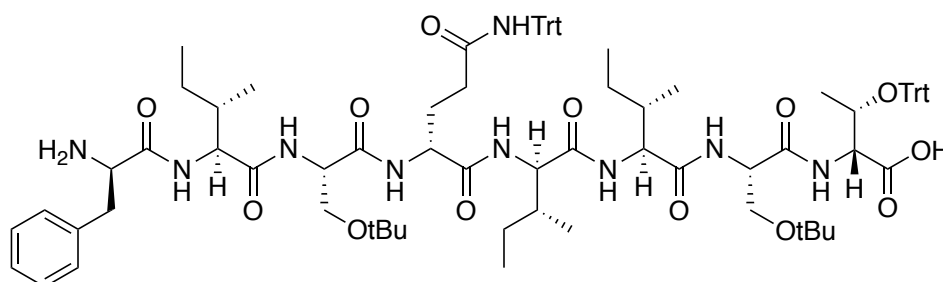
6.3.8.1 Synthesis of cyclic Ac-tAKI macrocycle (207) via D-Thr loading on safety-catch resin. Peptide 217 was also synthesised using this procedure.



4-Sulfamylbutyryl Rink resin (0.65 mmol/ g , 385 mg, 0.25 mmol, 1 eq) was added to a plastic sintered SPE cartridge (6 mL) and swollen in DMF (3 mL) for 0.5 hours, before being drained. Separately, a solution of Fmoc-D-Thr(Trt)-OH (438 mg, 0.75 mmol, 3 eq) and 1-Melm (60 μL , 0.75 mmol, 4 eq) in DMF/ DCM (1:4, 3

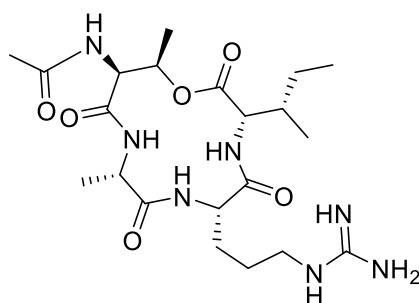
mL) was prepared and added to the resin. The reaction was shaken at room temperature for 10 minutes, before DIC (118 μ L, 0.75 mmol, 3 eq) was also added. The reaction was sealed and shaken overnight at room temperature, before being washed with DMF (3 x 10 mL), MeOH (3 x 10 mL) and DCM (3 x 10 mL). The reaction was repeated once more as previously, washed and dried *in vacuo*. 20% piperidine/DMF (3 mL) was added to the resin and shaken at room temperature for 30 minutes, before 20% acetic anhydride/DMF (3 mL) was added and reacted in the same way. After washing as previously, Trt deprotection was achieved by adding 1% TFA/DCM (3 mL) and shaken at room temperature for 45 minutes. A solution of Fmoc-Ile-OH (247 mg, 0.7 mmol, 4 eq), and DMAP (9 mg, 0.07 mmol, 0.4 eq) in DMF (3 mL) was prepared and added to the resin, before addition of DIC (0.11 mL, 0.7 mmol, 4 eq) into the same mixture. This was sealed and shaken at room temperature for 2 hours before being drained and washed as previously. Conversion to ester was determined by ESI MS and HPLC. Automation on the Biotage Alstra was used to achieve the next two amino acid couplings and final Fmoc-deprotection, using standard conditions as described in Section 6.3.1. The N-terminus was reprotected by addition of a solution of Mmt-Cl (31 mg, 0.1 mmol, 4 eq), DIPEA (35 μ L, 0.2 mmol, 8 eq) in DCM (anhydrous), by microwaving at 35 $^{\circ}$ C, 1 bar, 25W for 2 hours, before being washed with NMP (3 x 5 mL). To the resin, NMP (800 μ L) and DIPEA (43.5 μ L, 10 eq, 0.25 mmol) were added before also adding iodoacetonitrile (45 μ L, 0.625 mmol, 25 eq) that had been filtered through a plug of basic alumina. This was sealed and shaken at room temperature for 24 hours. After washing with NMP (3 x 5 mL), a solution of DIPEA/DMF (1:1) was added to the resin and this was shaken for a further 24 hours. The solution was concentrated and submitted to 1% TFA/DCM for 30 minutes at room temperature. ESI MS revealed $m/z = 455$ in solution but the product **207** was not isolated.

6.3.8.2 Synthesis of linear peptide H₂N-flS(OtBu)q(Trt)ilS(OtBu)t(Trt)-OH (261).



Peptide **261** was synthesised using the Biotage Alstra automated peptide synthesiser on a 0.1 mmol scale using standard conditions (Section 6.3.1). The linear peptide on resin was cleaved with TFA/TIS/H₂O (95:2.5:2.5, 2 mL) for 5 minutes, before the solution was filtered and concentrated *in vacuo*. The crude solution was diluted in MeCN/H₂O (1:1) and purified with RP-HPLC to yield the linear peptide **261** as a fluffy white solid (25.2 mg, 63% yield). LC-HRMS(ES⁺) at T_R = 2.52 found 1504.8492. C₈₈H₁₁₄O₁₃N₉ ([M+H]⁺) requires 1504.8530, Δ MW (ppm) = -2.5.

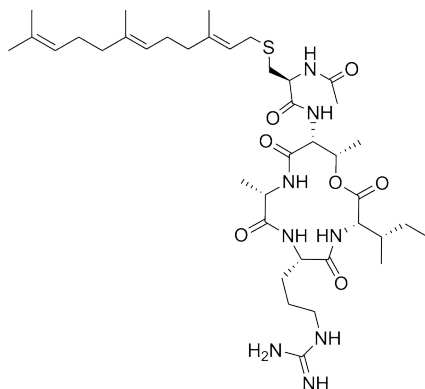
6.3.8.3 Synthesis of cyclic Ac-tARI macrocycle 290 via solution-phase cyclisation. Peptides 296 and 297 also synthesised using this procedure.



Wang resin (0.90 mmol/ g, 222 mg, 0.2 mmol, 1 eq) was added to a sintered glass filtration vessel. A solution of Fmoc-Ala-OH (250 mg, 0.8 mmol, 4 eq) and DMAP (9.8 mg, 0.08 mmol, 0.4 eq) in DMF (1 mL) was then added, followed by DIC (125 μL, 0.8 mmol, 4 eq). The vessel was shaken at rt for 2 hours, before being washed with DMF (3 x 10 mL), MeOH (3 x 10 mL) and DCM (3 x 10 mL).

The resin was deprotected with 20% piperidine/DMF (0.5 mL) with stirring at room temperature for 0.5 hours. A solution of Fmoc-D-Thr-OH (204 mg, 0.6 mmol, 3 eq) in DMF (0.5 mL) with DIPEA (0.28 mL, 1.2 mmol, 6 eq) was then added to the resin and shaken at room temperature for one hour, before the solution was filtered and washed as previously. Deprotection with 20% piperidine/DMF (0.5 mL) was repeated as before. A solution of 20% acetic anhydride/DMF was added to resin and shaken at room temperature for 30 minutes, before washing as previously. A solution of Fmoc-Ile-OH (282 mg, 0.8 mmol, 4 eq), and DMAP (10 mg, 0.08 mmol, 0.4 eq) in DMF (3 mL) was prepared and added to the resin, before addition of DIC (0.15 mL, 0.8 mmol, 4 eq) into the same mixture. This was sealed and shaken at room temperature for 2 hours before being drained and washed as previously. Conversion to ester was determined by ESI MS and HPLC. After a further deprotection with 20% piperidine/DMF as before, a solution of Fmoc-Arg(Pbf)-OH (388 mg, 0.6 mmol, 3 eq) and DIPEA (0.21 mL, 1.2 mmol, 6 eq) in DMF (4 mL) was added to the resin and shaken at room temperature for 1 hour. After a final Fmoc deprotection with 20% piperidine/DMF, a solution of 1% TFA/ DCM was added to the resin and shaken for 1 hour. The solution was then drained and collected, concentrated *in vacuo* and dissolved in H₂O/MeCN (1:1), before overnight lyophilisation. The crude linear peptide (12 mg, not isolated) was dissolved in DMF (1.6 mL) with DIPEA (16.7 µL, 0.096 mmol, 6 eq) and transferred to a syringe. HATU (12 mg, 0.1 mmol, 2 eq) was dissolved in DMF (4.25 mL) in an RBF with stirring. The peptide solution was added dropwise to the HATU solution over 20 minutes, then analysed by ESI MS and HPLC. After a final Pbf deprotection in TFA/TES/DCM (95:2.5:2.5, 1 mL) and purification with RP-HPLC, the cyclic peptide product **290** was obtained. See Table in Section 6.3.9 for data.

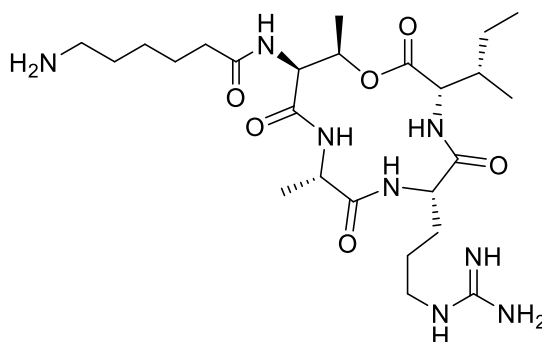
6.3.8.4 Synthesis of Farnesyl-Arg10bactin (357). Peptides 349-356 and 358-362 also synthesised using this procedure.



2-Chlorotrityl chloride resin **102** (1.51 mmol/g, 66 mg, 0.1 mmol, 1 eq) was added to an oven dried glass filtration vessel. Anhydrous DCM (2 mL) was added, and the resin allowed to swell for 20 minutes. Fmoc-Ala-OH (125 mg, 0.3 mmol, 3 eq) was then added, forming a suspension. DIPEA (0.14 mL, 0.6 mmol, 6 eq) was then also added and the vessel flushed with nitrogen. The reaction was shaken overnight at room temperature. The vessel was then drained and the resin washed with DMF (3 x 10 mL), MeOH (3 x 10 mL) and DCM (3 x 10 mL). The resin was deprotected with 20% piperidine/DMF (0.5 mL) with stirring at room temperature for 0.5 hours. A solution of Fmoc-D-Thr-OH (153 mg, 0.45 mmol, 3 eq) in DMF (0.5 mL) with DIPEA (0.21 mL, 0.9 mmol, 6 eq) was then added to the resin and shaken at room temperature for one hour, before the solution was filtered and washed as previously. Deprotection with 20% piperidine/DMF (0.5 mL) was repeated as before. A solution of Fmoc-Cys(Trt)-OH (175 mg, 0.3 mmol, 3 eq), HCTU (186 mg, 0.3 mmol, 3 eq) and DIPEA (0.14 mL, 0.6 mmol, 6 eq) in DMF (2 mL) was prepared and added to the resin. This was shaken at room temperature for one hour, before filtration and washes as previously. Deprotection (20% piperidine/DMF) was repeated. A solution of acetic anhydride (0.12 mmol, 1.2 eq) in DMF was added to resin and shaken at room temperature for 30 minutes, before washing as previously. A solution of Fmoc-Ile-OH (141 mg, 0.4 mmol, 4 eq), and DMAP (5 mg, 0.04 mmol, 0.4 eq) in DMF (2 mL) was prepared and added to the resin, before addition of DIC (0.075 mL, 0.4 mmol, 4 eq) into the same mixture. This was sealed and shaken at room temperature for 2 hours before being drained and washed as previously. Conversion to ester was determined by ESI MS and HPLC. After a further deprotection with 20%

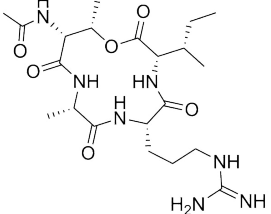
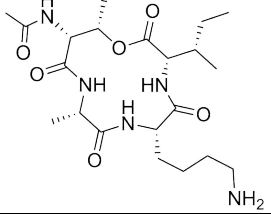
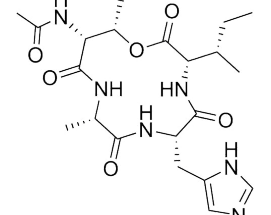
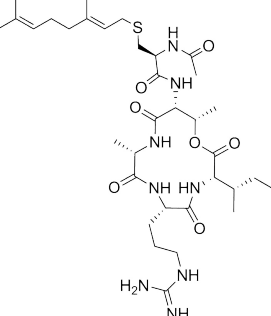
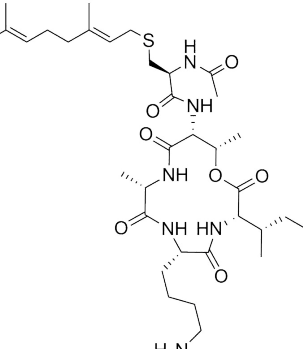
piperidine/DMF as before, a solution of Fmoc-Arg(Pbf)-OH (194 mg, 0.3 mmol, 3 eq) and DIPEA (0.14 mL, 0.6 mmol, 6 eq) in DMF (2 mL) was added to the resin and shaken at room temperature for 1 hour. After a final Fmoc deprotection with 20% piperidine/DMF, a solution of 1% TFA/ DCM was added to the resin and shaken for 10 minutes. The solution was then drained and collected, concentrated *in vacuo* and dissolved in H₂O/MeCN (1:1), before overnight lyophilisation. The crude linear peptide (59 mg, 0.05 mmol, 1 eq) was dissolved in DMF (6 mL) with DIPEA (0.052 mL, 0.3 mmol, 6 eq) and transferred to a syringe. HATU (38 mg, 0.1 mmol, 2 eq) was dissolved in DMF (13 mL) in an RBF with stirring. The peptide solution was added dropwise to the HATU solution over 20 minutes, then analysed by ESI MS and HPLC. The crude cyclised product (not isolated) was submitted to a solution of TFA/TES/EDT/DCM (90:2.5:2.5:5, 1 mL) for 2.5 hours at room temperature, before being concentrated *in vacuo* and precipitated with cold diethyl ether. The crude product was dissolved in DMF (1 mL) and to it Zn(OAc)₂·2H₂O (4 mg, 0.0185 mmol, 5 eq) was added. Farnesyl bromide (4 uL, 0.0148 mmol, 4 eq) was also added after filtration through a plug of basic alumina, and the reaction stirred at room temperature for 2 hours. Following purification by RP-HPLC, the final cyclic peptide product **357**. The crude prenylated cyclic peptide (Purification by RP-HPLC yielded the product **357** as a powdery white solid (4.3 mg, 5% yield). See Table in Section 6.3.9 for data.

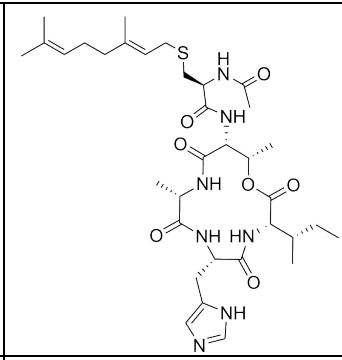
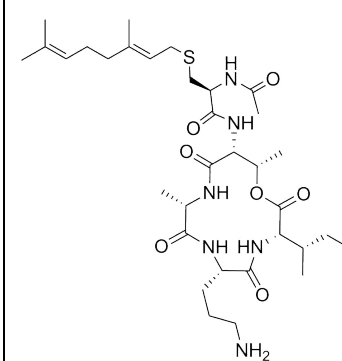
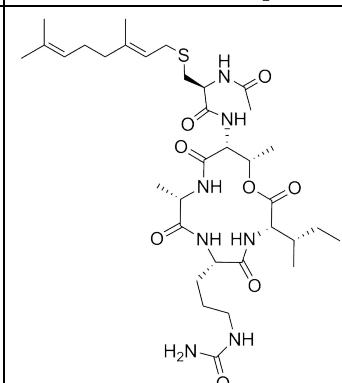
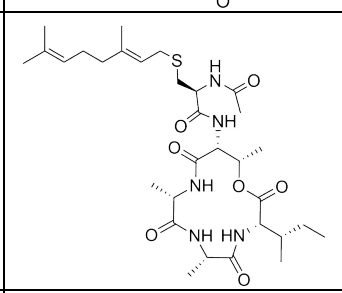
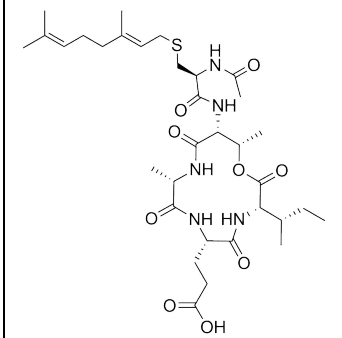
6.3.8.5 Synthesis of NH₂-Ahx-tARI .TFA (371). Peptide 372 also synthesised using this procedure.

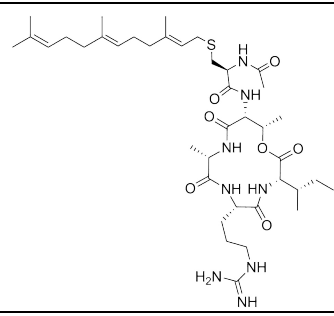
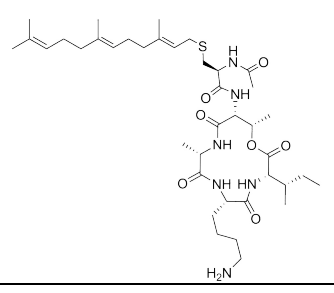
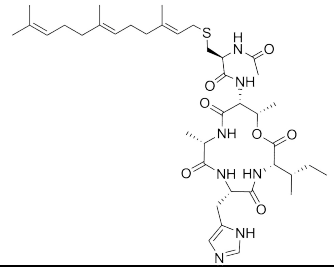
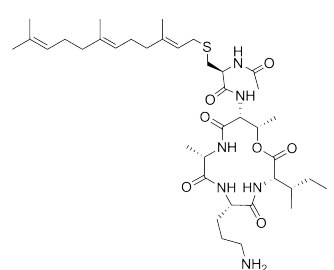
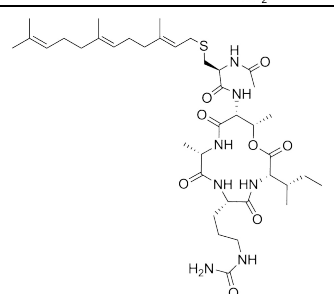
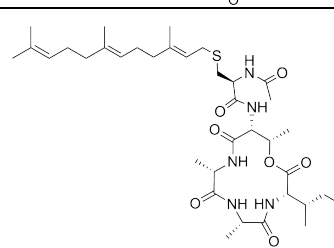


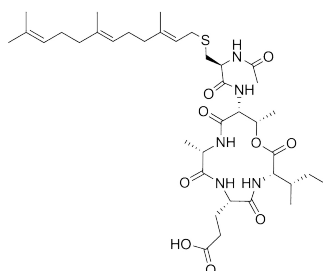
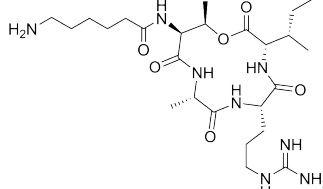
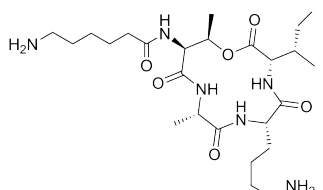
2-Chlorotrityl chloride resin **102** (1.51 mmol/g, 99 mg, 0.15 mmol, 1 eq) was added to an oven dried glass filtration vessel. Anhydrous DCM (2 mL) was added, and the resin allowed to swell for 20 minutes. Fmoc-Ala-OH (186.8 mg, 0.45 mmol, 3 eq) was then added, forming a suspension. DIPEA (0.21 mL, 0.9 mmol, 6 eq) was then also added and the vessel flushed with nitrogen. The reaction was shaken overnight at room temperature. The vessel was then drained and the resin washed with DMF (3 x 10 mL), MeOH (3 x 10 mL) and DCM (3 x 10 mL). The resin was deprotected with 20% piperidine/DMF (0.5 mL) with stirring at room temperature for 0.5 hours. A solution of Fmoc-D-Thr-OH (153 mg, 0.45 mmol, 3 eq) in DMF (0.5 mL) with DIPEA (0.21 mL, 0.9 mmol, 6 eq) was then added to the resin and shaken at room temperature for one hour, before the solution was filtered and washed as previously. Deprotection with 20% piperidine/DMF (0.5 mL) was repeated as before. A solution of Boc-Ahx-OH **369** (104 mg, 0.45 mmol, 3 eq), HCTU (186 mg, 0.45 mmol, 3 eq) and DIPEA (0.16 mL, 0.9 mmol, 6 eq) in DMF (2 mL) was prepared and added to the resin. This was shaken at room temperature for one hour, before filtration and washes as previously. A solution of Fmoc-Ile-OH (212 mg, 0.6 mmol, 4 eq), and DMAP (7.5 mg, 0.06 mmol, 0.4 eq) in DMF (2 mL) was prepared and added to the resin, before addition of DIC (0.094 mL, 0.6 mmol, 4 eq) into the same mixture. This was sealed and shaken at room temperature for 2 hours before being drained and washed as previously. Conversion to ester was determined by ESI MS and HPLC. After a further deprotection with 20% piperidine/DMF as before, a solution of Fmoc-Arg(Pbf)-OH (291 mg, 0.45 mmol, 3 eq) and DIPEA (0.21 mL, 0.9 mmol, 6 eq) in DMF (2 mL) was added to the resin and shaken at room temperature for 1 hour. After a final Fmoc deprotection with 20% piperidine/DMF, a solution of 1% TFA in DCM (1 mL) was added to the resin and shaken for 10 minutes. The solution was then drained and collected, concentrated *in vacuo* and dissolved in H₂O/MeCN, before overnight lyophilisation. Purification by RP-HPLC yielded the product **371** as a powdery white solid (3 mg, 36% yield). See Table in Section 6.3.9 for data.

6.3.9 Characterisation of peptides

Peptide (as HCl salt where applicable)		Pure yield (mg)	Yield (%)	Purity (%)	Peptide content	Calculated mass (Da)	Observed mass (Da)	Δ MW (ppm)
290		4	14	> 99 %	3.53 mg (88%)	484.2884 (M+H)	484.2900 (M+H)	3.3
297		3	2	> 99 %	0.39 mg (13%)	456.2822 (M+H)	456.2834 (M+H)	2.6
296		2.5	2	> 99 %	0.57 mg (23%)	465.2462 (M+H)	465.2462 (M+H)	0.0
350		5.2	12	> 99 %	1.93 mg (37%)	723.4227 (M+H)	723.4250 (M+H)	3.2
349		3.0	7	> 99 %	0.94 mg (31%)	695.4166 (M+H)	695.4200 (M+H)	4.9

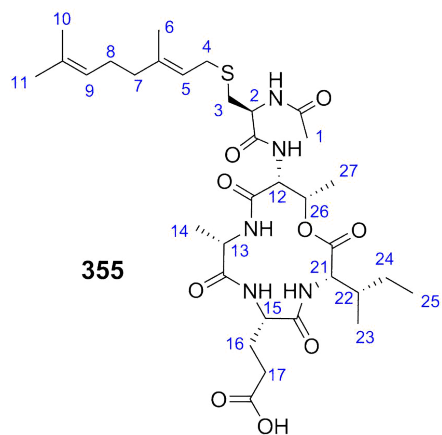
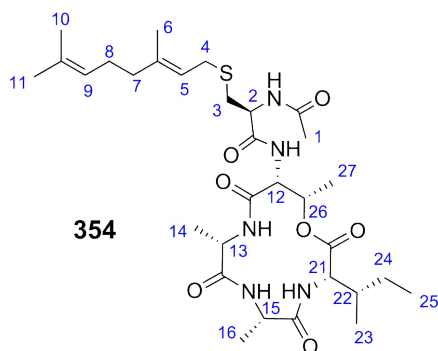
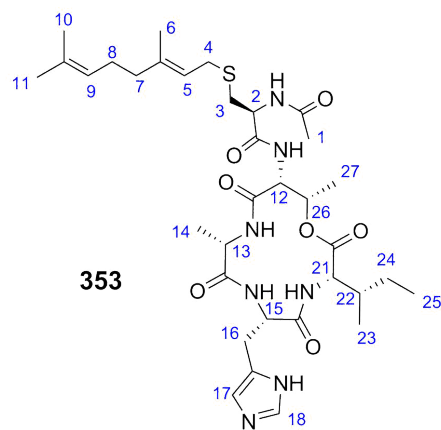
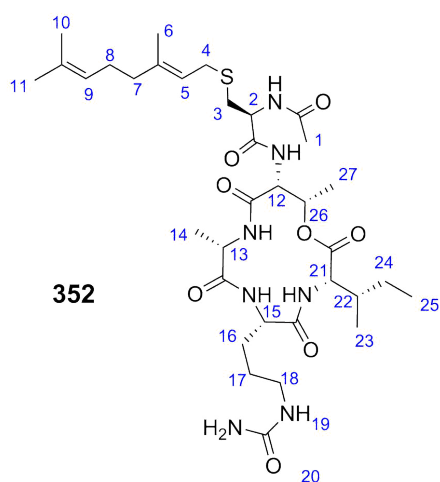
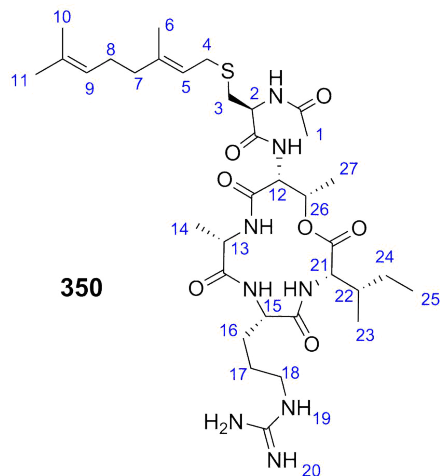
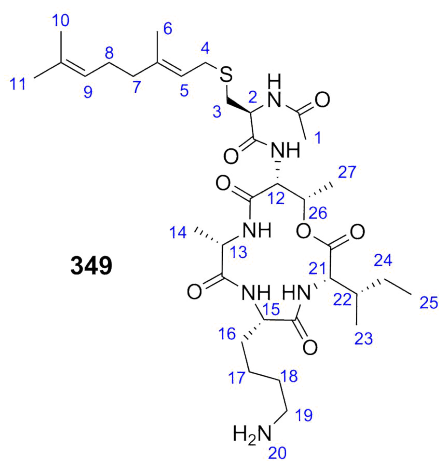
353		1.3	3	> 99 %	0.46 mg (35 %)	704.3805 (M+H)	704.3825 (M+H)	2.8
351		4.7	12	> 99 %	2.71 mg (57 %)	681.4009 (M+H)	681.4003 (M+H)	-0.9
352		2.8	7	> 99 %	2.39 mg (85%)	724.4068 (M+H)	724.4099 (M+H)	4.3
354		3.4	8	> 99 %	3.08 mg (91 %)	638.3608 (M+H)	638.3587 (M+H)	3.3
355		3.0	9	87 %	2.37 mg (79 %)	696.3642 (M+H)	696.3663 (M+H)	3.0

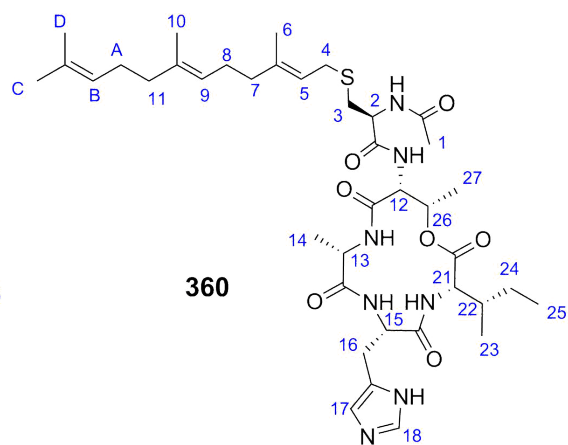
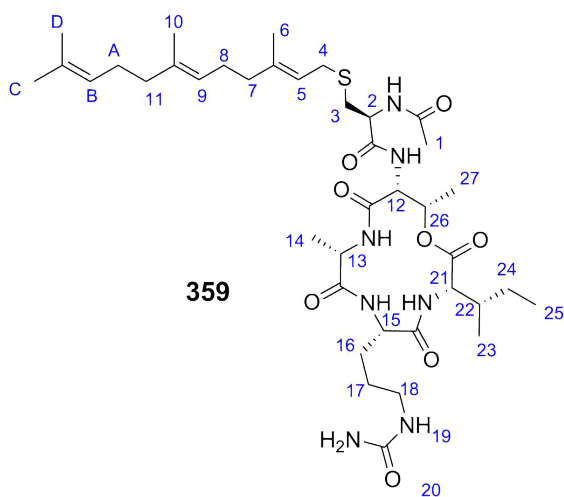
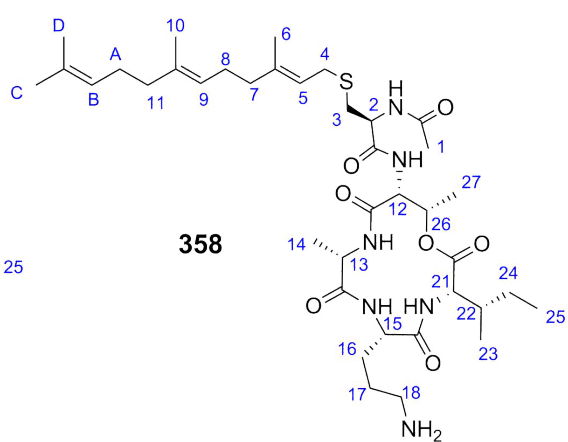
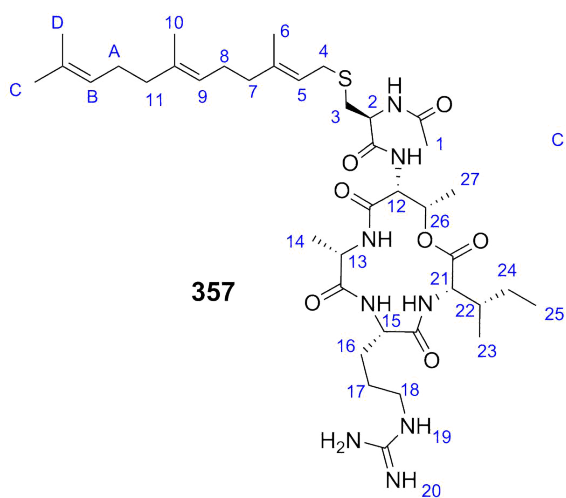
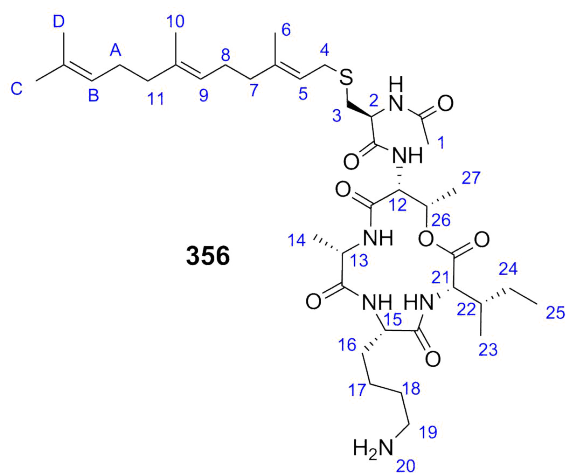
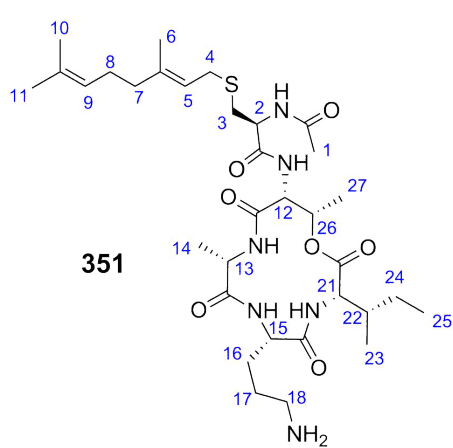
357		4.3	5	95 %	2.33 mg (54 %)	791.4853 (M+H)	791.4873 (M+H)	2.5
356		4.0	5	> 99 %	1.90 mg (48 %)	763.4792 (M+H)	763.4813 (M+H)	2.8
360		1.9	4	95 %	0.32 mg (17%)	772.4431 (M+H)	772.4462 (M+H)	4
358		3.0	7	> 99 %	2.71 mg (90 %)	749.4635 (M+H)	749.4639 (M+H)	0.5
359		4.5	5	98 %	2.37 mg (53 %)	792.4694 (M+H)	792.4731 (M+H)	4.7
361		2.6	7	> 99 %	1.88 mg (72 %)	706.4213 (M+H)	706.4241 (M+H)	4.0

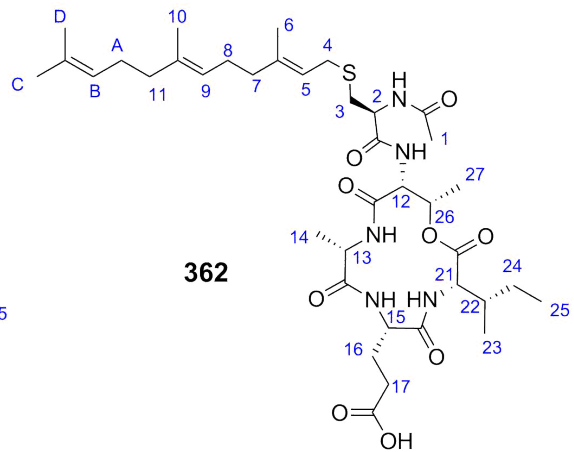
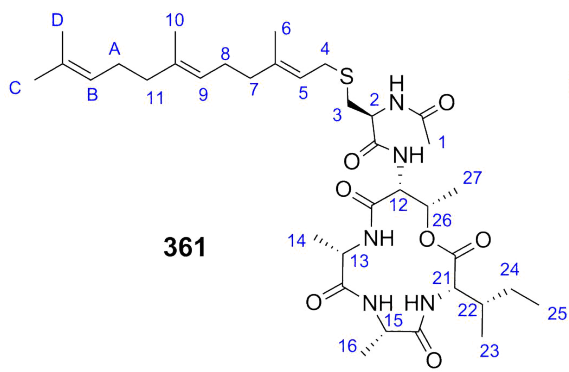
362		3.3	9	> 99 %	1.50 mg (45 %)	764.4268 (M+H)	764.4266 (M+H)	-0.3
371		2.1 mg	7	> 99 %	0.74 mg (35 %)	555.3619 (M+H)	555.3622 (M+H)	0.5
372		6.6 mg	22	> 99 %	5.0 mg (76 %)	527.3557 (M+H)	527.3564 (M+H)	1.3

6.3.9 NMR spectroscopy of peptides

All acetylated and prenylated peptide analogues were analysed by ^1H and COSY NMR, which all protons assigned where possible.







ID	10-residue	Prenyl	1	2	3	4	5	6	7	8
349	Arginine	Geranyl	2.14 (3H s)	4.61 (1H t, J=8)	3.04-2.95 (2H m)	3.40 (2H qd, J=8, 5)	5.34 (1H t, J=8)	1.78 (3H, s)	2.24-2.19 (2H m)	2.19-2.15 (2H m)
350	Lysine	Geranyl	2.09 (3H, s)	4.58 (1H t, J=7.5)	3.01 (2H t, J=6.5)	3.36-3.31 (2H m)	5.29 (1H t, J=8.5)	1.71 (3H s)	2.18-2.14 (2H m)	2.14-2.09 (2H m)
351	Ornithine	Geranyl	2.13 (3H s)	4.61 (1H t, J=7.5)	3.03-2.93 (2H m)	3.45-3.36 (2H m)	5.38-5.32 (1H, m)	1.78 (3H s)	2.23-2.19 (2H m)	2.19-2.15 (2H m)
352	Citrulline	Geranyl	not assigned	4.74-6.64 (1H) ²	3.14-3.07 (2H m)	3.56-3.47 (2H m)	5.46 (1H t, J=8)	1.90 (3H s)	2.35-2.30 (2H m)	2.30-2.26 (2H m)
354	Alanine	Geranyl	not assigned	4.43 (1H t, J=7.5)	2.83 (2H d, J=7)	3.26 (2H qd J=7.5, 2.5)	5.21 (1H t, J=7)	1.66 (3H s)	2.10-2.04 (2H m)	2.04-2.00 (2H m)
355	Glutamate	Geranyl	not assigned	4.59 (1H t, J=8)	3.04-2.96 (2H m)	3.45-3.35 (2H m)	5.34 (1H t, J=7.5)	1.78 (3H s)	2.24-2.16 (2H m)	2.24-2.16 (2H m)
357	Arginine	Farnesyl	2.13 (3H s)	4.65 (1H t, J=7.5)	3.35-2.98 (1H m) & 2.98-2.90 (1H m)	3.50-3.42 (1H m) and 3.38-3.32 (1H m)	5.29 (1H t, J=7.5)	1.75 (3H s)	2.15-2.10 (2H m)	2.02-1.97 (2H m)
356	Lysine	Farnesyl	2.06 (3H s)	4.76-4.75 (1H m) ⁷	2.90-2.80 (2H m)	3.33 (2H qd, J=13, 7.5)	5.24 (1H t, J=8)	1.70 (3H s)	2.13-2.05 (2H m)	2.08-2.02 (2H m)
358	Ornithine	Farnesyl	not assigned	4.52-4.45 (1H m) ⁶	3.04-2.89 (2H m)	3.49-3.39 (1H m) & 3.37-3.30 (1H m)	5.32-5.25 (1H, m)	1.75 (3H s)	2.12-2.04 (2H m)	2.01-1.95 (2H m)
359	Citrulline	Farnesyl	1.98 (3H s)	4.46 (1H t, J=7.5)	2.83 (2H d, J=7.5)	3.26 (2H d, J=8)	5.21 (1H t, J=8)	1.66 (3H s)	2.10-2.04 (2H m)	2.05-2.00 (2H m)
361	Alanine	Farnesyl	not assigned	4.35 (1H t, J=8)	3.66-3.50 (1H br m) & 2.85-2.74 (1H m)	3.26-3.15 (1H m) & 3.12-3.03 (1H m)	5.26-5.13 (1H br m)	1.61 (3H s)	2.08-2.01 (2H m)	2.00-1.94 (2H m)
362	Glutamate	Farnesyl	not assigned	4.58 (1H t, J=7.5)	2.98 (2H br d, J=7.5)	3.45-3.36 (2H m)	5.36 (1H t, J=7.5)	1.80 (3H s)	2.22-2.15 (2H m)	2.15-2.05 (2H m)

ID	10-residue	Prenyl	9	10	11	12	13	14	15	16
349	Arginine	Geranyl	5.21 (1H t, J=7)	1.77 (3H s)	1.70 (3H s)	4.87 (1H m) ²	4.24 (1H q, J=7.5)	1.55 (3H d, J=7)	4.48 (1H dd, J=9.5, 7.5)	1.95-1.85 (1H, m) and 1.79-1.74 (1H, m)
350	Lysine	Geranyl	5.16 (1H t, J=6.5)	1.69 (3H s)	1.63 (3H s)	4.75 (1H m) ²	4.18 (1H q, J=7.5)	1.49 (3H d, J=7.5)	4.43 (1H dd, J=9.5, 7)	1.95-1.89 (1H m) & 1.90-1.84 (1H m)
351	Ornithine	Geranyl	5.21 (1H t, J=6.5)	1.77 (3H s)	1.70 (3H s)	4.89 (1H m) ²	4.24 (1H q, J=7.5)	1.55 (3H d, J=7.5)	4.49 (1H dd, J=9.5, 6)	2.04-1.96 (1H m) & 1.87-1.80 (1H m)
352	Citrulline	Geranyl	5.32 (1H t, J=6)	1.89 (3H s)	1.89 (3H s)	not assigned	4.36 (1H q, J=7.5)	1.66 (3H d, J=7.5)	4.55 (1H dd, J=9.5, 6.5)	2.08-2.01 (1H m) & 1.81-1.73 (1H m)
354	Alanine	Geranyl	5.07 (1H t, J=5.5)	1.64 (3H s)	1.57 (3H s)	5.71-4.60 (1H m)	4.16-4.09 (1H m)	1.38 (3H d, J=7.5)	4.41-4.34 (1H m)	1.39 (3H d, J=7.5)
355	Glutamate	Geranyl	5.21 (1H t, J=6.5)	1.77 (3H s)	1.70 (3H s)	4.75 (1H m)	4.25 (1H q, J=7.5)	1.54 (3H d, J=7.5)	4.48 (1H dd, J=9.5, 6.5)	2.22-2.12 (2H m)
357	Arginine	Farnesyl	5.16-5.09 (1H m)	1.69 (3H s)	2.12-2.05 (3H m)	not assigned	4.26-4.21 (1H m)	1.56 (3H d, J=7)	4.49 (1H t, J=7.5)	2.01-1.94 (1H m) and 1.76-1.66 (1H m)
356	Lysine	Farnesyl	5.14-5.07 (1H m)	1.67 (3H s)	not assigned	4.73 (1H d, J=6)	4.09 (1H q, J=7.5)	1.45 (3H d, J=7)	4.36 (1H dd, J=10, 6)	not assigned
358	Ornithine	Farnesyl	5.16-5.09 (1H m)	1.68 (3H s)	not assigned	4.71-4.68 (1H m)	4.24 (1H q, J=7.5)	1.57 (3H d, J=7)	4.26-4.19 (1H m)	1.88-1.80 (1H m) and 1.85-1.76 (1H m)
359	Citrulline	Farnesyl	5.12-5.05 (1H m)	1.64 (3H s)	not assigned	4.72-4.63 (1H m)	4.09 (1H q, J=7)	1.41 (3H d, J=7.5)	4.30 (1H dd, J=9.5, 6.5)	1.55-1.49 (1H m) and 1.50-1.43 (1H m)
361	Alanine	Farnesyl	5.23-5.14 (1H m)	1.53 (3H s)	not assigned	4.76-4.55 (1H br m)	4.13-4.02 (1H m) ²	1.35 (3H d, J=7)	4.32 (1H q, J=7.5)	1.35 (3H d, J=7)
362	Glutamate	Farnesyl	5.27-5.19 (1H m)	1.79 (3H s)	not assigned	4.90-4.75 (1H br m)	4.27-4.23 (1H m) ²	1.54 (3H d, J=7.5)	4.49 (1H dd, J=9.5, 6.5)	not assigned

ID	10-residue	Prenyl	17	18	19	20	21	22	23	24
349	Arginine	Geranyl	3.34-3.25 (2H m)	not assigned	8.01 (2H br s)	8.01 (2H br s)	4.30 (1H d, J=8.5)	1.95-1.85 (1H, m)	0.98 (3H d, J=7.5)	1.61-1.52 (1H m) and 1.30-1.23 (1H m)
350	Lysine	Geranyl	3.01 (2H t, J=7.5)	not assigned	not assigned	\	4.23 (1H d, J=9)	1.89-1.84 (1H m)	0.92 (3H d, J=7)	1.55-1.50 (1H m) & 1.24-1.17 (1H m)
351	Ornithine	Geranyl	3.09 (2H t, J=7.5)	not assigned	\	\	4.30 (1H d, J=9)	1.97-1.87 (1H m)	0.99 (3H d, J=7)	1.62-1.52 (1H m) & 1.30-1.23 (1H m)
352	Citrulline	Geranyl	3.31 (2H t, J=7)	\	\	\	4.42 (1H d, J=8.5)	2.01.193 (1H m)	1.13-1.08 (3H m)	1.72-1.64 (1H m) & 1.42 -1.34 (1H m)
354	Alanine	Geranyl	\	\	\	\	4.16-4.10 (1H m)	1.79-1.72 (1H m)	0.90-0.82 (3H m)	1.52-1.42 (1H m) & 1.15-1.10 (1H m)
355	Glutamate	Geranyl	2.50 (2H t, J=7.5)	\	\	\	4.32 (1H d, J=8.5)	1.90-1.82 (1H m)	1.01-0.96 (3H m)	1.60-1.53 (1H m)and 1.31-1.22 (1H m)
357	Arginine	Farnesyl	3.33-3.26 (2H m)	not assigned	not assigned	not assigned	4.28 (1H d, J=9)	1.96-1.89 (1H m)	0.99-0.92 (3H m)	1.59-1.52 (1H m) and 1.28-1.22 (1H m)
356	Lysine	Farnesyl	2.91 (2H t, J=7.5)	not assigned	not assigned	\	4.14 (1H d, J=9)	1.93-1.85 (1H m)	0.89 (3H d, J=7)	1.55-1.47 (1H m) and 1.25-1.15 (1H m)
358	Ornithine	Farnesyl	3.07 (2H t, J=6.5)		\	\	4.27 (1H d, J=9)	1.82-1.74 (1H m)	1.00-0.92 (3H m)	1.63-1.57 (1H m) & 1.28-1.22 (1H m)
359	Citrulline	Farnesyl	3.05 (2H t, J=7)	1.83-1.72 (2H m)	\	\	4.15 (1H d, J=9)	1.83-1.74 (1H m)	0.86 (3H d, J=7)	1.51-1.42 (1H m) and 1.18-1.11 (1H m)
361	Alanine	Farnesyl	\	\	\	\	4.13-4.05 (1H m) ²	1.75-1.63 (1H m)	0.83-0.77 (3H m)	1.48-1.36 (1H m) & 1.12-1.01 (1H m)
362	Glutamate	Farnesyl	2.48 (2H t, J=7.5)	\	\	\	4.31 (1H d, J=9)	1.94-1.85 (1H m)	1.04-0.97 (3H m)	1.64-1.56 (1H m) & 1.33-1.23 (1H m)

ID	10-residue	Prenyl	25	26	27	A	B	C	D
349	Arginine	Geranyl	0.99 (3H t, J=6.5)	5.65 (1H qd, J=6.5, 2.5)	1.41 (3H d, J=6.5)	\	\	\	\
350	Lysine	Geranyl	0.90 (3H t, J=7.5)	5.60 (1H qd, J=6.5, 2.5)	1.35 (3H d, J=6.5)	\	\	\	\
351	Ornithine	Geranyl	0.98 (3H t, J=7.5)	5.64 (1H qd, J=6.5, 2)	1.41 (3H d, J=6.5)	\	\	\	\
352	Citrulline	Geranyl	1.13-1.08 (3H m)	5.77 (1H qd, J=6.5, 2.5)	1.52 (3H d, J=6.5)	\	\	\	\
354	Alanine	Geranyl	0.90-0.82 (3H m)	5.49 (1H qd, J=6.5, 2.5)	1.25 (3H d, J=6.5)	\	\	\	\
355	Glutamate	Geranyl	1.01-0.96 (3H m)	5.66 (1H qd, J=6.5, 2.5)	1.41 (3H d, J=6.5)	\	\	\	\
357	Arginine	Farnesyl	0.99-0.92 (3H m)	5.67-5.60 (1H m)	1.38 (3H d, J=6)	2.10-2.05 (2H m)	5.16-5.09 (1H m)	1.61 (3H s)	1.61 (3H s)
356	Lysine	Farnesyl	0.87 (3H t, J=7)	5.45 (1H qd), J=6.5, 2	1.23 (3H d, J=6.5)	not assigned	5.14-5.07 (1H m)	1.60 (3H s)	1.60 (3H s)
358	Ornithine	Farnesyl	1.00-0.92 (3H m)	5.64 (1H qd, J=7, 2)	1.38 (3H d, J=6)	not assigned	5.16-5.09 (1H m)	1.61 (3H s)	1.61 (3H s)
359	Citrulline	Farnesyl	0.86 (3H t, J=7)	5.49 (1H qd, J=6.5, 2.5)	1.24 (3H d, J=6.5)	not assigned			
361	Alanine	Farnesyl	0.86-0.79 (3H m)	5.51-5.41 (1H m)	1.21 (3H d, J=5.5)	not assigned	not assigned	not assigned	not assigned
362	Glutamate	Farnesyl	1.04-0.97 (3H m)	5.65 (1H qd, J=6.5, 2)	1.40 (3H d, J=6.5)	not assigned	5.27-5.19 (1H m) ³	1.72 (3H s)	1.72 (3H s)

6.4 MIC and MBC assays

6.4.1 Bacterial strains

Teixobactin analogues were examined against two lab reference strains for the antimicrobial susceptibility testing: *Staphylococcus aureus* ATCC 25923 and *Escherichia coli* ATCC 25922. These strains were used after thawing from -80°C frozen stock in the microbial genetics lab (University Of Leicester).

6.4.2 Microdilution method for susceptibility testing to antimicrobials

Müller–Hinton broth (MHB) medium containing 2x concentration of the highest concentration of the antimicrobial compound to be tested was made. For all compounds, 128 µg/ml was prepared for a final maximum concentration of 64 µg/ml). 200 µl of each compound was aliquoted into the wells of the first column of the plate, and two-fold serial dilutions of the compound were then performed along the row.

6.4.3 MIC and MBC Assays

Minimum inhibitory concentration (MIC) determination of the teixobactin analogues was performed as described by the Clinical and Laboratory Standards Institute (CLSI) guidelines, using broth microdilution method. These were initially performed singularly by Zaaima Al-Jabri, and later in triplicate by Megan De Ste Croix, both at Department of Genetics, University of Leicester. In short, each strain was streaked for a single colony on a fresh Müller–Hinton agar plates (Oxoid Ltd., Basingstoke, UK) and incubated at 37°C for 24 hours. Next day, a starting inocula of 1×10^5 CFU/ml of *Staphylococcus aureus* ATCC 25923 and *Escherichia coli* ATCC 25922 strains was aliquoted in 96-well plates containing serial dilutions of the Teixobactin or analogues in the range from 64 down to 0.125 µg/ml using Mueller-Hinton broth (Oxoid Ltd., Basingstoke, UK). Results were read with a Jenway (6705UV/Vis.) spectrophotometer after 18 hours of incubation at 37 °C.

Minimum bactericidal concentration (MBC) was determined by subculturing 10 μ l from each well without visible bacterial growth on Müller–Hinton agar plates (Oxoid Ltd., Basingstoke, UK). After 24 h of incubation at 37 °C, the dilution yielding three colonies or less was scored as the MBC.

7. References

1. A. Fleming, *Br. J. Ex. Pathol.*, 1929, **10**, 226-236.
2. A. Schatz, E. Bugle and S. A. Waksman, *Proc. Soc. Exp. Biol. Med.*, 1944, **55**, 66-69.
3. O. Genilloud, I. González, O. Salazar, J. Martín, J. R. Tormo and F. Vicente, *J. Ind. Microbiol. Biotechnol.*, 2011, **38**, 375-389.
4. K. Lewis, *Nat. Rev. Drug Discov.*, 2013, **12**, 371-387.
5. R. Fleischmann, M. Adams, O. White, R. Clayton, E. Kirkness, A. Kerlavage, C. Bult, J. Tomb, B. Dougherty, J. Merrick and e. al., *Science*, 1995, **269**, 496-512.
6. D. J. Payne, M. N. Gwynn, D. J. Holmes and D. L. Pompliano, *Nat. Rev. Drug Discov.*, 2007, **6**, 29-40.
7. E. D. Brown and G. D. Wright, *Nature*, 2016, **529**, 336-343.
8. D. N. Gilbert, R. J. Gidos, H. W. Boucher, G. H. Talbot, B. Spellberg, J. E. Edwards, M. Scheld, J. S. Bradley and J. G. Bartlett, *Clin. Infect. Dis.*, 2010, **50**, 1081-1083.
9. B. Bister, D. Bischoff, M. Ströbele, J. Riedlinger, A. Reicke, F. Wolter, A. T. Bull, H. Zähner, H.-P. Fiedler and R. D. Süssmuth, *Angew. Chem. Int. Ed.*, 2004, **43**, 2574-2576.
10. J. B. McAlpine, B. O. Bachmann, M. Pirae, S. Tremblay, A.-M. Alarco, E. Zazopoulos and C. M. Farnet, *J. Nat. Prod.*, 2005, **68**, 493-496.
11. Y.-Y. Liu, Y. Wang, T. R. Walsh, L.-X. Yi, R. Zhang, J. Spencer, Y. Doi, G. Tian, B. Dong, X. Huang, L.-F. Yu, D. Gu, H. Ren, X. Chen, L. Lv, D. He, H. Zhou, Z. Liang, J.-H. Liu and J. Shen, *Lancet Infect. Dis.*, 2016, **16**, 161-168.
12. T. R. Chen L, Kiehlbauch J, Walters M, Kallen A., *Morb. Mortal. Wkly. Rep.*, 2017, **66**, 33.
13. R. R. Roberts, B. Hota, I. Ahmad, I. I. R. D. Scott, S. D. Foster, F. Abbasi, S. Schabowski, L. M. Kampe, G. G. Ciavarella, M. Supino, J. Naples, R. Cordell, S. B. Levy and R. A. Weinstein, *Clin. Infect. Dis.*, 2009, **49**, 1175-1184.

14. W. M. M. Kirby, *Science*, 1944, **99**, 452-453.
15. M. Barber and M. Rozwadowska-Dowzenko, *Lancet*, 1948, **252**, 641-644.
16. C. L. Ventola, *Pharmacy and Therapeutics*, 2015, **40**, 277-283.
17. C. Janoir, V. Zeller, M. D. Kitzis, N. J. Moreau and L. Gutmann, *Antimicrob. Agents Chemother.*, 1996, **40**, 2760-2764.
18. J. Prystowsky, F. Siddiqui, J. Chosay, D. L. Shinabarger, J. Millichap, L. R. Peterson and G. A. Noskin, *Antimicrob. Agents Chemother.*, 2001, **45**, 2154-2156.
19. K. Hiramatsu, H. Hanaki, T. Ino, K. Yabuta, T. Oguri and F. C. Tenover, *Journal of Antimicrobial Chemotherapy*, 1997, **40**, 135-136.
20. S. Gardete and A. Tomasz, *J Clin Invest*, 2014, **124**, 2836-2840.
21. V. K. Viswanathan, *Gut Microbes*, 2014, **5**, 3-4.
22. M. Bergman, S. T. Nyberg, P. Huovinen, P. Paakkar and A. J. Hakanen, *Antimicrob. Agents Chemother.*, 2009, **53**, 912-917.
23. C.-E. Luyt, N. Bréchet, J.-L. Trouillet and J. Chastre, *Crit. Care*, 2014, **18**, 480.
24. M. J. Llewelyn, J. M. Fitzpatrick, E. Darwin, S. Tonkin-Crine, C. Gorton, J. Paul, T. E. A. Peto, L. Yardley, S. Hopkins and A. S. Walker, *Br. Med. J.*, 2017, **358**.
25. M. J. Martin, S. E. Thottathil and T. B. Newman, *Am. J. Public Health*, 2015, **105**, 2409-2410.
26. I. M. Gould and A. M. Bal, *Virulence*, 2013, **4**, 185-191.
27. J. G. Bartlett, D. N. Gilbert and B. Spellberg, *Clin. Infect. Dis.*, 2013, **56**, 1445-1450.
28. E. Power, *Clin. Microbiol. Infect.*, 2006, **12**, 25-34.
29. L. B. Rice, *J. Infect. Dis.*, 2008, **197**, 1079-1081.
30. H. W. Boucher, G. H. Talbot, J. S. Bradley, J. E. Edwards, D. Gilbert, L. B. Rice, M. Scheld, B. Spellberg and J. Bartlett, *Clin. Infect. Dis.*, 2009, **48**, 1-12.
31. J. M. A. Blair, M. A. Webber, A. J. Baylay, D. O. Ogbolu and L. J. V. Piddock, *Nat. Rev. Microbiol.*, 2015, **13**, 42-51.
32. O. o. I. D. Centers for Disease Control and Prevention, *Antibiotic resistance threats in the United States*, 2013, 2013.
33. M. Gross, *Curr. Biol.*, 2013, **23**, R1063-R1065.

34. C. C. S. Fuda, J. F. Fisher and S. Mobashery, *Cellular and Molecular Life Sciences*, 2005, **62**, 2617.
35. D. R. Schaberg, D. H. Culver and R. P. Gaynes, *Am. J. Med.*, 1991, **91**, S72-S75.
36. D. C. C. William B. Whitman, William J. Wiebe, *Proc. Natl. Acad. Sci. USA*, 1998, **95**, 6578-6583.
37. C. L. Sears, *Anaerobe*, 2005, **11**, 247-251.
38. M. G. Pinho, M. Kjos and J.-W. Veening, *Nat. Rev. Microbiol.*, 2013, **11**, 601-614.
39. J. F. Fisher, S. O. Meroueh and S. Mobashery, *Chem. Rev.*, 2005, **105**, 395-424.
40. H. U. Park, S. Suy, M. Danner, V. Dailey, Y. Zhang, H. Li, D. R. Hyde, B. T. Collins, G. Gagnon, B. Kallakury, D. Kumar, M. L. Brown, A. Fornace, A. Dritschilo and S. P. Collins, *Mol. Cancer Ther.*, 2009, **8**, 733-741.
41. L.-J. Zhang and R. L. Gallo, *Curr. Biol.*, 2016, **26**, R14-R19.
42. N. Bangalore, J. Travis, V. C. Onunka, J. Pohl and W. M. Shafer, *J. Biol. Chem.*, 1990, **265**, 13584-13588.
43. R. I. Lehrer, *Nat. Rev. Microbiol.*, 2004, **2**, 727-738.
44. U. H. N. Dürr, U. S. Sudheendra and A. Ramamoorthy, *Biochim. Biophys. Acta*, 2006, **1758**, 1408-1425.
45. K. De Smet and R. Contreras, *Biotechnol. Lett.*, 2005, **27**, 1337-1347.
46. D. I. Andersson, D. Hughes and J. Z. Kubicek-Sutherland, *Drug Resist. Update.*, 2016, **26**, 43-57.
47. M. S. Butler, K. A. Hansford, M. A. T. Blaskovich, R. Halai and M. A. Cooper, *J. Antibiot.*, 2014, **67**, 631-644.
48. M. A. Kohanski, D. J. Dwyer and J. J. Collins, *Nat. Rev. Microbiol.*, 2010, **8**, 423-435.
49. D. H. Williams, M. P. Williamson, D. W. Butcher and S. J. Hammond, *J. Am. Chem. Soc.*, 1983, **105**, 1332-1339.
50. J. C. J. Barna and D. H. Williams, *Annu. Rev. Microbiol.*, 1984, **38**, 339-357.
51. R. Leclercq, E. Derlot, J. Duval and P. Courvalin, *New Engl. J. Med.*, 1988, **319**, 157-161.

52. T. D. H. Bugg, G. D. Wright, S. Dutka-Malen, M. Arthur, P. Courvalin and C. T. Walsh, *Biochemistry*, 1991, **30**, 10408-10415.
53. J. Pootoolal, J. Neu and G. D. Wright, *Annu. Rev. Pharmacool. Toxicol.*, 2002, **42**, 381-408.
54. D. Meziane-Cherif, F. A. Saul, A. Haouz and P. Courvalin, *J. Biol. Chem.*, 2012, **287**, 37583-37592.
55. G. G. Zhanel, D. Calic, F. Schweizer, S. Zelenitsky, H. Adam, P. R. S. Lagacé-Wiens, E. Rubinstein, A. S. Gin, D. J. Hoban and J. A. Karlowsky, *Drugs*, 2010, **70**, 859-886.
56. J. W. Bennett, J. S. Lewis and M. W. Ellis, *Ther. Clin. Risk Manag.*, 2008, **4**, 31-40.
57. G. Candiani, M. Abbondi, M. Borgonovi, G. Romanò and F. Parenti, *Journal of Antimicrobial Chemotherapy*, 1999, **44**, 179-192.
58. R. G. Finch and G. M. Eliopoulos, *J. Antimicrob. Chemother.*, 2005, **55**, ii5-ii13.
59. S. Laohavaleeson, J. L. Kuti and D. P. Nicolau, *Expert Opin. Investig. Drugs*, 2007, **16**, 347-357.
60. A. Okano, N. A. Isley and D. L. Boger, *Proc. Natl. Acad. Sci. USA*, 2017, **114**, E5052-E5061.
61. J. Xie, J. G. Pierce, R. C. James, A. Okano and D. L. Boger, *J. Am. Chem. Soc.*, 2011, **133**, 13946-13949.
62. V. Yarlagadda, P. Akkapeddi, G. B. Manjunath and J. Haldar, *J. Med. Chem.*, 2014, **57**, 4558-4568.
63. H. S. R. Oscar P. Kuipers, Wyanda M. G. J. Yap, Hein J. Boot, Roland J. Siezen, and and W. M. d. Vos, *J. Biol. Chem.*, 1992, **267**, 24340-24346.
64. E. Breukink, I. Wiedemann, C. v. Kraaij, O. P. Kuipers, H.-G. Sahl and B. de Kruijff, *Science*, 1999, **286**, 2361-2364.
65. H. E. Hasper, B. de Kruijff and E. Breukink, *Biochemistry*, 2004, **43**, 11567-11575.
66. S. T. Hsu, E. Breukink, E. Tischenko, M. A. Lutters, B. de Kruijff, R. Kaptein, A. M. Bonvin and N. A. van Nuland, *Nat Struct Mol Biol*, 2004, **11**, 963-967.
67. M. Mota-Meira, G. Lapointe, C. Lacroix and M. C. Lavoie, *Antimicrobial Agents and Chemotherapy*, 2000, **44**, 24-29.

68. K. Fukase, M. Kitazawa, A. Sano, K. Shimbo, H. Fujita, S. Horimoto, T. Wakamiya and T. Shiba, *Tetrahedron Lett.*, 1988, **29**, 795-798.
69. W. a. H. J. N. Liu, *J. Biol. Chem.*, 1992, **267**.
70. L. Zhou, A. J. van Heel and O. P. Kuipers, *Front. Microbiol.*, 2015, **6**, 11.
71. J. Yuan, Z. Z. Zhang, X. Z. Chen, W. Yang and L. D. Huan, *Appl. Microbiol. Biotechnol.*, 2004, **64**, 806-815.
72. D. Field, P. M. O. Connor, P. D. Cotter, C. Hill and R. P. Ross, *Mol. Microbiol.*, 2008, **69**, 218-230.
73. B. Healy, D. Field, P. M. O'Connor, C. Hill, P. D. Cotter and R. P. Ross, *PLOS ONE*, 2013, **8**, e79563-e79563.
74. K. R. Meena and S. S. Kanwar, *BioMed Res. Int.*, 2015, **2015**, 1-9.
75. M. Ongena and P. Jacques, *Trends Microbiol.*, 2008, **16**, 115-125.
76. N. Bionda, J.-P. Pitteloud and P. Cudic, *Future Med. Chem*, 2013, **5**, 1311-1330.
77. J. H. Lakey and M. Ptak, *Biochemistry*, 1988, **27**, 4639-4645.
78. H. Y. Lam, Y. Zhang, H. Liu, J. Xu, C. T. T. Wong, C. Xu and X. Li, *J. Am. Chem. Soc.*, 2013, **135**, 6272-6279.
79. K. T. Nguyen, D. Ritz, J.-Q. Gu, D. Alexander, M. Chu, V. Miao, P. Brian and R. H. Baltz, *Proc. Natl. Acad. Sci. USA*, 2006, **103**, 17462-17467.
80. T. Kaeberlein, K. Lewis and S. S. Epstein, *Science*, 2002, **296**, 1127-1129.
81. L. L. Ling, T. Schneider, A. J. Peoples, A. L. Spoering, I. Engels, B. P. Conlon, A. Mueller, T. F. Schaberle, D. E. Hughes, S. Epstein, M. Jones, L. Lazarides, V. A. Steadman, D. R. Cohen, C. R. Felix, K. A. Fetterman, W. P. Millett, A. G. Nitti, A. M. Zullo, C. Chen and K. Lewis, *Nature*, 2015, **517**, 455-459.
82. D. Nichols, N. Cahoon, E. M. Trakhtenberg, L. Pham, A. Mehta, A. Belanger, T. Kanigan, K. Lewis and S. S. Epstein, *Appl. Environ. Microbiol.*, 2010, **76**, 2445-2450.
83. K. E. M. Michael A. D'Elia, Terry J. Beveridge, and Eric D. Brown, *J. Bacteriol.*, 2006, **186**, 8313-8316.
84. K. Y. Horii S., *J. Antibiot.*, 1968, **21**, 665-667.
85. H. K. Higashide E., Shibata M., Nakazawa K., *J. Antibiot.*, 1968, **21**, 126-137.

86. X. G. Li, X. M. Tang, J. Xiao, G. H. Ma, L. Xu, S. J. Xie, M. J. Xu, X. Xiao and J. Xu, *Mar Drugs*, 2013, **11**, 3875-3890.
87. Y. Hu, W. Yang, W. Wan, F. Shen, Z. Lei and D. Wang, *Appl Biochem Biotechnol*, 2012, **166**, 830-838.
88. O. I. Matsushashi M, Yoshiyama Y., *Agr. Biol. Chem.*, 1969, **33**, 134-137.
89. D. K. Farver, D. D. Hedge and S. C. Lee, *Ann Pharmacother*, 2005, **39**, 863-868.
90. S. E. A. a. R. P. E, *Antimicrob Agents Chemother*, 1990, **34**, 413-419.
91. M.-C. Lo, H. Men, A. Branstrom, J. Helm, N. Yao, R. Goldman and S. Walker, *Journal of the American Chemical Society*, 2000, **122**, 3540-3541.
92. P. Cudic, J. K. Kranz, D. C. Behenna, R. G. Kruger, H. Tadesse, A. J. Wand, Y. I. Veklich, J. W. Weisel and D. G. McCafferty, *Proc Natl Acad Sci U S A*, 2002, **99**, 7384-7389.
93. B. D. C. Cudic P., Kranz J.K., Kruger R.G., Wang A.J., Veklich Y.I., Weisel J.W., McCafferty D.G, *Chem Biol*, 2002, **9**, 897-906.
94. S. Tsuji, S. Kusumoto and T. Shiba, *Chem. Lett.*, 1975, 1281-1284.
95. L. Sanière, L. c. Leman, J.-J. Bourguignon, P. Dauban and R. H. Dodd, *Tetrahedron*, 2004, **60**, 5889-5897.
96. D. E. Olson, J. Y. Su, D. A. Roberts and J. Du Bois, *J Am Chem Soc*, 2014, **136**, 13506-13509.
97. A. M. Giltrap, L. J. Dowman, G. Nagalingam, J. L. Ochoa, R. G. Linington, W. J. Britton and R. J. Payne, *Org Lett*, 2016, **18**, 2788-2791.
98. K. Jin, I. H. Sam, K. H. Po, D. Lin, E. H. Ghazvini Zadeh, S. Chen, Y. Yuan and X. Li, *Nat Commun*, 2016, **7**, 12394.
99. J. Rudolph, F. Hannig, H. Theis and R. Wischnat, *Organic Letters*, 2001, **3**, 3153-3155.
100. W. Craig, J. Chen, D. Richardson, R. Thorpe and Y. Yuan, *Org Lett*, 2015, **17**, 4620-4623.
101. F. García-Martín, M. Quintanar-Audelo, Y. García-Ramos, L. J. Cruz, C. Gravel, R. Furic, S. Côté, J. Tulla-Puche and F. Albericio, *J. Comb. Chem.*, 2006, **8**, 213-220.
102. Y. E. Jad, G. A. Acosta, T. Naicker, M. Ramtahal, A. El-Faham, T. Govender, H. G. Kruger, B. G. de la Torre and F. Albericio, *Org Lett*, 2015, **17**, 6182-6185.

103. A. Parmar, A. Iyer, C. S. Vincent, D. Van Lysebetten, S. H. Prior, A. Madder, E. J. Taylor and I. Singh, *Chemical Communications*, 2016, **52**, 6060-6063.
104. S. A. H. Abdel Monaim, Y. E. Jad, G. A. Acosta, T. Naicker, E. J. Ramchuran, A. El-Faham, T. Govender, H. G. Kruger, B. G. de la Torre and F. Albericio, *RSC Adv.*, 2016, **6**, 73827-73829.
105. H. Yang, K. H. Chen and J. S. Nowick, *ACS Chem Biol*, 2016, **11**, 1823-1826.
106. S. A. H. Abdel Monaim, Y. E. Jad, E. J. Ramchuran, A. El-Faham, T. Govender, H. G. Kruger, B. G. de la Torre and F. Albericio, *ACS Omega*, 2016, **1**, 1262-1265.
107. A. Parmar, S. H. Prior, A. Iyer, C. S. Vincent, D. Van Lysebetten, E. Breukink, A. Madder, E. J. Taylor and I. Singh, *Chem Commun (Camb)*, 2017.
108. A. M. Burroughs, R. W. Hoppe, N. C. Goebel, B. H. Sayyed, T. J. Voegtline, A. W. Schwabacher, T. M. Zabriskie and N. R. Silvaggi, *Biochemistry*, 2013, **52**, 4492-4506.
109. B. Aillard, N. S. Robertson, A. R. Baldwin, S. Robins and A. G. Jamieson, *Org. Biomol. Chem.*, 2014, **12**, 8775-8782.
110. C. Nájera and J. M. Sansano, *Chem. Rev.*, 2007, **107**, 4584-4671.
111. M. J. Burk, M. F. Gross and J. P. Martinez, *J. Am. Chem. Soc.*, 1995, **117**, 9375-9376.
112. A. H. Jason, *Curr. Org. Chem.*, 2005, **9**, 657-669.
113. R. O. Duthaler, *Tetrahedron*, 1994, **50**, 1539-1650.
114. V. Tirayut, B. Worawan and S.-A. Yongsak, *Curr. Org. Chem.*, 2005, **9**, 1315-1392.
115. H. Nozaki, H. Takaya, S. Moriuti and R. Noyori, *Tetrahedron*, 1968, **24**, 3655-3669.
116. U. Schollkopf, *Pure. Appl. Chem.*, 1983, **55**, 1799-1806.
117. Y. N. Belokon, V. I. Bakhmutov, N. I. Chernoglazova, K. A. Kochetkov, S. V. Vitt, N. S. Garbalinskaya and V. M. Belikov, *J. Chem. Soc., Perkin Trans. 1*, 1988, 305-312.
118. Y. N. Belokon, N. I. Chernoglazova, C. A. Kochetkov, N. S. Garbalinskaya and V. M. Belikov, *J. Am. Chem. Soc.*, 1985, 171-172.

119. Z. Al Shuhaib, D. H. Davies, M. Dennis, D. M. Evans, M. D. Fletcher, H. Franken, P. Hancock, J. Hollinshead, I. Jones, K. Kähm, P. J. Murphy, R. Nash, D. Potter and R. Rowles, *Tetrahedron*, 2014, **70**, 4412-4419.
120. M.-C. Roux, R. Paugam and G. Rousseau, *J. Org. Chem.*, 2001, **66**, 4304-4310.
121. T. W. Baughman, J. C. Sworen and K. B. Wagener, *Tetrahedron*, 2004, **60**, 10943-10948.
122. M. Daniel, F. Blanchard, S. Nocquet-Thibault, K. Cariou and R. H. Dodd, *J. Org. Chem.*, 2015, **80**, 10624-10633.
123. P. R. Sultane, T. B. Mete and R. G. Bhat, *Tetrahedron Lett.*, 2015, **56**, 2067-2070.
124. J. D. A. Tyndall, T. Nall and D. P. Fairlie, *Chem. Rev.*, 2005, **105**, 973-1000.
125. M. Malesevic, U. Strijowski, D. Bächle and N. Sewald, *J. Biotechnol.*, 2004, **112**, 73-77.
126. N. Sayyadi, D. Taleski, S. Leesch and K. A. Jolliffe, *Tetrahedron*, 2014, **70**, 7700-7706.
127. L. Zhang and J. P. Tam, *Tetrahedron Lett.*, 1997, **38**, 4375-4378.
128. K. Haas, W. Ponikwar, H. Nöth and W. Beck, *Angew. Chem. Int. Ed.*, 1998, **37**, 1086-1089.
129. J. Illesinghe, C. X. Guo, R. Garland, A. Ahmed, B. van Lierop, J. Elaridi, W. R. Jackson and A. J. Robinson, *Chem. Commun.*, 2009, **0**, 295-297.
130. R. Jagasia, J. M. Holub, M. Bollinger, K. Kirshenbaum and M. G. Finn, *J. Org. Chem.*, 2009, **74**, 2964-2974.
131. V. V. Rostovtsev, L. G. Green, V. V. Fokin and K. B. Sharpless, *Angew. Chem. Int. Ed.*, 2002, **41**, 2596-2599.
132. R. M. Kohli, C. T. Walsh and M. D. Burkart, *Nature*, 2002, **418**, 658-661.
133. Y. Lee and R. B. Silverman, *Org. Lett.*, 2000, **2**, 3743-3746.
134. G. Sabatino, M. Chelli, S. Mazzucco, M. Ginanneschi and A. M. Papini, *Tetrahedron Lett.*, 1999, **40**, 809-812.
135. G. W. Kenner, J. R. McDermott and R. C. Sheppard, *J. Chem. Soc. D*, 1971, 636-637.
136. B. J. Backes and J. A. Ellman, *J. Org. Chem.*, 1999, **64**, 2322-2330.

137. B. J. Backes, A. A. Virgilio and J. A. Ellman, *J. Am. Chem. Soc.*, 1996, **118**, 3055-3056.
138. N. Wehofskey, N. Koglin, S. Thust and F. Bordusa, *J. Am. Chem. Soc.*, 2003, **125**, 6126-6133.
139. M. D. Gieselman, L. Xie and W. A. van der Donk, *Org. Lett.*, 2001, **3**, 1331-1334.
140. A. Díaz-Moscoso, J. M. Benito, C. Ortiz Mellet and J. M. García Fernández, *J. Comb. Chem.*, 2007, **9**, 339-342.
141. D. Maclean, R. Hale and M. Chen, *Org. Lett.*, 2001, **3**, 2977-2980.
142. L. Yang and G. Morriello, *Tetrahedron Lett.*, 1999, **40**, 8197-8200.
143. S. Kumarn, N. Chimnoi and S. Ruchirawat, *Org. Biomol. Chem.*, 2013, **11**, 7760-7767.
144. P. C. de Visser, N. M. A. J. Kriek, P. A. V. van Hooft, A. Van Schepdael, D. V. Filippov, G. A. van der Marel, H. S. Overkleef, J. H. van Boom and D. Noort, *J. Pept. Res.*, 2003, **61**, 298-306.
145. C. Qin, X. Bu, X. Wu and Z. Guo, *J. Comb. Chem.*, 2003, **5**, 353-355.
146. C. Qin, X. Zhong, X. Bu, N. L. J. Ng and Z. Guo, *J. Med. Chem.*, 2003, **46**, 4830-4833.
147. H. A. Lim, L. T. Tan and C. S. B. Chia, *Int. J. Pept. Res. Ther.*, 2013, **19**, 25-31.
148. L. Bourel-Bonnet, K. V. Rao, M. T. Hamann and A. Ganesan, *J. Med. Chem.*, 2005, **48**, 1330-1335.
149. A. Thakkar, T. B. Trinh and D. Pei, *ACS Comb. Sci.*, 2013, **15**, 120-129.
150. E. Fischer and E. Fourneau, *Ber. Dtsch. Chem. Ges.*, 1901, **34**, 2868-2877.
151. L. A. Carpino, M. Beyermann, H. Wenschuh and M. Bienert, *Acc. Chem. Res.*, 1996, **29**, 268-274.
152. C. A. G. N. Montalbetti and V. Falque, *Tetrahedron*, 2005, **61**, 10827-10852.
153. S. Yu, X. Pan, X. Lin and D. Ma, *Angew. Chem. Int. Ed.*, 2005, **44**, 135-138.
154. B. Neises and W. Steglich, *Angew. Chem. Int. Ed.*, 1978, **17**, 522-524.
155. C. Roses, C. Camo, K. Vogels, M. Planas and L. Feliu, *Org. Lett.*, 2016, **18**, 4140-4143.

156. W. Jiang, J. Wanner, R. J. Lee, P.-Y. Bounaud and D. L. Boger, *J. Am. Chem. Soc.*, 2003, **125**, 1877-1887.
157. Naveen and S. A. Babu, *Tetrahedron Lett.*, 2016, **57**, 5801-5807.
158. A. S. Culf, M. Čuperlović-Culf, D. A. Léger and A. Decken, *Org. Lett.*, 2014, **16**, 2780-2783.
159. I. Loke, N. Park, K. Kempf, C. Jagusch, R. Schobert and S. Laschat, *Tetrahedron*, 2012, **68**, 697-704.
160. S.-T. Chen, L.-C. Lo, S.-H. Wu and K.-T. Wang, *Int. J. Pept. Protein Res.*, 1990, **35**, 52-54.
161. M. Wang and P. J. Casey, *Nat. Rev. Mol. Cell Biol.*, 2016, **17**, 110-122.
162. N. Xu, N. Shen, X. Wang, S. Jiang, B. Xue and C. Li, *Sci. China Life Sci.*, 2015, **58**, 328-335.
163. S. L. Moores, M. D. Schaber, S. D. Mosser, E. Rands, M. B. O'Hara, V. M. Garsky, M. S. Marshall, D. L. Pompliano and J. B. Gibbs, *J. Biol. Chem.*, 1991, **266**, 14603-14610.
164. P. Casey, *Science*, 1995, **268**, 221-225.
165. S. S. Ivanov, G. Charron, H. C. Hang and C. R. Roy, *J. Biol. Chem.*, 2010, **285**, 34686-34698.
166. P. Mak, J. Pohl, A. Dubin, M. S. Reed, S. E. Bowers, M. T. Fallon and W. M. Shafer, *Int. J. Antimicrob. Agents*, 2003, **21**, 13-19.
167. N. A. Lockwood, J. R. Haseman, M. V. Tirrell and K. H. Mayo, *Biochem. J.*, 2004, **378**, 93-103.
168. Y. Hu, M. N. Amin, S. Padhee, R. E. Wang, Q. Qiao, G. Bai, Y. Li, A. Mathew, C. Cao and J. Cai, *ACS Med. Chem. Lett.*, 2012, **3**, 683-686.
169. J. D. Ochocki, U. Igbavboa, W. Gibson Wood, E. V. Wattenberg and M. D. Distefano, *Chem. Biol. Drug. Des.*, 2010, **76**, 107-115.
170. J. W. Wollack, N. A. Zeliadt, D. G. Mullen, G. Amundson, S. Geier, S. Falkum, E. V. Wattenberg, G. Barany and M. D. Distefano, *J. Am. Chem. Soc.*, 2009, **131**, 7293-7303.
171. T. Bonitz, F. Zubeil, S. Grond and L. Heide, *PLOS ONE*, 2013, **8**, e85707.
172. A. Grundmann, T. Kuznetsova, S. S. Afiyatullof and S.-M. Li, *ChemBioChem*, 2008, **9**, 2059-2063.
173. T. F. Andersen and K. Strømgaard, *Tetrahedron Lett.*, 2004, **45**, 7929-7933.

174. S. M. Dankwardt, D. B. Smith, J. A. Porco Jr and C. H. Nguyen, *Synlett*, 1997, **1997**, 854-856.
175. R. J. Bergeron and J. S. McManis, *J. Org. Chem.*, 1988, **53**, 3108-3111.
176. M. F. Richter, B. S. Drown, A. P. Riley, A. Garcia, T. Shirai, R. L. Svec and P. J. Hergenrother, *Nature*, 2017, **545**, 299-304.
177. D. M. Brown and P. Acred, *Br. Med. J.*, 1961, **2**, 197-198.
178. G. Quelever, P. Kachidian, C. Melon, C. Garino, Y. Laras, N. Pietrancosta, M. Sheha and J. Louis Kraus, *Org. Biomol. Chem.*, 2005, **3**, 2450-2457.
179. M. Jullian, A. Hernandez, A. Maurras, K. Puget, M. Amblard, J. Martinez and G. Subra, *Tetrahedron Letters*, 2009, **50**, 260-263.
180. P. Edman, *Nature*, 1956, **177**, 667-668.

